INPUT PROPERTIES OF FOUR POPULATIONS OF SPINOCEREBELLAR TRACT NEURONS IN THE CAT AND THE RAT THORACO-LUMBAR SPINAL CORD

Sony Shakya Shrestha

Thesis submitted in fulfillment for the degree of Doctor of Philosophy

Institute of Neuroscience and Psychology
College of Medical, Veterinary and Life Sciences
University of Glasgow
Glasgow, Scotland

July 2012

Dedication

To my most loving late Grandfather and my family

Summary

The cerebellum receives information from the hindlimbs through several populations of spinocerebellar tract neurons. Although the role of these neurons has been established in electrophysiological experiments, the relative contribution of afferent fibres and central neurons to their input, their organization and mechanisms of control of transmission has only been estimated approximately so far. The present study aimed to investigate the input properties of four populations of spinocerebellar tract neurons: dorsal spinocerebellar tract neurons located in Clarke´s column (ccDSCT) and in the dorsal horn (dhDSCT) and ventral spinocerebellar tract (VSCT) neurons including spinal border (SB) neurons. There were three major aims: (1) to investigate the excitatory inputs to four types of spinocerebellar tract neurons in the cat and rat thoraco-lumbar spinal cord; (2) to analyze the inhibitory inputs to four types of spinocerebellar tract neurons in the cat and rat thoraco-lumbar spinal cord; (3) to determine the origin of excitatory and inhibitory inputs to four types of spinocerebellar tract neurons in the cat and rat thoraco-lumbar spinal cord.

Two series of experiments were carried out. In the first series of experiments in cats, spinocerebellar tract neurons were identified electrophysiologically and labelled intracellularly with rhodamine-dextran and Neurobiotin. In the second series of experiments in rats, cells were labelled by retrograde transport of b-subunit of Cholera toxin (CTb) from the cerebellum. In addition, to address the third aim, reticulospinal (RetS) and corticospinal (CS) terminals were identified by anterograde transport of CTb from the caudal medulla and hindlimb sensory motor cortex respectively in rats along with labelling of spinocerebellar tract neurons by retrograde injection of Fluorogold in the cerebellum. Following this, immunohistochemistry was carried out.

The first aim was achieved by utilizing the difference in the immunohistochemistry of glutamatergic terminals of peripheral afferents and of central neurons with vesicular glutamate transporters, VGLUT1 or VGLUT2, respectively. All SB neurons with dominating inhibitory input from the periphery possessed very few VGLUT1

contacts and remarkably higher numbers of VGLUT2 contacts. In VSCT neurons with excitatory primary afferent input, the number of VGLUT1 contacts was relatively high although VGLUT2 contacts likewise dominated. In contrast, DSCT neurons were associated with numerous VGLUT1 contacts; ccDSCT neurons with strong input from group I afferents had higher density of VGLUT1 contacts than dhDSCT neurons with major input from group II and cutaneous afferents.

In order to fulfill the second aim, quantification of contacts formed by inhibitory axon terminals on spinocerebellar tract neurons along with excitatory terminals was carried out. Inhibitory axon terminals were characterised as either GABAergic, glycinergic or both GABAergic/glycinergic by using antibodies against vesicular GABA transporter (VGAT), glutamic acid decarboxylase (GAD) and gephyrin. Similarly, excitatory terminals were characterised by using combination of VGLUT1 and 2. The comparison revealed the presence of much higher proportions of inhibitory than excitatory contacts on SB neurons but similar proportions were found on VSCT, ccDSCT and dhDSCT neurons. In all types of cell, the majority of inhibitory terminals were glycinergic. The density of contacts was higher on somata and proximal in comparison with distal dendrites of SB and VSCT neurons but more evenly distributed in ccDSCT and dhDSCT neurons.

To achieve the third aim, a series of immunohistochemical reactions was performed to characterize contacts that originate from proprioceptors, different types of interneurons and descending RetS and CS pathways. Among the four populations of spinocerebellar tract neurons, ccDSCT neurons had the highest proportion of contacts formed by VGLUT1 terminals double labeled with parvalbumin (PV) which indicated that majority of direct excitatory sensory inputs to ccDSCT neurons are derived from proprioceptors. A small proportion of excitatory and inhibitory contacts on these neurons originated from Calbindin/ Calretinin/ PV expressing neurons. Quantitative analysis revealed that SB and VSCT neurons have significantly higher numbers of appositions from VGLUT2 expressing RetS axon terminals than DSCT neurons. A small proportion of the RetS contacts on these neurons were VGAT positive. In contrast, DSCT neurons had higher numbers of appositions made by CS axon terminals in comparison to SB and VSCT neurons.

The present findings provide a new basis for understanding the organization and functional connectivity of four populations of spinocerebellar tract neurons and strengthen previous indications of their functional differentiation. SB and VSCT neurons principally receive inputs from spinal and supraspinal neurons although direct input from primary afferents is also stronger in VSCT neurons. DSCT neurons have major direct input from primary afferents and also to some extent from the CS pathway but monosynaptic inputs from proprioceptors dominated in ccDSCT neurons and dhDSCT neurons have mixed proprioceptive and low threshold cutaneous afferent input.

Acknowledgement

Many people have directly or indirectly contributed to this work. To name them all would result in a directory worth of separate publication. Indeed, they know who they are, and they know that they share this work with me and hopefully they also know how much I am obliged to them.

While my intellectual debts are manifolds, I am especially grateful to my supervisor Professor David J Maxwell, Spinal Cord Research Group, Institute of Neuroscience & Clinical Psychology, College of Medicine, Veterinary and Life Sciences, University of Glasgow for his endless support and excellent guidance throughout my research period. I express my heartfelt gratitude to my collaborator Professor Elzbieta Jankowska, Department of Physiology, University of Gothenburg, Sweden for her continuous support and guidance during my visit to her laboratory for electrophysiology experiments. I also would like to thank Dr. Ingela Hammar for her help and hospitality during my Sweden visit. Moreover, I want to thank all the people in Professor Jankowska's group for their helpful nature.

My sincere gratitude also goes to Professor Andrew J Todd, Spinal Cord Research Group, Institute of Neuroscience & Clinical Psychology, College of Medicine, Veterinary and Life Sciences, University of Glasgow for his continuous encouragement and valuable inputs to my research work. I take an immense pleasure to acknowledge Dr. Anne Bannatyne and Dr. Erika Polgar for their help and expert guidance during my research work. An endless thanks goes to Mrs. Christine Watt and Mr. Robert Kerr for their technical support and their always welcoming nature. Special thanks go to my laboratory mates especially, Huma and Nazma for their constant support during my thesis work. There are other groups of individuals whose contributions to this work cannot go unmentioned. All the staffs of Spinal Cord Research Group including Biological Services Central Research Unit, with whom I worked closely, colleagues whose cooperation made this work worthwhile,

also deserve my heartfelt gratitude. I also want to thank all the cleaners and security people of West Medical Building for their friendly behaviour.

A special acknowledgement is due to Overseas Research Studentship Award Scheme and Glasgow University Postgraduate Scholarship awarding body for funding my PhD research. I am very thankful for their support and trust. My special thanks go to Carol and Paul for being a very good friend and supporting us whenever we needed.

Lastly, I cannot forget my parents and my loving husband Rajeev, whose never-ending support, trust and constant encouragement led to the accomplishment of this work.

Author's declaration

All the work in this thesis was carried out solely by the author apart from surgical procedures and electrophysiology. Professor David Maxwell contributed to this work by performing surgical procedures in rats. Professor Elzbieta Jankowska contributed to this work by performing surgical procedures and electrophysiological recordings in cats. This thesis has been composed by the author and has not been previously submitted for examination which has led to the award of a degree.

Signature:

Date:

Table of contents

List of Tables

List of Figures

List of Abbreviations

%	percentage
µA	microampere
µm	micrometer
3D	three dimensional
4-AP	4- amino-pyridine
5-HT	serotonin (5- hydroxytryptamine)
8-OH-DPAT	8- hydroxy-2-(di-n-propylamino)-tetralin
ABSM	anterior biceps and semimembranosus
AMPA	α-amino-3-hydroxy-5-methyl-4-isoxazolepropionic acid
ANOVA	analysis of variance
C	cervical
CB	calbindin
cc	Clarke's column
CCN	central cervical nucleus
CCT	cuneocerebellar tract
CIN	commissural interneurons
CR	calretinin
CS	corticospinal
CST	corticospinal tract
CTb	cholera toxin B subunit
CVLM	caudal ventrolateral medulla
DAB	3, 3'-diaminobenzidine
Dh	dorsal horn
DSCT	dorsal spinocerebellar tract
E-CCT	exteroceptive Cuneocerebellar tract
EPSP	excitatory post synaptic potential
FDL	flexor digitorum and hallucis longus
FRA	flexor reflex afferents
GABA	gamma-aminobutyric acid
GAD	glutamic acid decarboxylase

GDNF	glial derived neurotrophic factor
GFP	green florescent proteins
gm	gram
GS	gastrocnemius-soleus
HRP	horseradish peroxidase
i.p.	intra peritoneal
i.v.	intra-venous
Ig	immunoglobulin
IgG	immunoglobulin gamma
IPSP	inhibitory post synaptic potential
L	lumbar
LRN	lateral reticular nucleus
LVST	lateral vestibulospinal tract
M	molar
ml	milliliter
MLF	medial longitudinal fascicle
MLR	mesencephalic locomotor region
mm	millimeter
mM	millimolar
mV	milli-volt
MVST	medial vestibulospinal tract
NA	nor adrenaline
NK1	neurokinin-1
nm	nanometer
NMDA	N-methyl-D-Aspartate
ºC	degree Celsius
PB	phosphate buffer
PBS	phosphate buffer saline
PBST	phosphate buffer saline containing 0.3% trition
PBSt	posterior biceps and semitendinosus
P-CCT	proprioceptive cuneocerebellar tract
PL	plantaris

PSPs	post synaptic potentials
PT	pyramidal tract
PV	parvalbumin
Q	quadriceps
RetS	reticulospinal
RetST	reticulospinal tract
Rh	rhodamine
RS	rubrospinal
RSCT	rostral spinocerebellar tract
RST	rubrospinal tract
S	sacral
Sart	sartorius
SB	spinal border
SBC	spinal border cell
SD	standard deviation
SP	superficial peroneal
Th	thoracic
VGAT	vesicular GABA transporter
VGLUT	vesicular glutamate transporter
VS	vestibulospinal
VSCT	ventral spinocerebellar tract
VST	vestibulospinal tract
WGA	wheat germ agglutinin

1 Introduction

The spinocerebellar tract is a group of neurons that originate in the spinal cord and terminate in the cerebellum. Unlike other ascending tracts forwarding information from the spinal cord, they reach the cerebellum without any synaptic interruption. The spinocerebellar system has been considered as one of the principal target sites for afferent fibres innervating muscle receptors, cutaneous and joint receptors and, to some extent, the major descending pathways from the brain. Thus spinocerebellar tract neurons have been suggested as a key system for processing of proprioceptive and extereoceptive sensory information at the lowest levels in the nervous system where the functional connectivity between various sensory receptors, intraspinal and central neurons can be studied. It is well established that the spinocerebellar system consists of four direct tracts: the dorsal spinocerebellar tract (DSCT), the ventral spinocerebellar tract (VSCT), the rostral spinocerebellar tract (RSCT) and the cuneocerebellar tract (CCT). The DSCT and VSCT are considered to provide the major direct sensory projections from hindlimbs and lower part of the trunk to the cerebellum (Oscarsson, 1965) while the later two are regarded as their forelimb counterparts (Oscarsson and Uddenberg, 1965).

In this chapter, I have reviewed the literature available to date regarding the spinocerebellar pathways with a main focus on its hindlimb components. To aid our understanding of the control of transmission through this pathway, knowledge about the cerebellum and its functions, various identified spinal interneurons interposed in primary afferent pathways and the major descending pathways which have modulatory action on these neurons is a prerequisite. Therefore, this chapter is divided into four major sections. The first section focuses on the elementary organization and general characteristics of the spinocerebellar tracts; the second section provides an account of the cerebellum; the third section gives an overview of the general characteristics of functionally identified mammalian interneurons in the spinal cord and the last section describes the major descending pathways in the rat spinal cord.

1.1 Elementary organization and general characteristics of the spinocerebellar tracts

The introduction of retrograde tract tracing techniques with different tracers has provided neuroscientists with a selective retrograde labelling method for spinocerebellar tract neurons in the spinal cord (Matsushita and Hosoya, 1979; Matsushita *et al.*, 1979). Consequently, with the introduction of microelectrode techniques, the neurons of the spinocerebellar tract became a particularly interesting target for study along with spinal motoneurons. This is because the size of these cells is large enough for intracellular recording and both of them are direct targets for sensory input from muscle receptors. Based upon the axonal course of retrogradely labelled spinocerebellar tract neurons in the entire length of the spinal cord, various studies performed by using retrograde injection of horseradish peroxidase (HRP) into the cerebellum has resulted into a classification of these neurons into two major groups: the uncrossed spinocerebellar tract neurons and the crossed spinocerebellar tract neurons (Matsushita and Hosoya, 1979; Matsushita *et al.*, 1979). In the rat, the neurons forming the uncrossed tracts are located in the medial part of lamina VI of the cervical (C) segments between C2 to C8, the central part of lamina VII of C4 to C8, lamina V of C7 to L3 and Clarke's column (cc) whereas, the neurons forming the crossed tracts are located in the central cervical nucleus (CCN) of C1 to C3, the intermediate zone and the ventral horn of the lower thoracic (Th) and the lumbar (L) segments (Th11 to L3), and in the dorsal horn, the medial part of lamina VII and the ventrolateral part of the ventral horn of the sacral and caudal spinal cord (Matsushita and Hosoya, 1979). This organization is similar in cats (Matsushita *et al.*, 1979) and rats (Matsushita and Hosoya, 1979). A simplified diagram showing the origin of different populations of spinocerebellar tract neurons in the cat and the rat is shown in Figure 1-1. In the hindlimb component of spinocerebellar pathway, DSCT neurons belong to the uncrossed spinocerebellar tract neurons while VSCT comprises of the crossed spinocerebellar tract neurons (Matsushita and Hosoya, 1979; Matsushita *et al.*, 1979). In both the cat and the rat, different populations of neurons giving rise to DSCT and VSCT are distributed and organised in the similar manner, though there is some differences in the segmental

levels of appearance of the corresponding neuronal groups. DSCT neurons in the cc are present throughout Th2 to L4 segments in the cat (Matsushita *et al.,* 1979) while in the rat they are located in Th1 to L2 segments (Matsushita and Hosoya, 1979). Lamina V neurons (corresponding to dorsal horn component of DSCT in thoraco-lumbar segments; see below) are found from C7 to L6 segments in the cat (Matsushita *et al.,* 1979) whereas they extend from C7 to L3 segments in the rat (Matsushita and Hosoya, 1979). Similarly, the laterally located neurons in lamina VII and IX (SB neurons; see below) are most numerous in L2 to L6 segments in the cat (Matsushita *et al.,* 1979) which correspond to the laterally located neurons in Th11 to L3 segments in the rat (Matsushita and Hosoya, 1979). Further, the medially located group of neurons in lamina VII contributing to VSCT are found to extend from L2 to L5 segments in the cat (Matsushita *et al.,* 1979) which are equivalent to neurons in similar location extending from Th12 to L3 segments in the rat (Matsushita and Hosoya, 1979).

Figure 1-1 Diagram summarizing the origin of different populations of spinocerebellar tract neurons with uncrossed axons (left) and crossed axons (right)

***A*,** In the cat, uncrossed spinocerebellar tracts originate from neurons in the medial part of lamina VI (UC and CE), the central part of lamina VII (CE), lamina V (CE to LE), Clarke's column and medial lamina VI (LE), Crossed spinocerebellar tracts originate from neurons in the CCN, lamina VIII (UC to LE), medial part of lamina VII (L6 to Ca), lateral part of lamina VII and IX, lamina V (S and Ca), lamina VII and VIII (S and Ca). ***B*,** In the rat, uncrossed spinocerebellar tracts originate from neurons in the medial part of lamina VI (UC and CE), the central part of lamina VII (CE), lamina V (CE to LE) and Clarke's column. Crossed spinocerebellar tracts originate from neurons in the CCN, lamina VII (LE) and in the dorsal horn, the medial part of lamina VII and the ventrolateral part of the sacral and caudal spinal cord (S and Ca). UC, upper cervical; CE, cervical enlargement; Th, thoracic; LE, lumbar enlargement; S, sacral; Ca, caudal. Images are modified from Figure 11 in Matsushita *et al.*, 1979 and from Figure 6 in Matsushita and Hosoya, 1979.

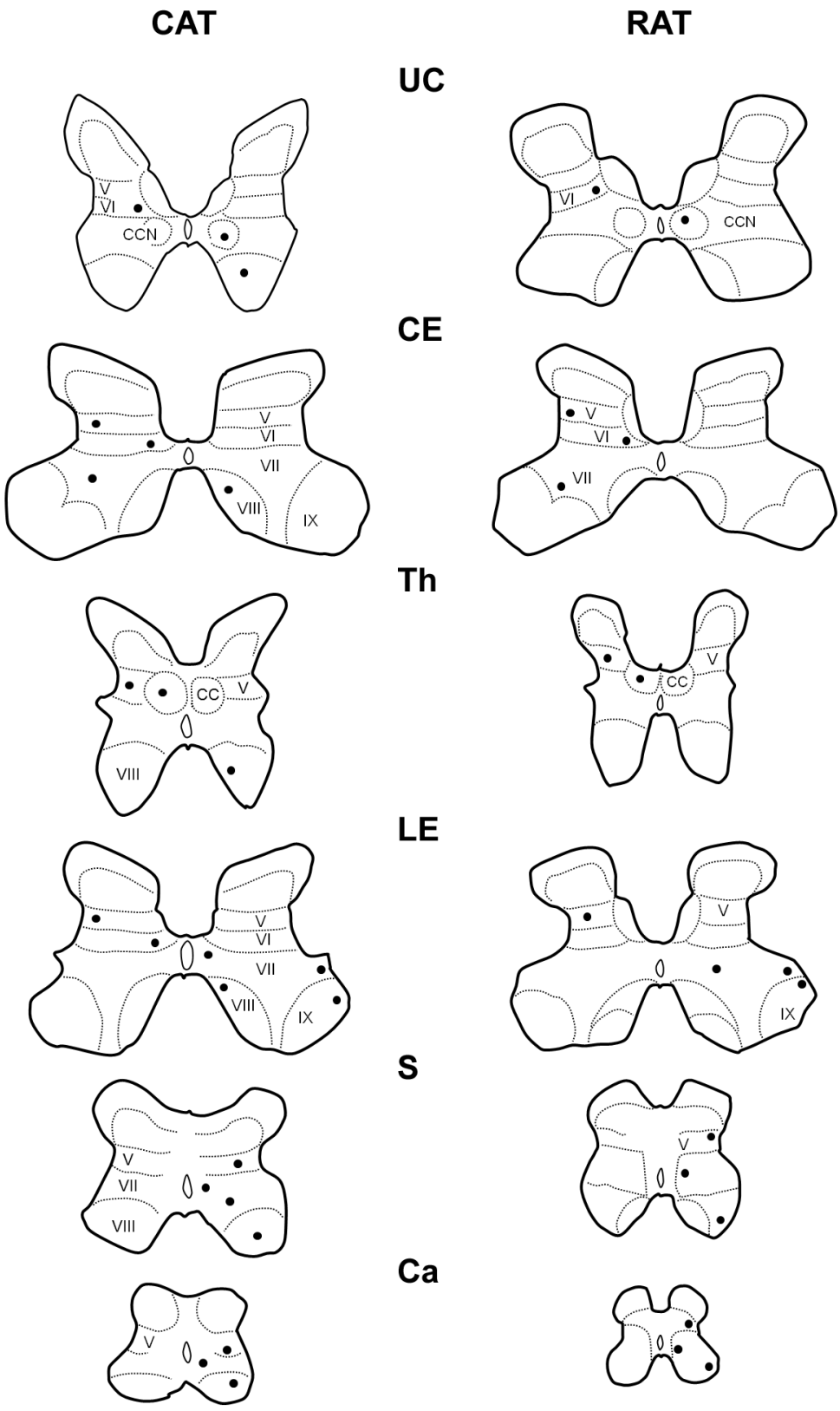
CAT
RAT
UC
V
VI
CCN
VI
CCN
CE
V
VI
VII
VIII
IX
V
VI
VII
Th
CC
V
VIII
CC
V
LE
V
VI
VII
VIII
IX
V
IX
S
V
VII
VIII
V
Ca
V

1.1.1 Dorsal Spinocerebellar tract (DSCT)

1.1.1.1 Anatomical location and general morphology

Classically, it was described that the cells of origin of DSCT reside in cc in Rexed's lamina VII (Rexed, 1954) which extends from the Th2 or Th3 segment to the L3 or more usually L4 segment of the spinal cord in cats (Boehme, 1968). The cytoarchitecture of cc in rats is significantly different from that of cats. The cells in cc in rats are smaller and more fusiform than those of cats and the column itself is more dorsoventrally flattened (Snyder *et al.*, 1978). However, the introduction of intracellular labelling of the neurons and development of anatomical tracers like wheat germ agglutinin (WGA)-HRP led to the identification of several other groups of neurons that also belong to DSCT although the axons from the cc form a major component of DSCT. This additional set of DSCT neurons were identified anatomically within the dorsal horn grey matter, dorsal and lateral to cc, from lamina IV to lamina VI in rats (Grant *et al.*, 1982) and electrophysiologically and anatomically in cats (Tapper *et al.*, 1975; Randic *et al.*, 1976; Edgley and Gallimore, 1988; Edgley and Jankowska, 1988). These neurons are found in the thoracic and lumbosacral segments of the spinal cord (Matsushita *et al.*, 1979; Matsushita, 1988; Matsushita and Yaginuma, 1989). The former group of neurons in cc which are major contributors of DSCT axons are referred as Clarke's column dorsal spinocerebellar tract (ccDSCT) neurons and the later group of neurons in the dorsal horn are termed as dorsal horn dorsal spinocerebellar tract (dhDSCT) neurons (Shakya-Shrestha *et al.*, 2012).

In general, with respect to dendritic and axonal morphology, DSCT cells of both origins are very similar (Edgley and Gallimore, 1988). Intracellular staining of HRP in physiologically identified neurons in cats has shown that both of these categories of cells have large somata with complex and extensive dendritic trees (Edgley and Gallimore, 1988; Walmsley and Nicol, 1990).

ccDSCT neurons are medium to large sized (Petras, 1977; Petras and Cummings, 1977; Randic *et al.*, 1981; Walmsley and Nicol, 1990) which are either multipolar star or spindle shaped (Matsushita *et al.*, 1979). Originally, Golgi studies in cats

suggested that the dendrites of these neurons are distributed predominantly in rostro-caudal direction within the nucleus (Boehme, 1968). Subsequent studies using intracellular labelling techniques in cats have revealed even more complex and extensive dendritic trees which extend beyond the boundaries of the nucleus but are confined mediolaterally (Randic *et al.*, 1981; Houchin *et al.*, 1983; Walmsley and Nicol, 1990). Furthermore, it has been proposed that the somata of ccDSCT neurons are organised somatotopically within the cc nucleus. For example, the ccDSCT neurons receiving input from gastrocnemius/ soleus are located more medially than those which have input from biceps femoris (Kuno *et al.*, 1973a).

dhDSCT neurons are located caudal to ccDSCT neurons and their cell bodies are distributed across the entire width of the dorsal horn close to the border of lamina IV and V (Edgley and Gallimore, 1988). Following intracellular injection of HRP on physiologically identified dhDSCT neurons in cats, Edgley and Gallimore (1988) have demonstrated that the cell bodies of these neurons are large like those of ccDSCT neurons and are considerably elongated in the rostro-caudal direction. The elongation of the dendrites is also in the rostro-caudal direction; the majority of them arborise dorsal to the cell body in laminae IV and V, and extend into lamina III. Their dendrites are also confined mediolaterally similar to those of ccDSCT neurons (Randic *et al.*, 1981; Houchin *et al.*, 1983).

1.1.1.2 Axonal projections and termination site in the cerebellum

In general, both the ccDSCT and dhDSCT have a similar pattern of axonal projections and cerebellar termination sites (Matsushita and Okado, 1981; Matsushita and Hosoya, 1982). The axons of both populations of DSCT neurons ascend exclusively in the ipsilateral side of the cord and occupy the dorsal part of lateral funiculus (Xu and Grant, 1994; Xu and Grant, 2005). They enter the cerebellum through the inferior cerebellar peduncle and terminate as mossy fibres almost exclusively in the ipsilateral cerebellar cortex (Oscarsson, 1965).

Studies using degeneration and electrophysiological approaches in cats have shown that the axons of DSCT neurons terminate in the intermediate region and in the

adjacent vermal region in the anterior lobe of the cerebellum (Lundberg and Oscarsson, 1960; Grant, 1962b; Coffey *et al.*, 1971). Subsequently, extensive anatomical studies by Matsushita's group have demonstrated various other regions in the cerebellum where spinocerebellar tract axons terminate. For example, one study in the cat using direct injection of HRP into the anterior lobe by removing the posterior part of the vermis has shown that the axons of DSCT neurons terminate in lobule I and II of the anterior lobe (Matsushita and Okado, 1981). Similarly, a study using the HRP method has also shown that DSCT neurons also project to lobule III and lobule V of the anterior lobe (Matsushita and Hosoya, 1982) and to lobule VIII of the posterior lobe vermis and the paramedian lobe in the cat (Matsushita and Ikeda, 1980). It is worth noting that in all of these studies, despite the categorization of two distinct components of the DSCT, retrogradely labelled neurons outside of the cc between laminae IV to V are more likely to be dhDSCT neurons. Anterograde labelling of mossy fibre terminals by injecting in different segments (C1-C4, Th3-Th4, Th4-Th7, L7-Sacral3) with WGA-HRP in the cat shows a similar projection field in the cerebellum (Matsushita *et al.*, 1984) and anterograde injection of biotinylated-dextran either in L1 to L3 or Th4 to Th9 segments in the rat revealed labelled DSCT axon terminals in the medial and interpositus cerebellar nuclei (Matsushita and Gao, 1997; Matsushita, 1999).

Various studies have suggested the existence of axon collaterals from DSCT neurons (Johansson and Silfvenius, 1977; Low *et al.*, 1986). Stimulation applied within the cerebellum and dorsolateral fascicle in the spinal cord activate cells in the Nucleus Z in the thalamus and a proportion of this action has been suggested to be from axon collaterals of DSCT neurons in cats (Johansson and Silfvenius, 1977). Complementing this evidence, another anatomical study based on double retrograde labelling in rats has demonstrated axonal collaterals from ccDSCT neurons (Low *et al.*, 1986). They have shown that most of the spinal afferents to nucleus Z are axon collaterals of ccDSCT neurons which have a smaller average diameter than that of DSCT neurons that do not project to the nucleus Z. On the other hand, although no initial axon collaterals are seen in dhDSCT axons, one of the studies proposed the possibility of collateral projections from these neurons in

the cat (Edgley and Jankowska, 1988), to the region of nucleus Z. Neurons in nucleus Z project to the ventrobasal thalamus and then to the somatosensory cortex (Landgren and Silfvenius, 1971). It has been shown that the majority of group I and II muscle afferents from the hindlimb in the cat project rostrally up to the dorsal columns in the upper lumbar segments or the lowest thoracic segments and very few reach the cervical levels (Fern *et al.,* 1988). Therefore as DSCT neurons transmit information from muscle afferents to the nucleus Z, this nucleus Z is believed to be a medullary relay nucleus contributing to the pathway for transmitting information from primary afferents from muscle spindle and Golgi tendon organs to the cerebral cortex and may have an important role in proprioception. Further, it is likely that DSCT has an important role in the conscious perception of limb position in addition to supplying the cerebellum with information from hindlimbs (Landgren and Silfvenius, 1970; Landgren and Silfvenius, 1971; Johansson and Silfvenius, 1977; McIntyre *et al.*, 1985).

1.1.1.3 Inputs and synaptic connections to neurons of origin of the DSCT

Studies on DSCT which began in the 1950s became the basis for the study of central proprioception. The term proprioception was first used by Sherrington (1906) which is used to describe the sensory information that contributes to the sense of self position and movement. This included different types of neurons and their projections relaying receptor-specific and highly localized sensory information to higher centres. Knowledge about the functional connectivity of neurons comprising DSCT helps in understanding the information transmitted from this pathway to the cerebellum. In this section, I have provided a detailed overview of different kinds of inputs to the neurons of cc and dorsal horn which constitute DSCT.

Excitatory inputs to ccDSCT neurons

Neurons of origin of ccDSCT receive excitatory inputs from various sources including muscle and cutaneous afferents and descending systems.

Excitatory inputs from primary afferents

ccDSCT neurons receive excitatory input from different types of receptors including muscle spindles (group Ia and II afferents), Golgi tendon organs (group Ib afferents), joint and cutaneous receptors (Lloyd and McIntyre, 1950; Laporte and Lundberg, 1956; Laporte *et al.*, 1956a; Laporte *et al.*, 1956b; Lundberg and Oscarsson, 1956; Jansen and Rudjord, 1965; Mann, 1971; Kuno *et al.*, 1973a; Kuno *et al.*, 1973b; Petras and Cummings, 1977). Earliest studies in cats using a combination of physiological identification of primary afferent fibres and labelling of ccDSCT neurons by retrograde injection in the cerebellum demonstrate the connections between them (Tracey and Walmsley, 1984; Walmsley *et al.*, 1985; Hongo *et al.*, 1987; Walmsley *et al.*, 1987). For example, Tracey and Walmsley (1984) have shown direct contacts made by both group Ia and Ib boutons on ccDSCT neurons. Their detailed anatomical examination provided evidence of wide variations in the size of the primary afferent terminals contacting ccDSCT neurons, some of which were extremely large, up to 25 µm in length. This feature was observed previously and the large boutons on ccDSCT neurons were named as “giant synapses” (Walmsley *et al.*, 1985). Previous evidence based on electron-microscopic studies in cc indicated that these giant boutons may contain multiple transmitter release sites (Réthelyi, 1970; Houchin *et al.*, 1983). However, the precise origin of these boutons was not described in those studies. Subsequently, similar evidence was provided by the ultrastructural analysis of identified HRP labelled Ia afferent terminals on HRP labelled ccDSCT neurons in cats (Walmsley *et al.*, 1985). Tracey and Walmsley (1984) also demonstrated contacts made by both Ia and Ib terminals on somata and dendrites of ccDSCT neurons, but the full contact pattern on the dendrites of these neurons was not investigated because of the very proximal labelling of dendrites following retrograde HRP labelling.

Direct monosynaptic excitatory connections between primary afferents and ccDSCT neurons as revealed by various studies at the light and electron microscopic level have later been confirmed by several lines of electrophysiological studies. These electrophysiological studies were mainly performed in cats and were based on the intracellular and extracellular recordings from the cell body of the particular

neuron. Earlier studies using intracellular recording of ccDSCT neurons showed strong monosynaptic activation following stimulation of primary afferents (Laporte *et al.*, 1956a; Laporte *et al.*, 1956b; Lundberg and Oscarsson, 1956; Eccles *et al.*, 1961b). Most of the electrophysiological research focused on the response of the cells to nerve stimulation, led to an elaborate set of divisions depending upon the main type of afferent input (Lundberg and Oscarsson, 1956; Lundberg and Oscarsson, 1960). According to those studies, ccDSCT neurons appear to fall into two classes, one with its main peripheral input from proprioceptors (proprioceptive subdivision) and the other with its main input from exteroceptors (exteroceptive subdivisions), although excitatory post synaptic potentials (EPSPs) are evoked from both muscle and cutaneous afferents in some cells. The majority of ccDSCT neurons belong to the proprioceptive subdivision. Thus neurons in the proprioceptive subdivision had their main excitatory input either from group Ia afferents from muscle spindles or group Ib afferents from Golgi tendon organs or both (Lundberg and Oscarsson, 1956; Lundberg and Winsbury, 1960; Eccles *et al.*, 1961b). Weak convergent input from group II afferents has been reported in some cells with group Ia and/ or group Ib inputs (Eccles *et al.*, 1961b). Furthermore, it has been shown that the predominant monosynaptic excitation of proprioceptive ccDSCT neurons originates from afferents in a single muscle nerve (Eccles *et al.*, 1961b; Kuno *et al.*, 1973a). The EPSPs generated in these neurons by stimulating group I afferents are generally large and are built up by several unitary EPSPs (Tracey and Walmsley, 1984; Walmsley, 1989). This has been suggested to be a consequence of extensive convergence of fibres from the same muscle nerves.

Furthermore, excitatory features of the synaptic inputs to ccDSCT neurons from primary afferents have been indicated by other studies (Maxwell *et al.*, 1990; Walmsley and Nicol, 1991). For example, a pharmacological study, using a technique of perfusion of the central canal to alter the ionic environment of ccDSCT neurons *in vivo,* demonstrated a complete block of the monosynaptic EPSP evoked by stimulation of gastrocnemius soleus with the passage of Kynurenate, an antagonist of excitatory amino acids (Walmsley and Nicol, 1991). In addition, evidence for a high intensity of glutamate antibody labelling in giant boutons in cc has been provided by an immunohistochemical study, which were presumed to be

group I muscle afferent terminals (Maxwell *et al.*, 1990). These studies provide direct evidence that the neurotransmitter released at the primary afferent synapse is glutamate. The summary of the various peripheral excitatory inputs from muscle and cutaneous afferents to this neuronal population as described above is shown in Figure 1-2 (A).

Excitatory inputs from descending pathways

Prior electrophysiological studies in cats have shown that the neurons of DSCT are activated by stimulation of descending corticospinal (CS) fibres (Hongo and Okada, 1967; Hongo *et al.*, 1967). These studies revealed that stimulation of either the cerebral cortical area or the contralateral pyramid resulted in transient excitation; however, the particular subdivision of DSCT neurons was not specified in these studies. Recently, monosynaptic excitatory actions on neurons of origin of ccDSCT from CS pathway have been shown based on physiological, pharmacological, anatomical and genetic approaches in a neonatal mouse model (Hantman and Jessell, 2010). This study showed that ccDSCT neurons are activated following stimulation of the dorsal columns which are blocked by combined exposure to α-amino-3-hydroxy-5-methyl-4-isoxazolepropionic acid (AMPA) and N-methyl-D-aspartate (NMDA) receptor antagonists. Such effect suggested that the CS inputs to ccDSCT neurons are glutamatergic. In addition, all the ccDSCT neurons identified by expression of the glial derived neurotrophic factor (Gdnf) gene have contacts made by green florescent proteins (GFP) terminals which selectively marked coticospinal axons in the spinal cord of Emx1::GFP BAC transgenic mice (Hantman and Jessell, 2010). Furthermore, Hammar and her group (2011) revealed disynaptic excitatory input to ccDSCT neurons from contralaterally descending reticulospinal (RetS) neurons in the medial longitudinal fasciculus (MLF). These different sources of descending excitatory drive to these neurons are summarized in Figure 1-2 (B).

Excitatory inputs to dhDSCT neurons

Excitatory inputs from primary afferents

Excitatory inputs to the dorsal horn component of DSCT neurons are significantly different than that of ccDSCT neurons. These neurons receive powerful monosynaptic excitation from group II muscle and cutaneous afferents but not from group I afferents (Edgley and Jankowska, 1988). Group II afferents innervating dhDSCT neurons originate from more than one muscle nerve, including those from muscles acting on different joints. Prior to this study, several earlier studies of DSCT neurons using recording from the ascending axons revealed several functional subsets of DSCT. One of these has convergence of input from group II muscle afferents and cutaneous afferents (Laporte *et al.*, 1956b; Lundberg and Oscarsson, 1956; Lundberg and Winsbury, 1960; Jansen and Rudjord, 1965). Even though, no systematic differentiation of this component from the ccDSCT neurons was made in those studies, this kind of input is characteristic of dhDSCT neurons and is never found in ccDSCT neurons. With respect to cutaneous inputs, dhDSCT neurons are stimulated by at least three classes of cutaneous afferents: slowly adapting receptors located in footpads, mechanoreceptors located on the hairy skin and flexor reflex afferents (FRA) (Mann, 1971). FRAs denote group II and III muscle afferents, joint and skin afferents which may jointly evoke excitation of ipsilateral flexors and inhibition of ipsilateral extensors as well as crossed extensor reflexes via polysynaptic reflex pathways (Eccles and Lundberg, 1959). Moreover, polysynaptic excitatory inputs to dhDSCT neuronal populations have been postulated in physiological studies (Eccles *et al.*, 1961b; Edgley and Jankowska, 1988; Krutki *et al.*, 2011). These studies reported infrequent EPSPs of longer latencies following stimulation of the hindlimb muscle nerves. Although Eccles and his group (1961b) did not specify the particular subset of DSCT neurons, Edgley and Jankowska (1988) and Krutki *et al.* (2011) revealed indirect excitatory inputs in dhDSCT neurons. Direct and indirect excitatory inputs from primary and cutaneous afferents to these neurons are summarized in Figure 1-3 (A).

Excitatory inputs from descending pathways

Earlier studies exploring the inputs from descending CS systems on DSCT neurons have reported the activation of particular DSCT units, following stimulation of cortical area (Hongo and Okada, 1967; Hongo *et al.*, 1967). As mentioned earlier, in these studies, particular subdivision of these neurons was not differentiated, however units analysed in these studies have excitatory inputs from high threshold muscle and cutaneous afferents, which resembles the characteristics of identified dhDSCT neurons. In contrast to ccDSCT neurons, no evidence has been provided for the activation of dhDSCT neuronal populations from RetS neurons descending from the MLF (Hammar *et al.*, 2011).

Inhibitory inputs to ccDSCT neurons

Inhibitory inputs from primary afferents

In addition to the wide range of excitatory inputs to ccDSCT neurons, there is evidence for the inhibition of these neurons from various sources (Eccles *et al.*, 1961b; Hongo *et al.*, 1983a; Jankowska and Puczynska, 2008). These neurons are inhibited following stimulation of both group Ia and Ib muscle afferents (Eccles *et al.*, 1961b). They reported longer latencies of inhibitory postsynaptic potentials (IPSPs) produced by muscle primary afferent volleys than monosynaptic EPSPs thus suggesting that such inhibition is mediated via inhibitory interneurons. Subsequently, other studies showed that the interneurons in pathways from both group Ia and Ib afferents inhibiting ccDSCT neurons also mediate inhibition of motoneurons (Hongo *et al.*, 1983a; Hongo *et al.*, 1983b). In these studies, it was revealed that IPSPs in ccDSCT neurons are evoked following stimulation of motor nuclei and in motoneurons by stimuli applied within cc. Hongo and colleagues (1983a) have also shown that the inhibitory effect evoked in ccDSCT neurons is mediated by interneurons located caudal to and also within the same segments as cc. Identified interneurons following intracellular injection of HRP, in this location project to motor nuclei (Czarkowska *et al.*, 1981; Jankowska *et al.*, 1981). Furthermore, only interneurons with input from group I afferents inhibiting

motoneurons project to the level of cc (Brink *et al.*, 1983; Hongo *et al.*, 1983a; Hongo *et al.*, 1983b). It has also been demonstrated that ccDSCT neurons are inhibited by group II muscle afferents, most of which is mediated by interneurons co-activated by both group I and II afferents and some by group II afferents only (Jankowska and Puczynska, 2008). These authors also concluded that this action of group I and II afferents on ccDSCT neurons is collateral to actions on motoneurons. Inhibitory inputs from primary afferents to these neurons are summarized in Figure 1-2 (A).

Inhibitory inputs from descending pathways

Inhibitory inputs to ccDSCT neurons also originate from descending CS neurons (Hongo and Okada, 1967; Hongo *et al.*, 1967; Hantman and Jessell, 2010). Early observations made by physiological studies have shown a prolonged inhibition of DSCT neurons following stimulation of the contralateral cerebral cortex and medullary pyramid (Hongo and Okada, 1967; Hongo *et al.*, 1967). This stimulation also inhibited the effects produced by group I afferents on these neurons. Similar evidence for cortically evoked inhibitory effect on these neurons has recently been provided by Hantman and Jessell (2010). Most ccDSCT neurons in their study exhibited inhibitory responses to dorsal column stimulation, an effect that was blocked by application of both bicuculline and strychnine which suggested the involvement of both gamma-aminobutyric acid (GABA) and glycine. In addition, the authors also reported the blockade of IPSPs on exposure to AMPA receptor antagonist and such effect was suggested to be generated due to inhibition of excitatory effects produced by CS neurons on inhibitory. Similarly, IPSPs of disynaptic latency are shown to be evoked by stimulation of RetS axons descending ipsilaterally in the MLF (Hammar *et al.*, 2011). A summary of the descending inhibitory inputs to these neurons is shown in Figure1-2 (B).

Inhibitory inputs to dhDSCT neurons

Inhibitory inputs from primary afferents

DSCT neurons in the dorsal horn are inhibited by stimulation of group II muscle afferents (Edgley and Jankowska, 1988). It has been shown that such inhibition is usually preceded by excitation and that IPSPs are evoked from same nerves which evoked EPSPs. All the IPSPs recorded in this study had longer latencies indicating that these neurons are inhibited by disynaptic connections. Furthermore, Edgley and Jankowska (1987a) have reported large extracellular field potentials in the location where the dhDSCT neurons are found which was generated by stimulation of group II muscle afferents in many hindlimb nerves. Supplementing this finding, the authors also demonstrated a large number of interneurons with characteristic dominant input from group II muscle afferents in the same location unlike the interneurons located in the ventral horn and intermediate zone which generally have input from group I and group II afferents together (Edgley and Jankowska, 1987b). Besides this, interneurons in this area also have input from cutaneous afferents. More recently, Krutki and colleagues (2011) have revealed an inhibitory postsynaptic effect produced by stimulation of motor nuclei on dhDSCT neurons which have a longer latency. They suggested that this inhibitory effect was a collateral action of inhibitory interneurons which also project to motoneurons. In addition, they also reported that such direct inhibitory action of premotor interneurons on dhDSCT neurons is much weaker than that in ccDSCT neurons although inhibition was evoked in a higher proportion of dhDSCT neurons than ccDSCT neurons. Such inhibitory input from group II afferents to these neurons is represented in Figure 1-3 (A).

Inhibitory inputs from descending pathways

Evidence for descending inputs to dhDSCT neurons is very scarce. However, attempts have been made in a recent study by Hammar and her group (2011) who demonstrated that dhDSCT neurons are inhibited by stimuli applied to RetS fibres

descending from the contralateral MLF which was mediated via inhibitory interneurons as represented in Figure 1-3 (B).

Action of various neuromodulators on DSCT neurons

In addition to evidence for excitatory and inhibitory actions of descending pathways to the DSCT neurons, there is also evidence for modulatory effects of descending systems mediated via different monoamines and other neuromodulators.

Differential actions of neuromodulators such as serotonin (5-hydroxytryptamine; 5-HT) and noradrenaline (NA) on these neurons have been discussed in several studies (Jankowska *et al.*, 1995b; Maxwell and Jankowska, 1996; Jankowska *et al.*, 1997). Quantitative light and confocal microscopic studies of dhDSCT neurons revealed substantial numbers of contacts made by 5-HT -immunofluorescent axon terminals on the somata and dendrites of these neurons (Jankowska *et al.*, 1995b). This input was suggested to originate either from stem axons and their collaterals or both myelinated and non-myelinated serotoninergic fibres (Jankowska *et al.*, 1995b). This study provided direct evidence about the possibility of direct postsynaptic action of 5-HT for modulating the activity of dhDSCT neurons although different indirect mechanisms might have been involved. Subsequently, evidence provided by this anatomical study was substantiated by another physiological study (Jankowska *et al.*, 1995a). In that study, synaptic excitation of dhDSCT neurons generated by group II afferents was depressed by ionphoretic application of 5-HT and 5-HT_{1A} agonist 8- hydroxy-2-(di-n-propylamino)-tetralin (8-OH-DPAT). On the other hand, synaptic activity of these neurons evoked by cutaneous afferents was enhanced in both the rat and the cat. Furthermore, contacts formed by 5-HT fibres were confirmed to be synaptic and therefore the modulatory action was generated by a post-synaptic effect (Maxwell and Jankowska, 1996). These studies show the alteration of the balance of input to dhDSCT neurons from group II afferents and cutaneous afferents by 5-HT although the mechanism underlying this is still unclear. However, Jankowska *et al.* (1995a) have proposed that the facilitatory and depressive actions of 5-HT on dhDSCT neurons might involve different combinations of transmitters, different membrane receptors including different sites of action.

Potential outcomes of such modulatory action, in particular depressive actions have been suggested. For example, Jankowska and her colleagues (1995a) proposed a distinct role in co-ordinating activity of spinal and supraspinal networks through dhDSCT neurons.

Similarly, NA also has modulatory effects upon the responses produced by muscle and cutaneous afferents on dhDSCT neurons (Jankowska *et al.*, 1997). Extracellular recording of these neurons during ionophoretic application of NA has shown the depressive effect on the actions produced by group II and cutaneous afferents in these neurons. However such responses evoked by both afferents were weakly affected by NA.

Following these studies of dhDSCT neurons, a similar attempt was made to study ccDSCT neurons. Extracellular recording of ccDSCT neurons and ionophoretic application of 5-HT has shown a facilitatory effect upon the actions produced by group I, II and cutaneous afferents on these neurons (Jankowska *et al.*, 1998). Subsequently, a study in cats using a combination of immunohistochemical and intracellular staining (with HRP or neurobiotin) of identified DSCT cells in cc revealed appositions made by 5-HT terminals on somata and dendrites of ccDSCT neurons (Pearson *et al.*, 2000). In addition responses evoked by muscle afferents on ccDSCT neurons are generally facilitated by NA while the effects generated by cutaneous afferents are depressed (Jankowska *et al.*, 1997).

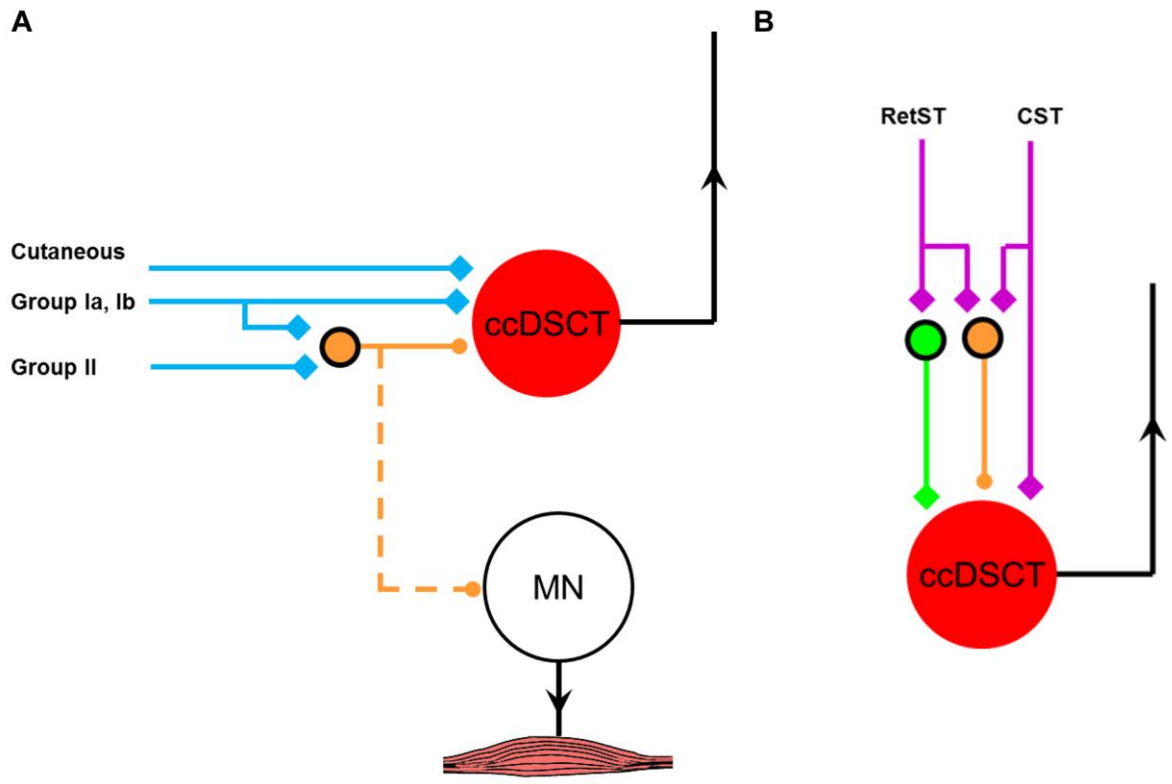

Figure 1-2 Summary of excitatory and inhibitory inputs to ccDSCT neurons

A, Schematic diagram representing ccDSCT neurons (red circles) receiving excitatory inputs from muscle and cutaneous afferents (blue lines and diamonds) and inhibitory inputs from muscle afferents mediated by inhibitory interneurons (orange circle) that have collateral projections (orange dotted line) to motoneuron. ***B***, Schematic diagram of monosynaptic descending excitatory inputs from RetST and CST (purple lines and diamonds), disynaptic excitatory input mediated via an excitatory interneuron (green circle) and inhibitory inputs relayed via an inhibitory interneuron (orange circle) to ccDSCT neurons. ccDSCT, Clarke's column dorsal spinocerebellar tract; CST, corticospinal tract; MN, motoneuron; RetST, reticulospinal tract.

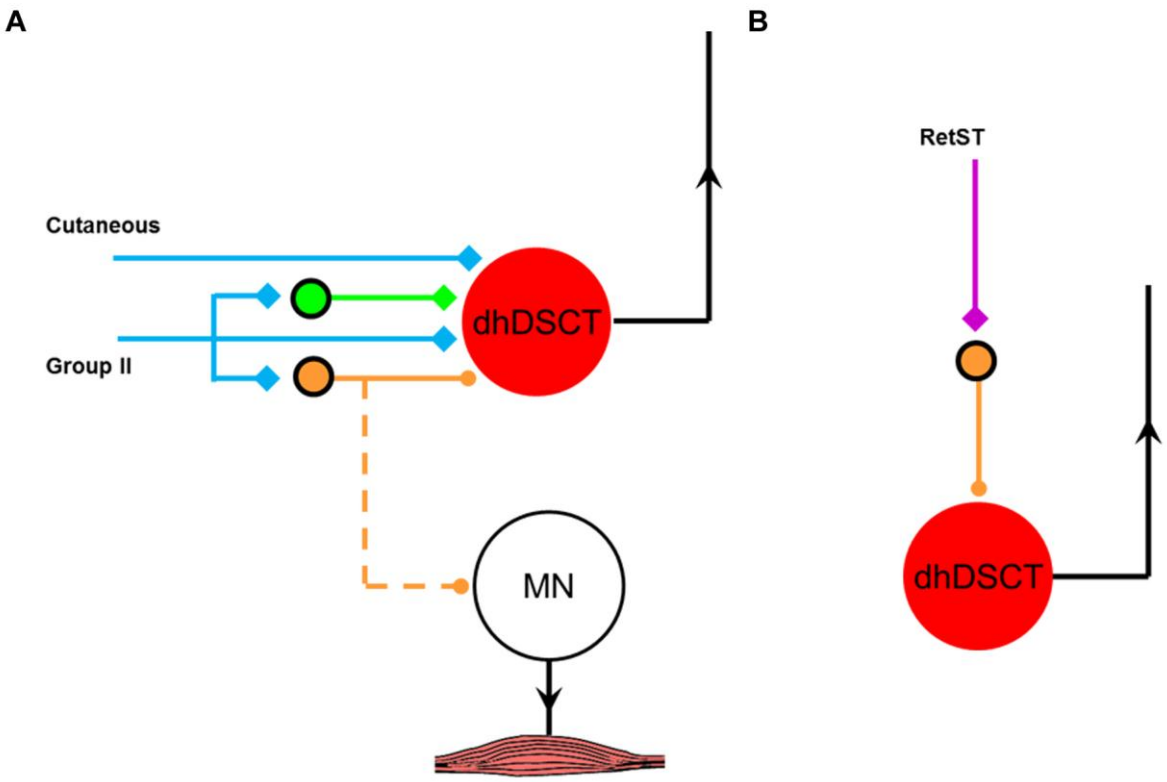

Figure 1-3 Summary of excitatory and inhibitory inputs to dhDSCT neurons

A, Schematic diagram representing dhDSCT neurons (red circles) receiving monosynaptic excitatory inputs from group II and cutaneous afferents (blue lines and diamonds), disynaptic excitatory inputs from group II afferents via excitatory interneuron (green circle) and inhibitory inputs from group II afferents mediated by inhibitory interneurons (orange circle) that have collateral projections (orange dotted line) to motoneuron. ***B***, Schematic diagram of disynaptic descending inputs from RetST (purple lines and diamonds) relayed via inhibitory interneuron (orange circle) to dhDSCT neurons. dhDSCT, dorsal spinocerebellar tract; MN, motoneuron; RetST, reticulospinal tract.

Finally, a study in rats has demonstrated the presence of neurokinin-1 (NK-1) receptors on the dhDSCT neurons (McGonigle *et al.*, 1996) and revealed appositions made by substance P immunoreactive profiles onto neurons which expressed NK-1 receptors. However, no NK-1 immunoreactivity was reported for ccDSCT and VSCT neurons and it was suggested that this kind of input to dhDSCT neurons might specifically influence transmission through the dhDSCT pathway which is well established to convey information from group II muscle afferents and low-threshold cutaneous afferents to the cerebellum (Edgley and Jankowska, 1988).

Functional role of DSCT

It has long been recognized that neurons contributing to DSCT forward proprioceptive information to the cerebellum and other parts of the brain. Since the predominant input to ccDSCT neurons is from group I afferents and also indirectly from group I and II afferents, they convey information about the change in muscle length, velocity and tension (Matthews, 1964). However, dhDSCT neurons with characteristic input from group II afferents respond to changes in muscle length only (Matthews, 1964). Therefore, DSCT as a whole is concerned with the limb movement or position. Both of these neuronal subsets have inhibitory input from disynaptic pathways mediated via the same interneurons that mediate inhibition of hindlimb motoneurons (Hongo *et al.*, 1983a; Hongo *et al.*, 1983b; Jankowska and Puczynska, 2008; Krutki *et al.*, 2011). Hence, several lines of evidence suggest that DSCT neurons have a vital role in monitoring inhibitory input to motoneurons which is mediated via premotor interneurons in reflex pathways from peripheral afferents. Additionally, it has been reported that the activity of DSCT neurons is inhibited during muscle contractions and that many DSCT neurons respond in the same way to muscle stretch and contraction (Osborn and Poppele, 1983). Furthermore, it has also been proposed that the DSCT neurons might function to integrate information on muscle stretches and contractions together with other kinds of information prior to forwarding this information to the cerebellum which could be used by the cerebellum to adjust motor activity (Bosco and Poppele, 2001). Despite ample evidence for convergence of input from muscle and cutaneous afferents, previous studies have showed that the firing pattern of

the DSCT neurons (identified by antidromic stimulation from the inferior cerebellar peduncle or the cerebellum) are modulated following changes in different limb kinematic parameters such as orientation of limb segments or the length and orientation of the whole limb (Bosco *et al.*, 1996) and movement direction (Bosco and Poppele, 1997; Bosco and Poppele, 1999). They showed change in the firing pattern depending on the changes in kinematic patterns of different limbs and joints. This evidence indicated that the activity of the DSCT encodes whole limb parameters. Moreover, modulation of the activity of ccDSCT neurons generated by both ipsilateral and contralateral limb movement has been revealed by recording activity from these ccDSCT neurons in anesthetised and decereberate cats (Poppele *et al.*, 2003). Although, this study has shown diversity (inhibitory or excitatory) in net effects from bilateral inputs to the DSCT cells, bipedal modulation was generally either in the same phase or in the opposite phase from the two limbs. It was further proposed following the elucidation of integration of bilateral sensory input by ccDSCT neurons that these neurons relay the information about the status of interlimb coordination to the cerebellum (Poppele *et al.,* 2003).

Recently, an additional functional role of ccDSCT neurons has been proposed by Hantman and Jessell (2010). These authors demonstrated a convergence of descending CS excitatory and inhibitory inputs to ccDSCT neurons. They suggested that ccDSCT neurons might modulate the proprioceptive input to the cerebellum and have functional role in motor planning and evaluation. Additionally, the demonstration of the collateral axons to nucleus Z makes these neurons an important candidate for a role in the conscious perception of limb position (Low *et al.*, 1986; Edgley and Jankowska, 1988).

1.1.2 Ventral Spinocerebellar Tract (VSCT)

1.1.2.1 Anatomical location and general morphology

The VSCT, located ventral to the DSCT originates principally from neurons located in the lateral region of the ventral horn at L3 to L6 segments of the spinal cord. These neurons are predominantly located along the lateral border of the ventral

horn and Cooper and Sherrington (1940) named these neurons as “Spinal border cells”. Different anatomical studies have also confirmed the presence of spinal border cells (SBCs) in various mammalian species including cats (Ha and Liu, 1968), rats and human (Burke *et al.*, 1971a). It has been suggested that SBCs are the major cells of origin of the VSCT (Burke *et al.*, 1971a). In addition to this, electrophysiological studies have demonstrated another group of cells in the lumbar enlargement which reside in the lateral region of the intermediate zone and the base and neck of the dorsal horn (Hubbard and Oscarsson, 1961; Hubbard and Oscarsson, 1962). Several studies utilizing microelectrode tracking, retrograde chromatolysis and retrograde HRP injection have been able to show that other neurons in the adjacent areas, principally the area more medial to the lateral border also give rise to fibres of VSCT (Hubbard and Oscarsson, 1962; Grant *et al.*, 1982; Bras *et al.*, 1988; Grant and Xu, 1988). The existence of these neurons which are functionally different from SB neurons has also been confirmed in recent studies (Jankowska *et al.*, 2010; Hammar *et al.*, 2011). Broadly, there are two major subpopulations of neurons whose axons constitute the VSCT; SBCs and the medially located neurons (Matsushita *et al.*, 1979). The neurons distributed in the lateral parts of laminae VII and IX are referred as SBCs or SB neurons while those found in the medial part of lamina VII are termed as VSCT (Ib-VSCT; see below) neurons.

SB neurons are present along the Th10 to L6 segments, most numerous in the L2 to L6 segment as revealed by retrograde labelling of HRP in the cat (Matsushita *et al.*, 1979) and Th11 to L3 segment in the rat (Matsushita and Hosoya, 1979). SB neurons in lamina IX are mainly localized to the dorsolateral and the ventrolateral nuclei (Grant *et al.*, 1982). Matsushita and his group (1979) have found two varieties of labelled SB neurons; large multipolar neurons of the motoneuron type and medium-sized spindle-shaped or triangular neurons. The later group of neurons are mainly shown to be confined in lamina IX.

The medially located VSCT neurons are principally found in the medial part of lamina VII of the L6 segment to the caudal segments (Matsushita *et al.*, 1979; Grant *et al.*, 1982; Grant and Xu, 1988). These neurons have similar soma size and shape as that of SB neurons (Matsushita *et al.,* 1979). Intracellular staining with HRP in

physiologically identified neurons in the cat revealed that cell bodies of VSCT neurons are large with dendrites radiating in various directions. The dendrites usually extend within lamina VII. Some of these dendrites also extend into lamina VI or VIII and sometimes in the white matter as well (Bras *et al.*, 1988). However, these studies did not differentiate between the two subsets of VSCT neurons with respect to their cell body location and dendritic plexus.

1.1.2.2 Axonal projections and termination sites in the cerebellum

The axons of both SB and VSCT neurons cross the midline near the level of the cell body and project via the ventral funiculus to ascend contralaterally through the ventrolateral fasciculus. The crossed axons then enter the cerebellum through the superior cerebellar peduncle (Oscarsson, 1965; Grant and Xu, 1988). Although these neurons are generally accepted to have crossed axons, within the cerebellum, the majority of the axonal projections recross to the ipsilateral side and terminate in different areas in both the anterior and the posterior lobe. The rest of the axons of these neurons terminate contralateral to the cell body of their origin (Matsushita and Hosoya, 1982; Matsushita *et al.*, 1984; Kim *et al.*, 1986; Yaginuma and Matsushita, 1986; Matsushita, 1988). Similarly, a study utilizing anterograde injection of WGA-HRP in the L5 segment of the spinal cord has shown an abundant number of labelled terminals of SB neurons on the side ipsilateral to the injection (Yaginuma and Matsushita, 1986). However, another study based on the unilateral retrograde injection in the paramedian lobule has demonstrated contralateral projections of SB neurons (Xu and Grant, 2005).

Several studies using the retrograde HRP technique have shown differential and overlapping cerebellar projections of these two populations of VSCT neurons. Following HRP injections in discrete lobules, many cells belonging to VSCT were labelled which included both SB and VSCT neurons. In the anterior lobe, the axons of SB neurons project to the lateral most part of the vermis and the intermediate-lateral regions of lobules II-V (Matsushita and Okado, 1981; Matsushita and Hosoya, 1982). Previous studies have shown abundant projections of these neurons in lobules III and IV and least in lobules II and V (Matsushita and Okado, 1981;

Matsushita and Hosoya, 1982). Projections from medially located VSCT population have also been found in these lobules. In the posterior lobe, the main projection area of SB neurons is in the paramedian lobule while that of medially located VSCT neurons is mainly in lobule VIII (Matsushita and Ikeda, 1980). Similarly, anterograde tract tracing in cats has also demonstrated axonal projections of SB neurons to the apical parts of lobules II-V (Yaginuma and Matsushita, 1986; Matsushita and Yaginuma, 1989). This anatomical evidence is supported by several lines of evidence from antidromic activation of VSCT neurons including SB neurons from the cerebellum (Lundberg and Oscarsson, 1962; Burke *et al.*, 1971a; Arshavsky *et al.*, 1978b).

Furthermore, a combination of intracellular recording and labelling of individual VSCT neurons with HRP has demonstrated the presence of collaterals from a specific group of these neurons (Bras *et al.*, 1988) which are mainly located in the middle part of lamina VII and are activated monosynaptically by group I muscle afferents. However, the neurons bordering the lateral funiculus are never shown to give off such collaterals (presumably SB neurons). All of the collaterals emerge in the contralateral ventral funiculus, enter the contralateral ventral horn at the same level of lamina VII or lamina VIII and give off the branches once they reach the grey matter.

1.1.2.3 Inputs and synaptic connections to neurons of origin of VSCT

It has been established for a long time that cells of origin of VSCT receive diversified inputs. Conclusions drawn from most of the earlier investigations were based upon three types of studies. Firstly, earlier studies based on recording the mass discharge of the entire tract generated by stimulation of Golgi tendon organ (Ib) afferents demonstrated monosynaptic connections between Ib afferents and VSCT neurons (Oscarsson, 1957). Secondly, VSCT neurons are excited and inhibited polysynaptically from FRA and some of them are monosynaptically activated by group Ib afferents when recording was done from single ascending axons identified by antidromic cerebellar stimulation (Lundberg and Oscarsson, 1962). Thirdly, neurons belonging to VSCT receive monosynaptic excitatory input from Ib afferents

and inhibitory inputs from FRA mediated via polysynaptic pathways (Eccles *et al.*, 1961a; Hubbard and Oscarsson, 1962). All of these studies led to a generalised assumption about VSCT neurons that these neurons forward homogeneous information to the cerebellum. However, in subsequent studies it became apparent that the inputs to these neurons are more complex than it was believed previously.

In addition, different functional sub-units of the neurons belonging to this tract have been defined though the complex organization of synaptic connections to them is yet to be clearly elucidated. It has been generally accepted that a group of VSCT neurons, located in the middle part of lamina V-VII (as defined above) mainly receive monosynaptic input from group Ib afferents (Eccles *et al.*, 1961a; Hubbard and Oscarsson, 1961; Hubbard and Oscarsson, 1962; Oscarsson, 1965) whereas another group of VSCT neurons, SBCs mainly receive monosynaptic input from group Ia afferents (Burke *et al.*, 1971a; Lundberg and Weight, 1971). Therefore on the basis of afferent inputs, VSCT neurons are divided into two major functional groups: Ib-VSCT neurons, receiving input from group Ib afferents and Ia-VSCT neurons (generally referred as SBC or SB neurons), with predominant input from Ia afferents (Oscarsson, 1965; Lundberg and Weight, 1971). Recently, the existence of further subsets of neurons within the populations of SB cells has been postulated (Jankowska *et al.*, 2010; Hammar *et al.*, 2011).

Excitatory inputs to SB neurons

Excitatory inputs from primary afferents

Earlier electrophysiological studies utilizing intracellular recordings in the cat have demonstrated monosynaptic EPSPs in SB neurons evoked by stimulation of group Ia afferents (Burke *et al.*, 1971a; Lundberg and Weight, 1971). This indicates that these neurons have direct connections with muscle afferents. However, other studies failed to show monosynaptic excitatory input from primary afferents in antidromically identified VSCT neurons, presumably SB neurons (Eccles *et al.*, 1961a) although the possibility of postsynaptic responses from untested nerves could not be excluded. Interestingly, Lundberg and Weight (1971)) suggested the

existence of a higher proportion of neurons without monosynaptic input from Ia afferents as they appeared to be more common in more rostral segments. In addition, Eccles and his group (1961a) demonstrated EPSPs of longer latency (di- or tri-synaptic) in SB neurons evoked by FRA stimulation. They reported that input from FRA is more common in SB neurons than in Ib-VSCT neurons. Similarly, polysynaptic EPSPs were shown to be generated in a proportion of SB neurons from Ib afferents (Lundberg and Weight, 1971). A recent study has demonstrated EPSPs of monosynaptic latency in VSCT neurons following stimulation of hindlimb motor nuclei (Jankowska *et al.*, 2010). The EPSPs recorded from these neurons matched EPSPs evoked in the respective motor nuclei following stimulation of muscle afferents. This action on VSCT neurons is likely to be mediated via premotor interneurons with inputs from group Ib/ II afferents which also have collateral actions on motoneurons. However, the particular subset of VSCT neurons was not specified in this study. A schematic representation of the excitatory inputs from primary afferents to SB neurons is shown in Figure 1-4 (A).

Excitatory inputs from descending pathways

There is evidence for direct and indirect connections between VSCT neurons including SB neurons and major descending systems (Baldissera and Weight, 1969; Baldissera and ten Bruggencate, 1976; Fu *et al.*, 1977; Hammar *et al.*, 2011; Jankowska *et al.*, 2011b; Jankowska *et al.*, 2011a). Two descending pathways, the vestibulospinal tract (VST) and RetST have monosynaptic connections with SB and VSCT neurons (Baldissera and Weight, 1969; Baldissera and Roberts, 1975). These pathways also have monosynaptic excitatory inputs to motoneurons (Grillner and Lund, 1968; Wilson and Yoshida, 1969; Grillner *et al.*, 1970) which imply that descending control from these pathways to SB neurons and motoneurons act in parallel to each other. Monosynaptic EPSPs can be evoked in a proportion of VSCT including SB neurons following stimulation of contralateral red nucleus (Baldissera and ten Bruggencate, 1976) which also forms monosynaptic connections with spinal interneurons (Hongo *et al.*, 1969; Hongo *et al.*, 1972). Furthermore, EPSPs of longer latency in VSCT neurons (both Ia and Ib VSCT neurons) generated by stimuli applied in the CS tract (CST) have also been reported (Fu *et al.*, 1977). These authors

showed that excitatory effects evoked by impulses from primary afferents were facilitated by stimulation of the CST. This effect was proposed to be mediated by the same interneurons which have convergence of input from the same primary afferents and CS neurons that evoke similar postsynaptic potentials in motoneurons.

Recently, a substantial number of further studies investigating the connections between different descending systems and VSCT neurons including SB neurons has emerged (Hammar *et al.*, 2011; Jankowska *et al.*, 2011a; Jankowska *et al.*, 2011b). Monosynaptic and disynaptic coupling between SB neurons and RetS neurons has been shown (Hammar *et al.*, 2011) which was based on intracellular recording of SB neurons following stimulation of RetS axons descending within the ipsilateral and contralateral MLF. This study also showed that the stimulation of group I and II afferents produced inhibition of the effects produced by the MLF stimulation on SB neurons. The authors emphasized that such actions indicates an important role of SB neurons in forwarding information on the actions of RetS neurons on spinal neurons.

This evidence has further been substantiated by observations which showed that SB and also VSCT neurons activated by stimulation of descending RetS axons are co-excited by stimulation of the mesencephalic locomotor region (MLR) and pyramidal tract (PT) (Jankowska *et al.*, 2011b). EPSPs evoked by MLR and PT stimulation are in parallel to the EPSPs generated by stimulation of RetS neurons in the MLF. Furthermore discharges in extracellular recording and PSPs in intracellular recording of SB (and VSCT) neurons are potently facilitated by stimulation of contralateral and ipsilateral pyramids. This effect is only reported for disynaptic excitation of these neurons from the RetS neurons (Jankowska *et al.*, 2011b) and it was proposed that this action is relayed by collaterals of RetS neurons which have direct connections with the MLR and PT neurons.

Reinforcing the evidence provided by Baldissera and ten Bruggencate (1976) for rubrospinal (RS) input to SB (and VSCT) neurons, it was shown that SB and VSCT neurons are activated by stimuli applied in the contralateral red nucleus in the cat (Jankowska *et al.*, 2011a). PSPs recorded from these neurons are of monosynaptic

as well as disynaptic latencies. The disynaptic action of RS neurons was suggested to be relayed by interneurons, as it was seen even after transection of RetS axons in the MLF. Moreover both facilitatory and inhibitory effects of RS neurons on the activity produced by RetS and/ or PT neurons recorded from SB neurons (also VSCT neurons) were observed. A schematic diagram summarizing the descending excitatory inputs to these neurons is shown in Figure 1-4 (B).

Excitatory inputs to VSCT (Ib-VSCT) neurons

Excitatory inputs from primary afferents

VSCT neurons are monosynaptically activated following stimulation of group Ib afferents (Eccles *et al.*, 1961a; Hubbard and Oscarsson, 1961; Hubbard and Oscarsson, 1962; Oscarsson, 1965). This is the main functional difference between SB neurons and VSCT neurons. Excitatory inputs mediated from polysynaptic pathways are similar to those of SB neurons (as described above in SB neurons) as summarised in Figure 1-5 (A).

Excitatory inputs from descending pathways

Earlier attempts to investigate the coupling between VSCT neurons and descending systems were based on physiological studies. As described above for SB neurons, previous studies did not differentiate between the subsets of VSCT neurons. Evidence has been provided for different supraspinal inputs to these neuronal populations. For example, monosynaptic EPSPs in VSCT neurons following stimulation of RetS axons descending from the contralateral MLF are reported to be more common than those evoked by ipsilaterally descending axons while ipsilaterally descending RetS input is more common in SB neurons (Hammar *et al.*, 2011). However origin of disynaptic linkage between these neurons and RetS neurons do not differ in this study since in both VSCT and SB neurons, disynaptic EPSPs and IPSPs are evoked from both the ipsilateral and the contralateral MLF. A summary diagram showing direct and indirect excitatory inputs from descending pathways to VSCT neurons is shown in Figure 1-5 (B).

Inhibitory inputs to SB neurons

Inhibitory inputs from primary afferents

It is well established that the predominant action of muscle afferents on VSCT neurons including both SB and Ib-VSCT neurons is inhibitory (Eccles *et al.*, 1961a; Lundberg and Weight, 1971). Inhibition is a common characteristic feature in all VSCT neurons. Polysynaptic inhibitory inputs from FRA are common in all SB neurons (Eccles *et al.*, 1961a) and disynaptic IPSPs from group I afferents are found in most SB neurons (Lundberg and Weight, 1971). IPSPs in more rostrally located SB neurons which do not have monosynaptic excitatory inputs from group Ia afferents are evoked from Ib afferents stimulation. However, caudally located SB neurons with monosynaptic excitatory inputs from group Ia afferents have IPSPs of disynaptic latency from both group Ia and Ib afferents (Lundberg and Weight, 1971). Furthermore, they also showed two additional features: i) Ia IPSPs in SB neurons from one of the muscle nerve usually followed Ia EPSPs generated by the same muscle nerve and ii) Ia EPSPs were followed by IPSPs evoked from Ia afferents from antagonist muscles in same SB neurons.

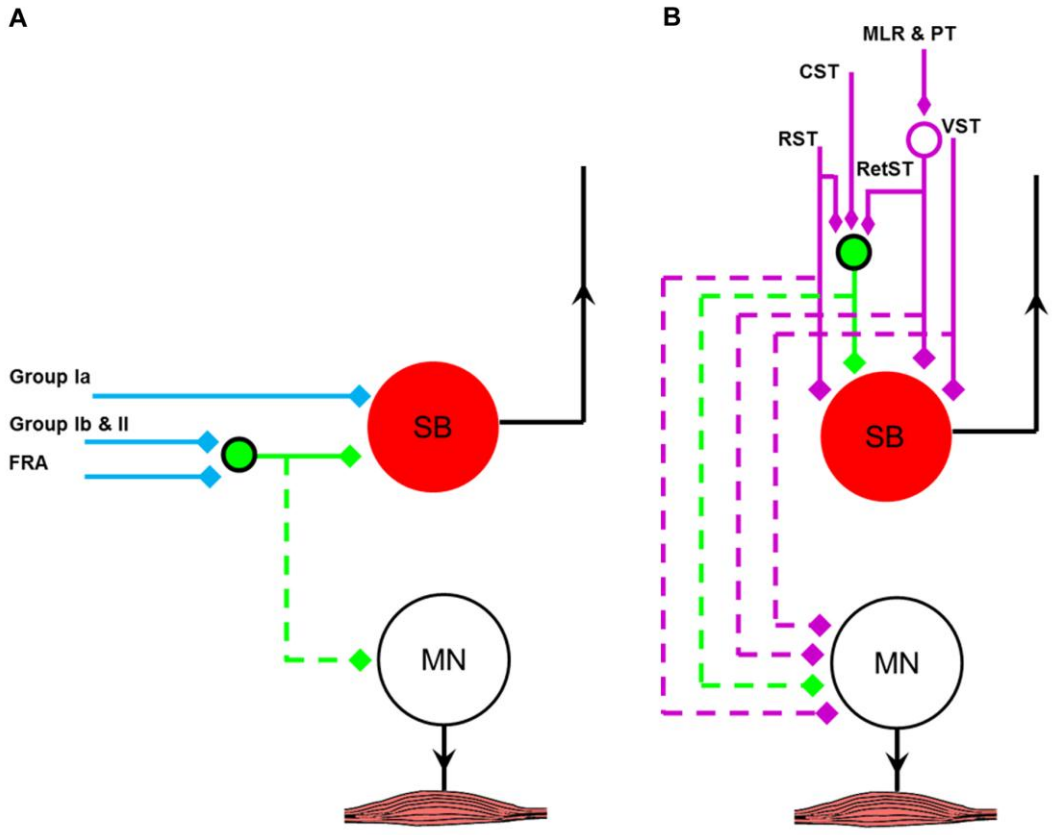

Figure 1-4 Summary of excitatory inputs to SB neurons

A, Schematic diagram representing SB neurons (red circles) receiving monosynaptic excitatory inputs from group Ia afferents (blue lines and diamond; common in caudal SB neurons) and disynapic excitatory inputs from muscle afferents and FRAs (blue lines and diamonds) mediated via excitatory interneurons (green circle) that have collateral projections (green dotted line) to motoneuron. ***B***, Schematic diagram summarizing SB neurons receive monosynaptic descending excitatory inputs from RST, RetST and VST (purple lines and diamonds), disynaptic excitatory input from RST, CST and RetST mediated via excitatory interneuron (green circle) and disynaptic excitatory inputs from MLR and PT (purple lines and diamonds) relayed via RetST neurons (purple circle). The dotted lines of corresponding color code represent collateral projections to motoneurons. CST, corticospinal tract; FRA, flexor reflex afferent; MLR, mesencephalic locomotor region; MN, motoneuron; PT, pyramidal tract; RetST, reticulospinal tract; RST, rubrospinal tract; SB, spinal border; VST, vestibulospinal tract.

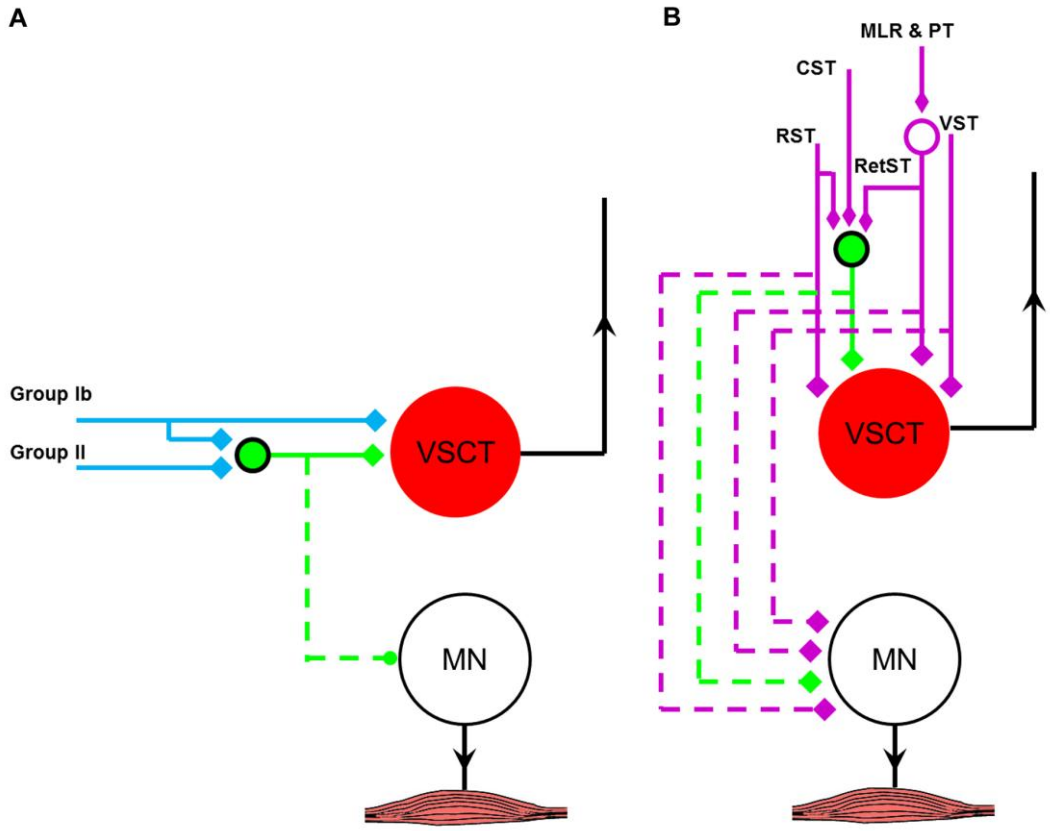

Figure 1-5 Summary of excitatory inputs to VSCT neurons

A, Schematic diagram representing VSCT neurons (red circles) receiving monosynaptic excitatory inputs from group Ib afferents (blue lines and diamonds) and disynapic excitatory inputs from group Ib/ II afferents mediated via excitatory interneurons (green circle) that have collateral projections (green dotted line) to motoneuron. ***B***, Schematic diagram summarizing VSCT neurons receiving monosynaptic descending excitatory inputs from RST, RetST and VST (purple lines and diamonds), disynaptic excitatory input from RST, CST and RetST mediated via excitatory interneuron (green circle) and disynaptic excitatory inputs from MLR and PT (purple lines and diamonds) relayed via RetST neurons (purple circle). The dotted lines of corresponding color code represent collateral projections to motoneurons. CST, corticospinal tract; MLR, mesencephalic locomotor region; MN, motoneuron; PT, pyramidal tract; RetST, reticulospinal tract; RST, rubrospinal tract; VSCT, ventral spinocerebellar tract; VST, vestibulospinal tract.

For the first feature of excitation and inhibition produced by the same nerve, it was postulated that the Ia excitatory action in VSCT cells including SB cells is related to the excitation of Ia inhibitory interneurons which in turn will cause inhibition of the same SB and VSCT cells (Lundberg, 1971). Lundberg (1971) further suggested that this effect is mediated via interneurons interposed in Ia inhibitory pathways to motoneurons. Subsequently, another study demonstrated depression of disynaptic IPSPs evoked from group Ia afferents in Ia-VSCT neurons following stimulation of ventral roots (Gustafsson and Lindstrom, 1973). This confirms that the inhibitory effect evoked in Ia-VSCT neurons (SB neurons) are collateral actions of Ia inhibitory interneurons which also provide inhibitory input to motoneurons.

Evidence for the inhibitory effect produced by Renshaw cells in both SB and VSCT neurons similar to that in motoneurons has also been found (Hultborn *et al.*, 1971a; Lindstrom and Schomburg, 1973; Lindstrom and Schomburg, 1974). Lindstrom and Schomburg (1973) have shown that impulses in ventral roots generated inhibition in VSCT cell which had group Ia excitatory inputs and that the same ventral roots evoked recurrent inhibition in motoneurons and Ia inhibitory interneurons which were also activated by Ia afferents of the same muscle as the VSCT cell. This indicated that IPSPs generated from Ia afferent stimulation in these cells are mediated by Ia inhibitory interneurons in addition to recurrent inhibition from motor axon collaterals through Renshaw cells.

Recently, such effects of other premotor interneurons on to VSCT neurons including the SB population have been re-explored in considerable detail (Jankowska *et al.*, 2010). This study has shown monosynaptic IPSPs in VSCT neurons from direct stimulation of motor nuclei which were evoked in parallel with disynaptic IPSPs from group Ib and II as well as group Ia afferents. This observation indicated that VSCT neurons, in addition to having inhibitory input from Ia inhibitory interneurons and Renshaw cells, also are depressed by other premotor interneurons interposed in inhibitory pathways from group Ib and group II afferents to motoneurons. A summary diagram of the inhibitory inputs from various peripheral and spinal sources to SB and VSCT neurons is shown in Figure 1-6 (A).

Inhibitory inputs from descending pathways

SB neurons in addition of having direct and indirect excitatory connections from descending pathways, are also subjected to inhibitory control from them. A study based on intracellular recording of VSCT neurons including SB neurons following stimulation of VST demonstrated inhibitory effects in these neurons, some of which were preceded by monosynaptic EPSPs (Baldissera and Roberts, 1975). This leads to the suggestion that this inhibitory action is mediated via interneurons and that the action of descending fibres on to SB and VSCT neurons reflects their action on motoneurons and interneurons. In the same study, IPSPs following stimulation of the MLF were also evoked in these neurons. In most of the neurons analysed, IPSPs of disynaptic latency were common, however, a small fraction of these neurons had monosynaptic linkage from axons descending in the MLF. Disynaptic linkage has also been proposed to be mediated via interneurons which also have collateral actions on to motoneurons. These effects are indicated to be common for both functional subunits of VSCT (SB and Ib VSCT neurons). Recently, Hammar and her group (2011) have demonstrated inhibitory actions of the MLF stimuli on these neurons but only disynaptic linkage was revealed from both ipsilaterally and contralaterally descending RetS axons from the MLF. Further, they proposed that IPSPs evoked in these neurons are mediated by common premotor interneurons interposed in inhibitory reflex pathways from group I and II afferents (Jankowska *et al.*, 2010).

Recently, it was shown that inhibition of SB and VSCT neurons evoked from the MLF stimulation is facilitated by preceding stimulation of the contralateral PT and MLR (Jankowska *et al.*, 2011b). IPSPs from RetS neurons in these neurons are generated by co-activation of other RetS collaterals and by fibres stimulated within the MLR and PTs which might have been relayed via inhibitory interneurons in the spinal level. Likewise, Jankowska and the group (2011b) have provided evidence for effects produced by the rubrospinal tract (RST) in which disynaptic IPSPs were recorded from VSCT neurons following stimulation within the red nucleus. This action persisted despite the transection of RetS axons within the MLF, and it was suggested that inhibition in VSCT neurons are relayed via inhibitory interneurons

activated by the RST. A summary of the descending inhibitory inputs to these neurons is shown in Figure 1-6 (B).

Inhibitory inputs to VSCT (Ib-VSCT) neurons

Inhibitory inputs from primary afferents

Inhibitory inputs to VSCT neurons from primary afferents are similar to that of SB neurons (see Figure 1-6 (A)) (Eccles *et al.*, 1961a; Lundberg, 1971; Lundberg and Weight, 1971; Jankowska *et al.*, 2010) (see above for details). However, minor distinctions from SB population have been observed (Eccles *et al.*, 1961a; Gustafsson and Lindstrom, 1973). For example, Eccles *et al.* (1961a) specified that Ib-VSCT neurons receive inhibitory inputs mainly from group Ia afferents. Similarly, it was demonstrated that a fraction of Ia IPSPs recorded in these cells are depressed by stimuli applied to ventral roots (Gustafsson and Lindstrom, 1973; Lindstrom and Schomburg, 1974). It was suggested that this action is generated by interneurons in recurrent inhibitory pathway from motor axon collaterals through Renshaw cells. Likewise, a recent study by Jankowska and colleagues (2010) reported that although both the populations of VSCT neurons have inhibitory inputs from group Ib and II afferents mediated via premotor interneurons which have collateral actions on motoneurons, the proportion of SB neurons with such input is relatively lower than that of Ib VSCT neurons.

Inhibitory inputs from descending pathways

As described earlier for SB neurons and summarized in Figure 1-6 (B), all the evidence to date for descending inhibitory control of this pathway was based on the concept that all the neurons belonged to the VSCT and functional subtypes were not considered. However, Hammar and her group (2011) have postulated that SB population of VSCT neurons might have divergent functions because of their distinct termination sites in the cerebellum (Matsushita and Ikeda, 1980; Matsushita and Yaginuma, 1989).

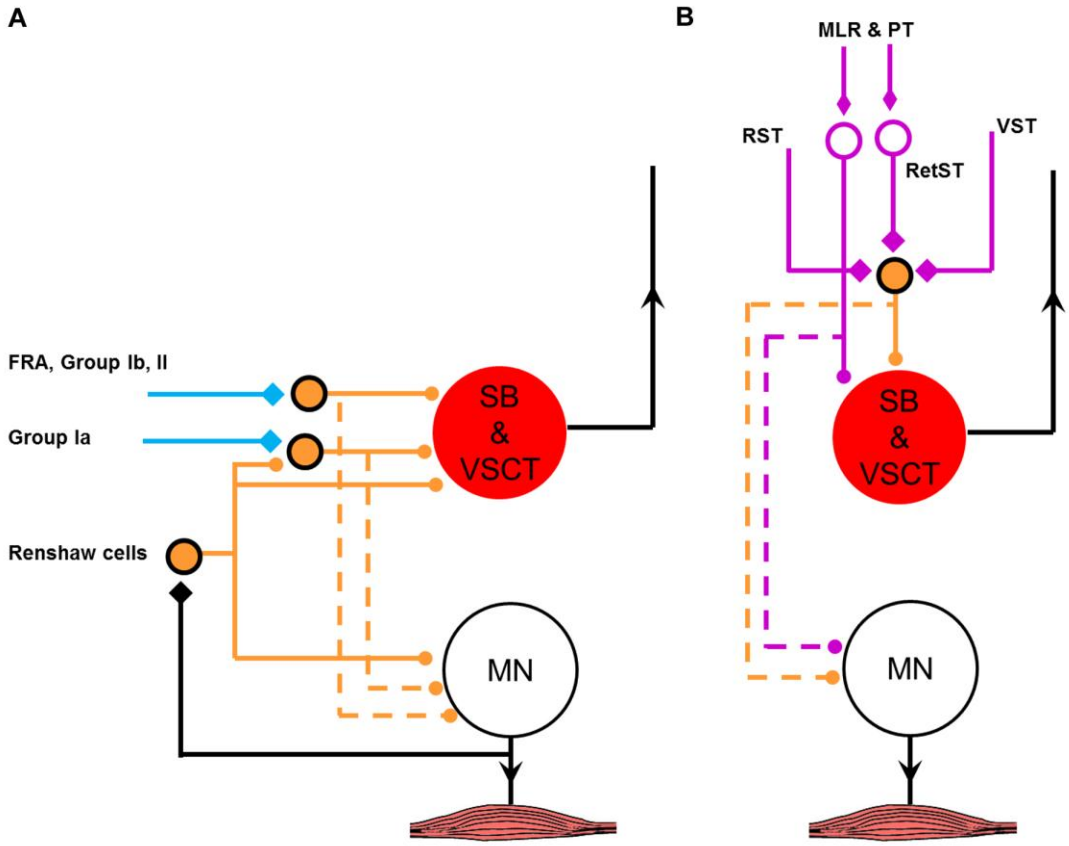

Figure 1-6 Summary of inhibitory inputs to SB and VSCT neurons

***A*,** Schematic diagram representing SB and VSCT neurons (red circles) receiving inhibitory inputs from group Ia, group Ib/ II afferents and FRAs (blue lines and diamond) relayed via inhibitory interneurons (orange circles) and recurrent inhibitory inputs from Renshaw cells (orange circle) that have collateral projections (orange dotted line) to motoneuron. ***B*,** Schematic diagram indicating SB and VSCT neurons receive inhibitory inputs from RST, RetST and VST (purple lines and diamonds) mediated via inhibitory interneuron, direct inhibitory input from RetST neurons (purple circle) and polysynaptic inhibitory inputs from MLR and PT (purple lines and diamonds) relayed via RetST neurons (purple circle) and inhibitory interneurons. The dotted lines of the corresponding colour code represent collateral projections to motoneurons. FRA, flexor reflex afferent; MLR, mesencephalic locomotor region; MN, motoneuron; PT, pyramidal tract; RetST, reticulospinal tract; RST, rubrospinal tract; SB, spinal border; VSCT, ventral spinocerebellar tract; VST, vestibulospinal tract.

Action of neuromodulators on VSCT neurons

In addition to the abundant evidence for excitatory and inhibitory effects of descending pathways on the VSCT neurons, a body of evidence for effects of monoamines and other neuromodulators has emerged (Hammar *et al.*, 2002; Hammar and Maxwell, 2002). For example, extracellular recording of Ib-VSCT neurons has shown both facilitation and depression of actions produced by group I afferents on these neurons following ionophoretic application of different types of 5-HT and NA agonists (Hammar *et al.*, 2002). Confocal and electron microscopic analysis has demonstrated immunoreactive varicosities of both 5-HT and NA in close apposition to both soma and dendrites of these neurons which were confirmed to be direct synaptic contacts (Hammar and Maxwell, 2002). Therefore their modulatory effects on VSCT neurons are likely to be mediated in part by direct postsynaptic actions (Hammar and Maxwell, 2002).

Functional role of VSCT

It has long been proposed that the functional role of VSCT neurons is to integrate and convey information on the stages of movement, or position of a limb, rather than on individual muscles (Oscarsson, 1965). Subsequently, evidence emerged for similarities and some distinct features between the two populations of VSCT neurons with respect to the afferent inputs, modulatory actions from descending pathways, connections with spinal neurons and their relationship with motoneurons (Eccles *et al.*, 1961a; Burke *et al.*, 1971a; Lundberg, 1971; Lundberg and Weight, 1971; Jankowska *et al.*, 2010; Hammar *et al.*, 2011; Jankowska *et al.*, 2011a; Jankowska *et al.*, 2011b). All these observations lead to the conclusion that the principal function of VSCT neurons is to provide the cerebellum with information on activity of interneuronal pathways to the motoneurons. These premotor interneurons are interposed in the pathways from primary afferents (group Ia, Ib and II afferents) and also from descending systems (as described above). However, attention has been paid to inhibitory inputs to these neurons; at present it is not known if they have a similar role in monitoring the excitatory interneuronal pathways to motoneurons. Nevertheless, VSCT neurons appear to compare

information on the degree of inhibition of motoneurons against the information on the excitatory reflex actions mediated via premotor interneurons in pathways from group Ia, Ib and II afferents (Lundberg, 1971; Jankowska *et al.*, 2010). This makes the VSCT neurons an important candidate to enable the cerebellum to adjust these reflex actions.

Furthermore, modulation of these neurons from the descending supraspinal systems (RetS, CS, RS and VS pathways), which have parallel actions on motoneurons also enables this pathway to play a vital role in allowing the cerebellum to adjust descending commands according to given circumstances (Baldissera and Roberts, 1975; Baldissera and Roberts, 1976; Baldissera and ten Bruggencate, 1976; Fu *et al.*, 1977; Hammar *et al.*, 2011; Jankowska *et al.*, 2011a; Jankowska *et al.*, 2011b). For example, as demonstrated by Hammar and her colleagues (2011), VSCT neurons integrate information from descending commands from RetS neurons which mirror those converging on to motoneurons and forward this information to the cerebellum. Similarly, VSCT neurons monitor descending commands for voluntary movements initiated by the PT as well as locomotor movements relayed by RetS neurons (Jankowska *et al.*, 2011b). In addition, this pathway is also suggested to be involved in predicting actions of RS neurons on motoneurons (Jankowska *et al.*, 2011a). A general consensus seem to emerge at present that the information carried by this pathway is of utmost importance for effective motor planning and preventing errors in centrally initiated movements before they are committed.

1.1.3 Cuneocerebellar Tract (CCT)

The CCT is a functional forelimb homologue of the DSCT (Grant, 1962a; Holmqvist *et al.*, 1963a). Studies in cats showed that the neurons of CCT terminate in the forelimb areas of the cerebellar cortex in a similar manner to those of DSCT neurons (Grant, 1962a). Like DSCT neurons, CCT has been categorized into two different components: one proprioceptive component, referred as proprioceptive CCT (P-CCT) and another exteroceptive component, called exteroceptive CCT (E-CCT) (Holmqvist *et al.*, 1963a). P-CCT originates from cell bodies in the external

cuneate nucleus whereas E-CCT is found to arise from neurons in the rostral part of the cuneate nucleus (Cooke *et al.*, 1971b). Both the components of CCT enter the cerebellum via the inferior peduncle and terminate in the same areas of the anterior lobe and paramedian lobule (Grant, 1962a). P-CCT neurons are monosynaptically activated by group I muscle afferents whereas E-CCT neurons receive di- and polysynaptic excitation from cutaneous afferents from various skin and muscle nerves (Holmqvist *et al.*, 1963a; Cooke *et al.*, 1971b).

Functionally, P-CCT consists of two subgroups: one which receives inputs mainly from muscle spindle primary afferents and another which receives inputs from both primary and secondary afferents, suggesting that P-CCT contains an additional path from group II afferents as is the case for DSCT (Cooke *et al.*, 1971a). However, in addition to similarities between CCT and DSCT neurons, they also have some distinct characteristics. For example, unlike DSCT neurons which have convergence of input from different nerves, P-CCT neurons receive excitatory inputs from only one nerve. Both P-CCT and proprioceptive component of DSCT are inhibited by group I afferents through disynaptic pathways (Cooke *et al.*, 1971a). Similarly, neurons of E-CCT, unlike DSCT neurons, do not have monosynaptic excitatory input from cutaneous afferents, they only have the disynaptic linkage between them (Lundberg and Oscarsson, 1960). Therefore the main function of these neurons is to forward information of proprioceptors and extereoceptors from the periphery to the cerebellum (Cooke *et al.*, 1971a).

1.1.4 Rostral Spinocerebellar Tract (RSCT)

The RSCT is a functional forelimb equivalent of the VSCT. The cell of origin of this tract differs from that of both DSCT and VSCT (Holmqvist *et al.*, 1963b; Oscarsson and Uddenberg, 1964). They differ from DSCT as RSCT originates from neurons located rostrally to the cc and located more ventrally, but they have uncrossed axons which differentiate them from axonal projections of VSCT neurons. In addition this tract is distinct from both DSCT and VSCT in reaching the cerebellum

through the inferior and middle cerebellar peduncles. In the cerebellum, they terminate mainly in the anterior lobe (Oscarsson and Uddenberg, 1964).

Electrophysiological studies in cats have revealed that some of their physiological properties resemble neurons of VSCT (Eccles *et al.*, 1961a; Holmqvist *et al.*, 1963b; Oscarsson and Uddenberg, 1965). RSCT neurons are monosynaptically activated from group Ib muscle afferents and polysynaptically excited by FRA. Like VSCT neurons, RSCT neurons also have extensive convergence of inputs from several muscles (Eccles *et al.*, 1961a; Oscarsson and Uddenberg, 1965). However, Oscarsson and Uddenberg (1965) reported that the EPSPs in RSCT neurons are evoked mono-, di- and poly-synaptically from group I afferents, whereas this input is exclusively monosynaptic in VSCT neurons. Likewise, they showed that inputs from FRA are predominantly excitatory in RSCT neurons but inhibitory in VSCT neurons.

1.2 Cerebellum

The cerebellum is considered as one of the most intriguing parts of the brain. It has been divided into different parts which have distinct roles in different behavioural aspects (D'Angelo, 2011): the vestibulo-cerebellum (includes flocculo-nodular lobe), the spino-cerebellum (represented by the vermis and the intermediate part of hemispheres) and the cerebro-cerebellum (corresponds to the lateral part of the cerebellar hemispheres). The vestibulo-cerebellum is involved in adjusting equilibrium and vestibulo-ocular reflexes. The spino-cerebellum regulates movement including feedback adjustments. The cerebro-cerebellum plays a crucial role in preparation, initiation and timing of motor acts. The cerebellar network is also divided into four main sections: the granular layer, the molecular layer, the deep cerebellar nuclei and the inferior olive (Ito, 2006). The molecular and granular layers compose the cerebellar cortex. The deep cerebellar nuclei form a part of the precerebellar nuclei and are the only output pathway of the cerebellar cortex. The inferior olive complex gives rise to the climbing fibres while the mossy fibres originate from various precerebellar nuclei and the spinocerebellar tract neurons.

The cerebellum has connections with the most important structures of the central nervous system, including brain stem, spinal cord, basal ganglia, thalamus and the cerebral cortex (Pijpers *et al.,* 2006; Glickstein *et al.,* 2009; Cerminara and Apps, 2010). It also has a characteristic double connectivity with central and peripheral structures (D' Angelo, 2011). A motor command generated in the cerebral cortex is sent to the motoneurons as well as to the cerebellum through the pontine nuclei. Similarly, sensory feedback generated by movement is transmitted back to the cerebellum through multiple pathways. Such cerebellar circuits generate signals which are relayed to deep cerebellar nuclei which are then transmitted to the thalamo-cortical circuit and to the premotor nuclei of the brain stem. All these signals enter the cerebellum through the mossy fibres a part from another pathway that originates from the inferior olive which generates the climbing fibres (Ito, 2006). Therefore, as spinocerebellar tract is one of the component of mossy fibres (Oscarsson, 1965), inputs to the neurons belonging to spinocerebellar tract and information forwarded by them to the cerebellum (as mentioned above) might form one of the basis to understand the function of the cerebellum in various activities including the motor activity. Recently, it has been proposed that one of the components of spinocerebellar tract neurons (SB neurons, in particular) have a special role in forwarding feedback information on descending commands relayed by RetS neurons to the cerebellum (Hammar *et al.,* 2010). Similarly, preliminary study by Hantman and Jessel (2010) has found the convergence of terminals of both DSCT and VSCT on the same cerebellar folia and these terminals were found frequently in proximity to the same granule neuron. This evidence highlights the involvement of the convergence of spinal inputs onto a common granule cell target for cerebellar processing. However, the cerebellum functions in a much more complex manner than predicted and knowledge on the operation of neuronal networks of the cerebellum is still poorly understood. New experimental tools are needed to investigate cerebellar network function and dynamics.

1.3 General characteristics of functionally identified mammalian interneurons in the spinal cord

The actions of both primary afferents and descending commands from the supraspinal system on ascending tract neurons including the spinocerebellar tracts and on motoneurons are primarily mediated by interneurons (Jankowska, 1992; Jankowska and Edgley, 2010). Interneurons are those neurons which have their axonal projections extending within only one of the enlargements or even one segment of the spinal cord or from one segment to another. Various electrophysiological and morphological studies done over more than a half century have shown the highly non-homogeneous nature of interneurons with respect to their size, dendritic trees, axonal projections, input and output properties and other features (Jankowska, 1992).

1.3.1 Group Ia inhibitory interneurons

Group Ia interneurons are one of the most completely defined mammalian interneuronal populations that mediate inhibition between flexor and extensor muscles in the disynaptic reflex arc in which one interneuron is interposed between group Ia muscle spindle afferents and motoneurons. Excitation of these interneurons by group Ia afferents from agonist muscles (extensor) causes inhibition of antagonist (flexor) motoneurons and vice versa. Therefore these interneurons mediate Ia reciprocal inhibition of antagonists (Jankowska, 1992). These interneurons are located mainly in the ventral part of lamina VII, just dorsal and medial to motor nuclei and have dominant input from group Ia afferents (Hultborn *et al.*, 1971b; Jankowska and Lindström, 1972). However, they affect motoneurons located a certain distance away as there is an evidence of their axonal projections extending up to one or two segments away from the cell body (Eccles *et al.*, 1957; Eccles and Lundberg, 1958). In addition to their exclusive monosynaptic activation from group Ia afferents, they are also effectively excited by group II afferents (Hultborn *et al.*, 1971b; Hultborn *et al.*, 1976b), FRAs (Hultborn *et al.*, 1971b; Fu *et al.*, 1975; Hultborn *et al.*, 1976b), neurons of intrinsic spinal locomotor and

scratch reflex networks (Feldman and Orlovsky, 1975) and by a number of descending tract neurons, for instance by VST neurons (Grillner and Hongo, 1972), CST neurons (Jankowska *et al.*, 1976) and RST neurons (Hultborn *et al.*, 1976c). Therefore, it is evident that they operate as last order interneurons in polysynaptic pathways from a variety of other peripheral and descending neuronal systems in addition to Ia muscle afferents (Hultborn *et al.*, 1971b; Jankowska and Lindström, 1972).

Their most characteristic source of inhibition is from Renshaw cells. Renshaw cells provide negative feed-back to motoneurons and also mediate recurrent inhibition of Ia inhibitory interneurons thus preventing very strong inhibition of antagonists which is important for the stability of various movements (Hultborn *et al.*, 1971a; Hultborn *et al.*, 1971b; Hultborn *et al.*, 1971c; Fedina and Hultborn, 1972). Another comparable source of inhibition of Ia interneurons is mutual inhibition. In this inhibition, interneurons causing Ia reciprocal inhibition from flexors to extensors and from extensors to flexors of a given joint inhibit each other (Hultborn *et al.*, 1976a). Moreover, actions of Ia interneurons are also modulated by supraspinal system (Hultborn *et al.*, 1976c).

Apart from direct and indirect actions of these interneurons on motoneurons, they also target other Ia inhibitory interneurons, neurons giving rise to VSCT (Lundberg and Weight, 1971; Hultborn *et al.*, 1976a). Therefore, Ia inhibitory interneurons adjust the excitability of motoneurons during variety of movements such as locomotion, scratch and centrally initiated movements (Jankowska *et al.*, 1976).

1.3.2 Group Ib interneurons

Group Ib interneurons are interneurons which have dominant source of peripheral input from Ib afferents from tendon organs (Jankowska, 1992). These interneurons are located in lamina VI and in the dorsal part of lamina VII, the region where the largest field potentials are evoked from group I afferents (Eccles *et al.*, 1954). The vast majority of them are monosynaptically activated by group Ib afferents; however disynaptic activation has also been reported (Harrison and Jankowska,

1985). Although Ib afferents from both extensors and flexors monosynaptically activate Ib interneurons, activation is more effective from extensors than that from flexors (Jankowska *et al.*, 1981; Harrison and Jankowska, 1985). Furthermore, convergence of Ia and Ib afferents or group II and Ib afferents is found in these interneurons (Jankowska *et al.*, 1981; Harrison and Jankowska, 1985; Jankowska and Edgley, 2010). In addition, these interneurons are also activated mono and di-synaptically from CS and RS neurons (Hongo *et al.*, 1972; Harrison and Jankowska, 1985).

In contrast to excitatory inputs, inhibitory control of these interneurons is principally mediated by mutual inhibition and inhibition from descending systems (Eccles and Lundberg, 1959; Lundberg *et al.*, 1978). Such mutual inhibition has been proposed to contribute to adjust the degree of negative feed-back to motoneurons (Lundberg *et al.*, 1978). These interneurons target a wide range of cells; motoneurons, other interneurons, other Ib interneurons in the disynaptic pathway to motoneurons, group II interneurons and ccDSCT neurons (Eccles *et al.*, 1961b; Hultborn *et al.*, 1971b; Lundberg, 1971; Harrison and Jankowska, 1985; Harrison *et al.*, 1986; Jankowska, 1992). Since these interneurons have dominant input from tendon organs operating at different joints, their main function is to co-ordinate activity of muscles operating at different joints (Lundberg *et al.*, 1975; Lundberg *et al.*, 1978; Harrison *et al.*, 1983). Moreover, as they also integrate other sensory and descending inputs, they are also proposed to have an important role in voluntary movements by adjusting the excitability of motoneurons (Jankowska, 1992).

1.3.3 Group II interneurons

Interneurons with a strong monosynaptic input from group II muscle afferents are referred as group II interneurons (Jankowska, 1992). They are mainly found in the grey matter of midlumbar segments (L4 and L5) of the lumbosacral enlargement. On the basis of their location, they are subdivided into three groups: those located in laminae IV-V are termed as dorsal horn group II interneurons; those found in lamina VI-VII are termed as intermediate zone group II interneurons and those in laminae

VIII are considered as lamina VIII group II interneurons (Maxwell *et al.*, 1997; Bannatyne *et al.*, 2003; Bannatyne *et al.*, 2006; Bannatyne *et al.*, 2009; Jankowska *et al.*, 2009). Individual interneurons are co-excited by group II afferents from both flexors and extensors (Edgley and Jankowska, 1987b; Lundberg *et al.*, 1987). Moreover, about 60% of these interneurons residing in intermediate zone/ ventral horn (but not those in dorsal horn) are also co-excited by group Ia and/ or group Ib afferents (Edgley and Jankowska, 1987b). The group II interneurons found in this area are also activated by the stimuli applied in the CST and the RST (Edgley *et al.*, 1988).

The main source of inhibitory input to group II interneurons including those in the dorsal horn originates from monoaminergic descending tract neurons (Andén *et al.*, 1966; Schomburg and Steffens, 1988). However, stimulation of other descending pathways (CST and RST) also evokes inhibition in them most probably mediated via other inhibitory interneurons (Edgley *et al.*, 1988). Like group Ia and Ib interneurons, these interneurons target various other neurons including motoneurons (Cavallari *et al.*, 1987; Bannatyne *et al.*, 2006), other group II interneurons (Edgley and Jankowska, 1987b) and different populations of spinocerebellar tract neurons such as VSCT (Lundberg and Weight, 1971) and dhDSCT neurons (Edgley and Jankowska, 1988). The primary function of these interneurons is to co-ordinate a variety of muscle activities of a limb and also co-ordinate muscle activity in various kinds of movements like locomotion and postural adjustments (Duysens *et al.*, 1980; Edgley and Jankowska, 1987a; Edgley and Jankowska, 1987b; Edgley *et al.*, 1988; Jankowska, 1992).

Recently, Jankowska and Edgley (2010) have proposed a distinct functional subdivision of interneurons which comprises of a group of premotor interneurons in the intermediate zone (lamina V-VII) with dominant input from group Ib afferents and also from group II afferents; to which a separate name has been assigned - “group I/ II interneurons”. These interneurons were originally referred as Ib interneurons (see above). However, the intermediate group II interneurons are also included in this reassessment (Jankowska and Edgley, 2010).

1.3.4 Commissural interneurons (CINs)

Commissural interneurons are a highly non-homogeneous group of neurons in the spinal cord with a characteristic feature of having axons which cross the midline and project to the contralateral grey matter and were first described by Ramon y Cajal (1909). Therefore, it is worth noting that CINs also include some of the interneurons which have already been discussed above.

The most reliably identified CINs that have been studied in detail include lamina VIII interneurons (Jankowska *et al.*, 2005). Lamina VIII CINs have been further subdivided into two subpopulations. The first population consists of CINs with monosynaptic inputs from group II muscle afferents (Jankowska *et al.*, 2005) and the second group are those with monosynaptic input from RetS neurons with or without inputs from VS neurons and/or group I afferents (Bannatyne *et al.*, 2003; Jankowska *et al.*, 2005; Jankowska, 2008). Both of these sub-populations of CINs include excitatory and inhibitory interneurons. Thus the two sub-populations of CINs are interposed in separate pathways as stimulation of group II afferents fail to evoke monosynaptic EPSPs in CINs with input from RetS neurons (second subpopulation) and vice versa (Jankowska *et al.*, 2005) but target cells of both populations are motoneurons and interneurons (Jankowska *et al.*, 2005). CINs with group II input mediate crossed stretch reflexes (crossed extensor and/ or flexor reflexes) which help in the reflex coordination of movements on both sides of the body (Jankowska *et al.*, 2005). Likewise, CINs with input from RetS/ VS/ group I afferents contribute to the coordination of movements on both sides of the body primarily during centrally initiated movements such as voluntary movements, locomotion and postural adjustment (Krutki *et al.*, 2003; Edgley *et al.*, 2004; Matsuyama *et al.*, 2004; Cabaj *et al.*, 2006; Jankowska *et al.*, 2006).

Other populations of CINs include: interneurons located in the dorsal horn (laminae IV-V) and the intermediate zone (lamina VII and within the border between laminae VII and VIII) (Jankowska *et al.*, 2009). CINs in the dorsal horn receive input from group II and skin afferents (Edgley and Jankowska, 1987b; Edgley *et al.*, 2003).

These interneurons are inhibitory and have axonal projections to the contralateral intermediate zone and the ventral horn both within and outside the motor nuclei (Bannatyne *et al.*, 2006). Another population of CINs in the intermediate zone is co-activated by group I and II muscle afferents (Czarkowska *et al.*, 1981; Jankowska *et al.*, 2009) which are exclusively excitatory (Bannatyne *et al.*, 2009).

1.4 Organization of the Descending pathways

Motor activity is a complex behaviour which is produced by various ascending pathways including spinocerebellar pathways, interneuronal circuits and descending supraspinal systems. The spinocerebellar pathway is modulated by various descending tract neurons as described earlier. Therefore, knowledge about the descending pathways is essential to understand their role in the control of transmission through the spinocerebellar pathway. Hence, the purpose of this section is to provide a brief overview of the neuroanatomical and functional properties of the major descending pathways at the level of spinal cord.

The fibres originating from supraspinal levels which descend to spinal cord participating in motor control systems is divided into two principal systems (Kuypers, 1964). One is the medial system, that includes RetS and VS pathways and another is the lateral system that includes CS and RS pathways.

1.4.1 Reticulospinal tract (RetST)

The RetS pathway is an extrapyramidal system which arises from the medial pontomedullary reticular formation and descends in the spinal cord. The medial pontomedullary reticular formation projections extend to the entire length of the spinal cord in the cat (Tohyama *et al.*, 1979b; Hayes and Rustioni, 1981), the opossum (Martin *et al.*, 1979b; Martin *et al.*, 1979a; Martin *et al.*, 1981) and the monkey (Kneisley *et al.*, 1978; Coulter *et al.*, 1979; Peterson, 1979) as revealed by retrograde tracer transport studies. The medial pontomedullary reticular formation gives rise to two major types of descending fibres – medial RetST and lateral RetST (Peterson, 1979).

The medial RetST originates from neurons found in the pons and the gigantocellular reticular nuclei (Ito *et al.*, 1970; Peterson *et al.*, 1975). The projections of these neurons descend through or close to the MLF which continue to the spinal ventromedial funiculus and terminate in laminae VI –IX at all levels of the spinal cord (Nyberg-Hansen, 1965; Petras, 1967). Anterograde tracing of single pontine RetS axon have shown that the axon collaterals arborize both ipsilaterally and bilaterally in lumbar enlargement of the cat spinal cord grey matter and terminate mainly in laminae VII and VIII. The pattern of terminal distribution from the same axon is similar at each segmental level (Matsuyama *et al.*, 1999).

The lateral RetST principally originates from neurons in the medullary reticular formation which are also called medullary RetS neurons. These neurons are found in the gigantocellular, parvocellular and paramedian reticular nuclei (Basbaum and Fields, 1979; Martin *et al.*, 1985). Their locations are also reported in dorsal and ventral medullary nuclei and in the retroambigus nucleus (Basbaum and Fields, 1979; Waltzer and Martin, 1984). The medullary RetS neurons which descend down to entire length of spinal cord are mainly located in the gigantocellular complex that includes the gigantocellular reticular nucleus, the dorsal paragigantocellular nucleus and the alpha and ventral parts. Anterograde degeneration following medullary lesions (Nyberg-Hansen, 1965; Peterson, 1979) and anterograde tracer transport (Basbaum *et al.*, 1978; Martin *et al.*, 1979b; Martin *et al.*, 1979a) have shown a bilateral course of their axons in the ventrolateral funiculus in the spinal cord. Collateral fibres of these neurons are distributed bilaterally with major arborization in laminae VI-VIII and also in lamina X at all levels of the spinal cord (Martin *et al.*, 1979a; Holstege and Kuypers, 1982). Furthermore, a recent retrograde tracing study has also demonstrated a substantial population of RetS neurons of gigantocellular reticular nucleus origin to be commissural in nature and project to both cervical and thoraco-lumbar segments in the rat (Reed *et al.*, 2008). However, most of the projections from the gigantocellular reticular nucleus are mainly found to be ipsilateral (Tohyama *et al.*, 1979a; Sakai *et al.*, 2009).

Neurons in the pontomedullary reticular formation are widely accepted to play a role in postural control and stability during reaching (Schepens and Drew, 2004) and

walking in cats (Prentice and Drew, 2001). Direct excitatory monosynaptic connections between RetS neurons and motoneurons of hindlimb (Grillner and Lund, 1968), neck and forelimb muscles (Wilson and Yoshida, 1969) are demonstrated electrophysiologically. Furthermore, a proportion of RetS neurons arising from gigantocellular complex are shown to be serotoninergic or peptidergic (Bowker *et al.*, 1981; Bowker *et al.*, 1982) and some make direct synaptic contacts with motoneurons (Holstege and Kuypers, 1987b; Holstege and Kuypers, 1987a). This kind of synaptic connectivity is proposed to be excitatory as stimulation of gigantocellular nucleus is shown to activate axial musculature (Robbins *et al.*, 1992). Similarly, iontophoretic application of 5-HT and certain peptides to motoneurons potentiates their excitability (Holstege and Kuypers, 1987b). Recently, combination of retrograde tracing and real-time reverse transcriptase polymerase chain reaction (PCR) analysis of single neurons descending to the spinal cord in the medullary gigantocellular reticular nucleus of the mouse has shown that these neurons are glutamatergic as they express mRNAs encoding for VGLUT2 (Martin *et al.*, 2011).

1.4.2 Vestibulospinal tract (VST)

Vestibulospinal projections descending from the vestibular nuclei to the spinal cord are a key system with a major role in the control of movement and posture. In mammals, classically it has been described that the VST is composed of two components- the medial VST (MVST) and the lateral VST (LVST) (Shinoda *et al.*, 2006). The MVST mainly originates from medial vestibular nuclei and joins bilaterally in the MLF. These fibres descend in the medial part of the ventral funiculus throughout cervical to mid thoracic segments of the spinal cord and terminate in spinal lamina VII (Nyberg-Hansen, 1964b). The axon terminals of these fibres are found to be both excitatory and inhibitory (Wilson and Peterson, 1978).

The LVST arises from the lateral vestibular nucleus and magnocellular portion of medial vestibular nuclei. The axons of LVST descend ipsilaterally (Nyberg-Hansen and Mascitti, 1964) and course in the ventral part of ventral funiculus projecting to

lumbar segments of the spinal cord and terminate in lamina VII and VIII (Holstege and Kuypers, 1982). These fibres have been proposed to be excitatory to all their target neurons which include motoneurons and lamina VIII neurons (Nyberg-Hansen and Mascitti, 1964). Antidromic (Akaike, 1983) and chromatolytic (Shamboul, 1980) studies following spinal lesions has shown that LVST fibres are organized somatotopically. The fibres originating from the dorsocaudal lateral vestibular nucleus project to hindlimb spinal levels whereas, those projecting from the magnocellular portion of medial vestibular nuclei reach neck and forelimb levels (Shamboul, 1980; Akaike, 1983).

Previous reports on different sizes, terminal arborizations and segment-specific termination patterns of VS axon collaterals in the cat have suggested diverse actions on interneurons and motoneurons located in different segments of the spinal cord (Rose *et al.*, 1996; Kuze *et al.*, 1999). MVST neurons innervate motoneurons in cervical segments which are responsible for mediating VS reflexes primarily controlling neck muscles while the LVST modulates motoneurons in both cervical and lumbar segments and mediates VS reflexes controlling the limbs (Wilson and Peterson, 1978; Shinoda *et al.*, 2006). Additionally, it has been reported that following stimulation of VS fibres, the activity of interneurons in cervical and lumbar segments in laminae VII-VIII is modulated (Wilson *et al.*, 1984; Suzuki *et al.*, 1985; Schor *et al.*, 1986). Furthermore, it has also been demonstrated that the axons of LVST have monosynaptic connections with interneurons in laminae VII-VIII in both the cervical and lumbar spinal cord (Grillner and Hongo, 1972; Alstermark *et al.*, 1987; Sugiuchi *et al.*, 1995). Similarly, Ia-inhibitory interneurons in laminae VI-VII (Hultborn *et al.*, 1976c) and group II activated mid-lumbar interneurons in laminae V-VII are also found to have monosynaptic input from the LVST (Davies and Edgley, 1994). Therefore, it is considered that VST neurons have an essential role in co-ordinating the diverse muscle actions that are required for the proper adjustment of posture and movement.

1.4.3 Corticospinal tract (CST)

The CST is the longest descending pathway in the central nervous system. The cells of origin of this tract are mainly located in the primary motor cortex and in the forelimb and hindlimb areas of the primary sensory cortex, throughout layer V (Miller, 1987). Anterograde tracing studies have differentiated the CST into five different components in the rat unlike in other species like cats and primates (Cheema *et al.*, 1984; Liang *et al.*, 1991; Brösamle and Schwab, 1997). The major component of this tract descends in the contralateral dorsal funiculus and rest of the fibres include the contralateral lateral CST, the contralateral intermediate CST located at the base of the contralateral dorsal horn of spinal grey matter and the ipsilateral dorsal and ventral CSTs. Neurons in the forelimb area of the sensorimotor cortex have the axonal projections which extend to the cervical enlargement, whereas those in the hindlimb sensorimotor cortex extend to the lumbar enlargement in the spinal cord (Li *et al.*, 1990). CS axon terminals are distributed in all spinal laminae contralateral to the cell of origin with the dense arborization in laminae III-VII and sparse projections in the ventral horn (Brown, 1971; Antal, 1984; Casale *et al.*, 1988; Liang *et al.*, 1991). Some axonal ramifications have also been reported in the medial part of the intermediate zone ipsilateral to the cortical injection site (Liang *et al.*, 1991). Furthermore, it has also been shown that the CST fibres project directly to the laminae I and II (Casale *et al.*, 1988; Liang *et al.*, 1991).

The distribution pattern of CS axon terminals in the intermediate zone and ventral horn of the spinal grey matter implies that this tract has a crucial role in the control of movement. The original evidence for the direct corticomotoneuronal connections was in primates with a role in fine motor control, particularly in the independent movement of the digits (Kuypers, 1960; Lawrence and Kuypers, 1968; Lawrence and Hopkins, 1976; Liang *et al.*, 1991; Curfs *et al.*, 1996). However, it is now evident from various tracing studies that this kind of connectivity exists in lower mammals like raccoons (Wirth *et al.*, 1974), the hamster (Kuang and Kalil, 1990) and the rat (Liang *et al.*, 1991; Curfs *et al.*, 1996) and electrophysiological

experiments indicate that this kind of corticomotoneuronal connectivity exists in the rat (Elger *et al.*, 1977).

The CS system is widely accepted as being glutamatergic as the neurons belonging to this system are immunoreactive to glutamate, aspartate or both (Giuffrida and Rustioni, 1989). Similarly subsequent study of the axon terminals of the CST has also demonstrated similar immunoreactivity to these amino acids suggesting that the CS terminals probably release these amino acids as neurotransmitters (Valtschanoff *et al.*, 1993).

1.4.4 Rubrospinal tract (RST)

The RST is one of the motor tracts that originate mainly from the neurons of the magnocellular region of the red nucleus (Massion, 1967; Shieh *et al.*, 1983). It has been shown that neurons in the ventrolateral part of the nucleus have axonal projections extending to the lumbar spinal cord whereas those residing in the dorsomedial region project to cervical segments (Daniel *et al.*, 1987; Strominger *et al.*, 1987) thus suggesting a somatotopic organization of this nucleus in the rat. This kind of organization has also been shown for the cat (Pompeiano and Brodal, 1957). However, there is evidence for projections of RS neurons to both cervical and lumbar regions of the spinal cord (Huisman *et al.*, 1981). It is a contralateral descending pathway as most of the axons cross in the ventral tegmental decussation which then run in the dorsal part of the lateral funiculus and terminate mainly in lamina V – VII of the spinal grey matter (Waldron and Gwyn, 1969; Antal *et al.*, 1992). This kind of terminal distribution pattern has been demonstrated in various species including the rat (Antal *et al.*, 1992), the cat (Holstege, 1987) and the monkey (Massion, 1967). However, anterograde and retrograde tracing combined with immunocytochemistry, has also revealed the presence of a small number of ipsilateral fibres which descended as far as the lumbar spinal cord in the rat (Antal *et al.*, 1992) and in the cat (Holstege, 1987). A projection of this tract to lamina IX within the cervical spinal cord of the rat has also been reported (Kuchler *et al.*, 2002).

It has been shown that RS neurons evoke excitatory actions on motoneurons controlling the musculature of hindlimbs (Hongo *et al.*, 1969). They are involved in the flexion of muscles, with effects causing excitation of flexor motoneurons (Arshavsky *et al.*, 1988) particularly of distal musculature (Kuchler *et al.*, 2002). However, this tract also evokes excitation of interneurons which in turn evokes EPSPs in flexor motoneurons and inhibition of extensor motoneurons (Hongo *et al.*, 1969). Antal and his colleagues (1992) have demonstrated connections of this tract with both the excitatory and inhibitory interneurons. Moreover, the majority of RS neurons are immunoreactive for glutamate which is also suggested to be released as a neurotransmitter by their terminals (Beitz and Ecklund, 1988).

1.5 Scope of the study

The DSCT, VSCT, CCT and RSCT are the four major well-defined anatomical and functional components of the spinocerebellar tract. The cerebellum receives information from hindlimbs via the DSCT and VSCT; and from forelimbs through the CCT and RSCT. Various anatomical and electrophysiological studies have demonstrated the complex organization of these tracts (DSCT and VSCT) and indicate a major role in proprioception with other supplementary functions including a contribution to centrally initiated voluntary and locomotor movements. Despite the potential importance of these tracts in proprioception, little is known about the synaptic organization of afferent input to spinocerebellar tract neurons and the mechanisms responsible for the control of afferent transmission through this pathway. Therefore, by investigating input properties of four different types of spinocerebellar tract neurons I believe that this information will provide better basis for understanding the processing of information at the spinal and supra-spinal levels.

1.6 Aims and Objectives

In view of the paucity of information about the synaptic organization of afferent input to different populations of spinocerebellar tract neurons as highlighted above,

I have investigated the input properties of these neurons in an attempt to fulfil the following aims:

- To investigate the excitatory inputs to four types of spinocerebellar tract neurons in the cat and rat thoraco-lumbar spinal cord.

- To analyze the inhibitory inputs to four types of spinocerebellar tract neurons in the cat and rat thoraco-lumbar spinal cord.

- To determine the origin of excitatory and inhibitory inputs to four types of spinocerebellar tract neurons in the cat and rat thoraco-lumbar spinal cord.

2 General Experimental procedures

The aim of this chapter is to give a detailed overview of the general experimental approaches used throughout the study to fulfil the three principal aims. Any specific experimental procedures performed while pursuing these investigations are explained in detail in the corresponding chapters.

All the experimental procedures on rats were conducted according to British Home Office legislation and were approved by the University of Glasgow Ethics committee. Experimental procedures on cats were approved by the Ethics Committee for Animal Research at the University of Gothenburg (Göteborgs Djurförsöksetiska Nämnd). All comply with National Institute of Health and European Union guidelines for animal care.

2.1 Surgical procedures and labelling of spinocerebellar tract neurons in the cat

2.1.1 Surgical procedure

General anaesthesia was induced with sodium pentobarbital (Apoteksbolaget, Sweden; 40-44 mg/kg, i.p.) and maintained with intermittent doses of α-chloralose (Rhône-Poulenc Santé, France; 5 mg/kg; i.v., administered every 1-2 hours up to 30 mg/kg and every 2-3 hours up to 55 mg/kg thereafter). Additional doses of α-chloralose were given when motor reactions were evoked during dissection and when increases in continuously monitored blood pressure or heart rate were evoked by any experimental procedures. Atropine (Mylan AB, Sweden; 0.05-0.2 mg/ kg i.m) was also administered occasionally during preliminary surgical procedures to reduce tracheal secretion. During recordings, neuromuscular transmission was blocked by using pancuronium bromide (Pavulon, Organon, Sweden; about 0.2 mg/kg/h i.v.) and the animals were artificially ventilated. The effectiveness of synaptic transmission was increased by intravenous administration of 4-AP (4-amino-pyridine, Sigma, USA; 0.1-0.2 mg /kg, i.v). These doses were expected to result in a

plasma concentration of 4-AP of about 1 μM and could be compared to clinically used doses of 10 mg, corresponding to 0.14 mg/kg in a 70 kg patient with minimal side effects (Alvina & Khodakhah, 2010). 4-AP was expected to increase the duration of action potentials in presynaptic fibres and thereby enhance the release of transmitter from terminals and thus to increase the probability of synaptic activation.

Mean blood pressure was maintained at 100-140 mm Hg and the end-tidal concentration of CO_2 at about 4% by adjusting the parameters of artificial ventilation and the rate of a continuous infusion of a bicarbonate buffer solution with 5% glucose (Merk, Sweden; 1-2 ml/h/kg). Core body temperature was kept at about 38^{o} C by servo-controlled infrared lamps.

Laminectomy was performed to expose the spinal cord from the third to the sixth lumbar (L3-L6) segments, primarily over the dorsal columns, and at the level of the low thoracic (Th10-Th12) segments, over both the dorsal columns and the lateral funiculi. The dura mater remained intact except for small holes (about 1 mm^2) over the dorsal columns through which recording electrodes were inserted. The caudal part of the cerebellum was exposed to allow insertion of tungsten electrodes (30-200 kOhms) used to stimulate axons of spinocerebellar tract neurons to activate them antidromically and to stimulate RetS axons running in the MLF.

Cerebellar stimulation sites were located ipsilateral to the DSCT and contralateral to VSCT and SB neurons, just rostral to or within the Nucleus Interpositus (at Horsley-Clarke coordinates about P 7, L 3.0-3.5, H 0 to -1). Axons within the MLF were stimulated ipsilateral with respect to the location of the neurons recorded from. The stimuli were applied at Horsley-Clarke coordinates P 7-9, L 0.5-0.8, H about -5. The final electrode position was adjusted while recording descending volleys from the surface of the spinal cord at the Th11-Th12 level. The electrodes were left at locations from which distinct descending volleys were evoked at thresholds of 10-20 μA; they were near maximal at 50-100 μA for cerebellar stimulation sites and at 100-150 μA for MLF stimulation sites. At the end of the experiments these locations were marked by electrolytic lesions (0.2 mA for 10 s) and it was verified that they were within the areas targeted at. To this end the

medulla was sectioned in the coronal plane and the cerebellum parasagitally at 100 μm and the distribution of the marking lesions were observed.

In order to identify peripheral inputs, several left hindlimb nerves were dissected free over a few mm distances, transected and mounted on pairs of silver stimulating electrodes separated by about 5 mm with cathode proximal. They included: quadriceps (Q) and sartorius (Sart) branches of the femoral nerve mounted in subcutaneous cuff electrodes; the posterior biceps and semitendinosus (PBST), anterior biceps and semimembranosus (ABSM), sural, superficial peroneal (SP), gastrocnemius-soleus (GS), plantaris (PL) and/or flexor digitorum and hallucis longus (FDL) branches of the sciatic nerve mounted on pairs of silver electrodes in a paraffin oil pool.

2.1.2 Stimulation and recording

Peripheral nerves were stimulated with constant voltage stimuli at intensities expressed in multiples of threshold (T) for the activation of the most excitable fibres. Standard stimuli were supramaximal for group I and II afferents (5T) but their intensity was reduced to near threshold or to 1.5T when latencies of PSPs recorded in the neurones indicated that these PSPs might have been evoked by group Ia or both group Ia and Ib afferents, to verify their origin. Afferent volleys following these stimuli (recorded from the cord dorsum at the L5 segmental level) were used to determine the central latencies of postsynaptic potentials (PSPs) recorded once neurons had been penetrated. Latencies <1 ms and about 1.5 – 2.5 ms indicated monosynaptic actions of group I and II afferents respectively, provided that the EPSPs were evoked by successive stimuli without signs for temporal facilitation. The spinocerebellar tract neurons were searched in the area where the field potentials were generated by different nerves (see below in criteria for identification). Intracerebellar axonal branches of tract neurons were stimulated by using 0.2 ms long constant current pulses at intensities ≤ 100 μA. Axons of these neurons within the ipsilateral or contralateral funiculus at the Th11-Th12 level were stimulated extradurally, with 2 silver ball electrodes in contact with its surface,

using constant current pulses of 100-500 μA. The stimulators used (designed by E. Eide, D. Magnusson and N. Pihlgren, University of Gothenburg) allowed the use of square constant voltage or constant current pulses via inbuilt isolation units, setting the constant voltage stimuli in multiples of threshold for activation of nerve fibres. The cerebellar and thoracic stimuli served to select neurons projecting to the cerebellum. Antidromic activation was first ascertained extracellularly and subsequently confirmed intracellularly, even if only blocked IS or M antidromic spikes could be recorded in strongly depolarised neurons where the spike generating mechanisms were inactivated during ionophoresis of intracellular markers.

2.1.3 Criteria for identification of different populations of spinocerebellar tract neurons and labelling

The spinocerebellar tract neurons were identified on the basis of antidromic activation from the cerebellum as well as a number of additional criteria specific for each population of neurons.

DSCT neurons were searched in the L3-L4 segments. Antidromic activation of these neurons was from the ipsilateral lateral funiculus at Th12-Th13. Antidromically activated neurons that were found at the medial border of the dorsal horn at depths of 2-2.5 mm from the surface of the dorsal columns at which large field potentials were evoked from group I muscle afferents at thresholds < 2T and latencies of ≤ 1 ms, i.e. corresponding to the location of Clark´s column were classified as ccDSCT neurons. dhDSCT neurons were found more laterally and more superficially, at 1.2 – 1.8 mm from the surface of the dorsal columns and often caudal to Clarke's column. In this area, large synaptic field potentials were evoked by group II, but not group I muscle afferents (Edgley and Jankowska, 1987a). In addition, dhDSCT neurons in these segments have a characteristic input from group II muscle afferents and cutaneous afferents (Edgley and Jankowska, 1988); from muscle nerves at 3-5T and latencies of 2-3 ms and from cutaneous afferents at minimal latencies of 1-2 ms (Edgley and Jankowska, 1988).

VSCT neurons were searched in the L4 and L5 segments. Antidromic activation of these neurons was from the contralateral lateral funiculus at Th12-Th13. The SB subpopulation of antidromically activated neurons were identified by their location within a 100-200 μm wide strip at the border between the lateral funiculus and the ventral horn (usually at depths 1.8-2.2 mm from the surface of the lateral funiculus at an angle of 10-20^{o} from vertical) and by their monosynaptic input from RetS neurons (MLF; Hammar *et al.,* 2011) and inhibitory input from group I and high threshold muscle afferents (Burke *et al.,* 1971; Lundberg and Weight, 1971). When present, excitatory input from primary afferents was evoked from group Ia afferents, but only SB neurons with exclusive inhibitory input from peripheral nerves were selected because of the growing evidence for their diverse functions (Hammar *et al.*, 2011; Jankowska *et al.*, 2011b). More medially distributed VSCT (Ib-VSCT) neurons were identified by their location at depths 2.4-3.9 mm from the surface of the dorsal columns (along vertical tracts), at which focal field potentials were evoked from both group I and II, or only group II muscle afferents (Hammar *et al.*, 2002), and by their characteristic input properties: excitatory from group Ib afferents and inhibitory from group I and high threshold muscle afferents (Eccles *et al.*, 1961a). Representative examples of PSPs from each of these four neuronal populations are shown in Figure 3-1. When the neurons were recorded from extracellularly prior to penetration, a collision test was performed to ensure that the shortest latency spike potentials were indeed evoked antidromically. The spikes were classified as evoked antidromically when they collided with spike potentials evoked by stimulation of a peripheral nerve at a critical time interval. In intracellular records a constant latency, usually coinciding with the descending volleys induced by the cerebellar and Th stimuli, lack of preceding EPSPs and the appearance of these spikes at an all-or-none fashion were used as criteria for antidromic activation.

Once the neurons were identified and penetrated, they were labelled intracellularly by ionophoresis from the same micropipettes ("sharp", with tips broken to about 1.5 μm, impedance of 7-20 MΩ) that were used for extracellular and intracellular recording. As in a previous study (Liu *et al.,* 2010a), the

micropipettes were filled with a mixture of equal proportions of 5% tetramethylrhodamine-dextran (Molecular probes, Inc, Eugene, USA) and 5% Neurobiotin (Vector laboratories, UK) in saline or potassium chloride (Merk, Sweden; KCl: pH 6.5) and ejected by passing 5-10 nA of positive constant current for up to 15 minutes, or as long as PSPs were recorded from the neuron. At the conclusion of the experiments, a lethal dose of pentobarbital was administered to the animals and they were perfused through the descending aorta (after having transected the venacava), initially with physiological saline (under 150-180 mm Hg pressure) and subsequently with paraformaldehyde (Merk, Sweden; 4%) in 0.1M phosphate buffer (Merk, Sweden; PB) (under 100-130 mm Hg pressure). Blocks of lumbar spinal cord containing labelled cells were removed and placed initially in the same fixative (for 8 hours at 4° C) and then in PB or in 30% sucrose (VWR, Sweden) in PB. Dura and pia mater were removed from the spinal cord blocks.

2.1.4 Revealing Neurobiotin and Rhodamine labelled cells

The spinal cord blocks and were rinsed in 0.1 M PB, three times for 10 minutes each, and flat-embedded in 3% agar in distilled water. The tissue blocks (L3 – L6 segments) were then cut into 50 µm thick transverse sections with a Vibratome (Oxford instruments, Technical products international Inc. USA). Serial sections were collected and stored in 0.1 M PB. These sections were immediately immersed free-floating in 50% ethanol for 30 minutes to enhance antibody penetration. Thereafter the sections were washed three times with 0.1M phosphate buffered saline that contained 0.3 M sodium chloride (Sigma-Aldrich, UK; NaCl) in PBS, 10 minutes each and mounted in the same serial order with anti-fade medium, Vectashield (Vector Laboratories, UK) on glass slides. The sections were examined for labelled spinocerebellar tract neurons with a fluorescence microscope and those containing labelled neurons were taken off the glass slides on which they were mounted and collected in serial order. These sections were washed three times in PBS, 10 minutes each. They were then incubated free-floating in Avidin-Rhodamine (1:1000, Jackson ImmunoResearch, UK) for 3 hours to reveal the detailed processes of the intracellularly Neurobiotin-Rhodamine labelled neurons. Following three 10

minute washes in PBS, the sections were mounted in Vectashield on glass slides. Sections were re-scanned using a fluorescence microscope and those containing well labelled neurons were processed for immunohistochemistry. Details of specific immunohistochemical procedure for each part of the study are given in the respective chapters. A schematic representation of experimental procedures in cats is shown in Figure 2-1.

2.2 Surgical procedures and labelling of spinocerebellar tract neurons in the rat

2.2.1 Surgical procedure

Sprague Dawley rats (Harlan, Bicester, UK; 250-350 g) were deeply anesthetized with intraperitoneal injections of Ketamine (Boehringer Ingelheim Vetmedica, Inc., USA) and Xylazine (Bayer Plc, UK) (0.1ml/ 100 gm; 2:1). The animals were then fixed in a stereotaxic frame during surgical procedures under strict aseptic conditions. The skin at the back of the head was cut in a midline and the skull was exposed. A small burr hole was made unilaterally in the skull through dura targeting the respective inter-aural anterior-posterior and medio-lateral co-ordinates, to expose the dorsal surface of the cerebellum. Glass micropipette with tip diameters of 20 µm filled with 0.2 µl Cholera toxin B subunit (CTb, 1%) (Sigma-Aldrich, Co., UK) in distilled water was aligned with this burr hole. The micropipette was then lowered and its tip was inserted into the cerebellum at a targeted dorso-ventral co-ordinates. CTb was injected by pressure (1-5 psi) using Pico injector (World Precision Instruments, USA). The micropipette was left in place for 5 minutes after injection to prevent backflow of CTb. The exposed surface was sutured and the animals were recovered from anesthesia which usually takes 2-4 hrs displaying exploratory behaviour and starting to drink. Following a six day postoperative survival period, animals were re-anesthetized with Pentobarbitone (Sigma-Aldrich, UK; 1ml, 200 mg/ ml i.p.) and were perfused with mammalian ringer solution followed by 4% paraformaldehyde (Sigma-Aldrich, UK) in 0.1M PB (Sigma-Aldrich, UK) through the left ventricle. The spinal cord and brain were removed and post-

fixed in the same fixatives for 8 hours at 4°C. The cerebellum and brainstem were kept in fixative for 1-2 days and cut coronally at 100 µm thickness in freezing microtome for histological examination of the injection site. Spinal cord blocks were prepared from T12 to L3 segments on the basis of dorsal roots which were then rinsed several times in 0.1M PB. All segments were cut into 50µm thick transverse sections with a Vibratome. The cerebellum and spinal cord sections were placed immediately in an aqueous solution of 50% ethanol for 30 minutes to enhance antibody penetration.

2.2.2 Identification of injection site

Injection sites were visualized by using 3, 3'-diaminobenzidine (Sigma-Aldrich, UK; DAB) as a chromogen. Sections were incubated in goat anti- CTb (List Quadratech, USA; 1:50000) for 48 hours and then rinsed three times in PBS which was followed by a reaction with secondary antibody of biotinylated anti-goat IgG (Jackson Immunoresearch, USA; 1:500) for 3 hours at room temperature. Sections were washed three times in PBS and incubated in avidin-horseradish peroxidase (HRP) (Sigma-Aldrich, UK; 1:1000) for 1 hour. Finally, hydrogen peroxide plus DAB was applied for a period of approximately 15 minutes to reveal immunoreactivity at the injection sites which was golden brown in colour. The same procedure was applied for selected spinal cord sections to determine the anatomical location of retrogradely labelled cells. During this time, the sections were monitored constantly. The sections of the brain and the spinal cord were then mounted on the gelatin coated slides after which they were fixed with fixative vapour (formalin) overnight. Sections were dehydrated, cleared and coverslip was applied. After this, the sections were observed with a transmission light microscope and photographed digitally with AxioCam camera (Carl ZEISS, Inc, Germany) using AxioVision 4.8 software (ZEISS, Germany). The location of the injection site was determined with reference to the stereotaxic rat brain atlas of Paxinos and Watson (1997). A schematic representation of rat experiments is shown in Figure 2-2.

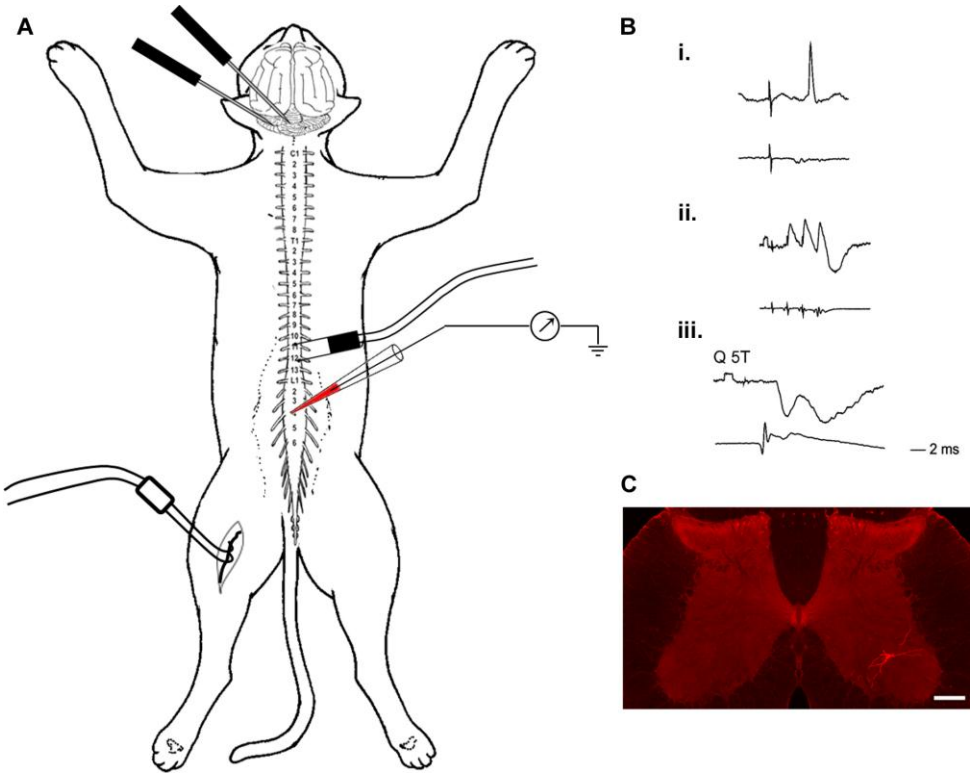

Figure 2-1 Schematic diagram of electrophysiological identification and labelling of spinocerebellar tract neurons in the cat

***A*,** Spinocerebellar tract neurons were identified by antidromic stimulation from the cerebellum (just rostral to or within the Nucleus Interpositus), excitation/ inhibition following stimulation of different hindlimb nerves and descending inputs from the MLF. Axons of these neurons within the ipsilateral or contralateral funiculus at the Th11-Th12 level were stimulated extradurally, with 2 silver ball electrodes in contact with its surface. Once the cells were identified, intracellular recording was done and cells were labelled intracellularly by ionophoresis with a mixture of equal proportions of tetramethylrhodamine-dextran and neurobiotin. ***B*,** Intracellular recording of one of the identified cells showing i) antidromic spikes following stimulation of the cerebellum ii) EPSPs evoked by MLF stimulation iii) IPSPs generated by stimulation of hindlimb nerves. In each pair of traces, the upper trace is an intracellular record from the cell indicated (negativity downward) and the lower trace is from the cord dorsum (negativity upward). *C*, A low power image of the neurobiotin filled cell revealed by Avidin-rhodamine reaction. Scale bar = 200μm. EPSP, excitatory post synaptic potential; IPSP, inhibitory post synaptic potential; MLF, medial lateral funiculus; Th, thoracic.

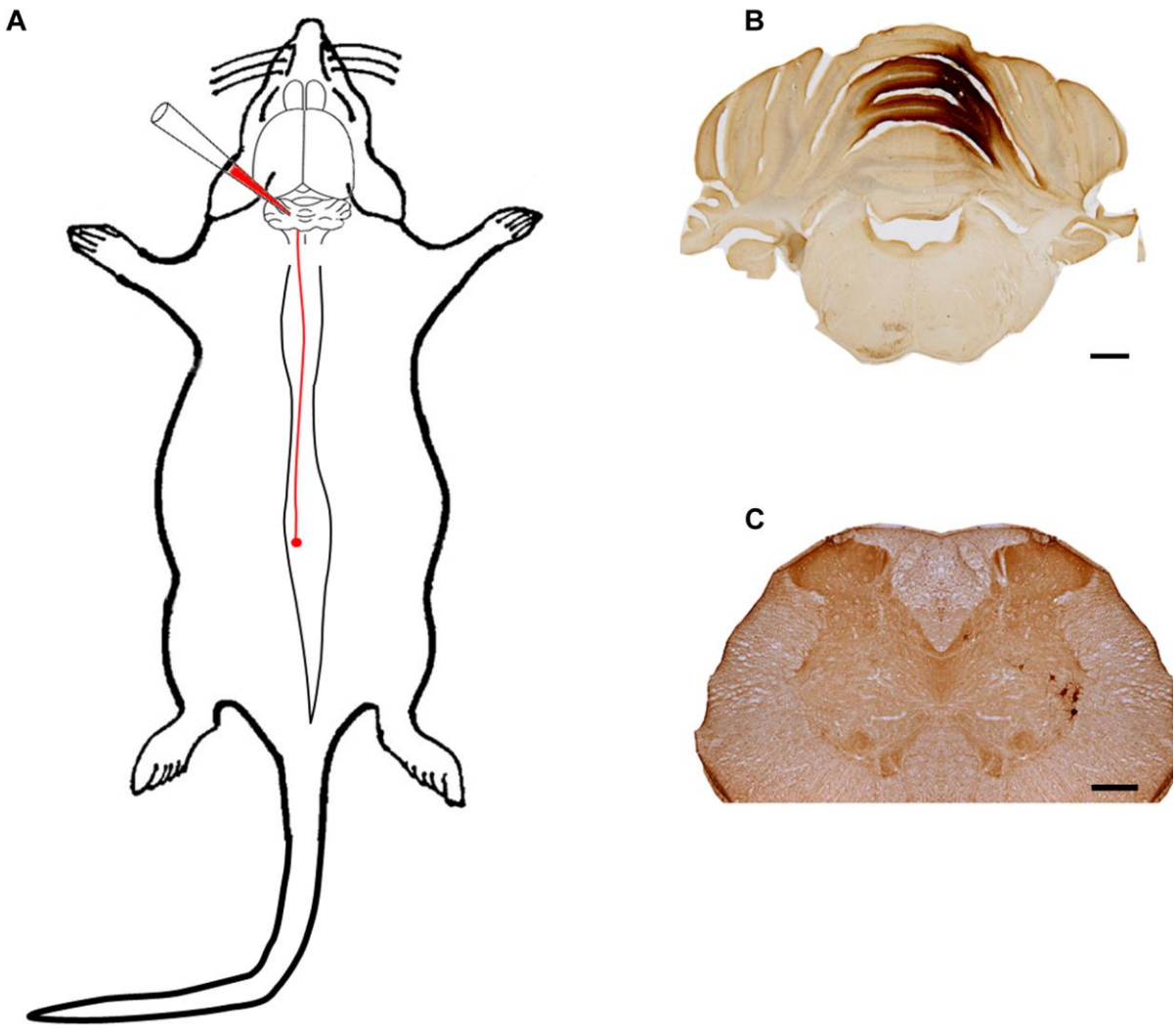

Figure 2-2 Schematic diagram of retrograde labelling of spinocerebellar tract neurons in the rat

A, Spinocerebellar tract neurons were labelled by retrograde transport of CTb following injection into the cerebellum. ***B***, A photomicrograph showing injection site in the targeted region of the cerebellum. Scale bar = 100 μm. ***C***, A photomicrograph of the spinal cord section showing the different anatomical locations of the retrogradely labelled spinocerebellar tract cells. Scale bar = 200 μm.

2.3 Tissue processing and Multiple immunolabelling for confocal microscopy

Spinal cord sections were processed for multiple immunolabelling for confocal microscopy. This technique allows the identification of more than one antigen in the same section of the spinal cord. To address the aims of the present study, various antigens were used which include transporters, neurotransmitters and receptors. This technique involves two principal steps:

1. The first step involves incubation of spinal cord sections in unlabelled primary antibodies that were raised in different species. Generally mixture of two or three primary antibodies derived from different species was used that binds to the target antigen in the tissue.

2. The second step involves incubation of sections in the species specific fluorophore conjugated secondary antibodies. Generally, the secondary antibody is an immunoglobulin (IgG) raised in donkey which is raised against the IgG of the animal species in which the primary antibody has been raised. Binding of these species specific secondary antibodies to specific primary antibodies can be readily detected by means of the fluorophore coupled to it.

Once these two steps are complete, following rinses, sections are mounted and are ready to be scanned with confocal laser scanning microscope. Individual antigens targeted for study can be independently visualised by the immunoreactivity of corresponding fluorophore-coupled secondary antibody. Images obtained from the same optical section can either be visualised in individual colours or can be merged in order to study the relative spatial distribution of the respective antigens and their relationship with each other. For example, contacts made by different axon terminals on identified cells can be analysed from the three channel images obtained from confocal microscope as represented in Figure 3-3 in chapter 3.

It is also possible to use a fourth antibody if it is raised against a different species in the same section by a sequential incubation technique. This process requires two additional steps. Hence, the overall procedure includes: 1) incubation of the section in cocktail of primary antibodies; 2) incubation in the secondary antisera cocktail; 3) scanning of the region of interest in the respective section; 4) sequential incubation with additional primary antibody; 5) incubation in species specific secondary antibody (this antibody will have one of the fluorophores which has already been used); 6) re-location and re-scanning of the area of interest which has already been scanned previously; 7) comparison of the scans obtained before and after sequential incubation allows detection of extra labelling in the corresponding channel which represents immunoreactivity for the sequentially added antibody. This procedure is usually performed to examine any double labelling in the same axon terminal. Therefore, it is visualised with additional colour due to the mixture of two different fluorophores. For example, if the axon terminal before sequential incubation is immunoreactive for one antibody which is displayed as blue and after sequential incubation, it also was labelled with additional antibody which is visualised in red then additional red structures will represent immunoreactivity for this antibody as shown in Figure 5-7 in chapter 5.

2.4 Confocal microscopy, reconstructions and analysis

The confocal laser scanning microscopes used in the present study are the Radiance 2100 microscope (Bio-Rad, UK) and the LSM 700 confocal microscope (Ziess, Gemany). The Radiance 2100 microscope was equipped with three lasers: blue diode (405 nm) argon multiline, green Helium Neon (543 nm) and red diode (637 nm). LSM 700 microscope was equipped with Argon multi-line, 405 nm diode, 561 nm solid state and 633 nm Helium Neon lasers. These lasers allowed scanning of sections that had different structures labelled with the secondary antibodies, each of which is coupled to a different fluorophore. Table 2-1 shows the excitation-emission wavelengths of different fluorophores conjugated with different secondary antibodies used.

Sections containing cell bodies and dendrites of intracellularly labelled cat neurons were initially scanned at low power (X20 lens, zoom factor 1.2) and this image was used as a frame of reference for the location of labelled processes within each section and to make preliminary reconstructions of the cells. Following this, individual cells were scanned at a higher magnification by using a X40 oil immersion lens at zoom factor of 2 at an increment of 0.5 μm. Series of confocal images were gathered and a montage was constructed for each cell. Usually the processes of cells extended within 6 or 7 sections and 60-80 series of images were collected from each section.

Table 2-1 Excitation-emission wavelength of the fluorophore used

Fluorophore	Excitation (λ)	Emission (λ)
Rhodamine-red (Rh Red)	543	591
Alexa-fluor 488 (Alexa488)	488	517
Cyanine 5.18 (Cy-5)	635	665
Dylight 649	652	670
Dylight 488	493	518
Avidin Rhodamine (AV-Rh)	570	590
Avidin Pacific blue (AV-PB)	410	455

Retrogradely labelled rat spinocerebellar tract neurons were examined ipsilaterally to the injection site. Sections from Th12 to L3 segments were firstly scanned at low power (X 10 lens, zoom factor 1) and these images were used as a frame of reference to categorize the neurons into different populations based on their anatomical location in the spinal cord grey matter. Sections containing well labelled neurons were then scanned with the confocal microscope by using a X 40 oil immersion lens with a zoom factor of 2 at 0.5 μm intervals.

Cells were reconstructed three dimensionally by using Neurolucida 9.14 (MicroBrightField Inc, USA) for Confocal software (MicroBrightField Inc, USA) and contacts on the labelled cells were mapped. Reconstructions were always started

from the stacks of single optical section containing the cell body. Once the reconstruction of the cell body was complete, dendritic processes were systematically added and contacts were plotted and recorded simultaneously with appropriate markers from the subsequent stacks until the dendritic tree was fully reconstructed. Only contacts in close apposition to the cell in the same focal plane and with no intervening black pixel space were counted.

Contact densities were calculated using data generated by Neurolucida and expressed as numbers of contacts per unit area (100 μm^2) of neuronal surface. The surface area of the cell body was estimated by measuring the perimeter of each labelled cell body from projected confocal images using Image J 1.4.3.67 software (National Institutes of Health, USA) and calculating the surface area of an equivalent sphere. The distribution of contacts was analysed using Sholl analysis with Neurolucida Explorer 9.14 (MicroBrightField Inc, USA). The number of contacts within series of 25 µm concentric spheres from the centre of the cell body of each cell was expressed as numbers per 100 µm of dendritic length. Numbers of contacts within each sphere were averaged for the four types of cell and shown as Sholl plots.

2.5 Statistical analysis

Data were expressed as mean ± standard deviation (SD). Multi-group comparisons were made by using one way Analysis of Variance (ANOVA) followed by a *post hoc* Tukey's analysis as appropriate and two variable comparisons among the same population was made by using Student's *t* test. A $p < 0.05$ was considered to be statistically significant (Prism 4.0.3).

3 Excitatory inputs to four types of spinocerebellar tract neurons in the cat and the rat thoraco-lumbar spinal cord.

3.1 Introduction

A first step towards understanding the role of the cerebellum in the control of movements is to determine the nature of the information forwarded to it. Therefore, the spinocerebellar tracts have a pivotal role in this control process. Electrophysiological studies of input to the four main populations of lumbar spinocerebellar tract neurons have revealed considerable differences between them. DSCT neurons were primarily found to carry information about peripheral events, subpopulations of these neurons monitoring input from different types of receptors including muscle spindles, Golgi tendon organs, joint and cutaneous receptors (Oscarsson, 1965; Edgley and Jankowska, 1988). However, even though input to individual DSCT neurons is drawn from fairly restricted receptive fields, information carried by the whole population of these neurons has been found to reflect whole limb kinematics (Bosco and Poppele, 2001). Direct input to VSCT neurons likewise originates from several categories of afferents, but input to individual neurons is drawn, as a rule, from several muscles (Oscarsson, 1965; Burke *et al.*, 1971a; Lundberg and Weight, 1971). In addition VSCT neurons monitor activity of spinal interneuronal networks (Lundberg, 1971) and descending commands to a much greater extent (Hammar *et al.*, 2011) than activity of peripheral afferents. For instance, DSCT neurons in cc were found to receive direct excitatory input from CST neurons (Hantman and Jessell, 2010) but only indirect excitatory input from RetS neurons (Hammar *et al.*, 2011), while VSCT neurons are excited both directly and indirectly by RetS, VS, CS and RS neurons (Baldissera and Roberts, 1976; Hammar *et al.*, 2011; Jankowska *et al.*, 2011b). However, in electrophysiological experiments the relative contribution of afferent fibres and central neurons to the input of subpopulations of VSCT and DSCT neurons could only be estimated approximately. For instance, even if a high proportion of the SB

subpopulation of VSCT neurons appeared to be primarily inhibited following stimulation of hindlimb muscle nerves (Burke *et al.*, 1971a; Lundberg and Weight, 1971), it could not be excluded that low threshold afferents from other parts of the body and/or slower conducting high threshold muscle or skin afferents evoked synaptic actions nor that those coinciding with IPSPs evoked by faster conducting lower threshold afferents remained undetected. Conversely, as input from only some descending tract neurons to DSCT neurons has been investigated so far, it could not be excluded that other descending neurons or intraspinal neurons provided major input to them.

Hence, one of the main aim of the present study was to compare the relative contribution of primary afferents and central neurons to excitatory synaptic input to two populations of DSCT and two populations of VSCT neurons: 1) DSCT neurons located in cc with their main input from group Ia afferents (ccDSCT neurons); 2) DSCT neurons located in the dorsal horn with input from group II afferents and skin afferents but not group I afferents (dhDSCT neurons; Edgley and Jankowska, 1987a); 3) VSCT neurons located in the medial part of lamina VII, with excitatory peripheral input mainly from group Ib afferents (Ib-VSCT neurons; which will be referred to as VSCT neurons throughout the study) and 4) VSCT neurons located at the border between the white and grey matter in the ventral horn, with excitatory peripheral input mainly from group Ia afferents, or apparently devoid of such input (which will be referred to as spinal border, SB, neurons). SB neurons with negligible input from primary afferents have been of particular interest because of recent indications that their main function might be different from those of other spinocerebellar tract neurons - to forward information not so much about input to spinal neurons as about the probability of activation of motoneurons by descending commands (Hammar *et al.*, 2011; Jankowska *et al.*, 2011b).

In order to achieve this aim, two series of experiments were carried out. In the first series of experiments in cats, spinocerebellar tract neurons were initially identified and characterized electrophysiologically. Representative neurons of the four populations were then injected with a mixture of rhodamine-dextran and Neurobiotin (see details in chapter 2, section 2.1). The second series of

experiments was performed in rats by utilizing the fact that the organization of the various subpopulations of spinocerebellar tract neurons, in terms of location and axonal projections, is the same in the cat and the rat, a part from the differences in the segmental levels of appearance of the neuronal groups (Matsushita and Hosoya, 1979; Matsushita *et al.*, 1979). The neurons were searched in equivalent anatomical locations and segments as for the cat (see chapter 1, section 1.1). The features of neurons analysed in the cat could thus be compared to features of corresponding rat neurons identified according to their anatomical location by retrograde transport of CTb, injected into the cerebellum (see details in chapter 2, section 2.2). In both species glutamatergic nerve terminals in contact with labelled neurons were analysed immunohistochemically. In order to differentiate between terminals of different origin, antibodies against vesicular glutamate transporter 1 (VGLUT1) to label primary afferent terminals (Varoqui *et al.*, 2002; Todd *et al.*, 2003; Alvarez *et al.*, 2004) and against vesicular glutamate transporter 2 (VGLUT2) to mark axon terminals of spinal interneurons and most descending tract neurons with the exception of the CST (A. Du Beau, S. Shakya Shrestha and D. J. Maxwell, In press) were used. As shown previously the distribution of VGLUT1 and VGLUT2 terminals in cat spinal cord grey matter is very similar to that in rat spinal cord, although the patterns of the expression of these two markers were originally investigated in rat spinal cord only (Varoqui *et al.*, 2002; Todd *et al.*, 2003). Furthermore, all cat excitatory interneurons studied previously expressed VGLUT2 but never VGLUT1 (Bannatyne *et al.*, 2009).

3.2 Methods

All experimental procedures were approved by the Ethics committee as mentioned in General experimental procedures (Chapter 2).

3.2.1 Experimental procedures on cats

The study was carried out on a sample of 23 neurons labelled in 6 adult cats weighing 2.5-3.8 Kg (2-5 cells from each animal). Surgical procedures, stimulation, identification and labelling of the four populations of spinocerebellar tract neurons in all animals were carried out following the procedures mentioned in detail in General experimental procedures (Chapter 2, Section 2.1).

3.2.2 Experimental procedures on rats

Four adult male Sprague Dawley rats (Harlan, Bicester, UK) weighing between 250 – 350g were deeply anesthetized and surgery was performed following the procedures described in detail in General experimental procedures (Chapter 2, Section 2.2). Retrograde injection with CTb (200 nl, 1%) was done at inter-aural co-ordinates -4.2 mm (anterior-posterior) and +2.0 mm (medio-lateral) at a dorso-ventral co-ordinate of +4.5 mm in the cerebellum (Paxinos and Watson, 1997). The injection site was identified by using DAB as a chromogen and the location of the targeted site was determined with reference to the stereotaxic rat brain atlas (Paxinos and Watson, 1997) as described previously (see chapter 2, Section 2.2).

3.2.3 Immunohistochemical procedures

Transverse sections of 50 µm thickness of L3 – L6 segments of the cat and Th12 – L3 segments of the rat (see rationale in section 3.1; also large number of four populations of spinocerebellar tract neurons were found in these segments which was consistent throughout four animals used) were prepared following procedure mentioned in Chapter 2 (Section 2.1 and 2.2). Intracellularly labelled neurons with

Neurobiotin and Rhodamine were first revealed using Avidine-Rhodamine reaction and sections containing well labelled cells were selected with a florescence microscope. Both the cat and rat sections were then processed for immunohistochemistry. Selected sections containing intracellularly labelled neurons were washed firstly several times in PBS and then incubated in a combination of the following primary antibodies: guinea pig anti-VGLUT1 and rabbit anti-VGLUT2 for 72 hours at 4° C. Following several washes in PBS, the sections were incubated in a combination of secondary antibodies coupled to Cy 5 and Alexa 488 for 3 hours at room temperature to identify VGLUT1 and VGLUT2 terminals respectively. All antibodies were diluted in PBS containing 0.3% Trition (Sigma-Aldrich, UK) (PBST) (see Table 3-1 for details of antibodies used). The sections were then mounted in Vectashield.

Retrogradely labelled rat spinocerebellar tract neurons were identified by the presence of CTb transported from injection sites and grouped into different populations based on their anatomical locations. Three colour immunofluorescence was performed on these sections with guinea pig anti-VGLUT1 and rabbit anti-VGLUT2 antibodies (see rat sections in Table 3-1) using the same procedures as for cat neurons.

3.2.4 Confocal microscopy, reconstruction and analysis

In both series of experiments, the sections were scanned using three channels of a confocal laser scanning microscope as described in Chapter 2 (Section 2.4). Serial sections containing entire cell bodies and dendrites of intracellularly labelled cat neurons and retrogradely labelled rat neurons ipsilateral to the injection site were scanned and images were collected from each section as described previously. VGLUT1 immunoreactive terminals were imaged as blue, while VGLUT2 terminals were green.

Cells were reconstructed three dimensionally by using Neurolucida for Confocal software and VGLUT1 and VGLUT2 contacts on the labelled cells were mapped and recorded. Contact densities were calculated using data generated by Neurolucida

and expressed as numbers of contacts per unit area (100 μm^2) of neuronal surface. In intracellularly labelled cells, the distribution of contacts was analysed using Sholl analysis with Neurolucida Explorer (see details in Chapter 2, Section 2.4).

3.2.5 Statistical analysis

Data were expressed as mean ± SD. Multi-group comparisons were made by using an one way ANOVA followed by a *post hoc* Tukey's analysis as appropriate and two variable comparisons among the same population was made by using Student's *t* test. A $p < 0.05$ was considered to be statistically significant.

Table 3-1 Summary of the primary and secondary antibody combinations and concentrations used.

	Primary antibody combination	Primary antibody concentration	Supplier	Secondary antibody combination	Secondary antibody concentration	Supplier
Cat	gp/ rbt VGLUT1	1:5000	Chemicon, Harlow, UK/ Synaptic systems	Cy-5	1:100	Jackson ImmunoResearch, West Grove, USA
	rbt VGLUT2	1:5000	Chemicon, Harlow, UK	Alexa 488	1:500	Molecular Probes, Eugene, USA
Rat	mo CTb	1:250	A. Wikström, University of Gothenburg	Rh. Red	1:100	Jackson ImmunoResearch, West Grove, USA
	gp VGLUT1	1:5000	Chemicon, Harlow, UK	Cy-5	1:100	Jackson ImmunoResearch, West Grove, USA
	rbt VGLUT2	1:5000	Chemicon, Harlow, UK	Alexa 488	1:500	Molecular Probes, Eugene, USA

All secondary antibodies were raised in donkey and conjugated to Rh. Red, Rhodamine Red; Cy-5, Cyanine 5.18; Alexa 488, Alexa-fluor 488; gp, guineapig; rbt, rabbit; mo, mouse; CTb, B- subunit of cholera toxin; VGLUT, Vesicular glutamate transporter

3.3 Results

3.3.1 Glutamatergic terminals on intracellularly labelled cat neurons

3.3.1.1 Samples of spinocerebellar tract neurons

In total, a sample of 23 well labelled spinocerebellar tract neurons that showed no evidence of damage following the injection of the markers was used for quantitative comparison of the numbers of glutamatergic terminals. The neurons included 6 SB neurons (cells 1- 6), 3 VSCT neurons (cells 7- 9), 3 ccDSCT neurons (cells 10 -12) and 3 dhDSCT neurons (cells 13- 15) for comparison of distribution of VGLUT1 and VGLUT2 contacts on the same cells. An additional eight cells were analysed for VGLUT1 contacts only (cells a-h); these were 3 ccDSCT, 3 dhDSCT and 2 VSCT cells used for inter-population comparisons on the whole sample of neurons.

Individual neurons antidromically activated from within or close to the Nucleus Interpositus were classified into four subpopulations on the basis of coupling between primary afferents and these neurons and according to their anatomical location in the lumbar grey matter, as described earlier (see chapter 2, section 2.1). Electrophysiological recordings from 4 neurons representative of the two populations of VSCT and the two populations of DSCT neurons are shown in Figure 3-1. The records illustrate antidromic activation from the cerebellum (in the middle panels) of all of these neurons. Furthermore, they illustrate strong inhibition from muscle afferents from the quadriceps nerve in SB (cell 3) and VSCT (cell 8) neurons and a lack of excitatory input from this nerve in the majority of SB neurons and some VSCT neurons (in the left panels). Peripheral excitatory input from the tested muscle nerves was not detected in 5 of the 6 SB neurons whereas excitatory input from at least one muscle nerve was evoked in all VSCT neurons. The records also illustrate the much shorter latencies of excitation of ccDSCT neurons (cell 12) following quadriceps stimulation when compared with dhDSCT (cell 13) neurons;

these were compatible with actions evoked by group I and group II afferents respectively.

The locations of cell bodies of these neurons are indicated in Figure 3-2. Cell bodies of SB neurons (red circles) were located within the most lateral part of the grey matter in lamina VII while cell bodies of VSCT neurons (green circles) were within more medial parts of lamina VII. The cell bodies of ccDSCT neurons (purple circles) were located within cc whereas dhDSCT neurons (blue circles) had their cell bodies in either lamina V or VI. The locations of the cell bodies of the 15 cells which were analysed for both VGLUT1 and VGLUT2 are indicated by closed circles whereas open circles indicate locations of the cell bodies of the eight cells analysed for VGLUT1 only. Both the location and morphology of the labelled neurons was fully consistent with the classification of these cells based on their input.

3.3.1.2 To what extent is excitatory input to different populations of spinocerebellar tract neurons monosynaptic from primary afferents and to what extent it is from other neurons?

As specified in the introduction, immunoreactivity against VGLUT1 or VGLUT2 was used as an indication of peripheral afferent or central origin of the terminals in contact with the labelled neurons (see Discussion for an evaluation of this rationale). The results summarised in Table 3-2 and illustrated in Figures 3-3 to 3-5 reveal strikingly different patterns of VGLUT1 and VGLUT2 axonal contacts on SB, VSCT, ccDSCT and dhDSCT neurons. Examples of confocal microscope images revealing immunocytochemical properties of axon terminals contacting labelled neurons (one from each group) are shown in Figure 3-3A, 3-3B, 3-3C and 3-3D respectively.

Figure 3-3A shows confocal microscope images of VGLUT2 immunoreactive axon terminals in contact with the cell body and dendritic trunk of a SB neuron (cell 1). Few VGLUT1 positive axon terminals contacted this or other SB cells. In contrast, both VGLUT1 and VGLUT2 positive terminals were found in contact with the cell body and dendrites of VSCT neurons, as illustrated in Figure 3-3B (cell 8). Although

both kinds of contacts were also found on ccDSCT and dhDSCT neurons, for most DSCT neurons the majority of the contacts were formed by VGLUT1 terminals and, in the case of ccDSCT neurons, very few contacts were formed by VGLUT2 axon terminals. Figures 3-3C and 3-3D show confocal microscope images of VGLUT1 and VGLUT2 immunoreactive axon terminals in contact with the cell body and dendritic trunk of a ccDSCT neuron (cell 10) and a dhDSCT neuron (cell 14), respectively. Figure 3-3C also illustrates the much lower density of VGLUT2 labelling within cc than in the neuropil just ventral to it. Generally Figure 3-3 illustrates that there is a good correspondence between the density of VGLUT1 and VGLUT2 positive terminals associated with the analysed spinocerebellar tract neurons and the concentration of these terminals within the regions of the grey matter where they are located (Alvarez *et al.*, 2004).

The differences in the number of VGLUT1 and VGLUT2 positive terminals in contact with the four populations of spinocerebellar tract neurons became even more marked when overall distribution of these terminals on the soma and along the whole dendritic tree of the four populations was compared. Reconstructions of the distribution of VGLUT1 and VGLUT2 immunoreactive axon terminals on individual cells analysed for both of these terminals are shown in Figure 3-4 and those analysed for VGLUT1 only are shown in chapter 5, Figure 5-2.

These reconstructions illustrate: (i) that VGLUT2 contacts are distributed on both somata and dendrites of SB neurons; (ii) that the overwhelming majority of VGLUT1 contacts are on somata of VSCT neurons while VGLUT2 contacts are concentrated on dendrites, especially distally; (iii) that VGLUT1 contacts are distributed on both somata and dendrites of ccDSCT neurons and; (iv) that mixed VGLUT1 and VGLUT2 contacts are distributed on both somata and dendrites of dhDSCT neurons.

3.3.1.3 Quantitative comparison of coverage of VGLUT1 and VGLUT2 terminals on intracellularly labelled SB and VSCT neurons

A quantitative analysis of the density of VGLUT1 and VGLUT2 terminals associated with cell bodies and dendrites was performed for each class of cell. The results are

summarized in Table 3-2 and in Figure 3-5A and B. The overall average density (i.e. on both soma and dendrites) calculated per 100 μm^2 of SB neurons was more than 200 times lower for VGLUT1 than for VGLUT2 contacts (0.02 ± 0.01 and 2.92 ± 0.25 respectively). This difference was statistically highly significant (Student *t*- test, $p < 0.0001$). For VSCT neurons the average contact density per 100 μm^2 was only about 5 times lower for VGLUT1 than for VGLUT2 contacts (0.43 ± 0.16 and 2.04 ± 0.66 respectively) but this difference was also statistically significant (Student *t*-test, $p < 0.01$).

Comparison of the overall coverage densities on SB and VSCT neurons revealed a weak statistically significant difference for VGLUT2 contacts ($p < 0.05$; ANOVA), the density being on average 1.5 - 2 times higher on SB neurons. No statistically significant difference ($p > 0.05$) was found between the overall densities of VGLUT1 contacts on these two populations of VSCT neurons even though the average density of VGLUT1 contacts on VSCT neurons was 15 times higher than on SB neurons.

The density of VGLUT1 and VGLUT2 contacts for individual neurons given in Table 3-2 and a Sholl analysis for these cells in Figure 3-6 provide a quantitative measure of the differences illustrated in Figure 3-4. Both the table and Sholl analysis show that much higher proportions of VGLUT2 relative to VGLUT1 terminals were found on somata and dendrites of SB and VSCT neurons, although differences in the densities were greater on the dendrites when compared with somata (about 150 times versus 100 times for SB neurons and about 7 times versus 2.5 times for VSCT neurons). Synaptic actions of VGLUT2 terminals therefore may be evoked within all compartments of the dendritic trees of SB and VSCT neurons whereas actions of VGLUT1 terminals are focused upon proximal dendrites.

3.3.1.4 Quantitative comparison of coverage of VGLUT1 and VGLUT2 terminals on intracellularly labelled ccDSCT and dhDSCT neurons

In ccDSCT neurons, the overall average density of VGLUT1 per 100 μm^2 was more than 10 times higher than VGLUT2 contacts (2.78 ± 0.65 and 0.15 ± 0.11,

respectively). This difference was statistically significant (Student *t*-test, $p < 0.0001$). In the dorsal horn population of DSCT neurons (dhDSCT), the overall average surface density of VGLUT1 was less than twice higher than of VGLUT2 contacts (1.74 ± 0.33 and 0.98 ± 0.29 respectively). Also this difference was statistically significant (Student *t*-test, $p < 0.05$).

Differences in the overall contact density of VGLUT2 terminals on ccDSCT and dhDSCT neurons were not found to be statistically significant but ccDSCT neurons showed significantly higher number of VGLUT1 contacts ($p < 0.01$) than dhDSCT neurons. Diagrams in Figure 3-5A and B also show that the overall contact density of VGLUT1 terminals was significantly higher on ccDSCT neurons than on either dhDSCT, VSCT or SB neurons and that the overall contact density of VGLUT2 terminals was significantly higher on SB than on either VSCT, dhDSCT, ccDSCT neurons.

Both the quantitative data of individual neurons in Table 3-2 and Sholl analysis in Figure 3-6 show that the differences in densities of VGLUT1 and VGLUT2 terminals on ccDSCT neurons were more apparent on dendrites than on somata (about 16 times versus 8 times) but the differences on somata were found in only 2 out of 3 cells. These differences were even smaller on dendrites of dhDSCT neurons (about 2 times, in 2 out of 3 cells), and were not apparent on somata.

Taken together the present results indicate that the distribution of VGLUT1 and VGLUT2 contacts within each class of cat spinocerebellar tract neuron is characteristic and differs from the distribution in other classes.

3.3.2 Glutamatergic terminals on retrogradely labelled rat neurons

A representative photomicrograph of a CTb injection site in the cerebellum and reconstructions of injection site for all four animals is shown in Figure 3-7. The injection of CTb into the cerebellum yielded unilateral, well defined injection sites that were surrounded by a shell of diffuse CTb staining. A total of 80 spinocerebellar tract neurons were analysed in rats that included 24 ccDSCT

neurons, 21 dhDSCT neurons, 18 SB neurons and 17 VSCT neurons. The first criterion for selection was strong labelling of both cell bodies and dendritic trees at distances of at least 35 μm from the soma (average distance of 164.23 μm). The second criterion was a location equivalent to the location of intracellularly labelled spinocerebellar tract neurons in cats. As shown in Figure 3-8, SB neurons were classified as those with cell bodies located within the most lateral part of the grey matter in lamina VII (red circles) and VSCT neurons as those located within more medial parts of lamina VII (green circles). Likewise, ccDSCT and dhDSCT neurons were classified as those located within cc (purple circles) or outside cc in either lamina V or VI (blue circles).

Examples of confocal microscope images for each of these neuronal populations are shown in Figure 3-9. As in the cat, they illustrate the preferential contacts of VGLUT2 immunoreactive terminals on SB neurons and the location of these neurons were within the region of the grey matter where there was much higher density of VGLUT2 than VGLUT1 immunoreactive terminals. In contrast, ccDSCT neurons show preferential contacts of VGLUT1 immunoreactive contacts, the location within the region of the grey matter with a much higher density of VGLUT1 than VGLUT2 immunoreactive terminals.

3.3.2.1 Quantitative comparison of coverage of VGLUT1 and VGLUT2 terminals on retrogradely labelled SB and VSCT neurons

A quantitative comparison of the density of VGLUT1 and VGLUT2 immunoreactive terminals contacting SB neurons reveals a significantly higher density of VGLUT2 contacts in comparison to VGLUT1 contacts (Student *t*- test, $p < 0.0001$). The overall average density of VGLUT1 and VGLUT2 contacts calculated per 100 μm^2 of SB neurons was 0.02 ± 0.01 and 1.10 ± 0.21 respectively. In contrast the average overall densities of VGLUT1 and VGLUT2 contacts on VSCT neurons were 0.13 ± 0.07 and 0.80 ± 0.65 per 100 μm^2 respectively. This difference was also statistically significant (Student *t*- test, $p < 0.05$).

Although these VSCT neurons have a higher number of VGLUT1 contacts relative to SB neurons, comparison of the overall contact densities on SB and VSCT was not

significantly different ($p > 0.05$; ANOVA see Figure 3-5C and 3-5D). Similarly, no statistically significant difference ($p > 0.05$; ANOVA) was found between the overall contact density of VGLUT2 on these two populations of neurons.

3.3.2.2 Quantitative comparison of coverage of VGLUT1 and VGLUT2 terminals on retrogradely labelled ccDSCT and dhDSCT neurons

The overall average density of VGLUT1 and VGLUT2 contacts on ccDSCT neurons was 0.68 ± 0.19 and 0.16 ± 0.07 per 100 μm^2. This difference was highly significant (Student *t*- test, $p < 0.001$). In contrast, in dhDSCT neurons, the overall average contact density of VGLUT1 terminals was 0.21 ± 0.04 and that of VGLUT2 was 0.36 ± 0.13 per 100 μm^2 of the neuron. This difference was also statistically significant (Student *t*- test, $p < 0.05$).

Comparison of the overall contact densities on ccDSCT and dhDSCT neurons revealed a strong statistically significant difference for VGLUT1 terminals ($p < 0.001$; ANOVA) whereas differences in the overall contact density of VGLUT2 terminals were not significant (cf data for cat cells above).

3.3.3 Comparison of cat and rat contacts

Comparison of the coverage by VGLUT1 and VGLUT2 terminals of spinocerebellar tract neurons in the cat and in the rat in Figure 3-5 and Table 3-2 & 3-3 reveals two main features. Firstly, the overall contact densities of VGLUT1 as well as VGLUT2 immunoreactive terminals were 3-4 times lower on rat neurons. Possible reasons for this difference are discussed below. Secondly, there is a similar pattern of relative contact densities between each class of neuron in both species (Figure 3-5); i.e. from the lowest densities of VGLUT1 terminals on SB neurons to the highest densities on ccDSCT neurons and from the highest densities of VGLUT2 terminals on SB neurons to the lowest densities on ccDSCT neurons.

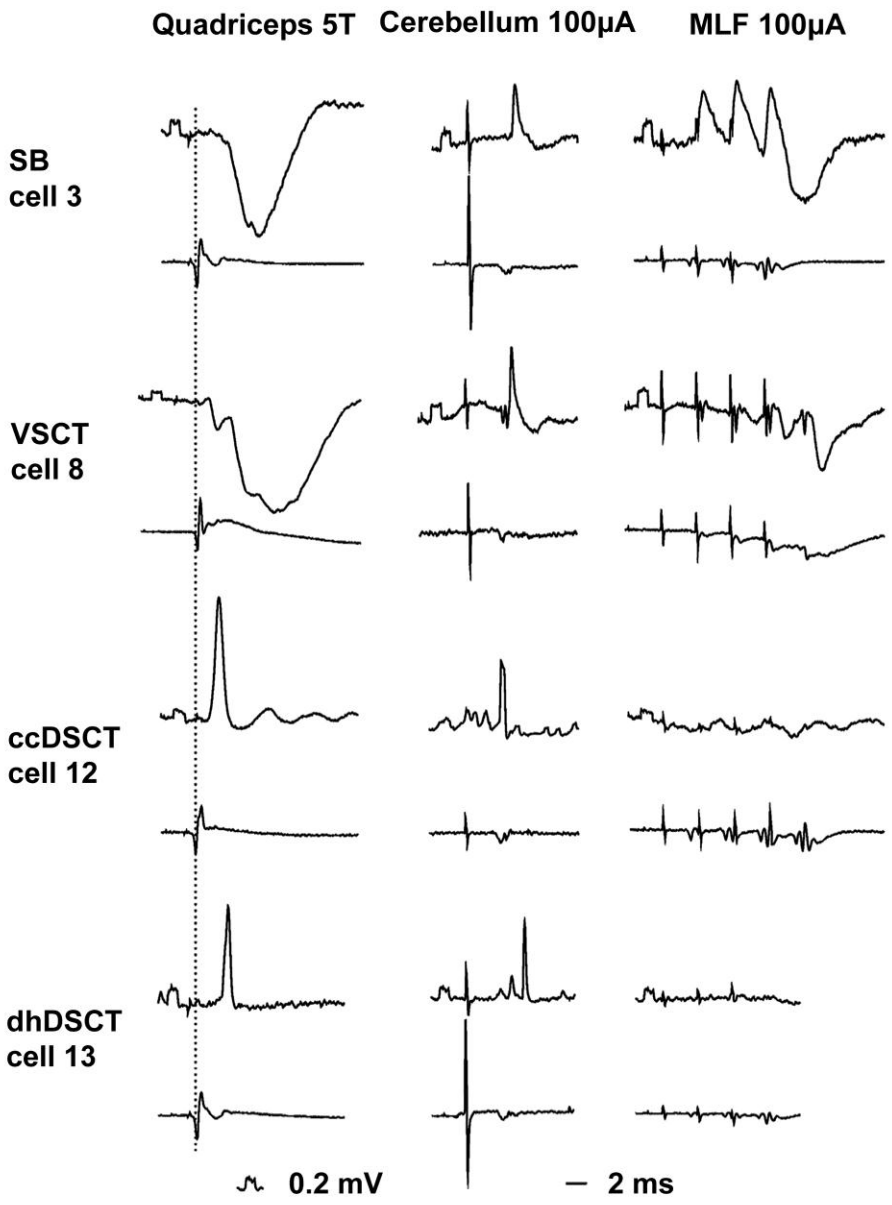

Figure 3-1 Representative examples of PSPs used to identify the four different populations of lumbar spinocerebellar tract neurons analysed morphologically.

In each pair of traces, the upper trace is an intracellular record from the cell indicated (negativity downward) and the lower trace is from the cord dorsum (negativity upward). All of the illustrated postsynaptic potentials in the left column were evoked by stimuli applied to the quadriceps nerve at 5 times threshold (5T). The dotted line indicates the afferent volleys. All rectangular calibration pulses at the beginning of traces are 0.2 mV.

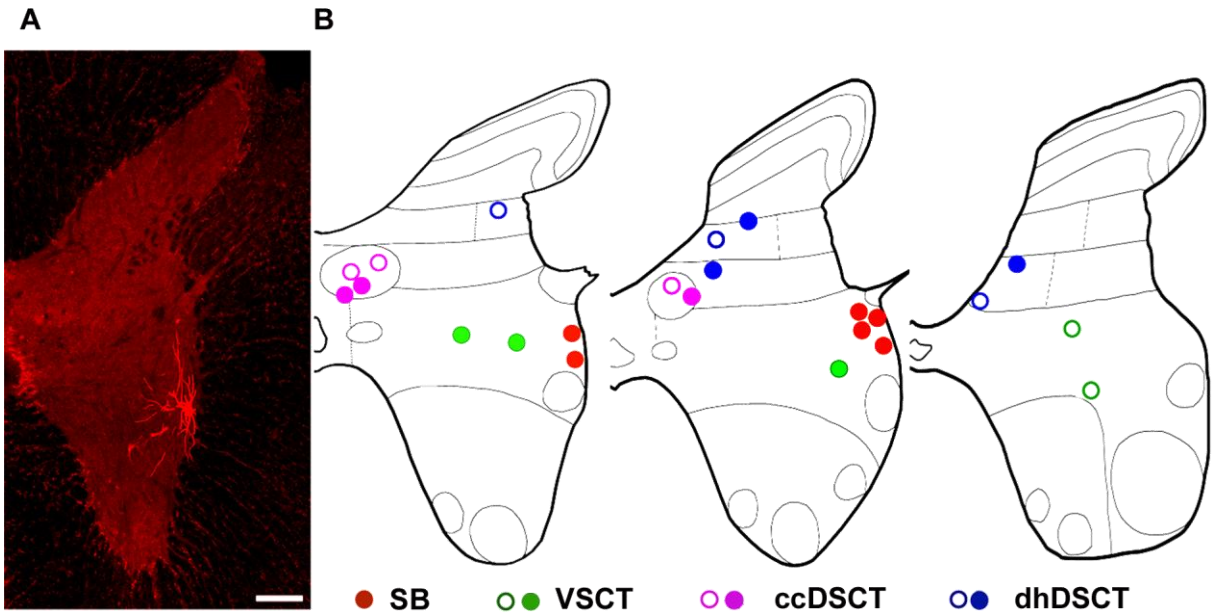

Figure 3-2 Locations of 23 intracellularly labelled spinocerebellar tract neurons

A*,** A low-magnification image of a transverse section of the L3 segment of the spinal cord showing the location of one of the SB neurons (cell 5). ***B*,** Diagrams illustrating the locations of cell body of all 23 cells in the L3, L4 and L5 segments respectively. Closed circles indicate location of the 15 cells which were analysed for both VGLUT1 and VGLUT2 while the open circles are for the 8 additional cells which were analysed for VGLUT1 only. Scale bar in ***A 200 μm.

Figure 3-3 Immunohistochemical characteristics of VGLUT1 and VGLUT2 axon terminals in contact with intracellularly labelled spinocerebellar tract neurons

A-D*,** Single optical sections through the cell bodies of representative SB (Cell 1), VSCT (Cell 8), ccDSCT (Cell 10) and dhDSCT (Cell 14) neurons showing the presence of VGLUT1 (blue) and VGLUT2 (green) immunoreactive terminals. The cell body and dendrites of intracellularly labelled cells are in red. ***A1-A4; B1-B4; C1-C4 and D1-D4*,** Projected images of dendritic trunks from cells shown in ***A*, *B*, *C and ***D*** respectively (areas encompassed in the boxes) illustrating contacts made by VGLUT1 and VGLUT2 immunoreactive terminals with the cell indicated by arrow heads and arrows respectively. Note differences in the density of VGLUT1 and VGLUT2 immunoreactive terminals within different regions of the grey matter shown in ***A-D*** and especially the high density of VGLUT1 and low density of VGLUT2 within Clarke's column shown in ***C***. Scale bar in ***A-D*** = 10 μm. Scale bar in ***A1-A4*, *B1-B4*, *C1-C4*** and ***D1-D4*** = 5 μm.

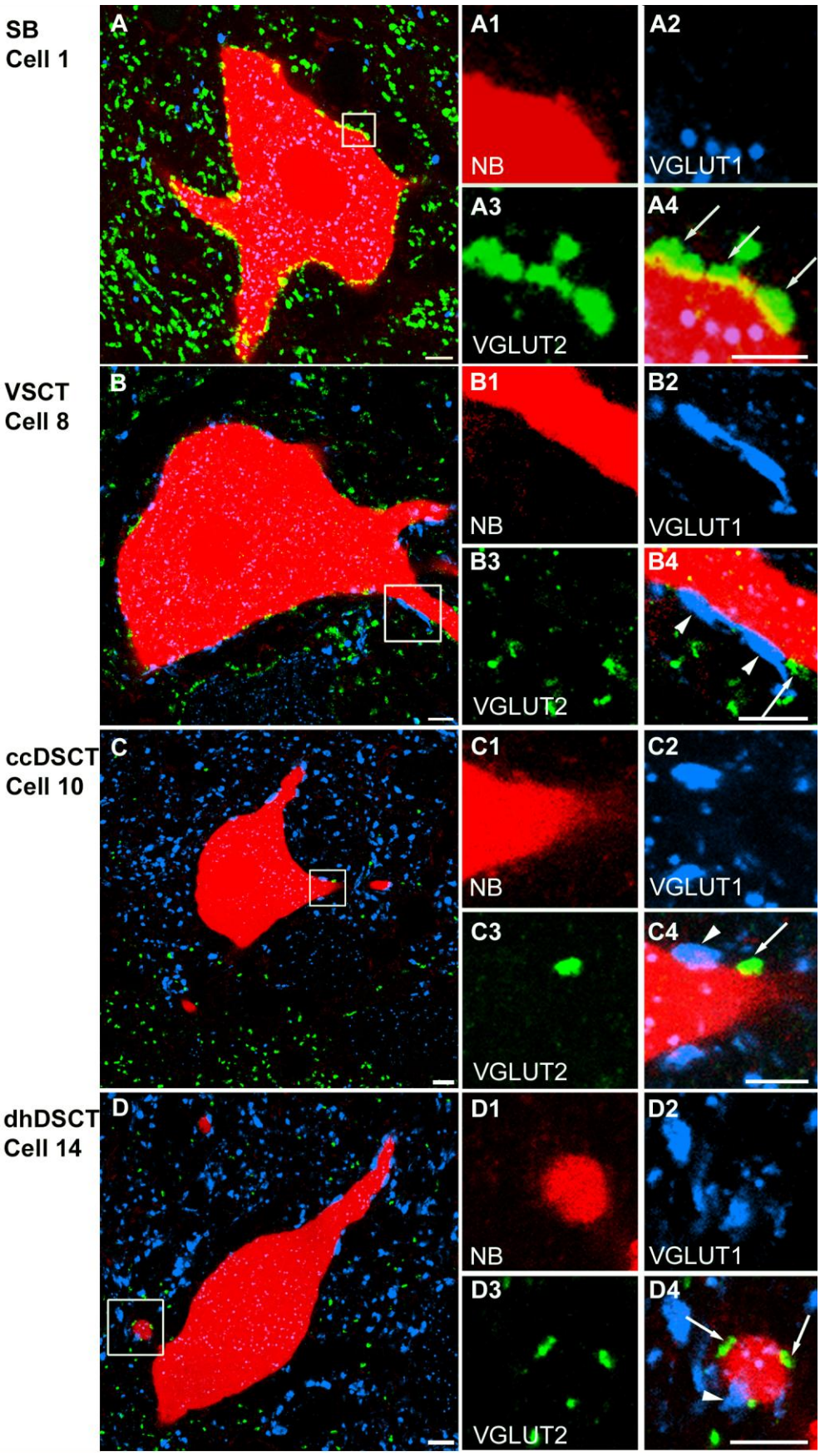
SB
Cell 1
A
A1
NB
A2
VGLUT1
A3
VGLUT2
A4
VSCT
Cell 8
B
B1
NB
B2
VGLUT1
B3
VGLUT2
B4
ccDSCT
Cell 10
C
C1
NB
C2
VGLUT1
C3
VGLUT2
C4
dhDSCT
Cell 14
D
D1
NB
D2
VGLUT1
D3
VGLUT2
D4

Figure 3-4 Reconstructions of spinocerebellar tract neurons illustrating the four different types of distribution patterns of VGLUT1 and VGLUT2 contacts

Reconstructions of 15 spinocerebellar tract neurons analysed in the present study showing the distributions of VGLUT1 (green) and VGLUT2 (red) contacts throughout the dendritic trees. The reconstructions were made with Neurolucida for Confocal. All the small images without contacts plotted show the reconstructions of respective cells. Cell body and dendrites are shown in light grey. Scale bars = 50 μm for reconstructions with contacts plotted and 100 μm for reconstructions without contacts. All are oriented such that the midline is to the left and the lateral borders of the grey matter to the right, as in Figure 3-2.

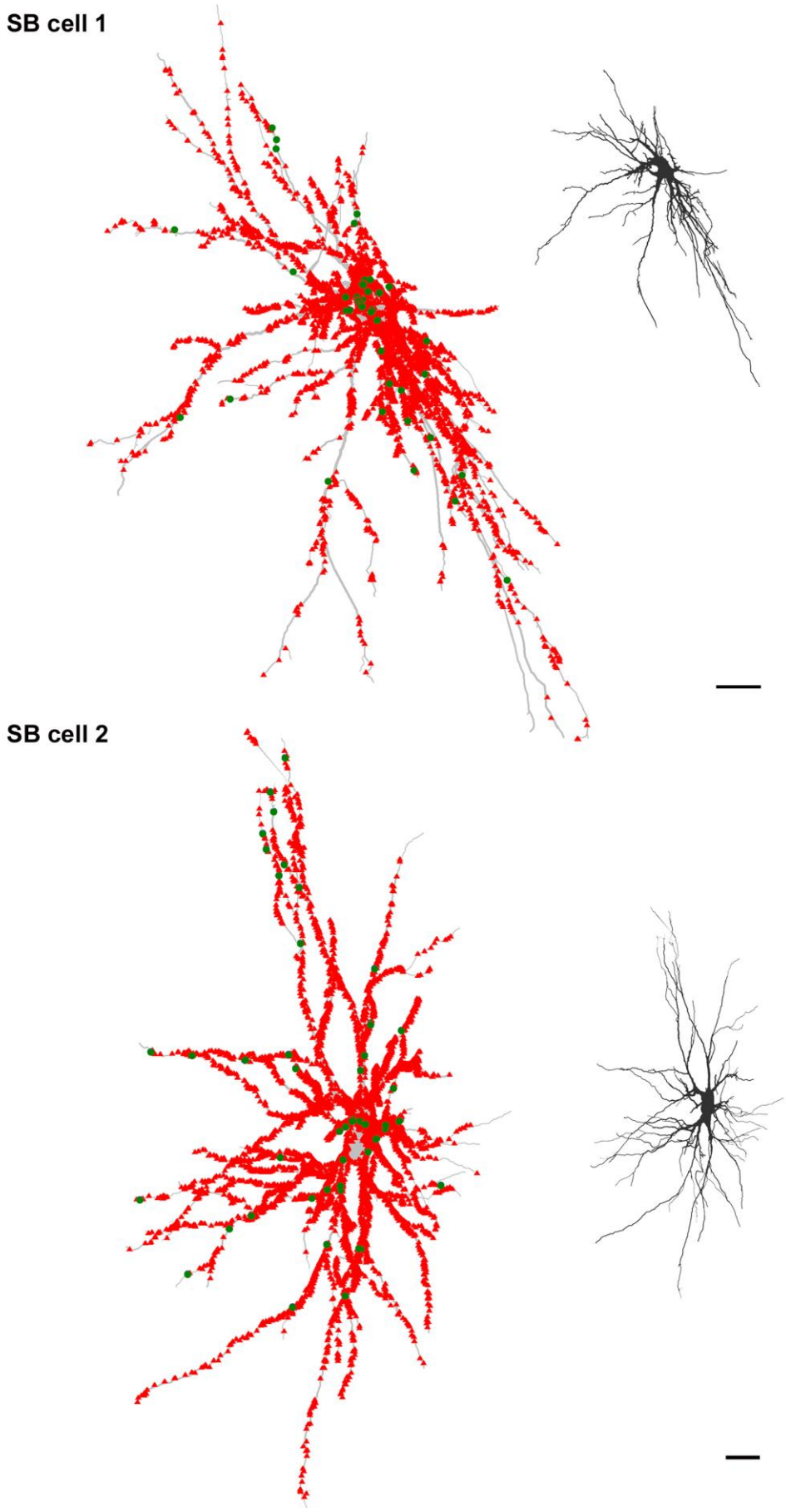
SB cell 1
SB cell 2

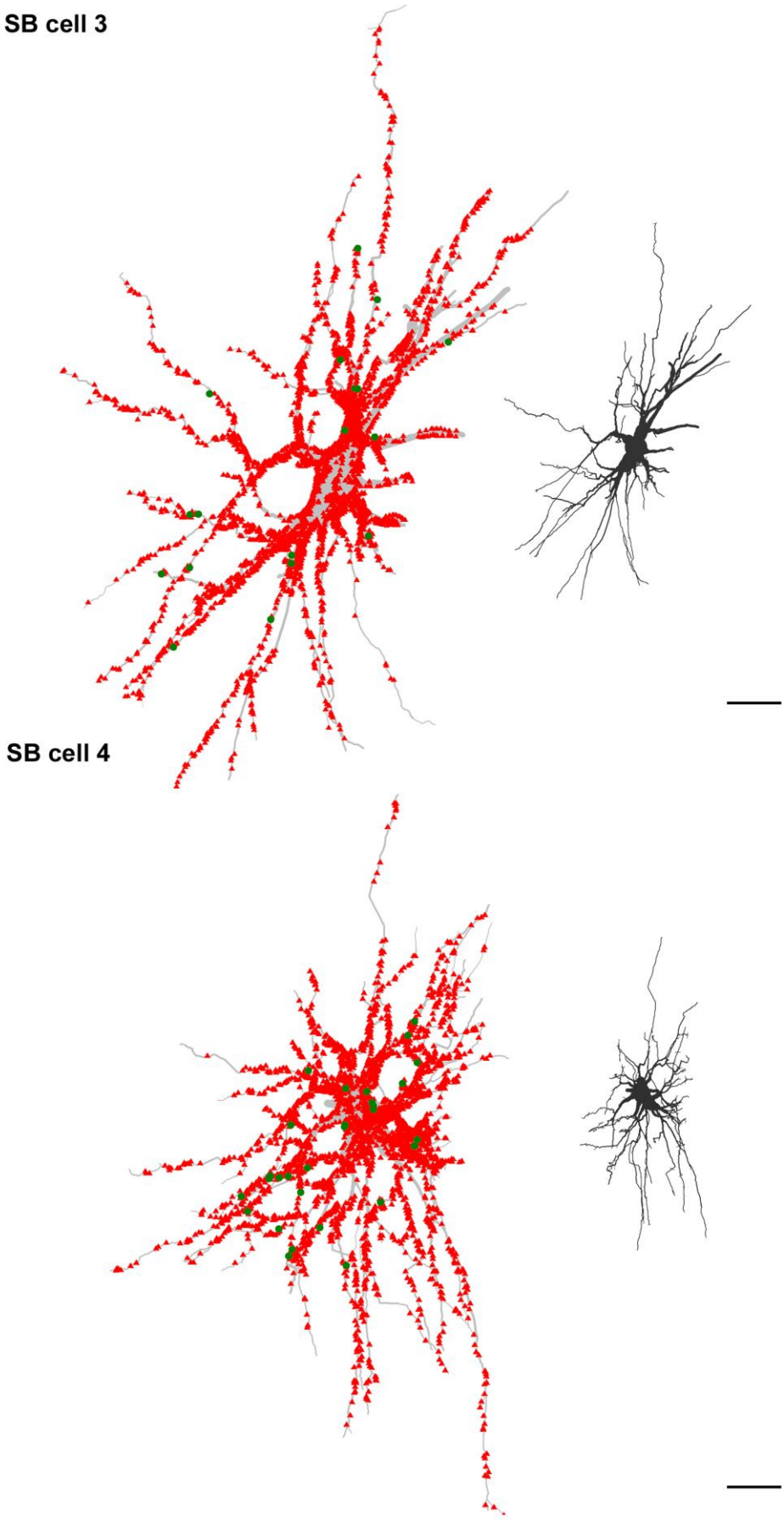
SB cell 3
SB cell 4

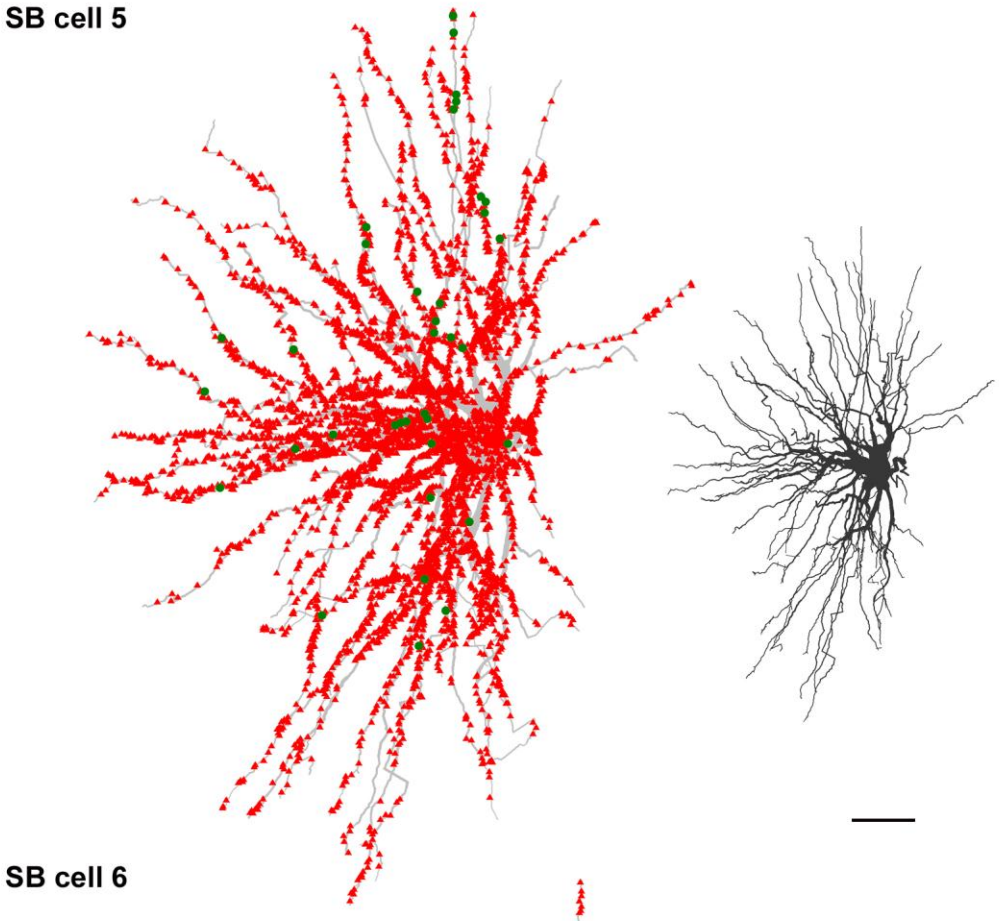
SB cell 5

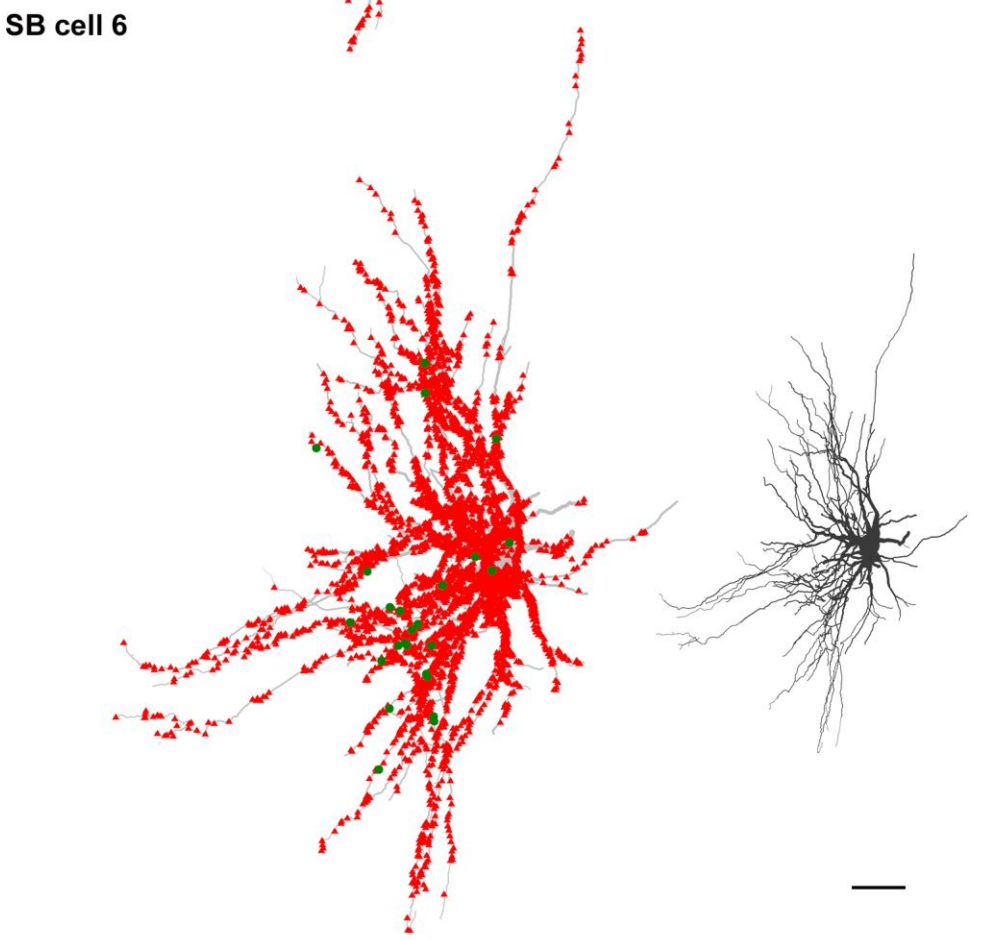
SB cell 6

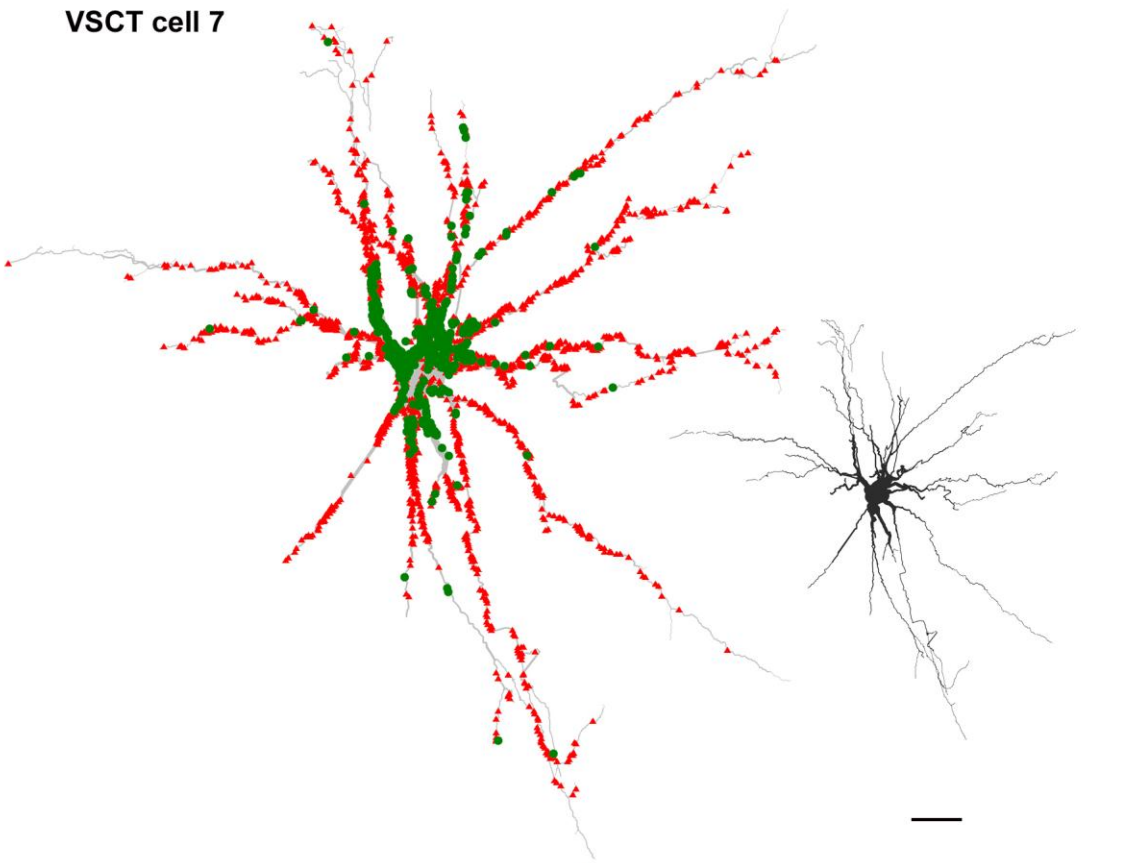
VSCT cell 7

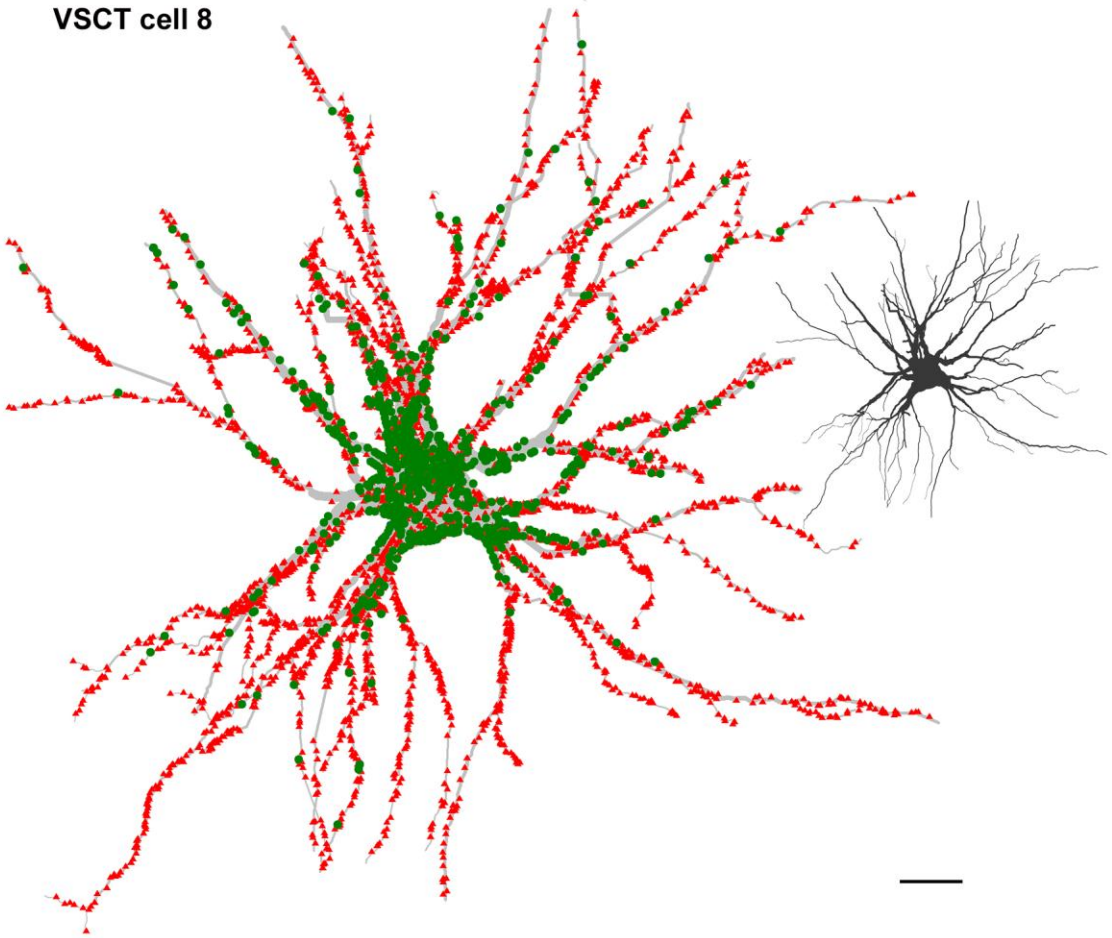
VSCT cell 8

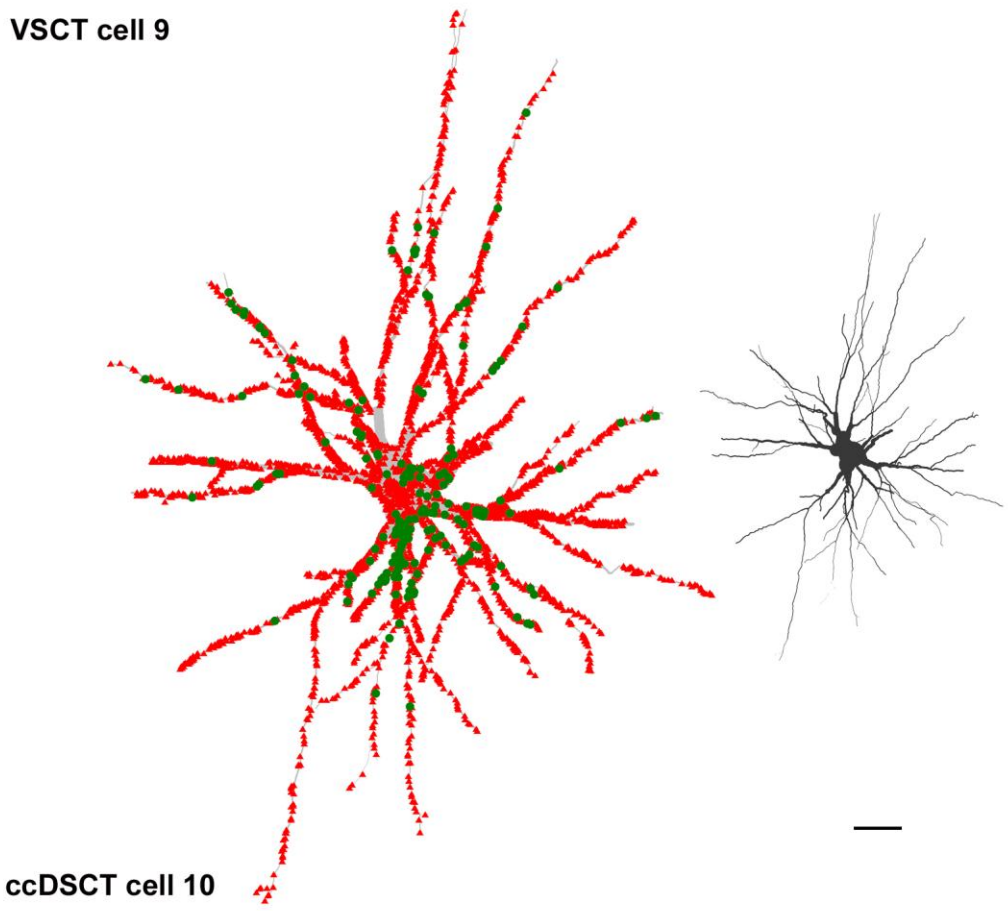
VSCT cell 9
ccDSCT cell 10

ccDSCT cell 11

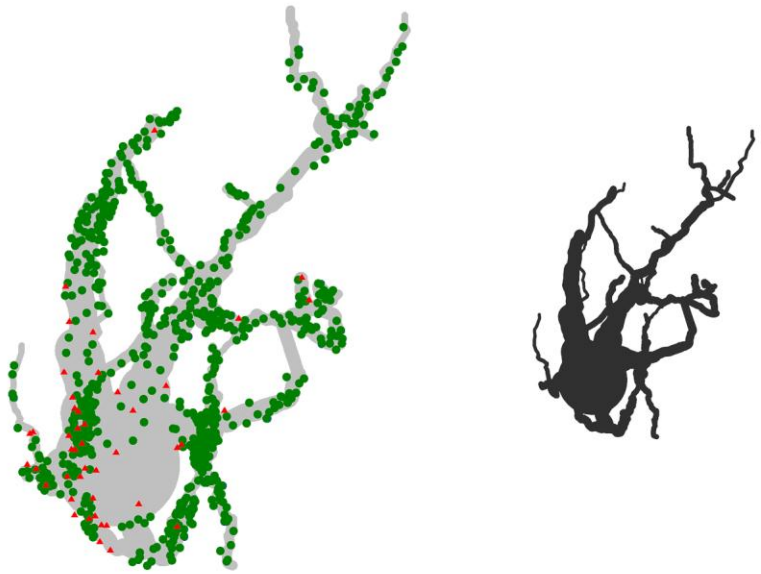

ccDSCT cell 12

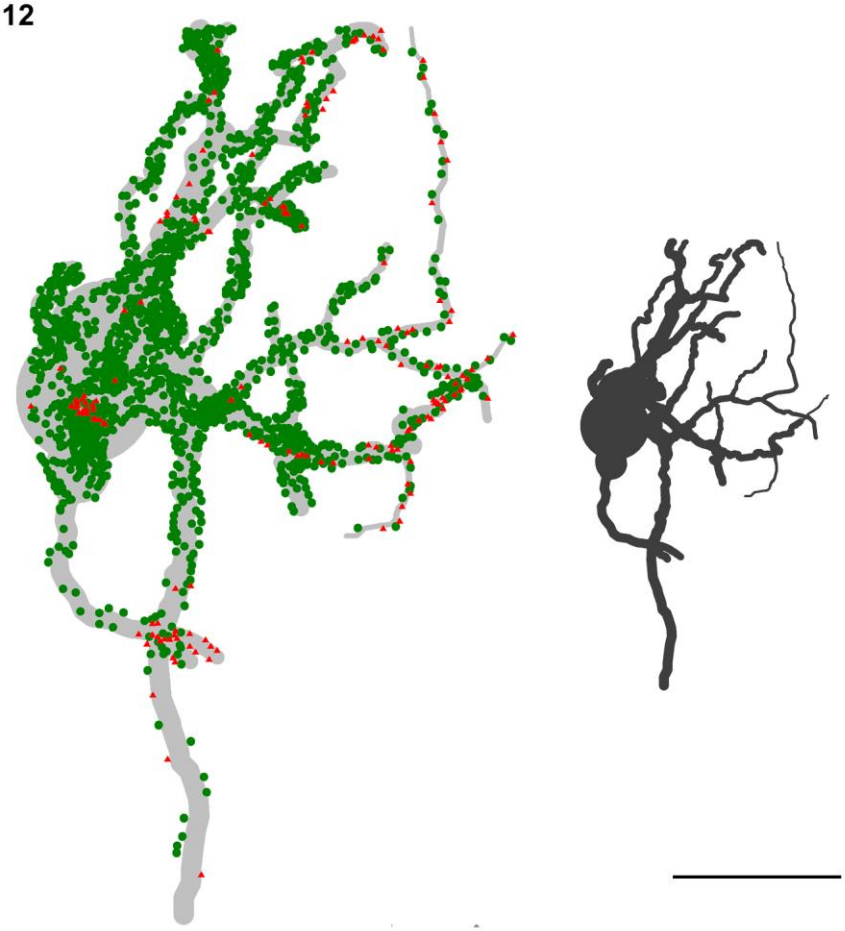

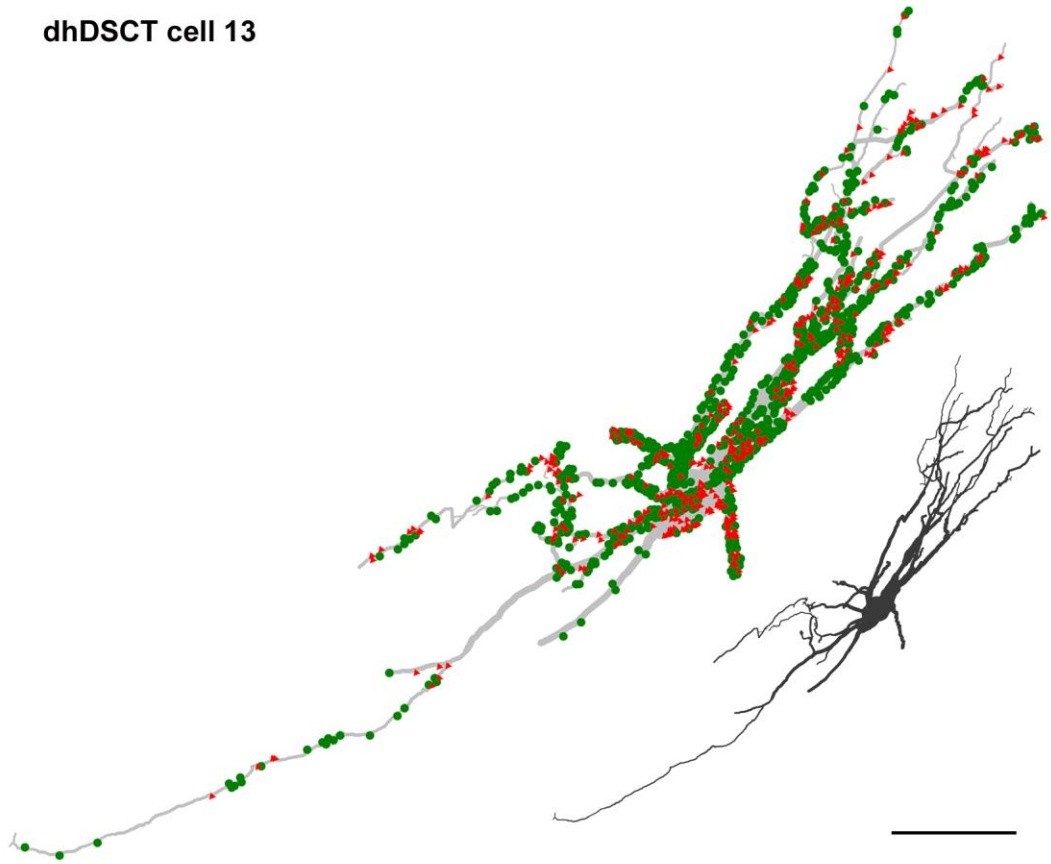
dhDSCT cell 13

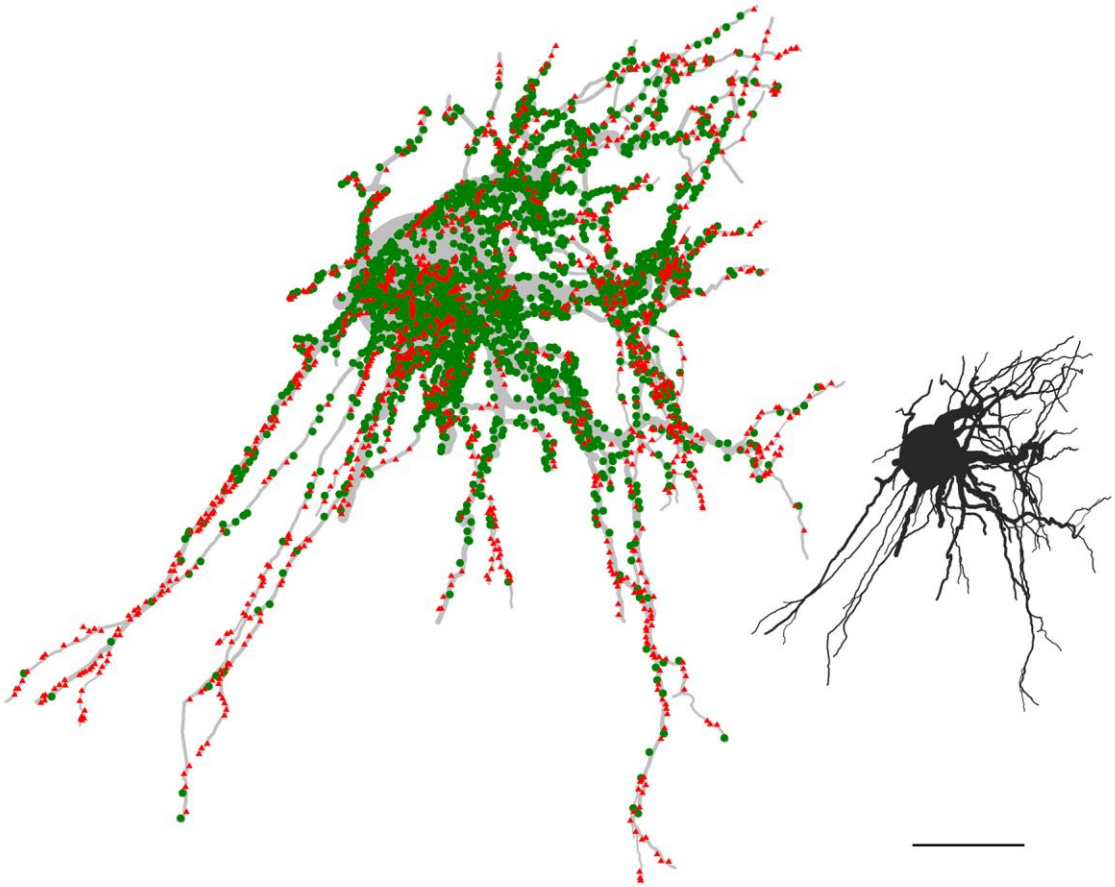
dhDSCT cell 14

dhDSCT cell 15

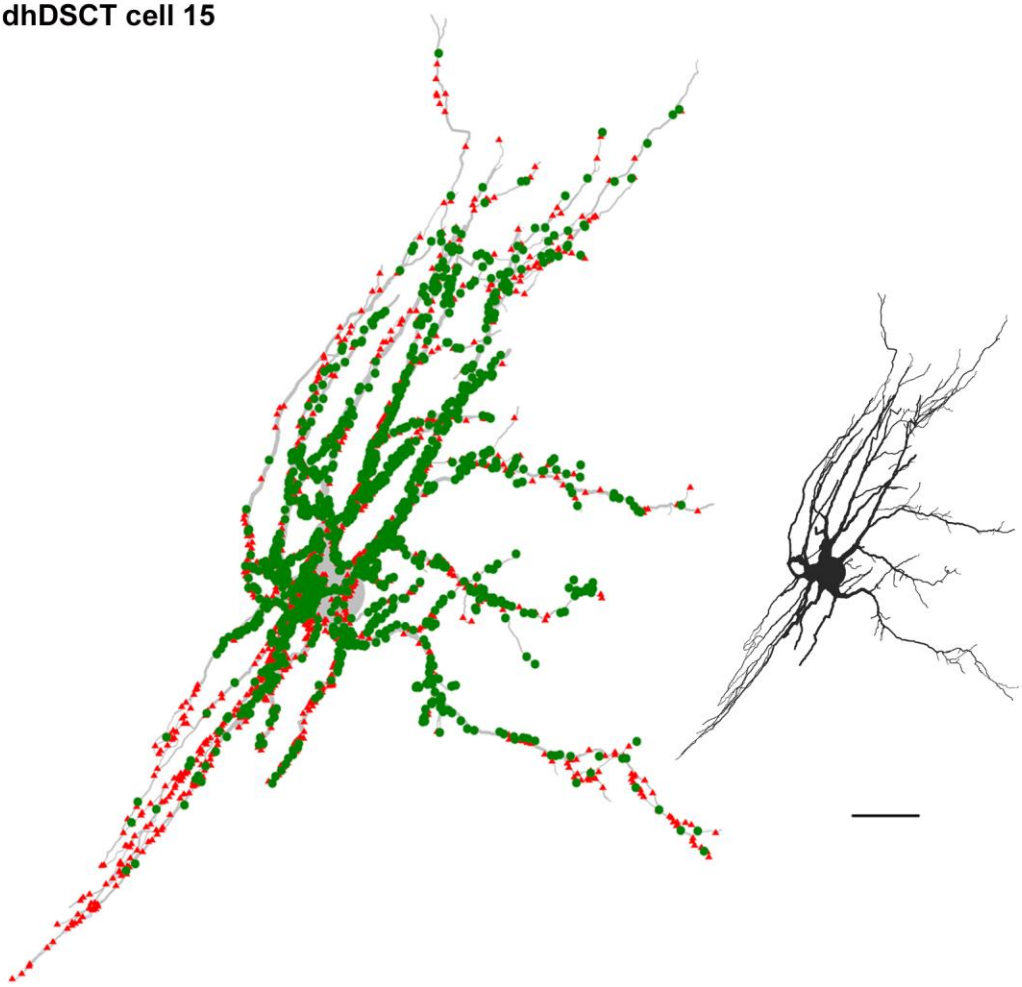

Figure 3-5 Comparison between the contact density of VGLUT1 and VGLUT2 axon terminals in different populations of spinocerebellar tract neurons

***A*,** Differences in the overall contact density of VGLUT1 terminals/ 100 μm^2 for the four different populations of spinocerebellar tract neurons in the cat. The contact density in ccDSCT neurons is significantly different from that on dhDSCT neurons ($p < 0.01$), VSCT neurons ($p < 0.001$) and SB neurons ($p < 0.001$). Similarly, the overall contact density on dhDSCT neurons is significantly different from that of VSCT neurons ($p < 0.001$) and SB neurons ($p < 0.001$). ***B*,** Differences in the contact density of VGLUT2 terminals/100 μm^2 in different populations of spinocerebellar tract neurons in the cat. The contact density in SB neurons is significantly different than in VSCT ($p < 0.05$), dhDSCT ($p < 0.001$) and ccDSCT ($p < 0.001$) neurons. The contact density on VSCT neuron is also significantly different from dhDSCT ($p < 0.05$) and ccDSCT ($p < 0.001$) neurons. All experiments were carried out in 6 cats (23 cells). Data presented as mean ± SD. ***C*,** Differences in the overall contact density of VGLUT1 terminals/ 100 μm^2 in four different populations of spinocerebellar tract neurons in the rat. The contact density in the ccDSCT neurons is significantly different from that on dhDSCT neurons ($p < 0.001$), VSCT neurons ($p < 0.001$) and SB neurons ($p < 0.001$). ***D*,** Differences in the contact density of VGLUT2 terminals/100 μm^2 in different populations of spinocerebellar tract neurons in the rat. The contact density in SB neurons is significantly different than in dhDSCT ($p < 0.05$) and ccDSCT ($p < 0.05$) neurons. All experiments were carried out in 4 rats (80 cells). Data presented as mean ± SD. * denotes $p < 0.05$; ** denotes $p<0.01$ and *** denotes $p < 0.001$.

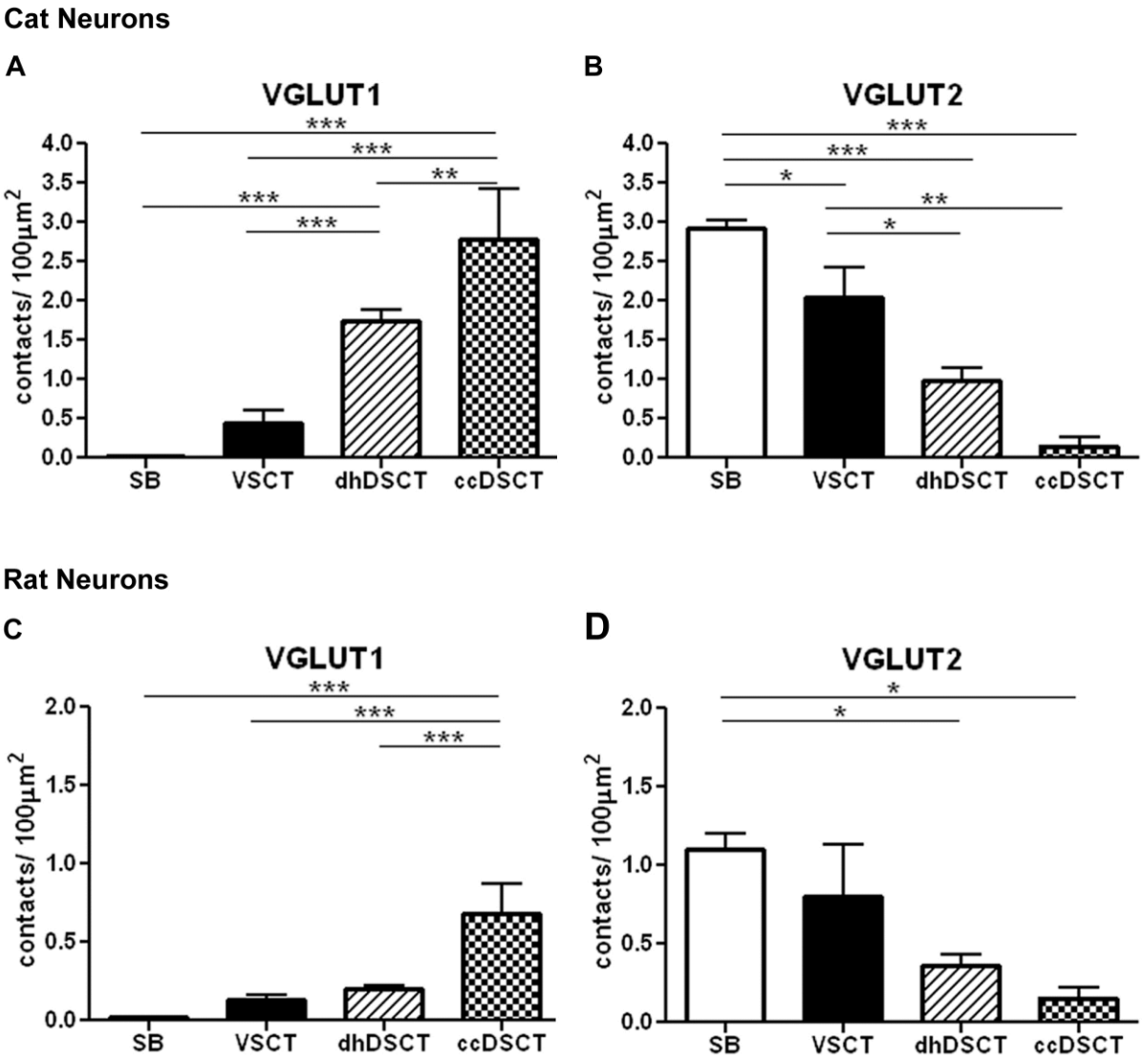
Cat Neurons
A
VGLUT1
contacts/ 100µm2
SB
VSCT
dhDSCT
ccDSCT
B
VGLUT2
Rat Neurons
C
VGLUT1
D
VGLUT2

Figure 3-6 Bar charts derived from Sholl analysis

Comparison of the mean numbers of VGLUT1 and VGLUT2 terminals forming contacts with different populations of intracellularly labelled spinocerebellar tract neurons ***A*****,** SB neurons (cells 1 to 6), ***B*****,** VSCT neurons (cells 7 to 9 and cell a & b), ***C*****,** ccDSCT neurons (cells 10 to 12 and cells c to e) and ***D***, dhDSCT neurons (cells 13 to 15 and cells f to h). The plots show the mean numbers of contacts per 100 µm of dendritic length contained within concentric spheres with radii which increase in 25 µm from the centre of the cell body. Bars represent the standard deviations.

A. SB

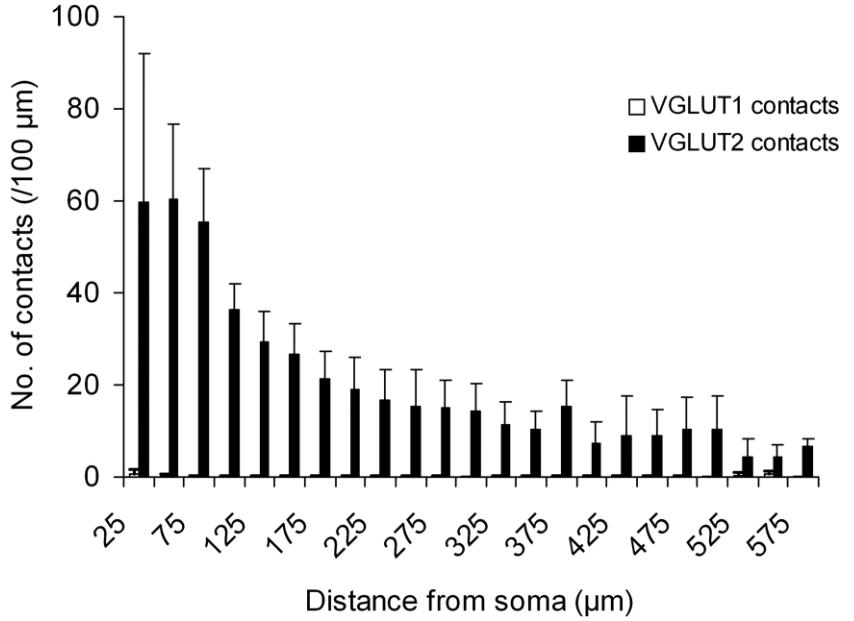
100
80
60
40
20
0
No. of contacts (/100 µm)
VGLUT1 contacts
VGLUT2 contacts
25
75
125
175
225
275
325
375
425
475
525
575
Distance from soma (µm)

B. VSCT

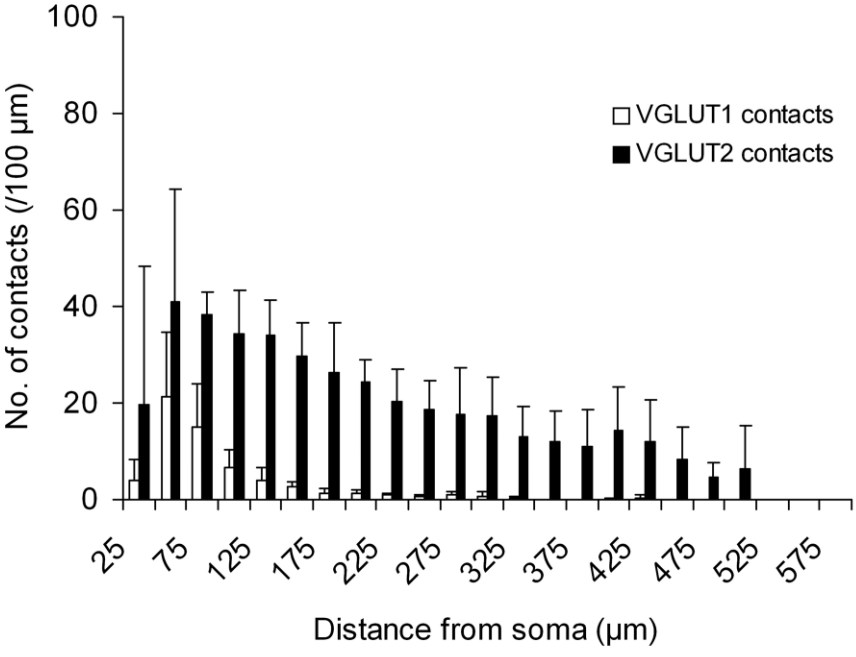
100
80
60
40
20
0
No. of contacts (/100 µm)
VGLUT1 contacts
VGLUT2 contacts
25
75
125
175
225
275
325
375
425
475
525
575
Distance from soma (µm)

C. ccDSCT

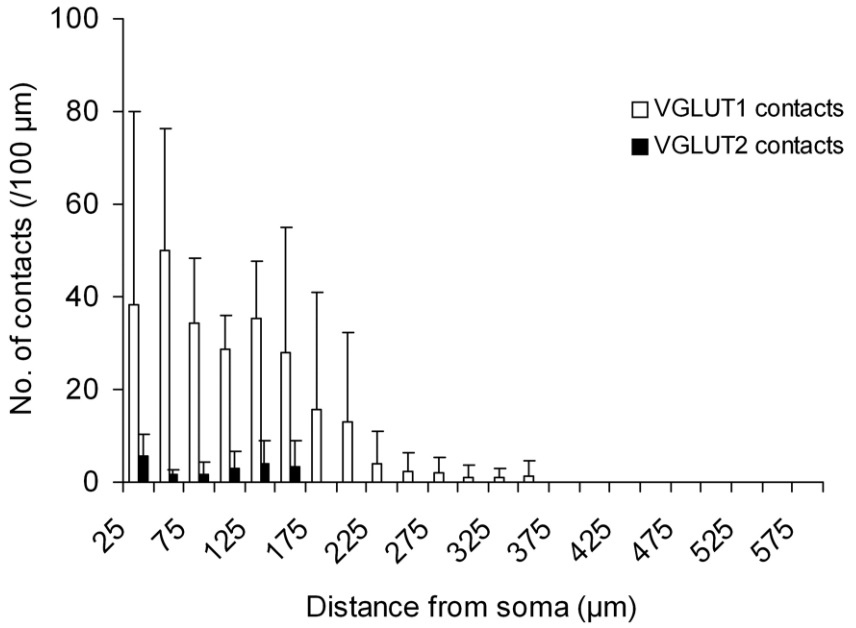

D. dhDSCT

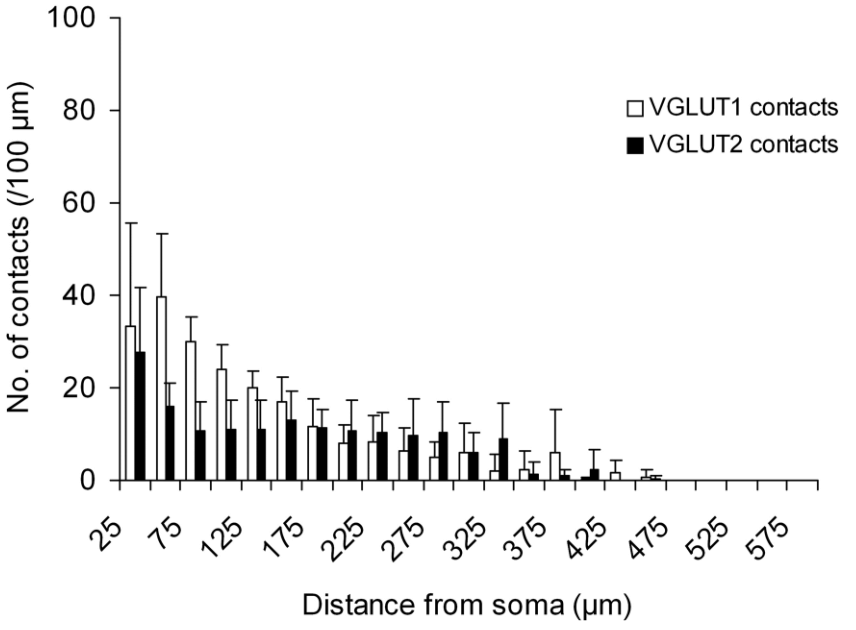

Figure 3-7 Photomicrograph and reconstruction of a representative section of the rat brain illustrating an injection site in the cerebellum

A*,** A photomicrograph of a coronal section of the rat brain showing an injection site in the cerebellum. ***B-E*,** Reconstruction of the injection sites for all 4 animals. The black shaded area shows the CTb injection site and the grey shaded area shows the maximum spread of the CTb projected on a schematic drawing based on the atlas of Paxinos and Watson (1997). Scale bar in ***A 100 µm.

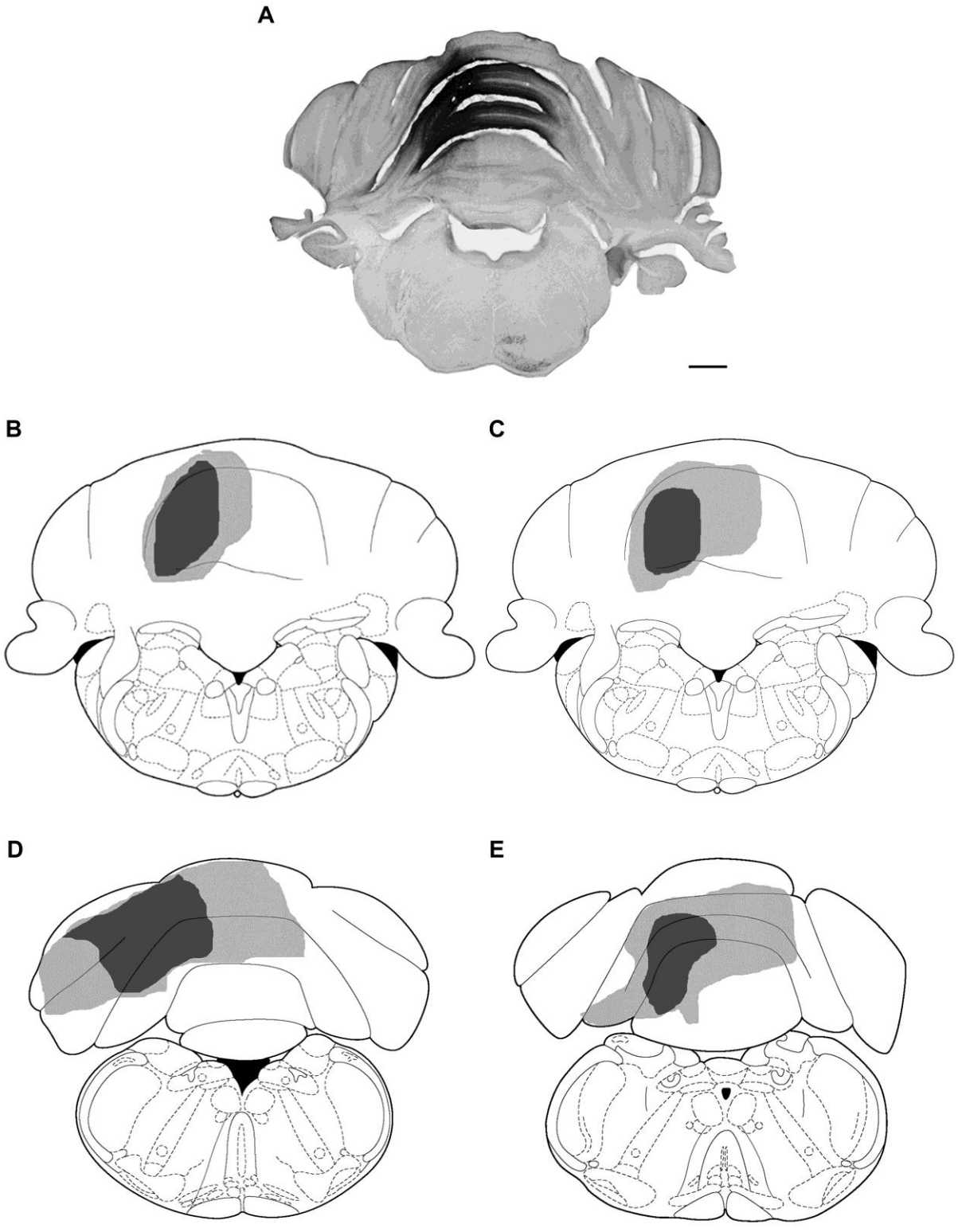
A
B
C
D
E

Figure 3-8 Locations of 80 analysed spinocerebellar tract neurons labelled retrogradely

A*,** A photomicrograph of a transverse section of the L3 segment of the rat spinal cord showing the location of one of the SB neurons (1), VSCT neurons (2) and dhDSCT neurons (3) identified by retrograde transport of CTb. ***B & C*,** Diagrams illustrating the locations of cell bodies of 80 cells analysed in the Th12 and Th13 segments and L1, L2 and L3 segments respectively. Scale bar in ***A 200 μm.

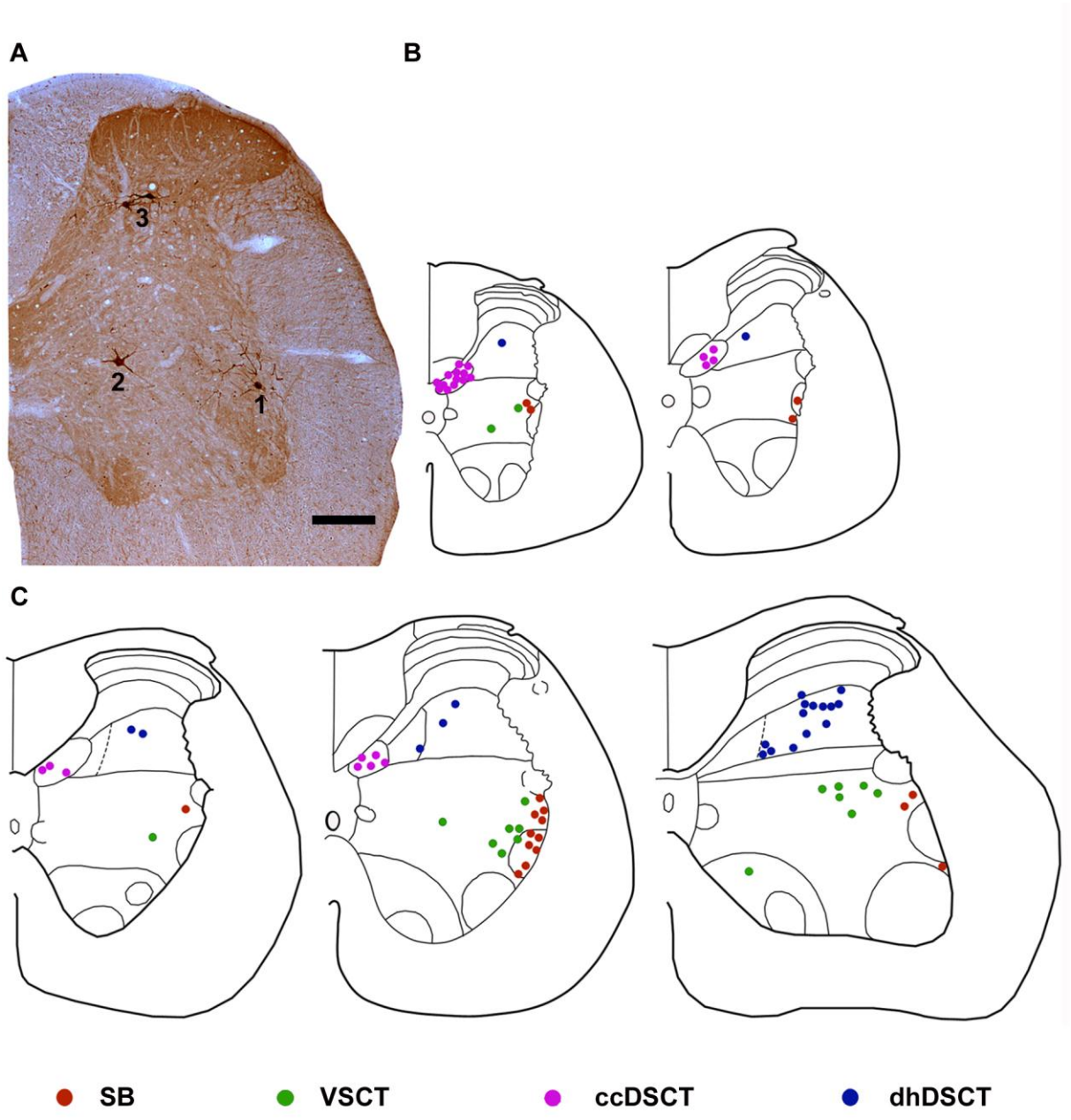
A
B
3
2
1
C
SB
VSCT
ccDSCT
dhDSCT

Figure 3-9 Immunohistochemical characteristics of VGLUT1 and VGLUT2 axon terminals in contact with retrogradely labelled rat spinocerebellar tract neurons

A1-A4; B1-B4; C1-C4 and D1-D4, Single optical sections through the cell bodies of representative SB, VSCT, ccDSCT and dhDSCT neurons illustrating the contacts made by VGLUT1 (blue) and VGLUT2 (green) immunoreactive terminals indicated by arrow heads and arrows respectively. The cell body and dendrites of retrogradely labelled cells are in red. Note differences in the density of VGLUT1 and VGLUT2 immunoreactive terminals within different regions of the grey matter shown in ***A-D*** and especially the high density of VGLUT1 and low density of VGLUT2 within Clarke's column shown in ***C***. Scale bar in ***A-D*** = 10 μm.

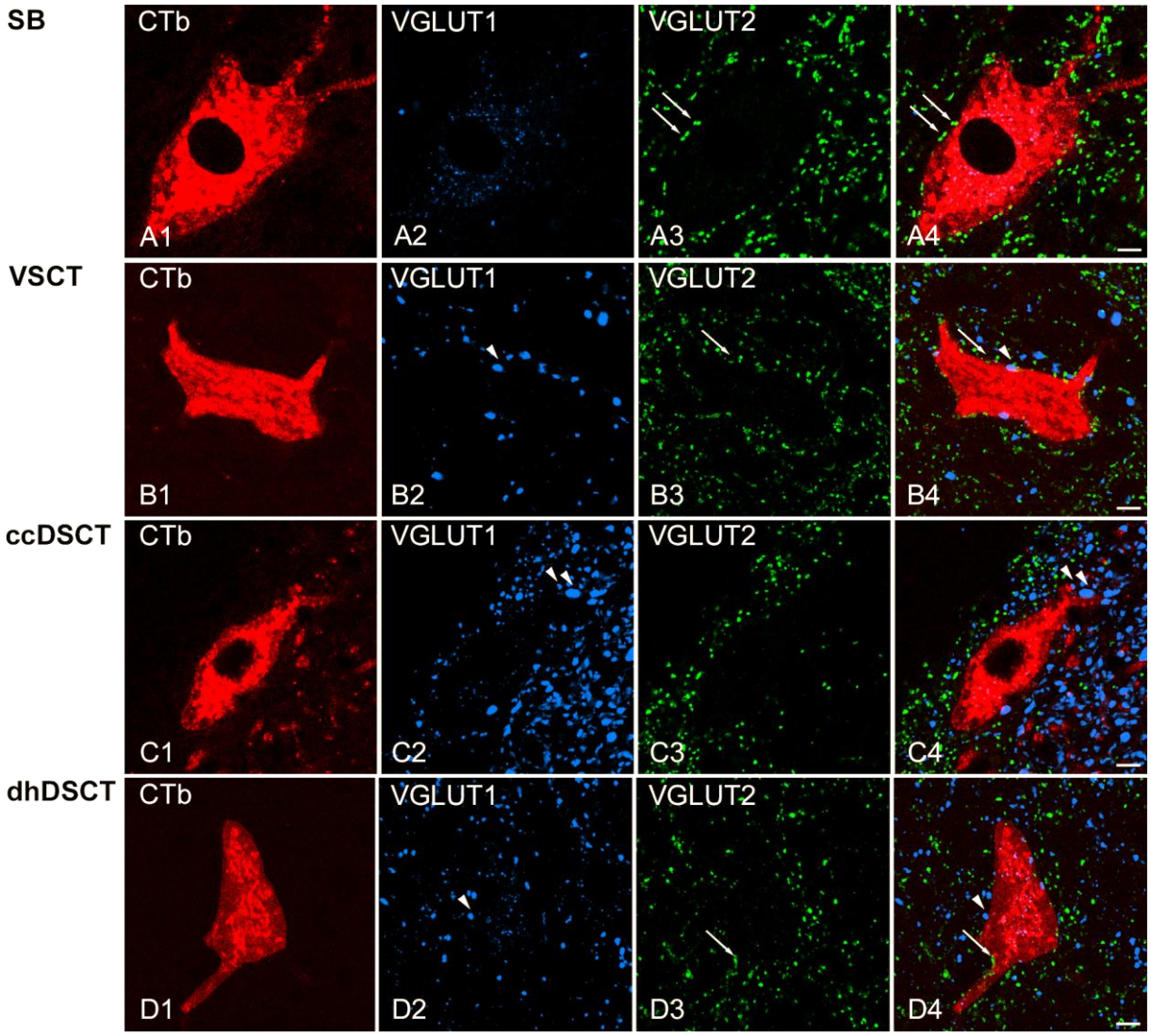
SB
CTb
VGLUT1
VGLUT2
A1
A2
A3
A4
VSCT
CTb
VGLUT1
VGLUT2
B1
B2
B3
B4
ccDSCT
CTb
VGLUT1
VGLUT2
C1
C2
C3
C4
dhDSCT
CTb
VGLUT1
VGLUT2
D1
D2
D3
D4

Table 3-2 The number and densities of VGLUT1 and VGLUT2 axon terminals in apposition with the cell bodies and dendrites of different populations of intracellularly labelled spinocerebellar tract neurons in cats

Populations of Spinocerebellar tract neurons	Cell	Contacts (total number)		Soma					Dendrite					
				Contacts (n)		Surface area (μm^2)	Density (n/ 100 µm2)		Contacts (n)		Total dendritic length (µm)	Surface area (μm^2)	Density (n/ 100 µm2)	
		VGLUT1	VGLUT2	VGLUT1	VGLUT2		VGLUT1	VGLUT2	VGLUT1	VGLUT2			VGLUT1	VGLUT2
SB														
	Cell 1	43	4413	5	148	14214.43	0.04	1.04	38	4265	15639.80	137176.29	0.03	3.11
	Cell 2	52	5006	0	85	22147.44	0.00	0.38	52	4921	13857.60	135472.01	0.04	3.63
	Cell 3	18	3461	0	119	18231.61	0.00	0.65	18	3342	10494.30	117120.97	0.02	2.85
	Cell 4	29	3350	4	127	10151.65	0.04	1.25	25	3223	12178.20	95415.10	0.03	3.38
	Cell 5	36	4998	0	140	11333.18	0.00	1.24	36	4858	21372.70	171956.71	0.02	2.83
	Cell 6	25	4605	0	170	9853.31	0.00	1.73	25	4435	17415.00	145863.22	0.02	3.04
Mean							**0.01**	**1.05**					**0.02**	**3.14**
SD							**0.02**	**0.48**					**0.01**	**0.31**
VSCT														
	Cell 7	451	2057	24	20	15813.27	0.15	0.13	427	2037	10821.80	88947.60	0.48	2.29
	Cell 8	843	3731	110	208	23494.96	0.47	0.89	733	3523	16532.80	237681.10	0.31	1.48
	Cell 9	185	4132	5	90	14158.38	0.04	0.64	180	4042	1894.50	136782.27	0.13	2.96
	Cell a*	627	–	36	–	14947.19	0.24	–	591	–	4874	53863.5	1.10	–
	Cell b*	489	–	25	–	18555.2	0.13	–	464	–	7102.7	108068	0.43	–
Mean							**0.21**	**0.55**					**0.49**	**2.24**
SD							**0.16**	**0.39**					**0.37**	**0.74**
ccDSCT														
	Cell 10	1213	24	27	2	10804.80	0.25	0.02	1186	22	2504.90	44898.72	2.64	0.05
	Cell 11	721	45	6	5	4567.81	0.13	0.11	715	40	2166.70	25711.70	2.78	0.16
	Cell 12	1708	162	85	1	9317.87	0.91	0.01	1623	161	2805.50	53763.82	3.02	0.30
	Cell b*	1245	–	44	–	5859.13	0.75	–	1201	–	2188.9	25757.44	4.66	–
	Cell c*	1355	–	86	–	7118.77	1.21	–	1259	–	3624.5	49684.52	2.53	–
	Cell d*	3049	–	124	–	15951.52	0.78	–	1570	–	7667.2	82986.78	1.89	–
Mean							**0.67**	**0.05**					**2.92**	**0.17**
SD							**0.41**	**0.05**					**0.93**	**0.13**
dhDSCT														
	Cell 13	1082	403	7	29	6404.21	0.11	0.45	1075	374	5630.80	55767.37	1.93	0.67
	Cell 14	2276	1211	267	90	14347.69	1.86	0.63	2009	1121	9198.60	90628.60	2.22	1.24
	Cell 15	1291	1274	52	111	12466.69	0.42	0.89	1239	1163	10979.20	98521.86	1.26	1.18
	Cell e*	1137	–	33	–	10127.78	0.33	–	1104	–	6016.4	56847.3	1.94	–
	Cell f*	2221	–	120	–	16828.68	0.71	–	2094	–	8841.8	98492.42	2.13	–
	Cell g*	2058	–	39	–	16924.57	0.23	–	2019	–	9829.3	100458.97	2.01	–
Mean							**0.61**	**0.66**					**1.91**	**1.03**
SD							**0.65**	**0.22**					**0.34**	**0.31**

* Neurons analysed for VGLUT1 only.

Table 3-3 The number and densities of VGLUT1 and VGLUT2 axon terminals in apposition with the cell bodies and dendrites of different populations of retrogradely labelled spinocerebellar tract neurons in rats

Populations of Spinocerebellar tract neurons	Animal	No. of Cells	Contacts (total number)		Soma					Dendrite					
					Contacts (n)		Surface area (μm^2)	Density (n/ 100 µm2)		Contacts (n)		Total dendritic length (µm)	Surface area (μm^2)	Density (n/ 100 µm2)	
			VGLUT1	VGLUT2	VGLUT1	VGLUT2		VGLUT1	VGLUT2	VGLUT1	VGLUT2			VGLUT1	VGLUT2
SB															
	Rat 1	3	2	126	1	20	6859.79	0.01	0.29	1	106	374.00	5050.97	0.02	2.10
	Rat 2	3	1	71	1	17	3766.96	0.03	0.45	0	54	107.70	2018.07	0.00	2.68
	Rat 3	7	2	125	1	36	7070.03	0.01	0.51	1	89	155.51	3769.65	0.03	2.36
	Rat 4	5	0	123	0	40	6755.2	0.00	0.59	0	83	136.24	3166.41	0.00	2.62
Mean								**0.01**	**0.46**					**0.01**	**2.44**
SD								**0.01**	**0.13**					**0.01**	**0.27**
VSCT															
	Rat 1	4	24	52	10	11	7015.04	0.14	0.16	14	41	260.63	6875.58	0.20	0.60
	Rat 2	4	8	39	2	5	5004.42	0.04	0.10	6	34	267.05	5277.05	0.11	0.64
	Rat 3	3	2	94	1	33	5448.27	0.02	0.61	1	61	130.17	2857.12	0.04	2.14
	Rat 4	6	6	112	2	23	4860.67	0.04	0.47	4	89	207.18	3987.45	0.10	2.23
Mean								**0.06**	**0.33**					**0.11**	**1.40**
SD								**0.06**	**0.24**					**0.07**	**0.90**
ccDSCT															
	Rat 1	5	39	6	12	2	4602.70	0.26	0.04	27	4	107.74	3436.65	0.79	0.12
	Rat 2	7	31	8	12	3	2740.30	0.44	0.11	19	5	118.94	1939.90	0.98	0.26
	Rat 3	5	40	10	17	4	3004.15	0.57	0.13	23	6	51.14	1186.31	1.94	0.51
	Rat 4	7	37	6	8	2	3341.03	0.24	0.06	29	4	85.89	1723.13	1.68	0.23
Mean								**0.38**	**0.09**					**1.35**	**0.28**
SD								**0.15**	**0.04**					**0.55**	**0.16**
dhDSCT															
	Rat 1	5	17	18	6	7	4208.02	0.14	0.17	11	11	172.58	4285.35	0.26	0.26
	Rat 2	7	6	10	1	2	1812.43	0.06	0.11	5	8	110.40	1498.88	0.33	0.53
	Rat 3	6	11	25	2	5	2504.78	0.08	0.20	9	20	127.80	2454.00	0.37	0.81
	Rat 4	3	4	15	1	4	2229.03	0.04	0.18	3	11	80.6	1816.72	0.17	0.61
Mean								**0.08**	**0.16**					**0.28**	**0.55**
SD								**0.04**	**0.04**					**0.09**	**0.23**

3.4 Discussion

The major finding of the present study was significant differences in patterns of excitatory axonal contacts on four populations of spinocerebellar tract neurons in cats and rats as summarised in Table 3-2, 3-3 and Figure 3-5.

It is well established that VGLUT1 and VGLUT2 are the transporters which are present in the axons of glutamatergic neurons within the spinal cord and that all myelinated primary afferent terminals in the grey matter of lumbar spinal cord, with the exception of those in lamina I, express VGLUT1 (Varoqui *et al.,* 2002; Todd *et al.,* 2003; Alvarez *et al.,* 2004). Terminals of spinal interneurons and most glutamatergic descending tract neurons express VGLUT2; the exception to this is the CST which contains VGLUT1 only (A. Du Beau, S. Shakya Shrestha and D. J. Maxwell, In press). Hence, the results of the present study substantiate the conclusion based on electrophysiological experiments (see Introduction) that SB neurons receive direct input mainly from intraspinal and supraspinal neurons. In contrast negligible or weak input via VGLUT2 immunoreactive terminals to ccDSCT neurons in the cat makes it unlikely that these neurons receive major input from non-primary afferent excitatory neurons, with the possible exception of CS neurons (Hantman and Jessell, 2010). The results of the current study also indicate that differences in input from primary afferents and from other excitatory intraspinal and supraspinal neurons to VSCT and dhDSCT neurons are much less marked and therefore may have equally powerful actions on these cells.

3.4.1 Methodological issues

The numbers of spinocerebellar tract neurons of the four kinds on which the analysis is based in this study are small but the sample of these neurons can be considered to be sufficiently representative because significant differences were found between each type while properties of neurons within them were reasonably consistent. The differences between the four types of spinocerebellar tract neurons were both qualitative and quantitative. Qualitative differences in the presence or absence and in the distribution of VGLUT1 and VGLUT2 positive terminals

illustrated in Figures 3-4 and 3-6 are in fact so striking that they hardly require quantitative analysis to substantiate them. The comparison of numbers of VGLUT1 and VGLUT2 positive terminals on SB and VSCT neurons (cats; Table 3-2, rats; Table 3-3 and Figure 3-5) accordingly showed very highly significant differences between them. Highly significant differences were also found between numbers of VGLUT1 or VGLUT2 positive terminals in contact with VSCT and DSCT neurons.

Criteria for classification on the basis of coupling between primary afferents and selected spinocerebellar tract neurons and according to anatomical location in the lumbar grey matter also require some comments. Properties of main populations of spinocerebellar tract neurons were previously outlined in electrophysiological and morphological studies in the cat. Using this knowledge individual neurons encountered during electrophysiological exploration of the spinal cord could reliably be classified into one of these populations. In addition it was possible to select subpopulations within a given group, in particular a subpopulation of SB cells with dominant inhibitory input from peripheral afferents and monosynaptic input from RetST neurons (Burke *et al.*, 1971a; Jankowska *et al.*, 2010; Hammar *et al.*, 2011) and subsequent verification of location and morphology of the labelled neurons fully confirmed original classifications.

The density of contacts on cat spinocerebellar tract cells was generally 3-4 times higher than that associated with rat cells. Whilst the reason for this difference is unclear at least part of the explanation is the incomplete labelling of dendritic arbors of retrogradely labelled cells. Sholl analysis of contacts on dendrites of cat neurons reveals that even the most distal parts of the dendrites are associated with substantial numbers of VGLUT1 and/or VGLUT2 terminals (see below). As the surface area of the dendrites is small, the mean values of contact densities will therefore be higher in the cat. Contact densities on rat dendrites were found to be considerably lower than those associated with cat dendrites whereas contact densities on cell bodies of both species were similar (see Tables 3-2 and 3-3). Nevertheless differences have been also found in the densities of contacts on the soma; for example rat dhDSCT somata had considerably lower densities for VGLUT1 and VGLUT2 when compared with their cat counterparts. It should be noted that

cell bodies of all types of rat spinocerebellar tract neurons are smaller than those in the cat and therefore they may require less excitatory drive to activate them.

3.4.2 Different excitatory axonal contact pattern on different populations of spinocerebellar tract neurons

3.4.2.1 SB and VSCT neurons

Morphological analysis in the present study revealed that VSCT neurons have much higher numbers of contacts from VGLUT1 immunoreactive terminals than SB neurons in both cats and rats. They also show that there are no reasons to assume that SB neurons with dominating inhibitory input from low threshold afferent fibres in the main branches of the sciatic nerve might receive direct excitatory input from higher threshold afferents in the same nerves or from afferent fibres from other parts of the body (e.g. from the most distal or most proximal parts of the limbs or from trunk that were not tested; see section 3.1).

However, this conclusion may be valid only for a fraction of feline SB neurons located in the L3-L4 segments where only IPSPs can be evoked from stimulated muscle nerves (Burke *et al.*, 1971; Jankowska *et al.*, 2010; Hammar *et al.*, 2011). As a higher proportion of more caudally located SB neurons were found to be monosynaptically excited by group I afferents (Burke *et al.*, 1971), a greater density of VGLUT1 positive terminals would be predicted to be present on these neurons.

Differences in direct input from primary afferents are also relevant to the problem of subdivision of VSCT neurons into SB and more medially located subpopulations (see section 3.1). The borderlines between these subpopulations are not very sharp, whether in terms of location or of synaptic input predominantly from group Ib or group Ia afferents, but the present results support this functional subdivision and are compatible with differential activation of VSCT and SB neurons and their proposed functions (Lundberg, 1971; Hammar *et al.*, 2011) as well as their differential projections to the cerebellum (Matsushita and Ikeda, 1980; Matsushita and Hosoya, 1982; Matsushita and Yaginuma, 1989).

The number of VGLUT2 terminals in contact with VSCT and SB neurons likewise differed, both in the cat and in the rat, but the reasons for this difference are less clear. Previous electrophysiological studies have revealed that both SB and VSCT neurons are sometimes di- and poly- synaptically excited from muscle, tendon organ and cutaneous afferents (Eccles *et al.*, 1961a; Lundberg and Oscarsson, 1962; Lundberg, 1971) so that VGLUT2 terminals could originate from excitatory interneurons mediating indirect actions of peripheral afferents upon these neurons. Eccles *et al.* (1961a) have shown that the polysynaptic EPSPs from FRA are much more common in SB neurons than in Ib VSCT neurons. The finding of the present study in context of SB neurons is highly consistent with findings of Eccles *et al.* (1961a) showing majority of inputs from VGLUT2 expressing terminals. Recently, it has been shown that disynaptic EPSPs in VSCT neurons including SB neurons are mediated by collateral actions of excitatory premotor interneurons with input from group I/ II afferents (Jankowska *et al.*, 2010). Therefore, these premotor interneurons are also likely to be the source of VGLUT2 terminals on these neurons. However, descending tract fibres provide direct excitatory input to both SB and VSCT neurons (Baldissera and ten Bruggencate, 1976; Hammar *et al.*, 2011) and could be another source of VGLUT2 immunoreactive terminals (A. Du Beau, S. Shakya Shrestha and D. J. Maxwell, In press). Excitatory interneurons contacting SB and VSCT neurons might include interneurons located in the intermediate zone with group I/II inputs and ipsilateral terminations outside motor nuclei in addition to those within motoneuron pools (Bannatyne *et al.*, 2009). Another potential source of VGLUT2 contacts might be the excitatory dorsal horn interneurons with group II inputs which were shown to have VGLUT2 expressing axons projecting to the intermediate zone (Bannatyne *et al.*, 2006). However, these interneurons are less likely to be involved in relaying indirect actions of RetS neurons because majority of contacts on them are made by VGLUT1 positive terminals and there are very few from VGLUT2 terminals, thus indicating that they receive inputs mainly from primary afferents (Liu *et al.*, 2010a). Indirect excitatory actions of RetS neurons are more likely to be mediated by lamina VIII commissural interneurons projecting to areas outside motor nuclei, including medial and lateral lamina VII and VIII which are known to have VGLUT2 immunoreactive terminals (Jankowska *et al.*, 2009).

3.4.2.2 Clarke´s column and dorsal horn DSCT neurons

Electrophysiological and morphological studies have established that two functionally distinct populations of cell form components of DSCT: ccDSCT and dhDSCT (Edgley and Jankowska, 1988; Bosco and Poppele, 2001), but that both receive strong monosynaptic input from primary afferents; ccDSCT neurons mainly from group I afferents (Eccles *et al.*, 1961b) and dhDSCT neurons from group II and cutaneous afferents (Edgley and Jankowska, 1988). Some disynaptic excitatory actions were also postulated (Eccles *et al.*, 1961b; Edgley and Jankowska, 1988; Krutki *et al.*, 2011). However, the paucity of VGLUT2 contacts on ccDSCT neurons makes it unlikely that any major excitatory input is provided to them by interneurons in neuronal pathways that have not been explored in electrophysiological experiments. This conclusion is consistent with the observations made by Krutki *et al.* (2011) who were able to evoke disynaptic EPSPs in dhDSCT cells but not in ccDSCT cells following stimulation applied within motor nuclei. Furthermore, the paucity of VGLUT2 contacts on ccDSCT neurons suggests that it is unlikely that they are involved to any major extent in processing information from supraspinal neurons with the exception of CS neurons which constitute an additional source of input to ccDSCT neurons at least in mice (Hantman and Jessell, 2010). Nevertheless, a small fraction of VGLUT2 contacts on ccDSCT neurons might have derived from RetS neurons as disynaptically evoked EPSPs following stimulation of descending RetS axons was revealed by Hammar and collegues (2011).

3.4.3 Differential distribution of VGLUT1 and VGLUT2 contacts

Sholl analysis in the intracellularly labelled cat neurons shown in Figure 3-6 reveals that VGLUT2 contacts were concentrated around proximal dendrites of SB and VSCT neurons whereas VGLUT1 contacts dominated on the proximal dendrites of DSCT neurons. There is limited information on distribution patterns of excitatory terminals associated with other spinal neurons. In a study by Liu *et al.* (2010a) on intermediate zone interneurons, it was found that VGLUT1 terminals predominated on both inhibitory and excitatory cells and were most concentrated around proximal

dendrites. Excitatory cells were almost devoid of VGLUT2 terminals whereas inhibitory cells had relatively low densities of VGLUT2 contacts that were evenly distributed throughout their dendritic trees. As a similar pattern of distribution was identified for VGLUT1 terminals in contact with DSCT cells, this may represent a pattern for primary afferent input. The consequences of the differential distribution of VGLUT1 and VGLUT2 contacts for the efficiency of synaptic actions evoked from different sources cannot be predicted until more is known about characteristics of the synaptic contacts and cable properties of dendrites of both ascending tract cells and interneurons in which such differences occur. However, one may expect different shape indices of EPSPs evoked at different distances from soma, including time to peak, half width, as well as the latency and amplitude, and differences in the linearity of summation and final effects on the spike generating region (Rall *et al.*, 1967; Rall, 1977; Korogod and Tyc-Dumont, 2010).

3.4.4 Functional considerations

The present findings provide a new basis for understanding the organization and functional connectivity of four populations of spinocerebellar tract neurons in the lumbar enlargement of the cat and in the thoraco-lumbar segments in the rat and strengthen previous indications of their functional differentiation. Putative excitatory connections of the four populations of neurons based on the present findings combined with information from previous studies are summarized in Figure 3-10.

Although, this simple circuit diagram has still uncovered functional circuitry mainly the inhibitory inputs to these particular groups of neurons, it can be interpreted to reasonable extent that the role of DSCT neurons is not limited to the integration of proprioceptive and extereoceptive sensory inputs. For instance, ccDSCT neurons also integrate cortical inputs (Hantman and Jessell, 2010) allowing predictions of the sensory consequences of motor acts from higher centres in anticipation of peripherally derived sensory feedback. However, very scarce input via VGLUT2 immunoreactive contacts in cats makes it unlikely that ccDSCT neurons are involved in relaying actions of intrinsic interneuronal networks. It is also unlikely that

rhythmic locomotor like activity reported in ccDSCT neurons (H. Hultborn, personal communication) can be attributed to actions of excitatory spinal networks. The current findings are in good agreement with the demonstration that VSCT neurons receive inputs from inhibitory premotor interneurons as well as sensory fibres and might therefore supply the cerebellum with information about activity in interneuronal pathways to motoneurons (Lundberg, 1971; Arshavsky *et al.*, 1972; Arshavsky *et al.*, 1984). They also provide convincing evidence that SB neurons, in which no excitatory actions are found from peripheral nerves, do indeed lack direct input from peripheral afferents. However, the considerable density of VGLUT2 immunoreactive contacts on VSCT and SB neurons is not matched by the widespread but relatively weak supraspinal input to them. Some intraspinal sources of excitatory input to these neurons have been discussed above, but many more would be expected. Lack of peripheral excitatory input to SB neurons has led to the conclusion that they forward information on spinal actions of descending commands depending on the degree of inhibition of motoneurons (Hammar *et al.*, 2011). This information as proposed by Hammar and her group (2011) can be of paramount importance in preventing errors in descending commands and thereby enabling the cerebellum to adjust these commands relayed by RetS neurons before errors are committed. However, even though the role of SB and VSCT neurons in monitoring actions of inhibitory premotor interneurons on motoneurons may be particularly important, excitatory inputs to these neurons mediated via yet undefined spinal neurons might likewise provide the cerebellum with important information.

In conclusion, although excitatory inputs to different populations of spinocerebellar tract neurons have been predicted on the basis of connections established in electrophysiological experiments, the existence of putative connectivity of these neurons has not been predicted morphologically. Therefore, the present study provides evidence that there are four different functional populations of spinocerebellar tract neurons relaying highly differentiated information to the cerebellum. If more about the connections between these neurons and different muscle and cutaneous afferents and interneurons interposed in different reflex pathways is known, this knowledge might be of particular importance to deepen understanding of motor control.

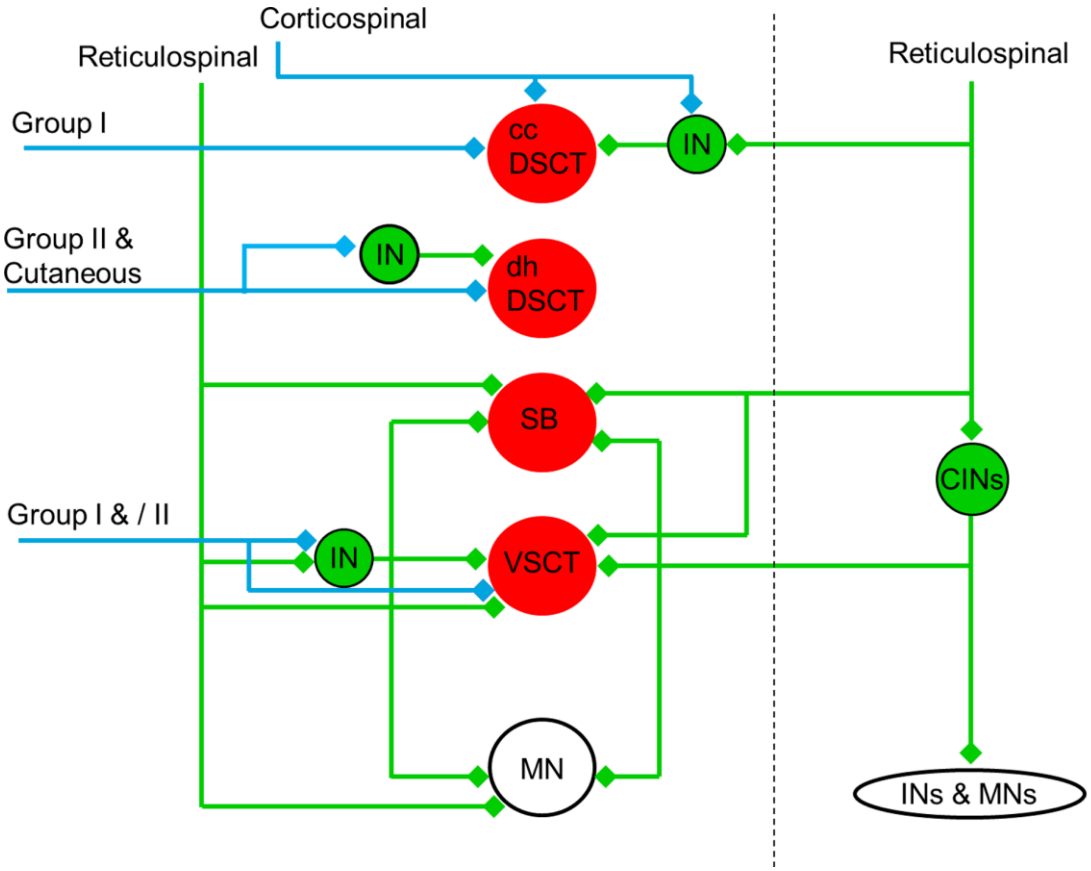

Figure 3-10 Putative excitatory contacts formed with the four different populations of lumbar spinocerebellar tract neurons

Red circles represent Clarke's column dorsal spinocerebellar tract neurons (ccDSCT); dorsal horn dorsal spinocerebellar tract neurons (dhDSCT), spinal border neurons (SB), Ib-ventral spinocerebellar tract neurons (VSCT). Green circles represent excitatory interneurons in reflex pathways to motoneurons (MN) activated by primary afferents and descending systems. Blue lines and diamonds represent neurons that express vesicular glutamate transporter 1 (VGLUT1) in their axon terminals. Green lines and diamonds represent neurons that express vesicular glutamate transporter 2 (VGLUT2) in their axon terminals. CINs, commissural interneurons; INs, interneurons; MNs, motoneurons.

4 Inhibitory inputs to four types of spinocerebellar tract neurons in the cat and the rat spinal cord

4.1 Introduction

It is well established that different populations of spinocerebellar tract neurons forward information from different sources (Oscarsson, 1965; Bosco and Poppele, 2001) to the cerebellum. This information is primarily provided by excitatory input which is modified by postsynaptic inhibition of various origins, as well as by presynaptic filtering. Previous studies have revealed that DSCT carries information about the peripheral events and VSCT primarily monitors the activity in spinal interneuronal pathways (Oscarsson, 1965; Bosco and Poppele, 2001). DSCT neurons, in addition to having fundamental role in integrating direct proprioceptive and exteroceptive information from periphery, are also under inhibitory control from muscle afferents. The strongest evidence to date is for the disynaptically evoked inhibition from both group Ia/ Ib muscle afferents and group II afferents (Lundberg and Oscarsson, 1960; Eccles *et al.*, 1961b; Hongo *et al.*, 1983b; Jankowska and Puczynska, 2008). More, recently, it has been demonstrated that this inhibition is direct action of premotor interneurons (Krutki *et al.*, 2011). However, in some spinocerebellar tract neurons inhibition may play a more essential role because a reduction or even arrest of firing in these neurons may be a source of information for their cerebellar target cells itself (Lundberg, 1971; Hammar *et al.*, 2011). This may apply particularly to the subpopulation of VSCT neurons in which peripheral input is mainly or almost exclusively inhibitory (Burke *et al.*, 1971a; Jankowska *et al.*, 2010; Shakya-Shrestha *et al.*, 2012). Postsynaptic and presynaptic inhibitory actions on various populations of spinocerebellar tract neurons may also vary as much as the excitatory ones, both in origin and degree (Burke *et al.*, 1971a; Lundberg and Weight, 1971; Edgley and Jankowska, 1988; Jankowska and Puczynska, 2008; Jankowska *et al.*, 2010; Krutki *et al.*, 2011). However, given the considerable number of studies on the diverse inhibitory input pattern of the different populations of spinocerebellar tract neurons, it is surprising that very little is known about the synaptic connections formed with these neurons. The aim

of the present study was therefore to supplement my previous investigation of excitatory input to four types of spinocerebellar tract neurons (Chapter 3) by making similar comparisons of inhibitory input to these neurons.

The first aim was to compare the number and the distribution of inhibitory (GABAergic and/ or glycinergic) and excitatory (glutamatergic) terminals in contact with these neuronal populations. This was done both on cat and rat neurons with a supplementary aim to compare these features in the two species. The second aim was to determine the proportion of contacts formed by glycinergic and GABAergic/ glycinergic terminals on these neuronal populations in the cat.

Spinocerebellar tract neurons in the cat were initially identified and characterized electrophysiologically. Representative neurons of the four populations were then injected with a mixture of rhodamine-dextran and Neurobiotin. In the rat the selection of the neurons was done by taking advantage of the similar location, organization and axonal projections of spinocerebellar tract neurons as in the cat as mentioned in chapter 3, section 3.1 (Matsushita and Hosoya, 1979; Matsushita *et al.*, 1979). Neurons labelled by retrograde transport of CTb injected into the cerebellum in the rat were therefore differentiated on the basis of their location.

4.2 Methods

The study was carried out on a sample of 20 neurons labelled in 8 adult cats and on 68 neurons labelled in four adult Sprague Dawley rats (Harlan, Bicester, UK). All experimental procedures were approved by the Ethics committee as mentioned in General experimental procedures (Chapter 2).

4.2.1 Experimental procedures on cats

Surgical procedures, stimulation, identification and labelling of the four populations of spinocerebellar tract neurons in all animals were carried out following the procedures mentioned in detail in General experimental procedures (Chapter 2, Section 2.1).

4.2.2 Experimental procedures on rats

Stereotaxic surgery was performed on four adult male Sprague Dawley rats (250 – 350g) following the procedures described in detail in General experimental procedures (Chapter 2, Section 2.2). Retrograde injection with CTb was done at inter-aural co-ordinates -4.2 mm (anterior-posterior) and +2.0 mm (medio-lateral) at a dorso-ventral co-ordinate of +4.5 mm in the cerebellum (Paxinos and Watson, 1997). Injection sites were identified by using DAB as a chromogen and the location of the targeted site was determined with reference to the stereotaxic rat brain atlas (Paxinos and Watson, 1997) as described previously (see chapter 2, Section 2.2).

4.2.3 Immunohistochemical procedures

L3 – L6 segments of the cat and Th12 – L3 segments of the rat (see rationale in section 3.1; also large number of four populations of spinocerebellar tract neurons were found in these segments which was consistent throughout four animals used) were cut into 50 µm thick transverse sections with a Vibratome and processed following the procedure described in (Section 2.1 and 2.2). Intracellularly labelled

neurons with Neurobiotin and Rhodamine were first revealed using Avidine-Rhodamine reaction and sections containing well labelled cells were selected. Cat and rat sections were then processed for immunohistochemistry.

AIM I: Comparison of the density and distribution of inhibitory and of excitatory terminals in contact with the four populations of spinocerebellar tract neurons

Data from 12 neurons in the cat and 68 neurons in the rat were used in this part of the study. In both cats and rats inhibitory and excitatory terminals in contact with labelled neurons were analysed immunohistochemically. In order to differentiate between them antibodies against vesicular GABA transporter (VGAT) which is known to be highly expressed in both GABAergic and glycinergic nerve endings (Burger *et al.*, 1991; McIntire *et al.*, 1997; Chaudhry *et al.*, 1998; Wojcik *et al.*, 2006; Aubrey *et al.*, 2007) and a combination of antibodies against VGLUT1 and VGLUT2 which should label most excitatory terminals (Varoqui *et al.*, 2002; Todd *et al.*, 2003; Alvarez *et al.*, 2004) were used. Selected sections containing intracellularly labelled neurons were first washed several times in PBS and thereafter incubated in a combination of primary antibodies containing rabbit anti-VGAT and guinea pig anti-VGLUT1+2 for 72 hours at 4° C. Following several washes in PBS, the sections were incubated in a combination of secondary antibodies coupled to Alexa 488 and Dylight 649 for 3 hours at room temperature to identify VGAT and VGLUT1+2 terminals respectively. They were then rinsed in PBS and were then mounted in Vectashield. All antibodies were diluted in PBST (see Table 4-1 for details of antibodies used). The sections were then mounted in Vectashield.

Retrogradely labelled rat spinocerebellar tract neurons were identified by the presence of CTb transported from injection sites and grouped into different populations based on their anatomical locations. Three colour immunofluorescence was performed on these sections with rabbit anti-VGAT and guinea pig anti-VGLUT1 + 2 antibodies (see rat sections in Table 4-1) using the same procedures as for cat neurons. In both series of experiments, the sections were scanned using three channels of a confocal laser scanning microscope (BioRad Radiance, UK). VGAT

immunoreactive terminals were imaged as green, while VGLUT1+2 terminals were blue.

AIM II. Comparison of proportions of glycinergic and GABAergic/ glycinergic terminals forming contacts with different populations of spinocerebellar tract neurons

Data from 8 additional neurons from cats were used for this comparison. GABA and glycine are the two major inhibitory neurotransmitters in the spinal cord. It is widely accepted that antibodies directed against glutamic acid decarboxylase (GAD) can be used as reliable markers for axon terminals using GABA as neurotransmitter (Kaufman *et al.*, 1991; Soghomonian and Martin, 1998) whereas antibodies against gephyrin have been established as markers of postsynaptic glycine and GABA receptor clusters (Todd *et al.*, 1995; Alvarez *et al.*, 1997). In order to examine whether the contacts formed by inhibitory terminals are glycinergic or GABAergic or both GABAergic/ glycinergic, we therefore incubated the cat spinal cord sections containing well labelled cells in the following combination of primary antibodies: rabbit anti-GAD and mouse anti-7A (which recognizes gephyrin; Pfeiffer *et al.*, 1984; Meyer *et al.*, 1995) for 72 hours at 4º C. Following several washes in PBS, the sections were incubated in a combination of secondary antibodies coupled to Dylight 649 and Alexa 488 for 3 hours at room temperature to identify GAD terminals and gephyrin puncta respectively. The sections were then rinsed in PBS and subsequently mounted in Vectashield. The sections were scanned using confocal laser microscopy and contacts were analysed as described in the section below. It was not possible to make an accurate estimate of the number of pure glycinergic contacts by counting and quantifying gephyrin puncta not apposed by GAD terminals because gephyrin labels multiple active sites associated with a single presynaptic bouton. However, it was possible to estimate the numbers of pure glycinergic contacts by utilizing quantitative data obtained for overall contact density of inhibitory terminals which were VGAT immunoreactive (see Aim 1) and deducting the overall contact density of terminals immunolabelled with GAD apposed to gephyrin puncta.

Table 4-1 Summary of the primary and secondary antibody combinations and concentrations used

		Primary antibody combination	Primary antibody concentration	Supplier	Secondary antibody combination	Secondary antibody concentration	Supplier
Cat	A	gp VGLUT1	1:5000	Chemicon, Harlow, UK	Dylight 649	1:500	Jackson ImmunoResearch, West Grove, USA
		gp VGLUT2	1:5000	Chemicon, Harlow, UK	Dylight 649	1:500	Jackson ImmunoResearch, West Grove, USA
		rbt VGAT	1:5000	Synaptic systems, UK	Alexa 488	1:500	Molecular Probes, Eugene, USA
	B	rbt GAD	1:1000	Sigma, UK	Dylight 649	1:500	Jackson ImmunoResearch, West Grove, USA
		mo Gephyrin (7a)	1:1000	Synaptic systems, UK	Alexa 488	1:500	Molecular Probes, Eugene, USA
Rat		gt CTb	1:5000	List (quadratech)	Rh. Red	1:100	Jackson ImmunoResearch, West Grove, USA
		gp VGLUT1	1:5000	Chemicon, Harlow, UK	Dylight 649	1:100	Jackson ImmunoResearch, West Grove, USA
		gp VGLUT2	1:5000	Chemicon, Harlow, UK	Dylight 649	1:500	Jackson ImmunoResearch, West Grove, USA
		rbt VGAT	1:5000	Synaptic systems, UK	Alexa 488	1:500	Molecular Probes, Eugene, USA

All secondary antibodies were raised in donkey and conjugated to Rh. Red, Rhodamine Red; Dylight 649, Alexa 488, Alexa-fluor 488; gp, guineapig; rbt, rabbit; gt, goat; mo, mouse; CTb, B- subunit of cholera toxin; VGLUT, Vesicular glutamate transporter; VGAT, Vesicular GABA transporter;GAD, Glutamic acid decarboxylase

4.2.4 Confocal microscopy, reconstruction and analysis

Serial sections containing cell bodies and dendrites of intracellularly labelled cat neurons were scanned using Radiance 2100 microscope and images were collected from each section as described in Chapter 2 (Section 2.4). Cells were reconstructed three dimensionally by using Neurolucida for Confocal software and contacts on the labelled cells were mapped. In order to fulfil the first aim, contacts formed by VGAT and VGLUT1+2 were counted and recorded while to achieve the second aim, appositions made by GAD and GAD apposed to gephyrin were plotted. Corresponding contact densities were calculated using data generated by Neurolucida and expressed as numbers of contacts per unit area (100 μm^2) of neuronal surface. The distribution of contacts in intracellularly labelled neurons was analysed using Sholl analysis with Neurolucida Explorer. The detailed process of reconstruction and analysis is given in Chapter 2 (Section 2.4).

Retrogradely labelled rat spinocerebellar tract neurons were scanned ipsilaterally to the injection site, categorised and stacks of images obtained were analysed with Neurolucida for Confocal software. Reconstructions of cells were made and, VGAT and VGLUT1+2 contacts were plotted on each reconstruction. Analysis of the contacts formed with these spinocerebellar tract neurons was performed in the same way as described above (see details in chapter 2, section 2.4) for the intracellularly labelled neurons in the cat.

4.2.5 Statistical analysis

Data were expressed as mean ± SD. Multi-group comparisons were made by using an one way ANOVA followed by a *post hoc* Tukey's analysis as appropriate and two variable comparisons among the same population was made by using Student's *t* test. A $p < 0.05$ was considered to be statistically significant.

4.3 Results

4.3.1 Comparison of the number and the distribution of inhibitory and excitatory terminals in contact with the four populations of spinocerebellar tract neurons

4.3.1.1 GABAergic/ Glycinergic and Glutamatergic terminals on intracellularly labelled cat neurons

Samples of spinocerebellar tract neurons

Analysis was done in 12 neurons from seven adult cats. This included 3 SB neurons (cells 1 - 3), 3 VSCT neurons (cells 4 - 6), 3 ccDSCT neurons (cells 7 - 9) and 3 dhDSCT neurons (cells 10 - 12) were selected.

Individual neurons were classified as belonging to four subpopulations of spinocerebellar tract neurons on the basis of antidromic activation by stimulation within or close to the Nucleus Interpositus, and from either the contralateral or ipsilateral lateral funiculus, on the basis of coupling between primary afferents and these neurons and according to their anatomical location in the lumbar grey matter, as described in Chapter 2, section 2.1). Series of electrophysiological recordings from 4 neurons illustrating the antidromic activation from the cerebellum and inhibitory postsynaptic potentials evoked from muscle nerves are shown in Figure 4-1. These records illustrate strong inhibition from group I (early) and group II (late) afferents in the SB (cell 2) and VSCT (cell 5) neurons, from mainly group I afferents in the ccDSCT (cell 9) and group II afferents in the dhDSCT (cell 11) neurons.

All neurons were located within midlumbar segments. The locations of cell bodies of these neurons within the L3, L4 and L5 segments are shown in Figure 4-2. The cell bodies of the SB neurons (red circles) were located within the most lateral part of the grey matter in lamina VII while the cell bodies of VSCT neurons (green circles) were within more medial parts of lamina VII. The cell bodies of the ccDSCT

neurons (purple circles) were contained within cc whereas the dhDSCT neurons (blue circles) had their cell bodies in either lamina V or VI. Both the location and morphology of analysed neurons was fully consistent with the categorization of these cells based on their physiological properties.

As described in the Methods (Section 4.2.3), immunoreactivity for VGAT was used to reveal inhibitory axonal terminals containing GABA and/or Glycine and a combination of antibodies against VGLUT1 and VGLUT2 which were raised against same species was used to reveal excitatory contacts independently of their source of origin. The results revealed marked differences in proportions and distribution of VGAT and VGLUT1+2 axonal contacts on the SB, VSCT, ccDSCT and dhDSCT neurons. These differences are apparent in examples of single optical sections of confocal images of axon terminals contacting these neurons shown in Figure 4-3.

Figure 4-3 illustrates that the majority of contacts on SB population of neurons are immunopositive for VGAT, especially on the cell body (Figure 4-3A). In contrast, similar proportions of VGAT and VGLUT1+2 positive terminals were found in contact with cell bodies and dendrites of VSCT neurons, as illustrated in Figure 4-3B and 4.3B4. Both kinds of contacts were also found on ccDSCT and dhDSCT cells although these contacts were to a greater extent on dendrites (Figure 4-3 C4 and D4) than on somata (Figure 4-3 C and D) where inhibitory contacts were more frequent.

Differences in the distribution of VGAT and VGLUT1+2 axon terminals based on reconstructions of contacts formed by these terminals over the cell bodies and the whole dendritic trees of individual neurons belonging to the four populations of these neurons are illustrated in Figure 4-4. Figure 4-5 shows the distribution of VGAT and VGLUT1+2 separately in the same neuron of each class. The emerging patterns of contacts on these neurons are (i) the overwhelming majority of VGAT contacts (green in Figure 4-4 and 4-5) and a smaller proportion of VGLUT1+2 contacts (red) on both soma and dendrites of SB neurons, (ii) similar proportions and more even distribution of VGAT and VGLUT1+2 contacts on soma and dendrites of VSCT, and dhDSCT neurons, (iii) a clustered distribution of these contacts on ccDSCT neurons, suggesting a higher density of excitatory contacts close to the

initial segment or on some dendrites and (iv) a generally smaller density of somatic contacts on ccDSCT neurons than on other neurons.

The results of quantitative comparison of distribution of VGAT and VGLUT1+2 contacts at different distances from the soma are summarised in Figure 4-6. They are based on Sholl analysis in which numbers of contacts in concentric areas around the soma are plotted against distances from the soma (see details in Chapter 2, Section 2.4). The four charts show that the density of VGAT and VGLUT1+2 contacts on proximal dendrites of SB and VSCT neurons was higher than of ccDSCT and dhDSCT neurons but similar at longer distances from soma. Sholl analysis also shows that the proportion of VGAT contacts within the first 75 μm was considerably higher than of VGLUT1+2 contacts for SB neurons, somewhat higher for VSCT and dhDSCT neurons and similar for ccDSCT neurons. A similar finding was also found for the initial axon segments of SB neurons where the contact density (2.19 ± 0.74 /100 μm^2) was almost twice that associated with the other three types of spinocerebellar tract neurons (VSCT= 1.41 ± 1.11; ccDSCT=1.15 ± 0.69; dhDSCT =1.28 ± 0.52 per 100μm^2; none of these values are significant). The details of the further quantitative comparisons are shown in Figure 4-7 and Table 4-2.

Quantitative comparison of coverage of VGAT and VGLUT1+2 terminals on intracellularly labelled SB and VSCT neurons

Table 4-2 summarizes data for the four populations of intracellularly labelled spinocerebellar tract neurons, including the number and density of VGAT and VGLUT1+2 terminals in contact with the soma and dendrites of individual neurons analysed in this study.

The overall average densities of VGAT and VGLUT1+2 contacts per 100 μm^2 of the soma and the dendritic tree of SB neurons were 5.84 ± 0.92 and 3.86 ± 0.73 respectively. The total contact density of VGAT terminals was thus 1.5 times greater than that of VGLUT1+2 terminals. This difference was statistically significant (Student's *t*- test, $p < 0.05$). The difference was even greater (2 times) for the soma. In contrast with SB neurons, VSCT neurons have similar overall

contact densities of VGAT and VGLUT1+2 terminals, 3.95 ± 0.63 and 3.62 ± 0.54 per 100 μm^2 even though there was a somewhat higher (1.25 times, not statistically significant) density of VGAT contacts for the soma. Therefore this comparison suggests that the main difference between SB and VSCT neurons was in the overall density of VGAT contacts, but as this difference was not statistically significant ($p > 0.05$; ANOVA) a firm conclusion could not be drawn.

Quantitative comparison of coverage of VGAT and VGLUT1+2 terminals on intracellularly labelled ccDSCT and dhDSCT neurons

ccDSCT neurons, displayed the lowest overall average densities of VGAT and VGLUT1+2 contacts, 2.50 ± 0.85 and 3.15 ± 1.16 per 100 μm^2 respectively and the difference between them was not statistically significant ($p > 0.05$). In dhDSCT neurons, the overall average densities of these terminals were also relatively low and not significantly different, with VGAT density of 2.76 ± 0.80 and VGLUT1+2 density of 3.48 ± 0.77 per 100 μm^2. Comparison of the contact densities of VGAT and VGLUT1+2 terminals on ccDSCT and dhDSCT neurons did not show any significant differences. However, as shown in Figure 4-7A and 4-7B, the overall contact density of VGAT terminals associated with SB neurons in the cat was significantly higher than that on either ccDSCT or dhDSCT neurons ($p < 0.01$; ANOVA). No such difference was found in the contact densities of VGLUT1+2 terminals among any of the population of neurons analysed in the current study. However, it should be noted that significant differences in densities of separately labelled VGLUT1 and VGLUT2 terminals were found in the preceding study (see Figure 5 in Shakya-Shrestha *et al.,* 2012 or Figure 3-5 in chapter 3).

The density and distribution of VGAT and VGLUT1+2 contacts for individual neurons presented in Figures 4-3 – 4-6 and in Table 4-2 show that synaptic actions of VGAT and VGLUT1+2 terminals may be evoked within all compartments of the dendritic trees of SB and VSCT neurons even though, as specified in previous chapter, it is more likely that the actions of VGLUT1 terminals are focused upon proximal dendrites and the highest densities of VGAT terminals are on soma and proximal dendrites. Taken together the present results indicate that the distribution of VGAT

and VGLUT1+2 contacts within each class of cat spinocerebellar tract neuron is characteristic and differs from the distribution in other classes.

4.3.1.2 GABAergic/ Glycinergic and Glutamatergic terminals on retrogradely labelled neurons in the rat

An example of a CTb injection site in the cerebellum and reconstructions of injection site for all four animals is shown in Figure 3-7 in chapter 3. In total, 68 spinocerebellar tract neurons labelled by retrograde transport of CTb were analysed in rats. These neurons included 20 ccDSCT neurons, 14 dhDSCT neurons, 17 SB neurons and 17 VSCT neurons. Two principal criteria were used for the selection of the labelled cells. The first criterion for selection was strong labelling of both cell bodies and dendritic trees at distances of at least 20 μm from the soma (average distance of 110.24 μm). The second criterion was a location equivalent to the location of intracellularly labelled spinocerebellar tract neurons in the cat as mentioned previously (see chapter 3). As shown in Figure 4-8, SB neurons were classified as those with cell bodies located within the most lateral part of the grey matter in lamina VII (red circles), whereas VSCT neurons were located within more medial parts of lamina VII (green circles). Likewise, anatomically ccDSCT and dhDSCT neurons were classified as those located within cc (represented by purple circles) or outside cc in either lamina V or VI (blue circles) respectively. Representative examples of confocal microscope images for each of these neuronal populations are shown in Figure 4-9.

Quantitative comparison of coverage of VGAT and VGLUT1+2 terminals on retrogradely labelled SB and VSCT neurons

Confocal microscopy analysis revealed that the overall average densities of VGAT and VGLUT1+2 contacts per 100 μm^2 of SB neurons in the rat were 1.10 ± 0.36 and 0.75 ± 0.34 per 100 μm^2 respectively whereas the average overall densities of VGAT and VGLUT1+2 contacts on VSCT neurons were 1.06 ± 0.77 and 0.86 ± 0.30 per 100 μm^2 respectively

Although these SB neurons have a higher numbers of VGAT contacts relative to VSCT neurons, comparison of the overall contact densities on SB and VSCT neurons was not significantly different ($p > 0.05$; ANOVA see Figure 4-7C and 4-7D). Similarly, no statistically significant difference ($p > 0.05$; ANOVA) was found between the overall contact density of VGLUT1+2 on these two populations of neurons (see preceding chapter for details of VGLUT1 and VGLUT2 contacts separately).

Quantitative comparison of coverage of VGAT and VGLUT1+2 terminals on retrogradely labelled ccDSCT and dhDSCT neurons

In ccDSCT neurons, the overall average densities of VGAT and VGLUT1+2 contacts were 0.39 ± 0.05 and 0.43 ± 0.20 per 100 μm^2 respectively. The overall mean contact densities of VGAT and VGLUT1+2 terminals in dhDSCT neurons were 0.44 ± 0.36 and 0.61 ± 0.24 per 100 μm^2 respectively. None of these differences were found to be statistically significant (Student's *t*- test, $p > 0.05$).

Comparison of the overall contact densities on ccDSCT and dhDSCT neurons similarly didn't show a statistically significant difference for both VGAT and VGLUT1+2 contacts on them ($p > 0.05$; ANOVA).

Table 4-3 summarizes data for the four populations of retrogradely labelled rat spinocerebellar tract neurons, including the number and density of VGAT and VGLUT1+2 terminals in contact with the soma and dendrites of these neurons. Together with Figure 4-7C and 4-7D it shows that the overall densities of VGAT and VGLUT1+2 terminals in the rat were at least 3-4 times lower than in the cat. However, the relative densities of these terminals indicate a similar pattern of distribution in cats and rats, from the highest densities of VGAT terminals on SB neurons to the lowest densities on ccDSCT neurons and similar densities of VGLUT1+2 terminals on all four populations of neurons.

4.3.2 Comparison of proportions of glycinergic and GABAergic/ glycinergic terminals forming contacts with different populations of spinocerebellar tract neurons

Following the quantification of contacts formed by VGAT terminals in different populations of spinocerebellar tract neurons as described above, 8 additional intracellularly labelled spinocerebellar tract neurons (a-h) from 3 cats were examined to define which inhibitory neurotransmitters were contained within the VGAT immunoreactive contacts. This was done by using markers for GABAergic terminals and glycine/ GABA receptors (see Table 4-1; Cat B). Examples of confocal images revealing the association of GABAergic terminals and gephyrin for each population of spinocerebellar tract neurons are shown in Figure 4-10 (A-D); GABAergic terminals apposed to gephyrin are indicated by arrow heads while gephyrin puncta occurring separately are indicated by arrows. Analysis of distribution of GAD terminals apposed to gephyrin (green) and GAD terminals which were not associated with gephyrin (red) revealed the great majority of GAD terminals in all spinocerebellar tract neurons formed synaptic contacts. Reconstructions of individual neurons analysed in this study are shown in Figure 4-11.

Analysis of the confocal microscope images revealed that in SB neurons, overall mean densities of contacts formed by GAD terminals apposed to gephyrin was 0.70 per 100 μm^2 and of those GAD terminals which were not associated with gephyrin was 0.02 per 100 μm^2. Similarly, in VSCT neurons, the density of the contacts made by GAD positive terminals associated with gephyrin puncta was 1.08 per 100 μm^2 and that of GAD terminals only was 0.02 per 100 μm^2. Hence, using data in Table 4-2 and the procedure of calculation described in the methods section (section 4.2.3, Aim II), the density of purely glycinergic axon terminals that apposed to SB and VSCT neurons was estimated as 5.12 and 2.85 per 100 μm^2 respectively.

In ccDSCT and dhDSCT neurons the overall contact densities of GAD immunolabelled terminals associated with gephyrin puncta were 1.64 and 1.45 per 100 μm^2 respectively while the densities of the appositions formed by GAD positive terminals

not associated with gephyrin were 0.12 and 0.01 per 100 $\mu m^{2.}$. On the basis of these data the density of contacts made by glycinergic terminals was estimated as 1.39 terminals per 100 μm^2 in ccDSCT neurons and as 2.02 terminals per 100 μm^2 in dhDSCT neurons.

Generally, taken together with the data on the overall density of VGAT contacts on the same populations of cells, the present results show that the majority of the contacts made by inhibitory terminals are likely to be made by glycinergic interneurons, albeit both GABA and glycine may act as co-transmitters in a proportion of glycinergic synapses.

Figure 4-1 Examples of records from the four populations of lumbar spinocerebellar neurons analysed morphologically.

In each pair of traces, the upper traces are intracellular records (averages of 10 or 20 single recordings) from the cells identified as indicated to the left, and the lower traces are from the cord dorsum. Panels in the left column illustrate antidromic activation following the cerebellar stimulation. Panels in the right column illustrate IPSPs evoked from muscle nerves by stimulation of both group I and II afferents in the quadriceps (Q) or deep peroneal (DP) nerves at intensity 5 times threshold (T) for group I afferents. The negativity is downward in intracellular records and upward in those from the cord dorsum. The dotted lines indicate the onset of the earliest group I and group II evoked potentials respectively. Rectangular calibration pulses at the beginning of traces are 0.2 mV.

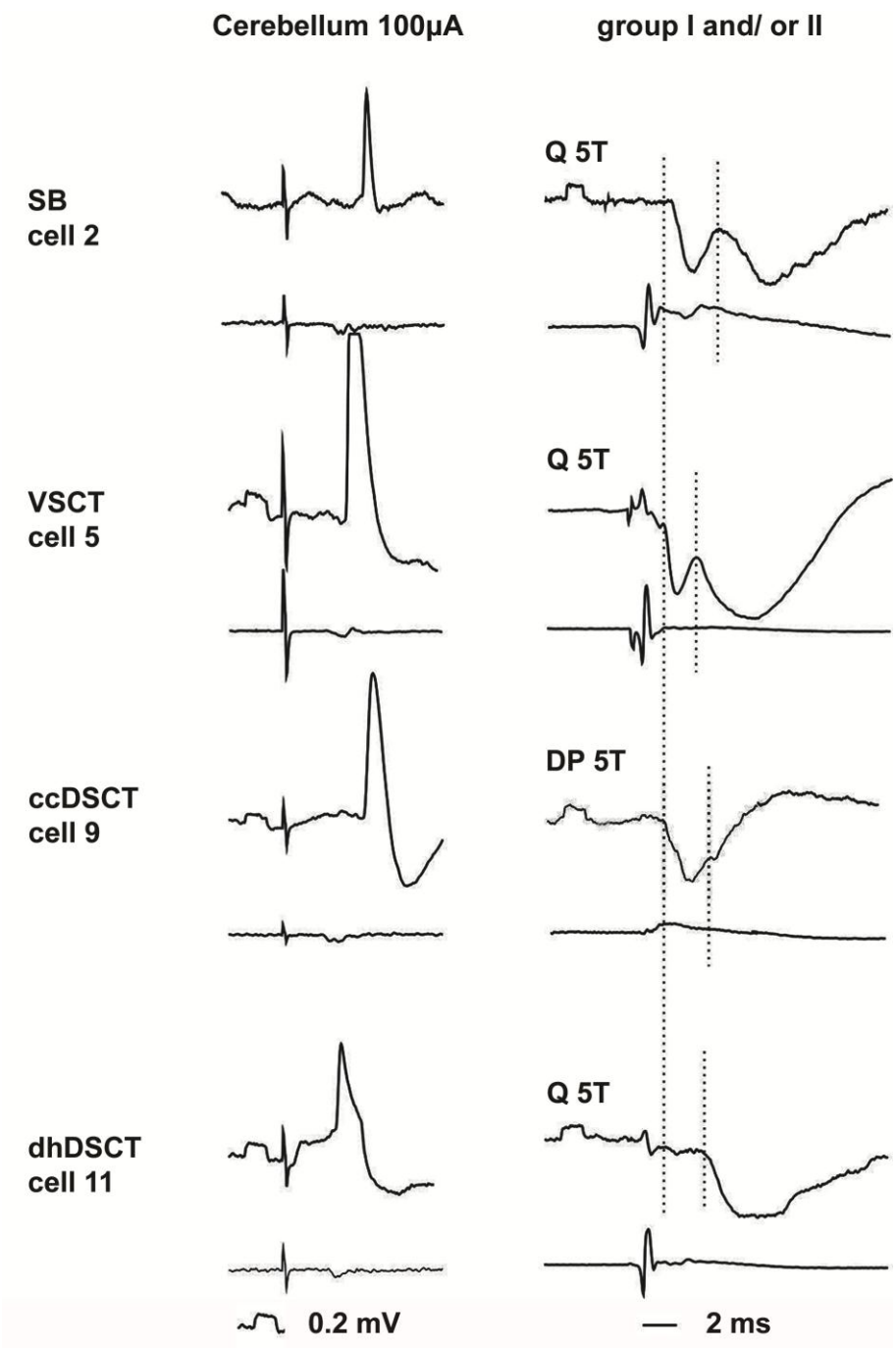
Cerebellum 100µA
group I and/ or II
SB
cell 2
Q 5T
VSCT
cell 5
Q 5T
ccDSCT
cell 9
DP 5T
dhDSCT
cell 11
Q 5T
0.2 mV
2 ms

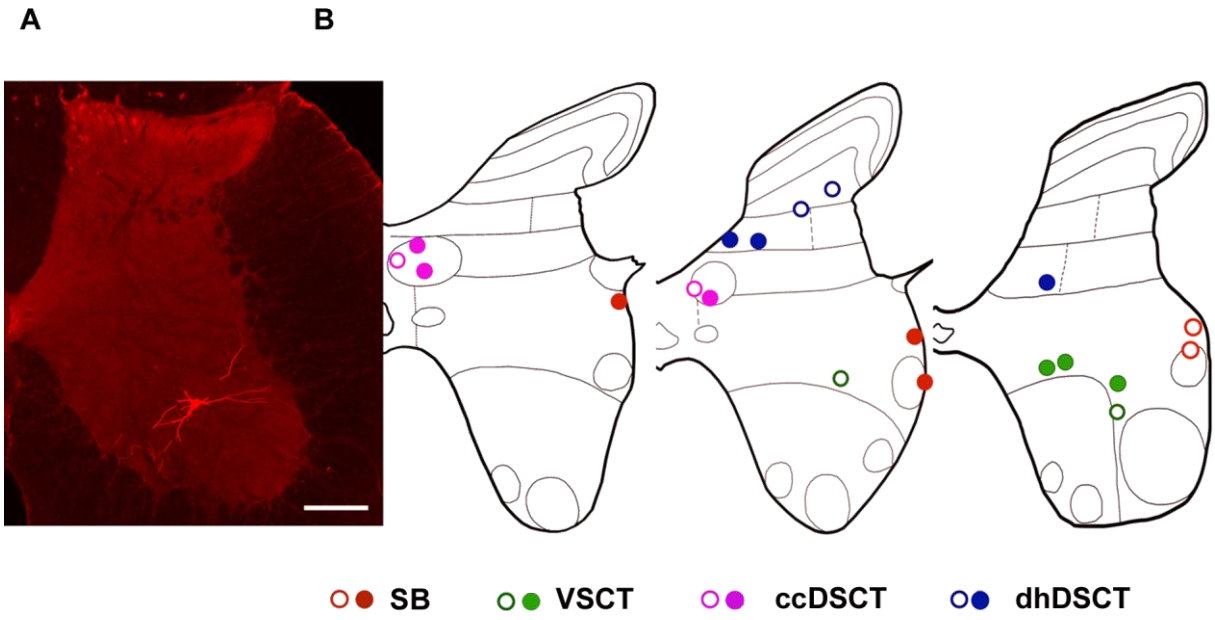

Figure 4-2 Locations of 20 intracellularly labelled spinocerebellar tract neurons

A*,** A low-magnification image of a transverse section of the L5 segment of the spinal cord showing the location of one of the VSCT neurons (cell 4). ***B*,** Diagrams illustrating the locations of cell bodies of all 20 cells in the L3, L4 and L5 segments respectively on contours of the spinal cord from (Rexed, 1954). Closed circles indicate location of the 12 cells analysed for both VGAT and VGLUT1+2 while open circles are for the 8 cells analysed for GAD and gephyrin. Scale bar in ***A 400 μm.

Figure 4-3 Immunohistochemical characteristics of VGAT and VGLUT1+2 axon terminals in contact with intracellularly labelled spinocerebellar tract neurons

A-D, Single optical sections through the cell bodies of representative SB (Cell 1), VSCT (Cell 4), ccDSCT (Cell 7) and dhDSCT (Cell 10) neurons showing the presence of VGAT (green) and VGLUT1+2 (blue) immunoreactive axon terminals. The cell body and dendrites of intracellularly labelled cells are in red. ***A1-A4; B1-B4; C1-C4 and D1-D4***, images of dendritic trunks from cells shown in ***A***, ***B***, ***C*** and ***D*** respectively (areas encompassed in the boxes) illustrating contacts made by VGAT and VGLUT1+2 immunoreactive terminals with the cell indicated by arrows and arrow heads respectively. Scale bar in ***A-D*** = 10 μm. Scale bar in ***A1-A4***, ***B1-B4***, ***C1-C4*** and ***D1-D4*** = 5 μm.

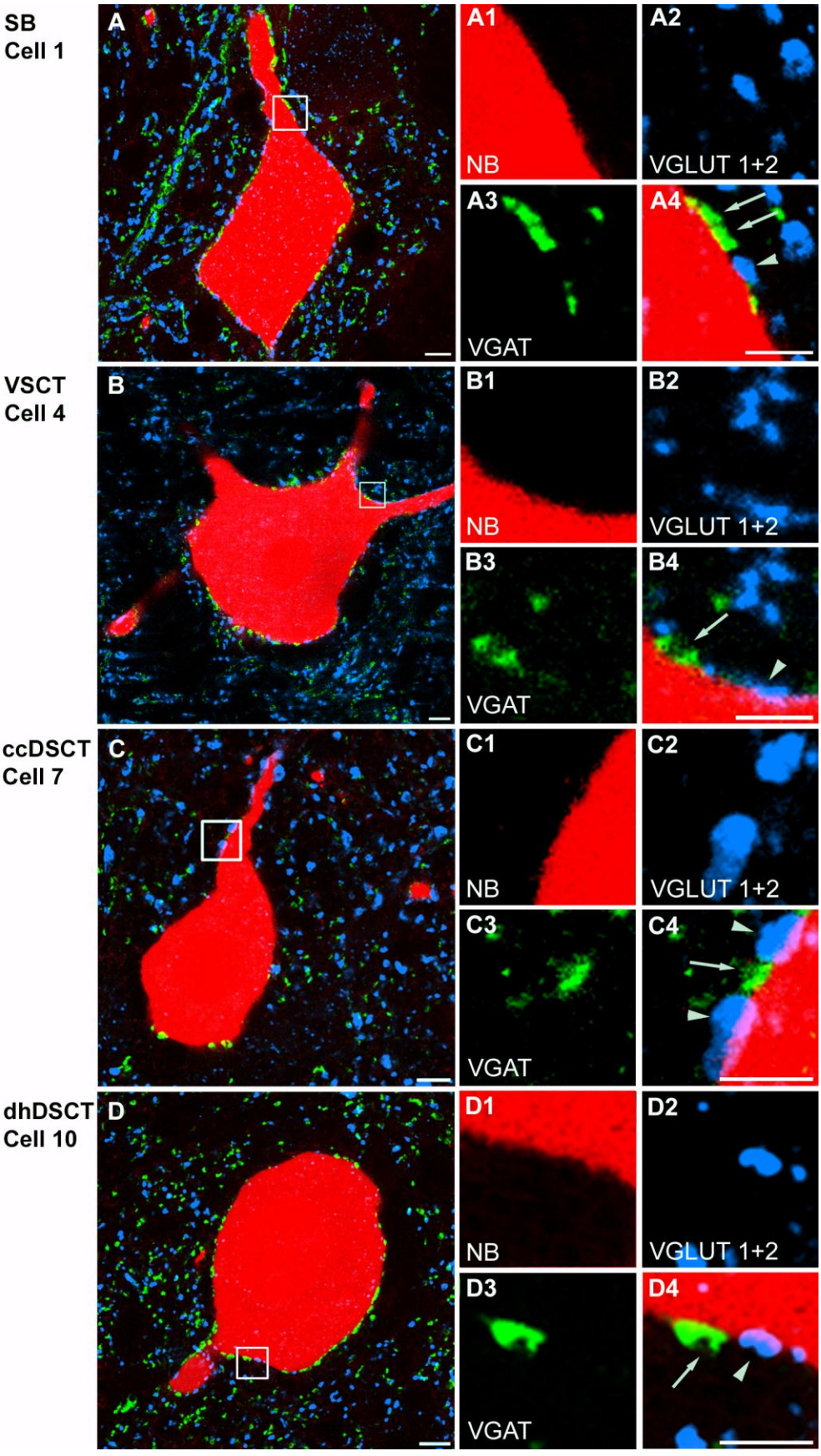
SB
Cell 1
A
A1
NB
A2
VGLUT 1+2
A3
VGAT
A4
VSCT
Cell 4
B
B1
NB
B2
VGLUT 1+2
B3
VGAT
B4
ccDSCT
Cell 7
C
C1
NB
C2
VGLUT 1+2
C3
VGAT
C4
dhDSCT
Cell 10
D
D1
NB
D2
VGLUT 1+2
D3
VGAT
D4

Figure 4-4 Reconstructions of spinocerebellar tract neurons illustrating different patterns of distribution of VGAT and VGLUT1+2 contacts

Reconstructions of 12 spinocerebellar tract neurons showing the distributions of VGAT (green) and VGLUT1+2 (red) contacts throughout the dendritic trees. The reconstructions were made with Neurolucida for Confocal. All the small images without contacts plotted show the reconstructions of respective cells. Cell body and dendrites are shown in light grey. Scale bars = 50 μm for reconstructions with contacts plotted and 100 μm for reconstructions without contacts. All the reconstructed neurons are oriented such that the midline is to the left and the lateral borders of the grey matter to the right, as in Figure 4-2.

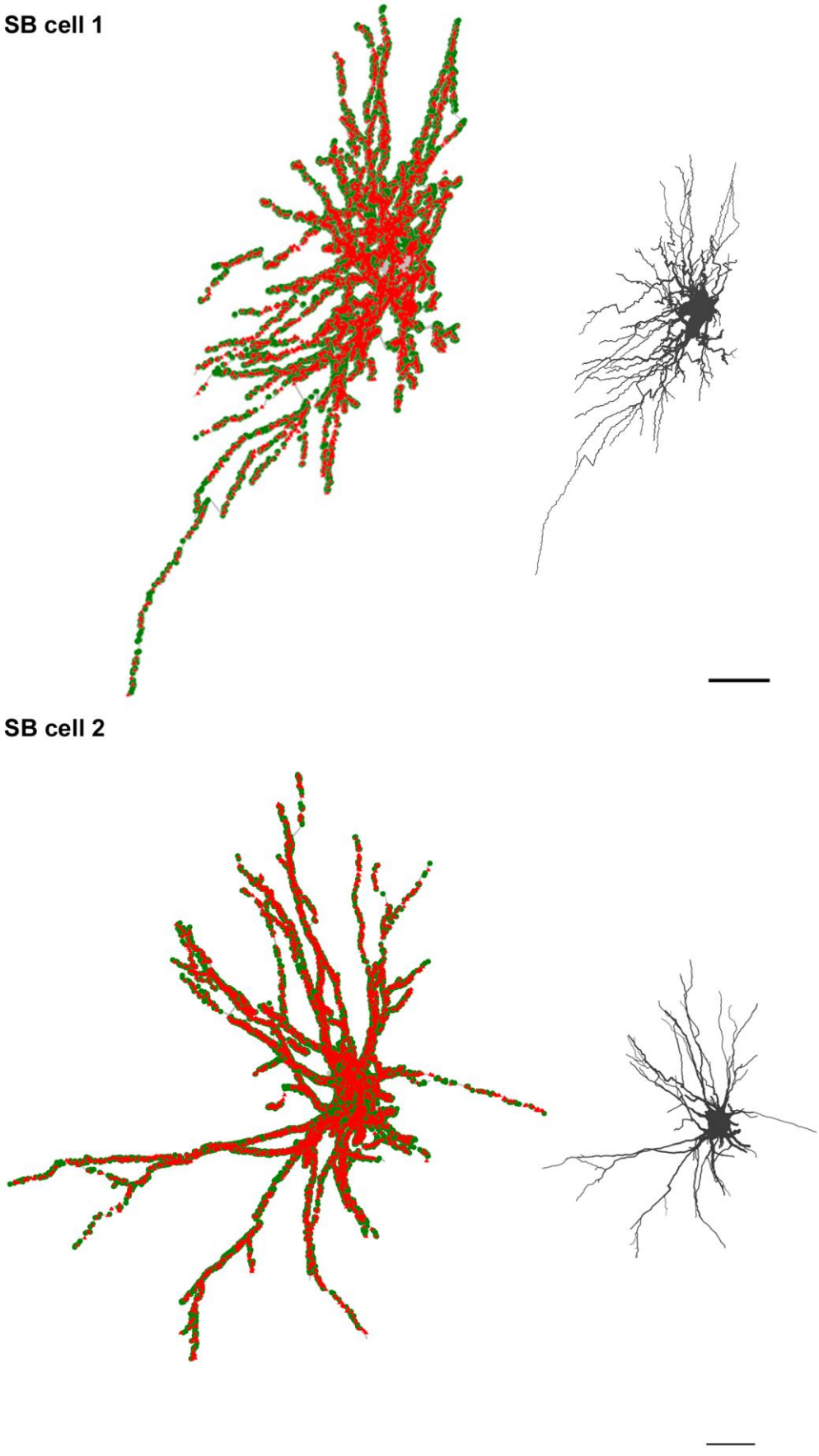
SB cell 1
SB cell 2

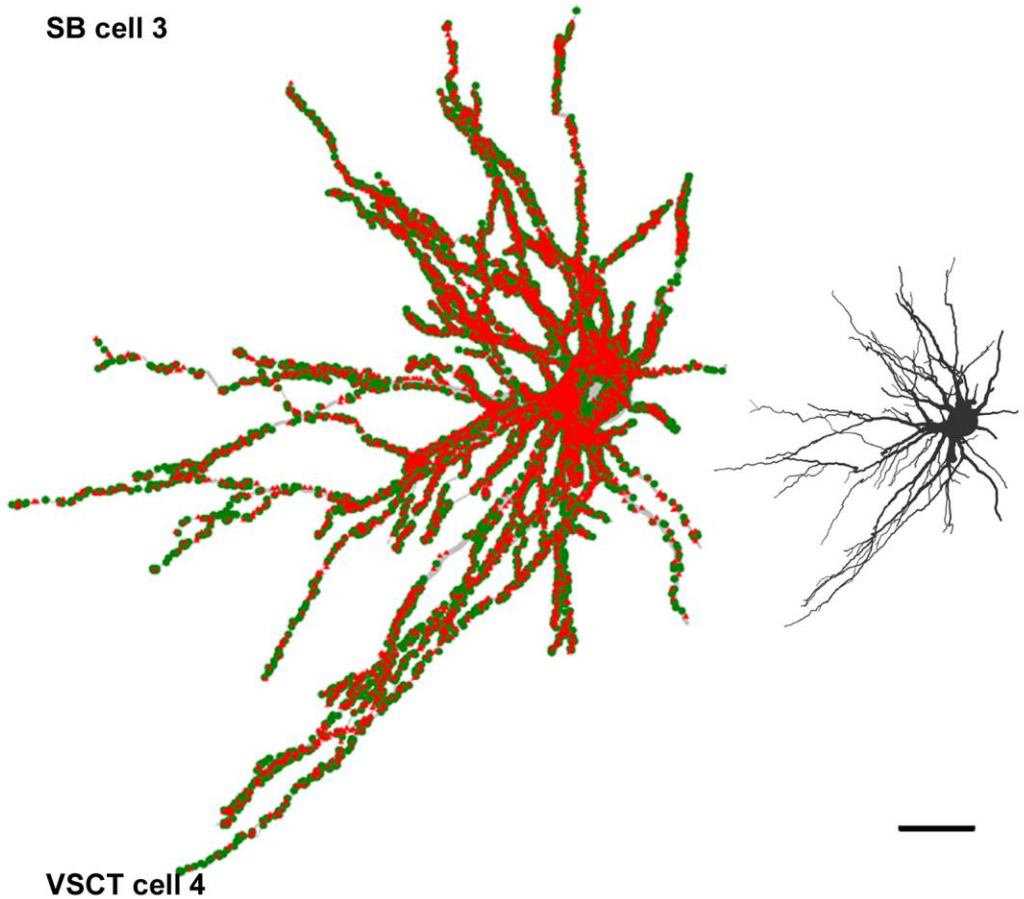
SB cell 3

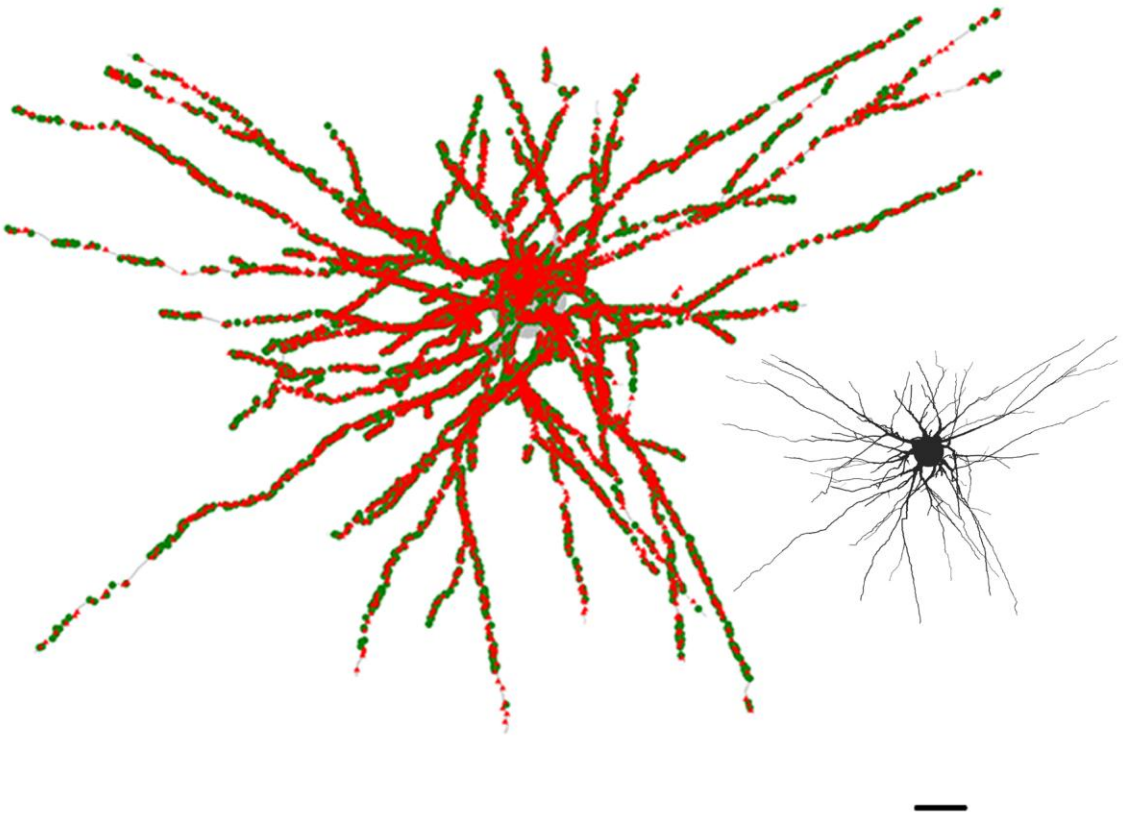
VSCT cell 4

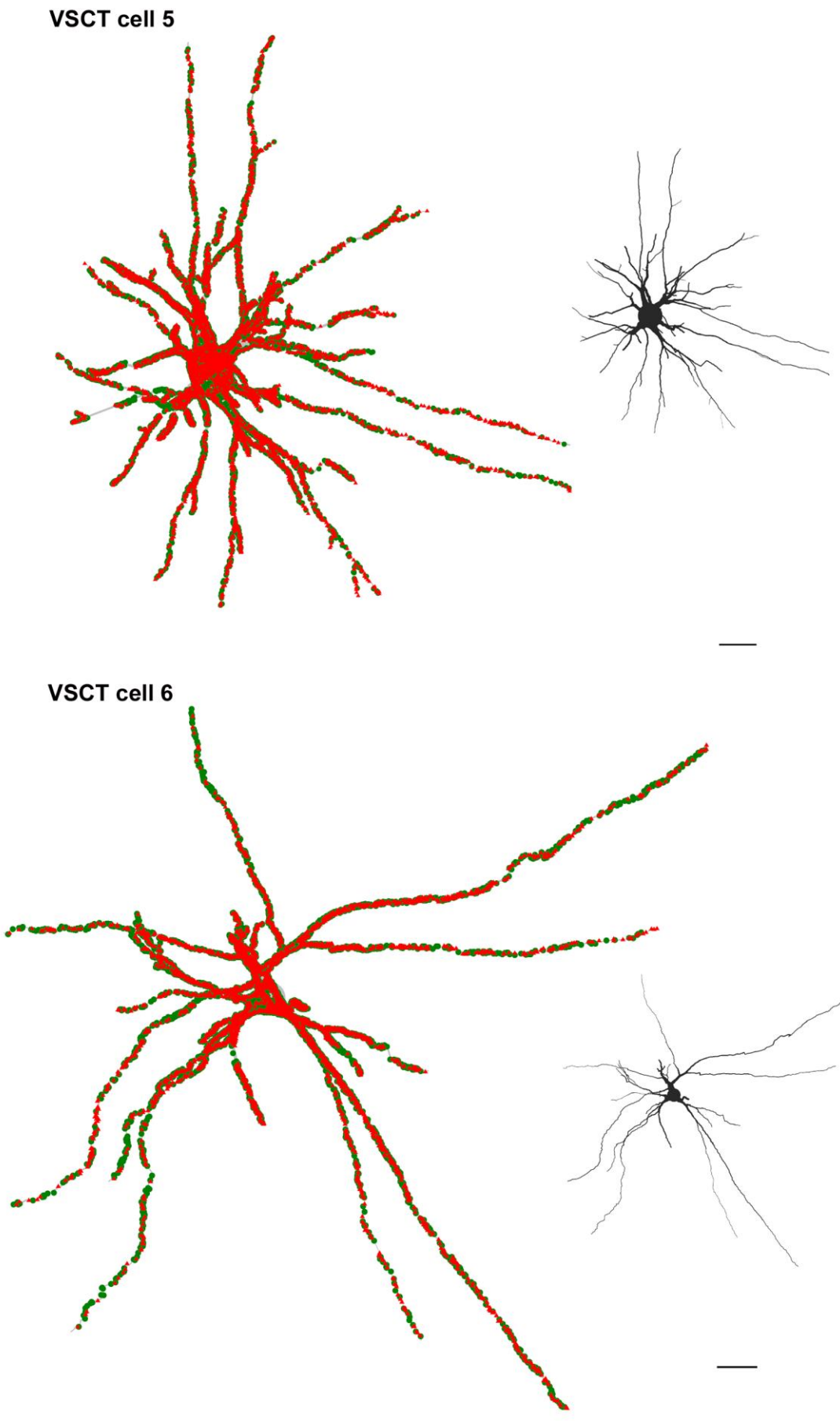
VSCT cell 5
VSCT cell 6

ccDSCT cell 7

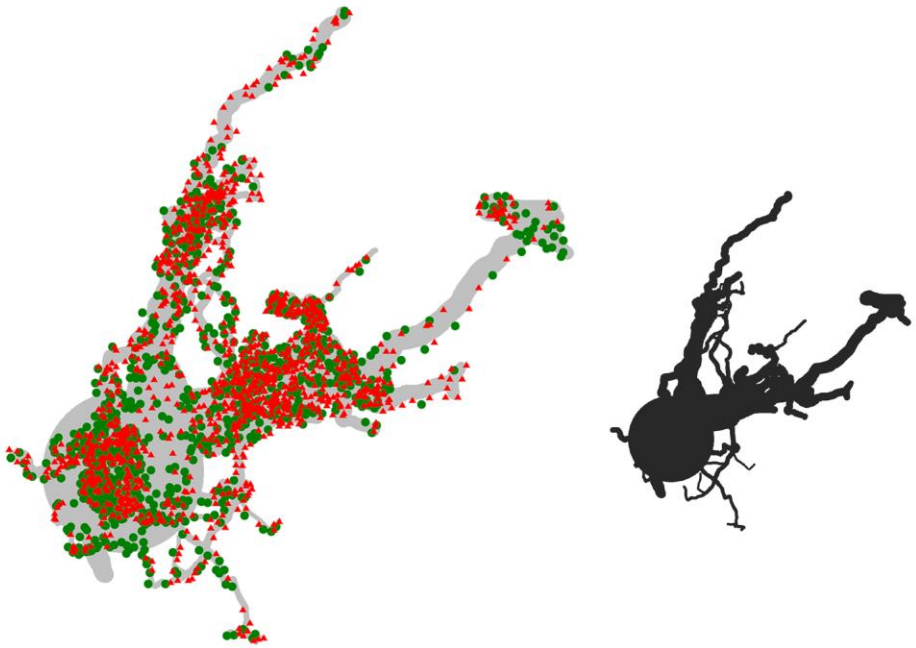

ccDSCT cell 8

ccDSCT cell 9

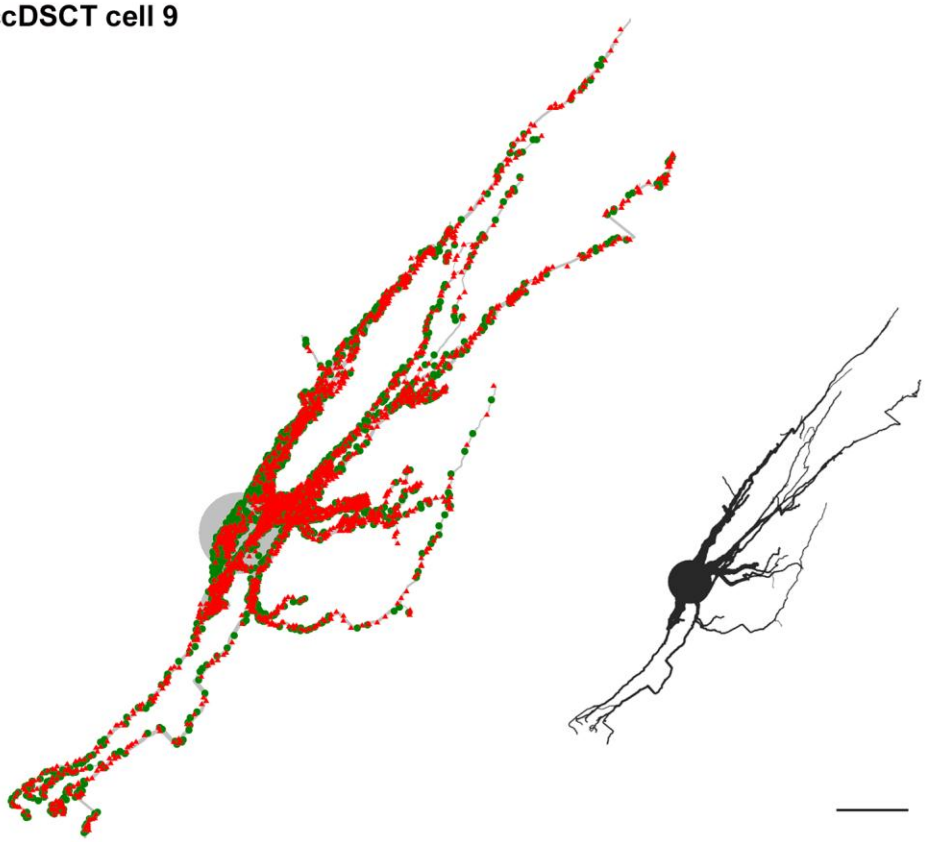

dhDSCT cell 10

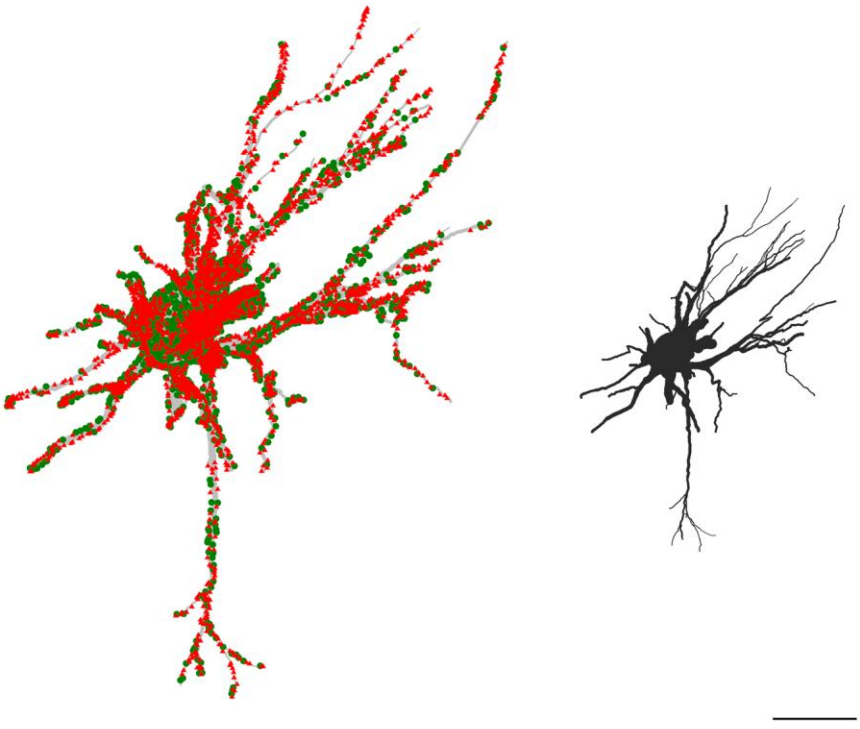

dhDSCT cell 11

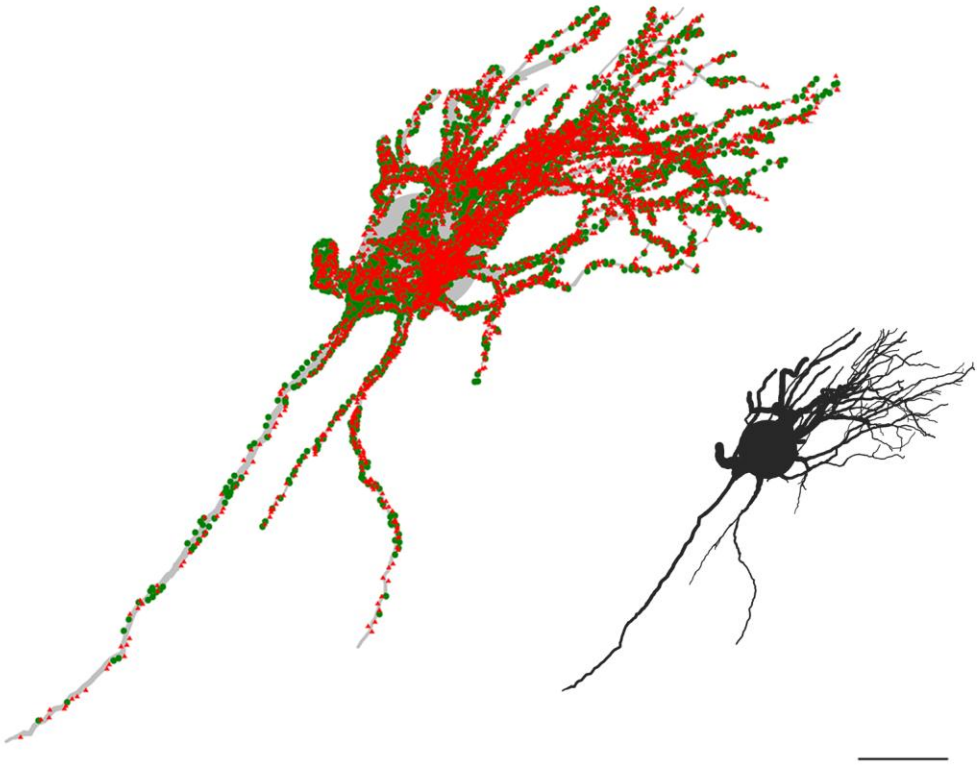

dhDSCT cell 12

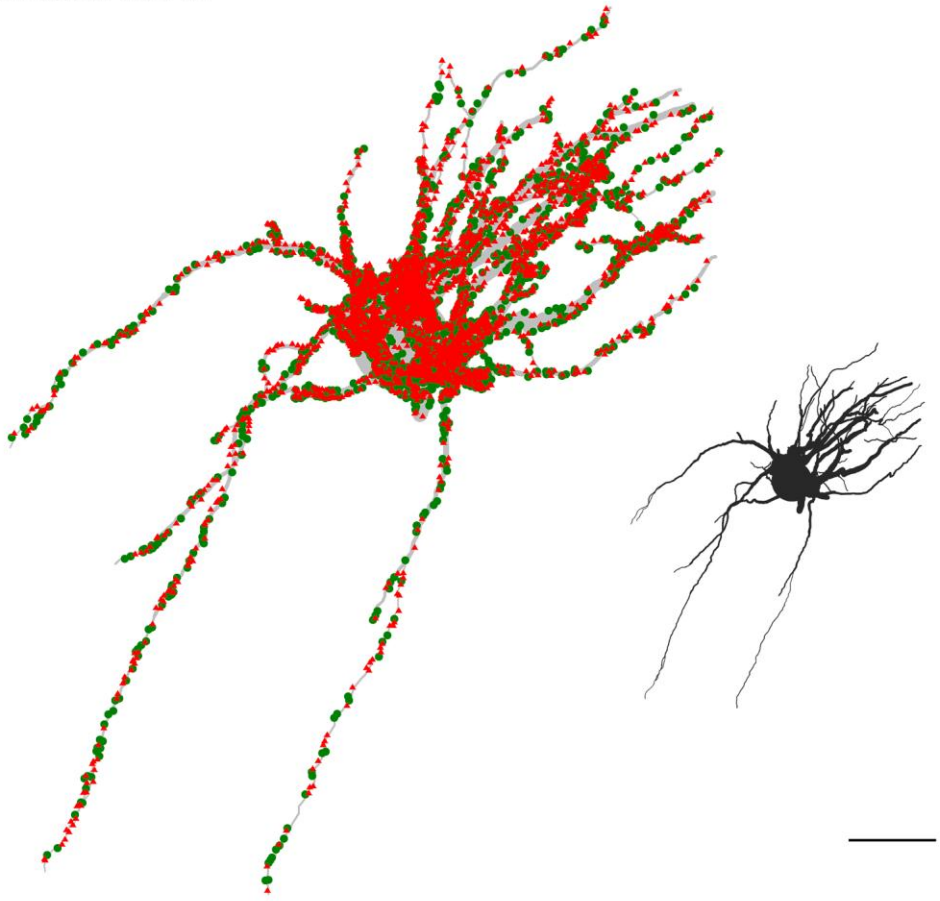

Figure 4-5 Distribution of VGAT and VGLUT1+2 contacts on reconstructions of SB, VSCT, ccDSCT and dhDSCT neurons

Distribution of VGAT (green) and VGLUT1+2 (red) contacts formed with somata and dendrites are illustrated on two dimensional projections of the same neuron of each class. The reconstructions were made with Neurolucida for Confocal. Cell bodies and dendrites are shown in light grey. Scale bars = 50 μm. All cells are oriented such that the midline is to the left and the lateral borders of the grey matter to the right, as in Figure 4-2. Note the more even distribution of both VGAT and VGLUT1+2 contacts on the soma and throughout the whole dendritic tree of SB and VSCT neurons and the patchy distribution of these contacts on both populations of DSCT neurons.

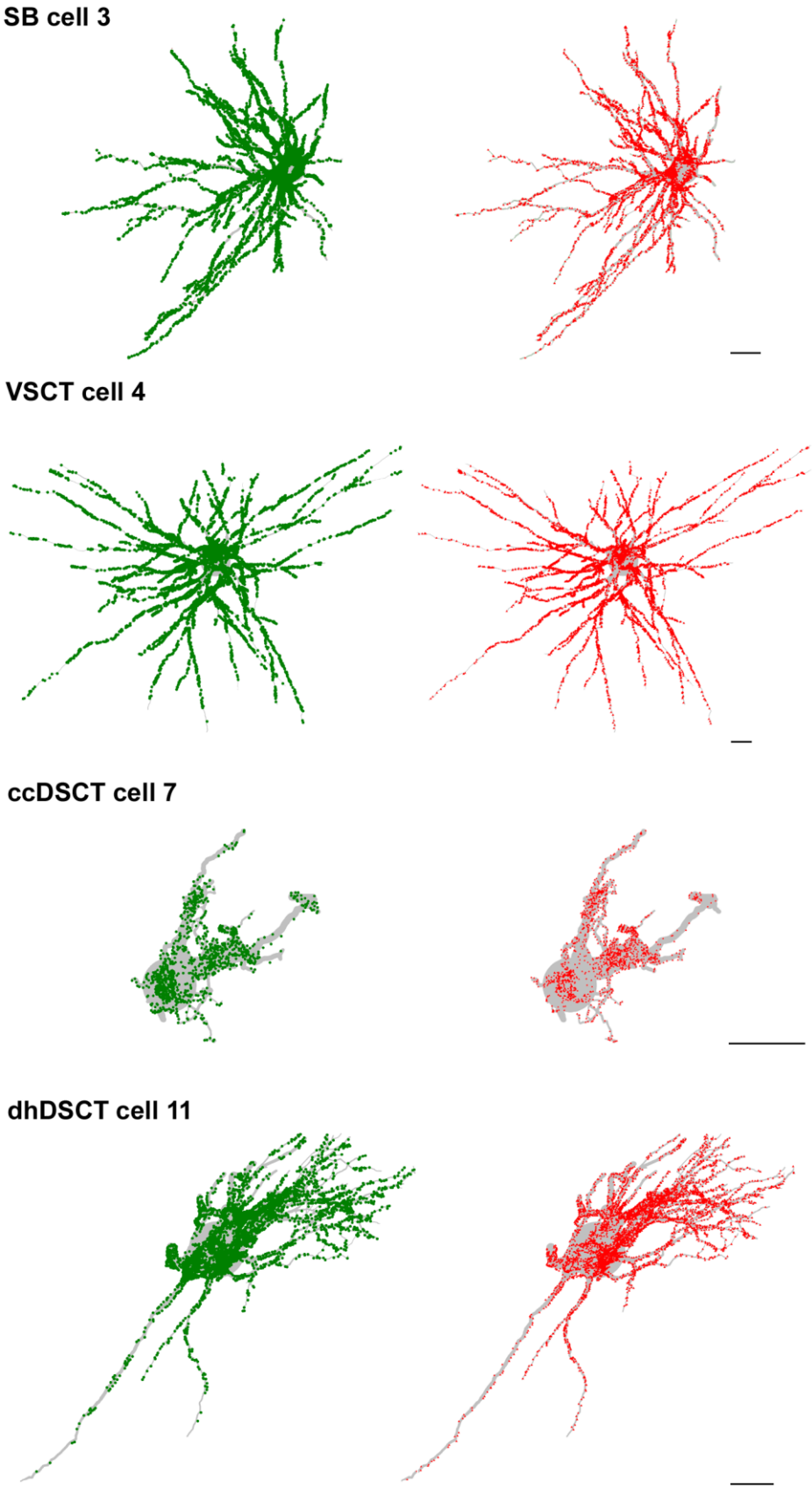
SB cell 3
VSCT cell 4
ccDSCT cell 7
dhDSCT cell 11

Figure 4-6 Comparison of distribution of VGAT and VGLUT1+2 terminals along dendrites

Mean numbers of VGAT and VGLUT1+2 terminals forming contact with different populations of intracellularly labelled spinocerebellar tract neurons at different distances from soma derived from Sholl analysis. ***A*,** SB neurons (cells 1 - 3), ***B*,** VSCT neurons (cells 4 - 6), ***C*,** ccDSCT neurons (cells 7 to 9) and ***D*,** dhDSCT neurons (cells 10 - 12). The plots show the mean numbers of contacts per 100 µm of dendritic length contained within concentric spheres with radii which increase in 25 µm from the centre of the cell body. Bars represent the standard deviations.

A. SB

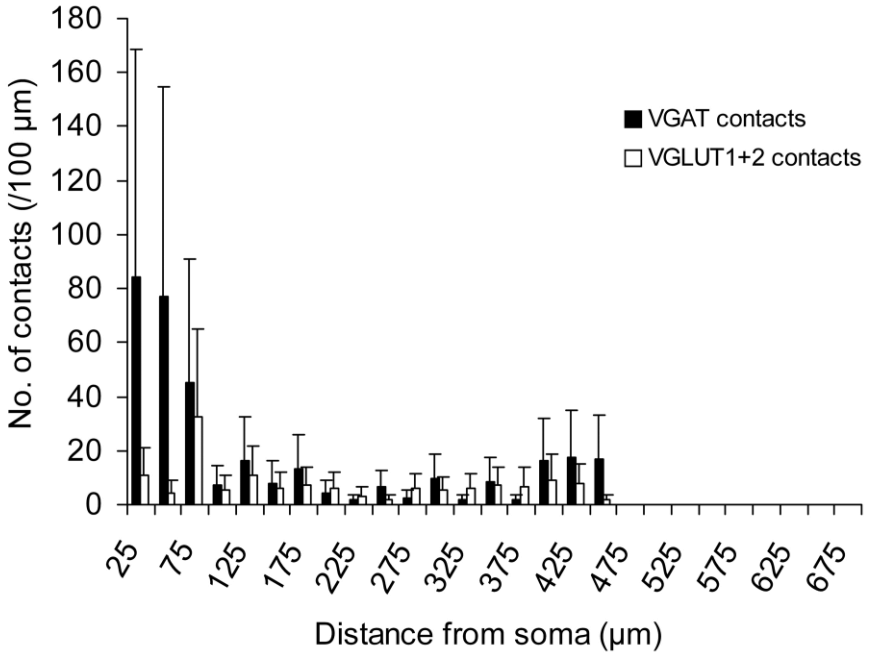
No. of contacts (/100 µm)
180
160
140
120
100
80
60
40
20
0
VGAT contacts
VGLUT1+2 contacts
25
75
125
175
225
275
325
375
425
475
525
575
625
675
Distance from soma (µm)

B. VSCT

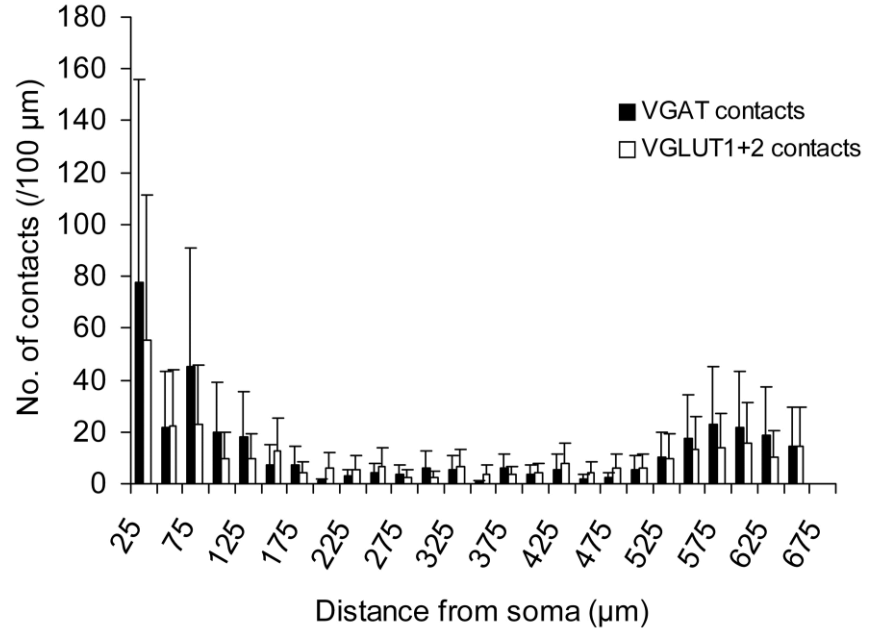
No. of contacts (/100 µm)
180
160
140
120
100
80
60
40
20
0
VGAT contacts
VGLUT1+2 contacts
25
75
125
175
225
275
325
375
425
475
525
575
625
675
Distance from soma (µm)

C. ccDSCT

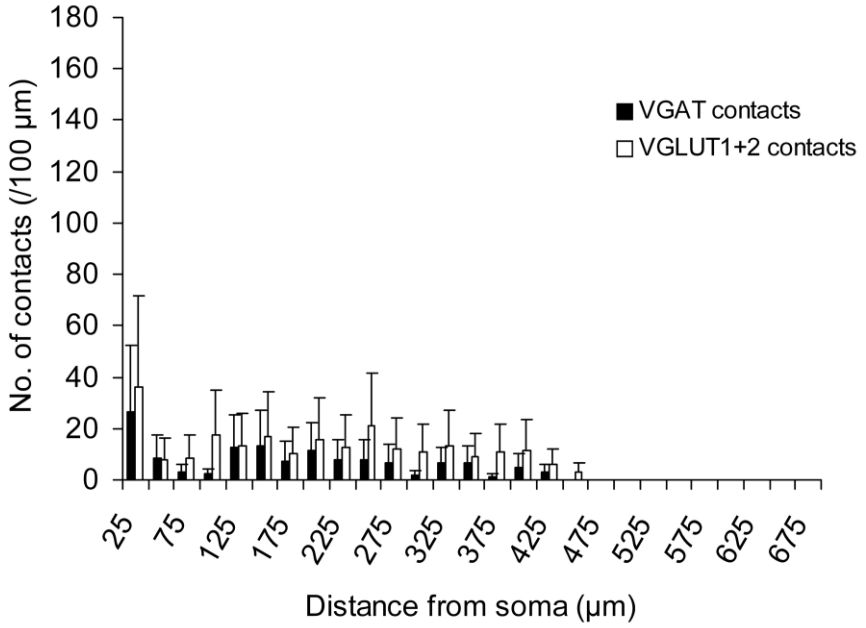

D. dhDSCT

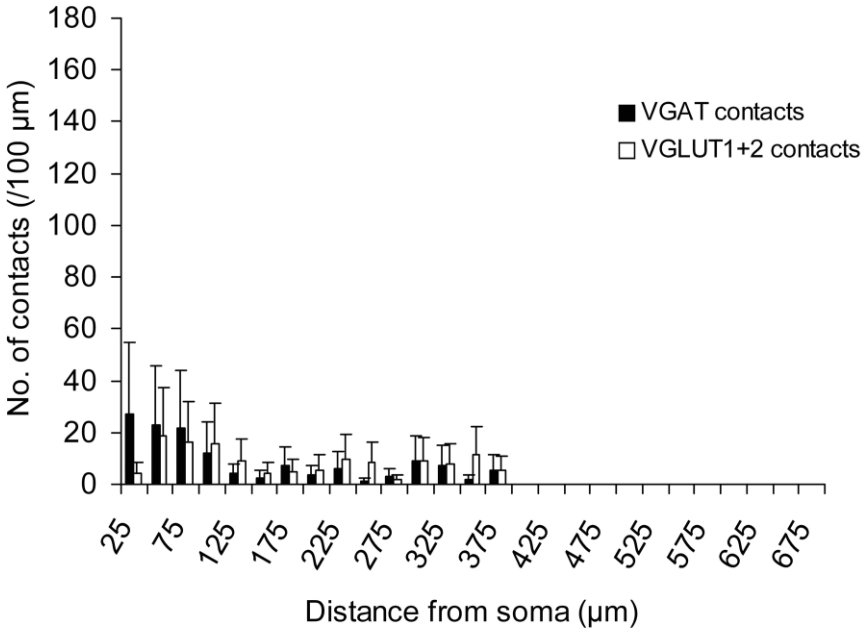

Figure 4-7 Comparison between contact densities of VGAT and VGLUT1+2 axon terminals in different populations of spinocerebellar tract neurons

***A and B*,** Differences in overall contact density of VGAT and VGLUT1+2 terminals /100 μm^2 for the four populations of spinocerebellar tract neurons in the cat. All experiments were carried out in 7 cats (12 neurons). Data presented as mean ± SD. ***C and D*,** Differences in the overall contact density of VGAT and VGLUT1+2 terminals/100 μm^2 in four populations of spinocerebellar tract neurons in the rat. All experiments were carried out in 4 rats (68 neurons). Data presented as mean ± SD. ** denotes $p<0.01$.

Cat Neurons

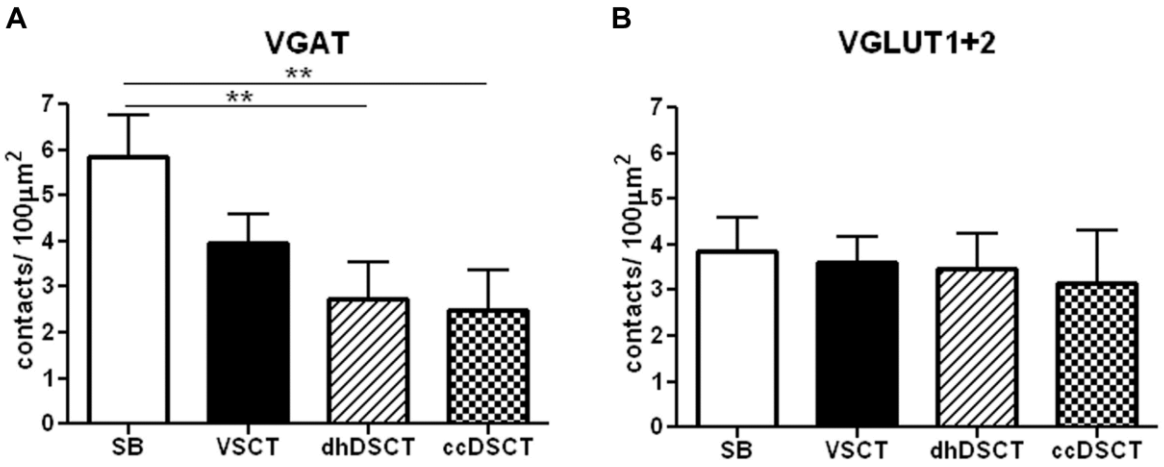

Rat Neurons

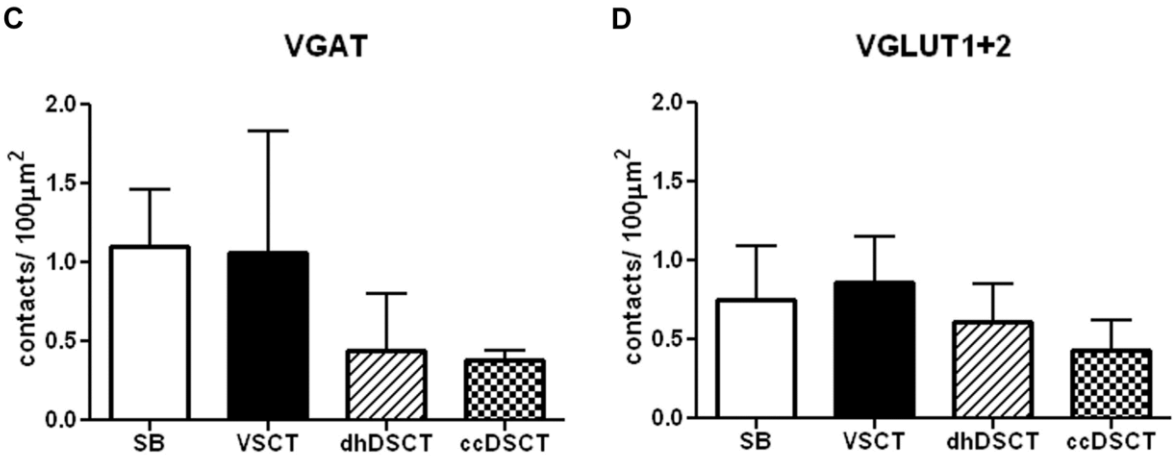

Figure 4-8 Locations of 68 analysed spinocerebellar tract neurons labelled retrogradely

A*,** Photomicrograph of a transverse section of the L1 segment of the rat spinal cord showing the location of SB neurons (1), VSCT neurons (2) and ccDSCT neurons (3) identified by retrograde transport of CTb. ***B* & *C*,** Diagrams illustrating the locations of cell bodies of 68 cells analysed in the Th12 and Th13 and in the L1, L2 and L3 segments respectively superimposed on contours of the spinal cord with Rexed´s laminae (Molander *et al.*, 1984). Scale bar in ***A 200 µm.

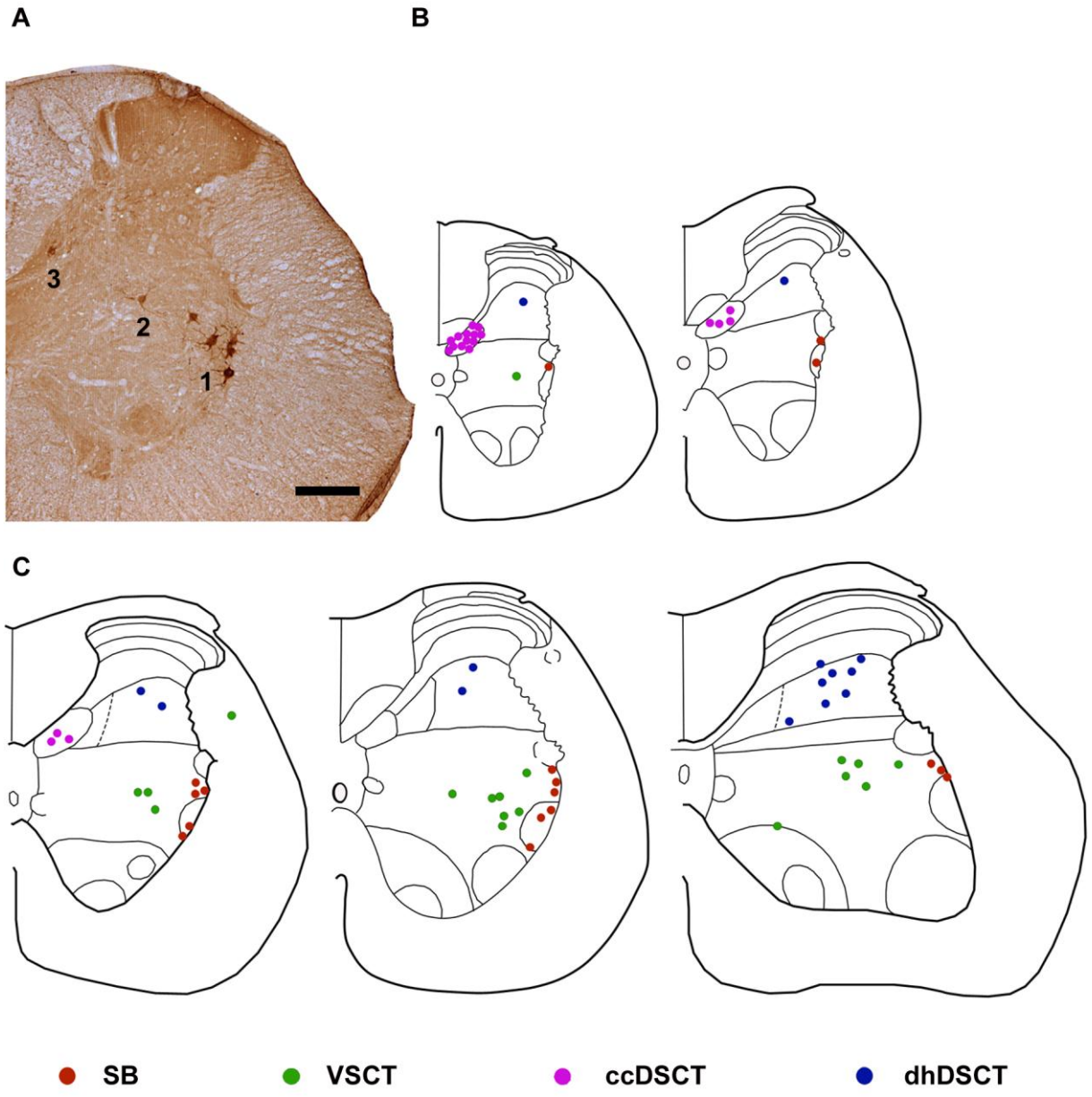
A
B
3
2
1
C
SB
VSCT
ccDSCT
dhDSCT

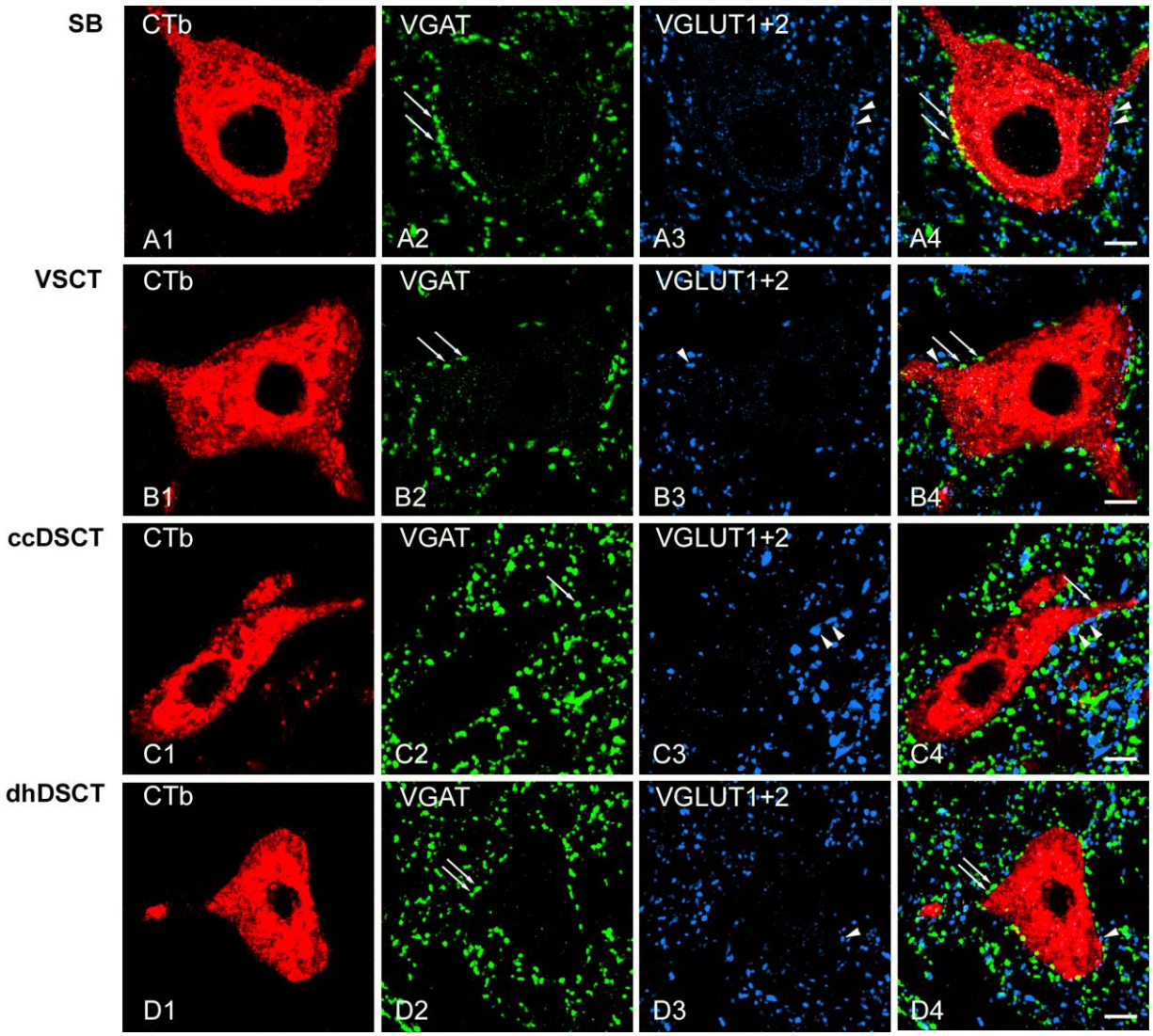

Figure 4-9 Immunohistochemical characteristics of VGAT and VGLUT1+2 axon terminals in contact with retrogradely labelled rat spinocerebellar tract neurons

A1-A4; B1-B4; C1-C4 and D1-D4, Single optical sections through the cell bodies of representative SB, VSCT, ccDSCT and dhDSCT neurons illustrating the contacts made by VGAT (green) and VGLUT1+2 (blue) immunoreactive terminals indicated by arrows and arrow heads respectively. The cell body and dendrites are in red. Scale bar in ***A-D*** = 10 μm.

Figure 4-10 Immunohistochemical characteristics of GAD axon terminals and Gephyrin puncta in apposition with intracellularly labelled spinocerebellar tract neurons

A-D, Single optical sections through the cell bodies of representative SB, VSCT, ccDSCT and dhDSCT neurons showing the presence of gephyrin puncta (green) and GAD (blue) immunoreactive axon terminals. The cell body and dendrites are in red. ***A1-A4***; ***B1-B4***; ***C1-C4 and D1-D4***, Projected images of cell bodies or dendritic trunks from cells shown in ***A***, ***B***, ***C*** *and* ***D*** respectively (areas encompassed in the boxes) illustrating contacts made by GAD immunoreactive terminals associated with gephyrin puncta and GAD negative gephyrin puncta associated with the cell indicated by arrowheads and arrows respectively. Note differences in the density of gephyrin associated with the surface of cell bodies and dendrites in all the four neuronal populations shown in ***A-D***. Scale bar in ***A-D*** = 20 μm. Scale bar in ***A1-A4***, ***B1-B4***, ***C1-C4*** and ***D1-D4*** = 5 μm.

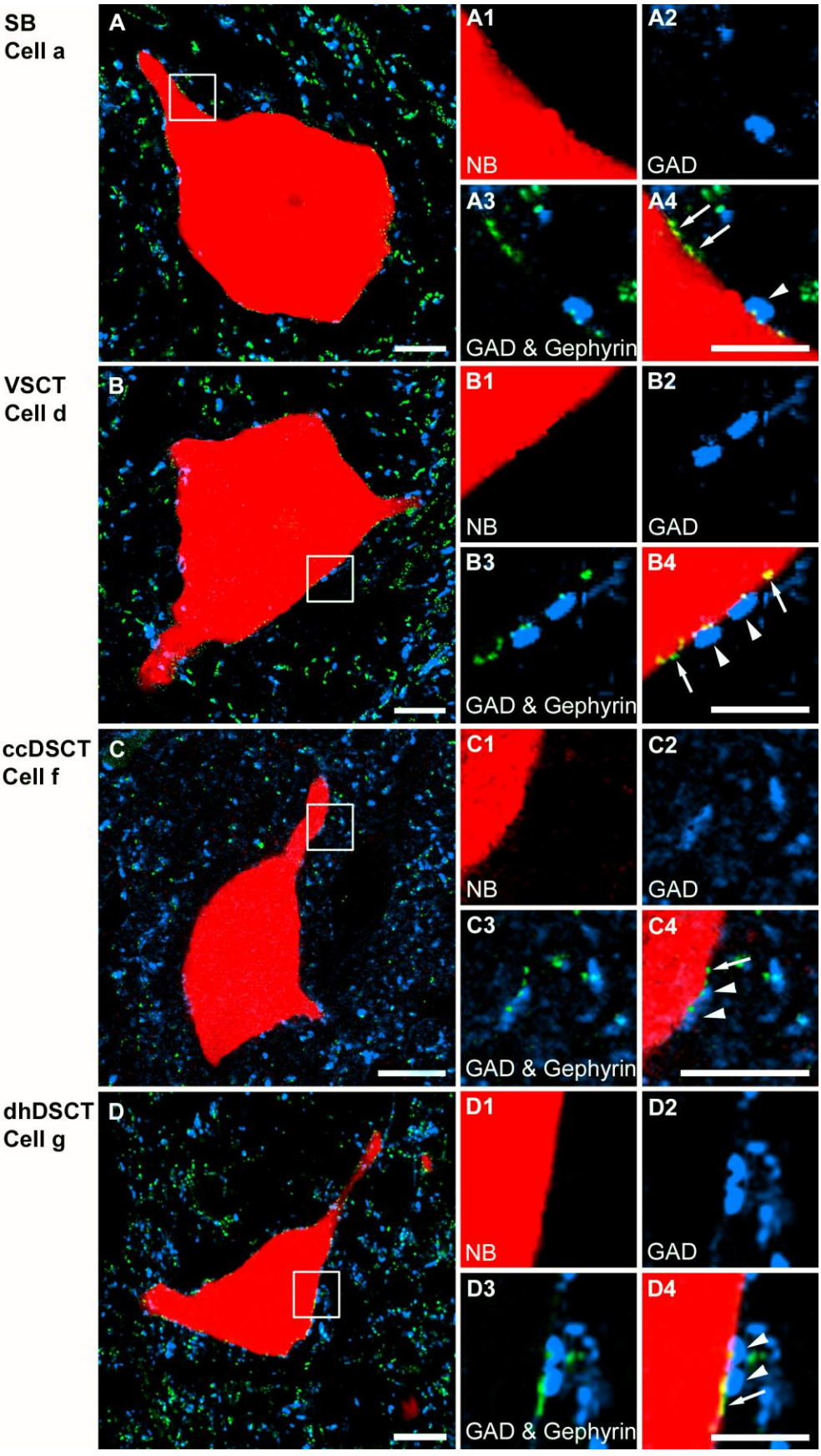
SB
Cell a
A
A1
NB
A2
GAD
A3
GAD & Gephyrin
A4
VSCT
Cell d
B
B1
NB
B2
GAD
B3
GAD & Gephyrin
B4
ccDSCT
Cell f
C
C1
NB
C2
GAD
C3
GAD & Gephyrin
C4
dhDSCT
Cell g
D
D1
NB
D2
GAD
D3
GAD & Gephyrin
D4

Figure 4-11 Reconstructions of distribution of GAD terminals associated with Gephyrin and GAD terminals only on four types of the spinocerebellar tract neurons

Reconstructions of spinocerebellar tract neurons showing the distributions of GAD terminals apposed to gephyrin puncta (green) and GAD terminals without association with gephyrin contacts (red) throughout the dendritic trees. The reconstructions were made with Neurolucida for Confocal. All the small images without contacts plotted show the reconstructions of respective cells. Cell body and dendrites are shown in light grey. Scale bars = 50 μm for reconstructions with contacts plotted and 100 μm for reconstructions without contacts. All are oriented such that the midline is to the left and the lateral borders of the grey matter to the right, as in Figure 4-2.

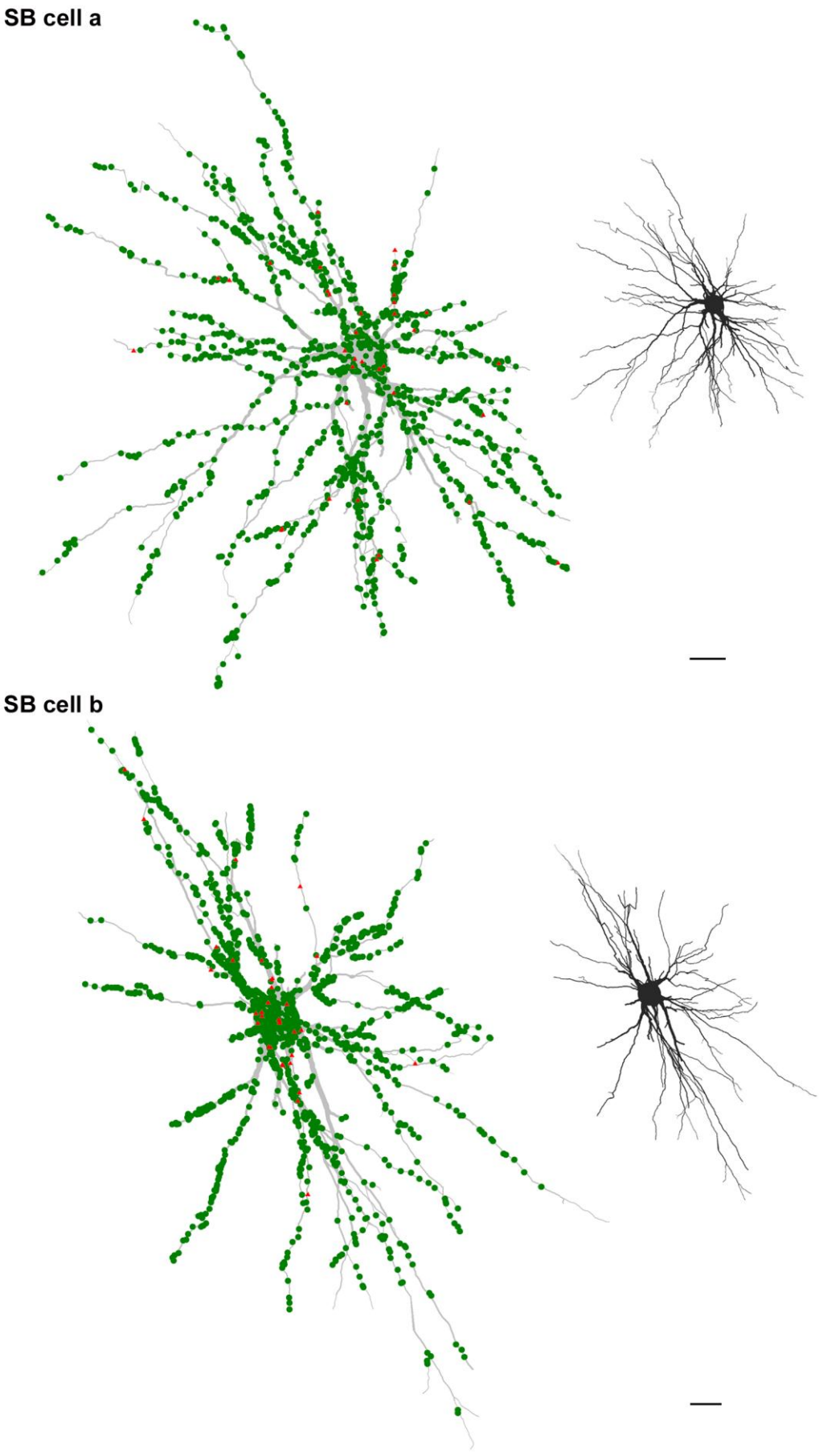
SB cell a
SB cell b

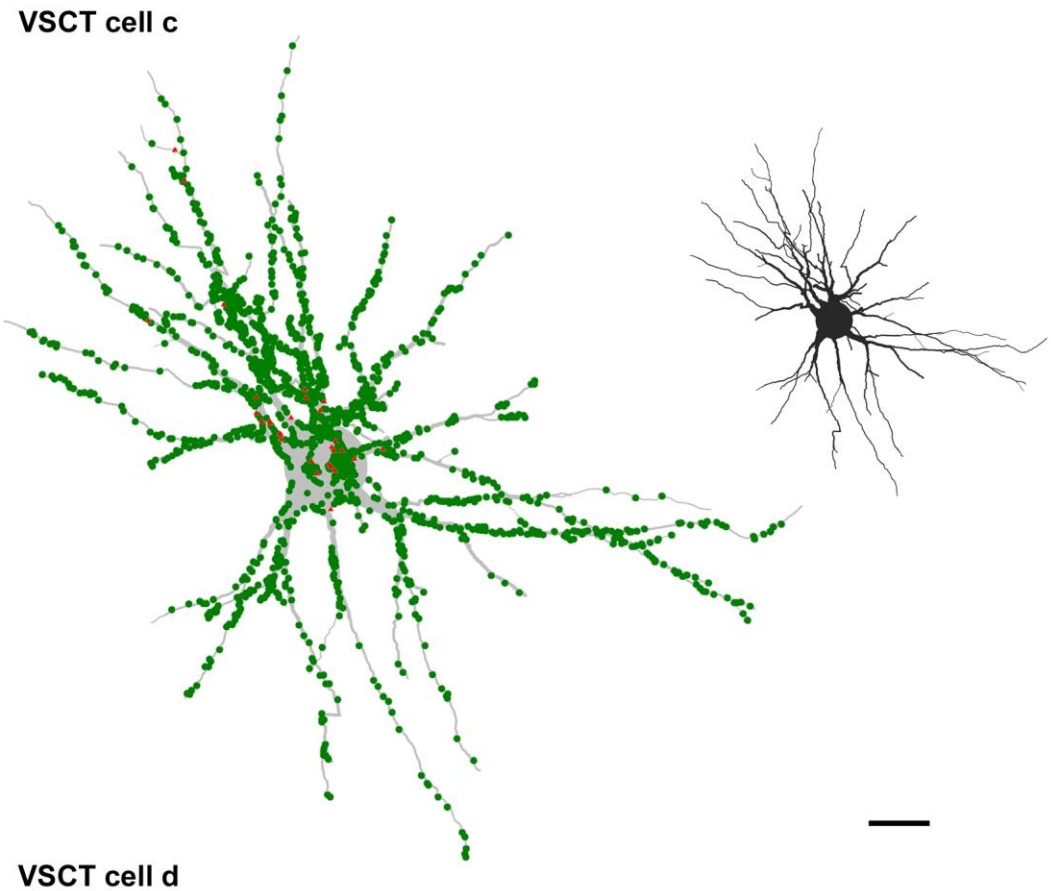
VSCT cell c

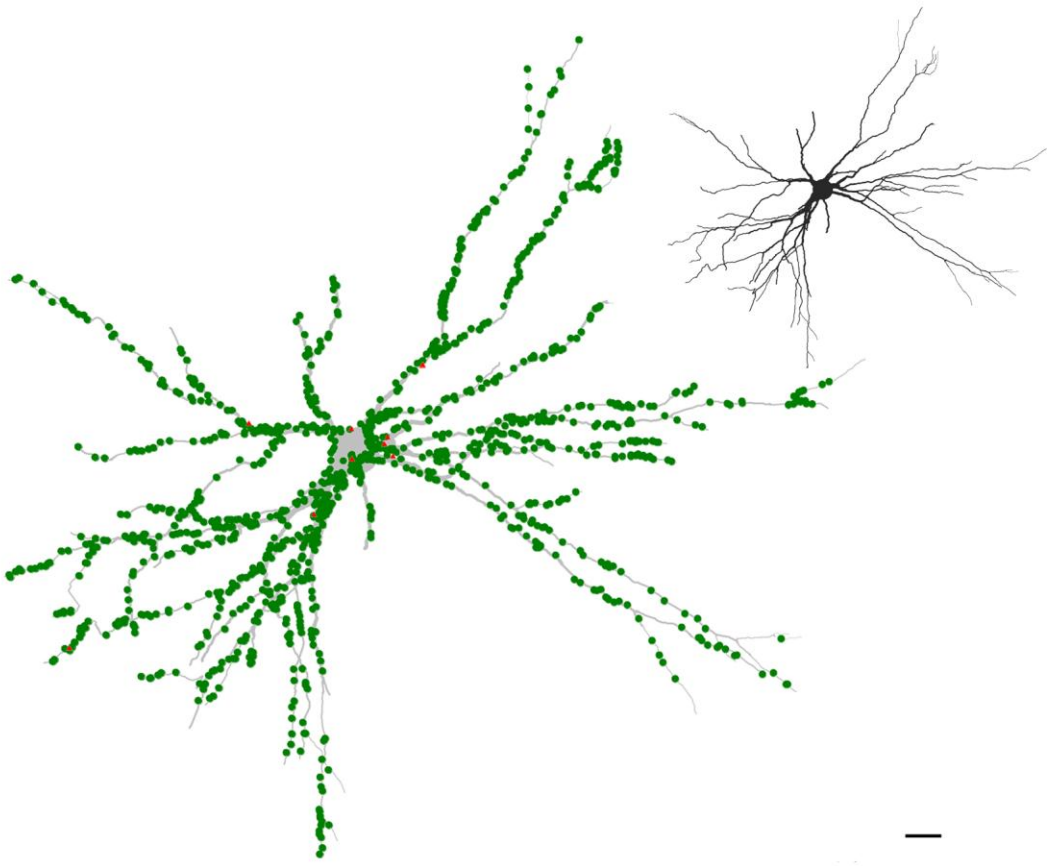
VSCT cell d

ccDSCT cell e

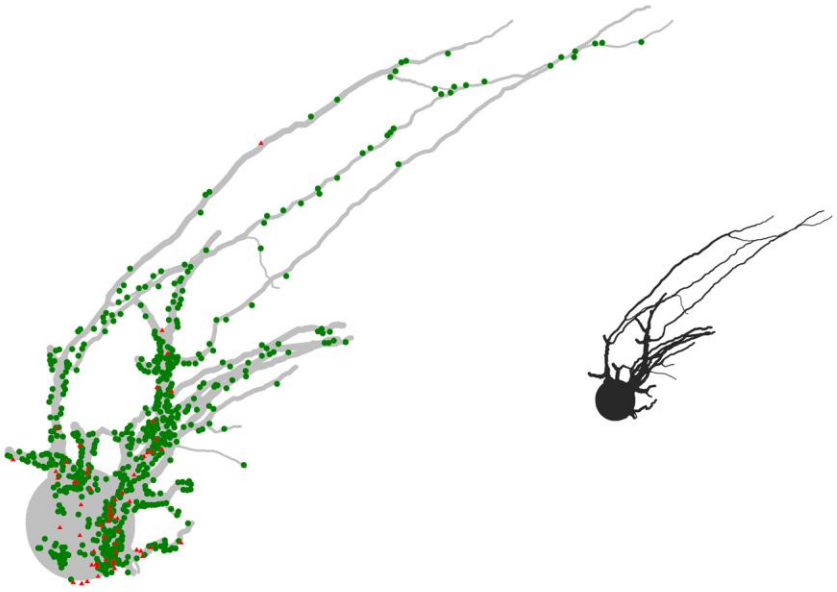

ccDSCT cell f

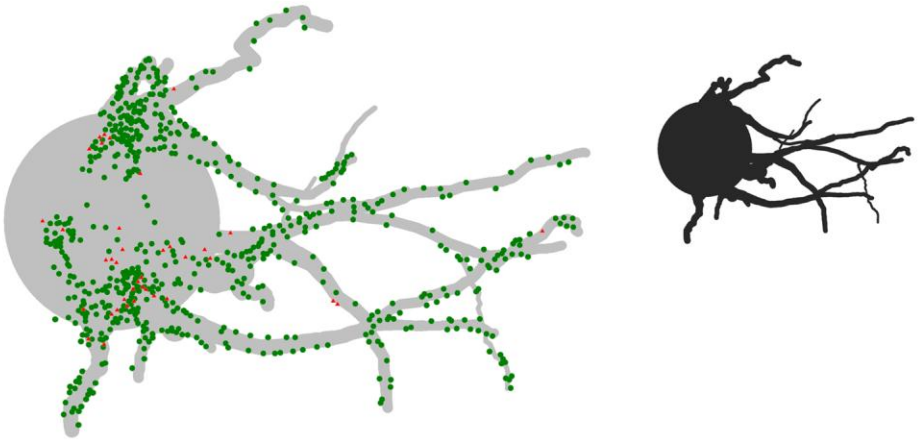

dhDSCT cell g

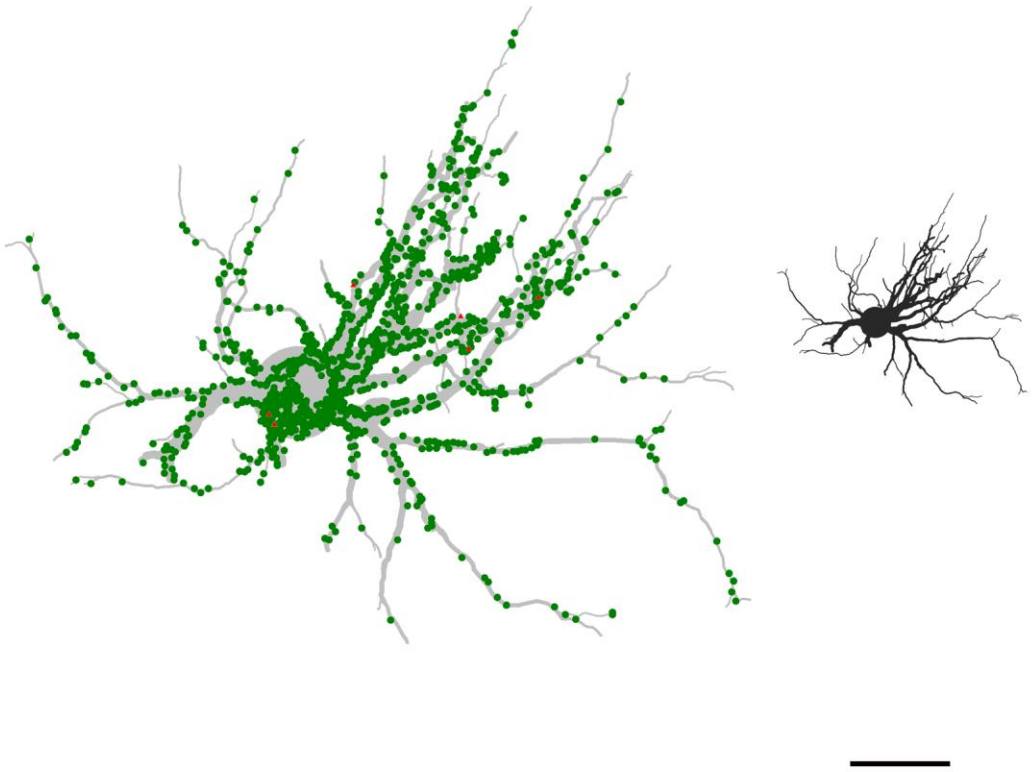

dhDSCT cell h

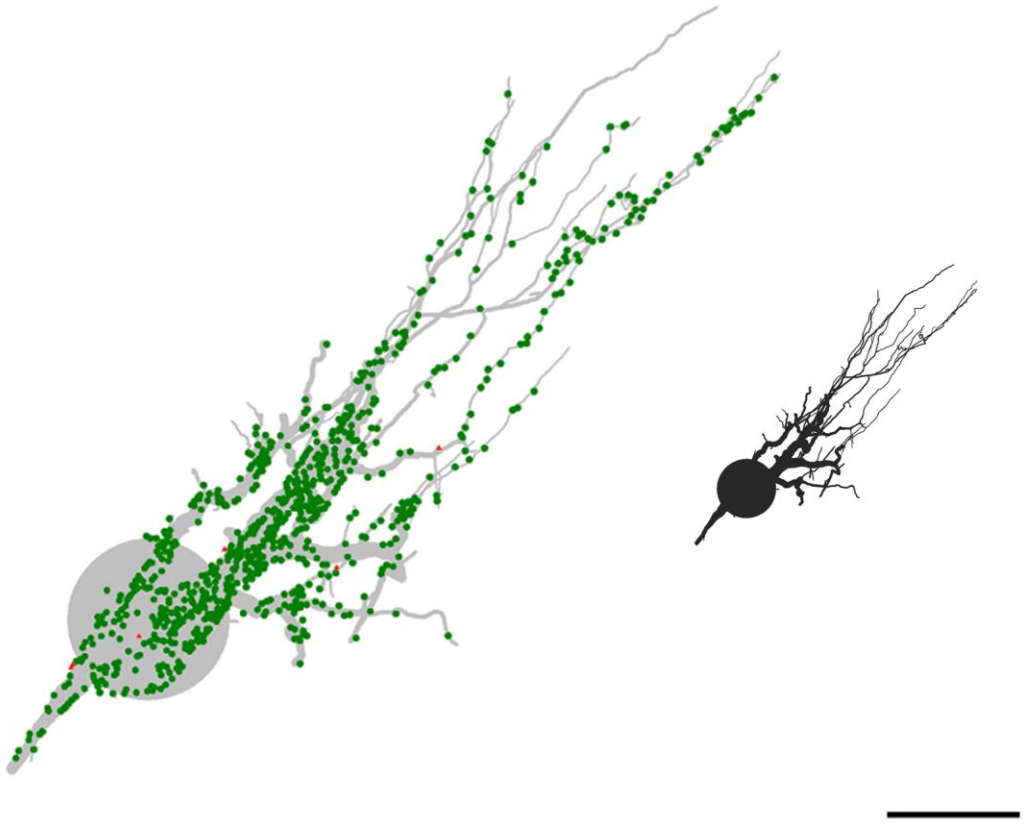

Table 4-2 The number and densities of VGAT and VGLUT1+2 axon terminals in apposition with the cell bodies and dendrites of different populations of spinocerebellar tract neurons in cats

Populations of Spinocerebellar tract cells	Cell	Contacts (total number)		Soma					Dendrite					
				Contacts (n)		Surface area (μm^2)	Density (n/ 100μm2)		Contacts (n)		Total dendritic length (μm)	Surface area (μm^2)	Density (n/ 100μm2)	
		VGAT	VGLUT1+2	VGAT	VGLUT1+2		VGAT	VGLUT1+2	VGAT	VGLUT1+2			VGAT	VGLUT1+2
SB														
	Cell 1	4864	3371	164	59	8260.33	1.99	0.71	4700	3312	9286.9	63472.452	7.40	5.22
	Cell 2	6160	3780	542	237	12445.91	4.35	1.90	5618	3543	9013.4	93367.21	6.02	3.79
	Cell 3	6026	4061	449	245	12436.47	3.61	1.97	5577	3816	10588.1	109762.29	5.08	3.48
Mean							**3.32**	**1.53**					**6.17**	**4.16**
SD							**1.21**	**0.71**					**1.17**	**0.93**
VSCT														
	Cell 4	5723	5446	286	144	20467.14	1.45	0.40	5427	5302	16815.9	153591.14	3.53	3.45
	Cell 5	5297	4655	435	416	21347.05	2.04	1.95	4862	4239	9049.1	110283.64	4.41	3.84
	Cell 6	3252	3002	235	228	8948.45	2.63	2.55	3017	2774	7172	62676.9	4.81	4.43
Mean							**2.04**	**1.63**					**4.25**	**3.91**
SD							**0.59**	**1.11**					**0.65**	**0.49**
ccDSCT														
	Cell 7	1000	1267	54	22	6081.86	0.89	0.36	946	1245	2019	22654.74	4.18	5.50
	Cell 8	1196	1306	110	52	10548	1.04	0.49	1086	1254		50451.69	2.15	2.49
	Cell 9	1543	2169	163	117	13919.93	1.17	0.84	1380	2052	5697.3	61025.78	2.26	3.36
Mean							**1.03**	**0.56**					**2.86**	**3.78**
SD							**0.14**	**0.25**					**1.14**	**1.55**
dhDSCT														
	Cell 10	2405	3104	443	196	12496.2	3.55	1.57	1962	2908	5141.6	66574.3	2.95	4.37
	Cell 11	3651	4245	446	278	17427.93	2.56	1.60	3205	3967	8229.2	90850.29	3.53	4.37
	Cell 12	2186	3052	244	330	18336.92	1.41	1.90	1942	2722	7459.3	99661.73	1.95	2.73
Mean							**2.51**	**1.69**					**2.81**	**3.82**
SD							**1.07**	**0.18**					**0.80**	**0.95**

Table 4-3 The number and densities of VGAT and VGLUT1+2 axon terminals in apposition with the cell bodies and dendrites of different populations of retrogradely labelled spinocerebellar tract neurons in rats

Populations of Spinocerebellar tract neurons	Animal	No. of Cells	Contacts (total number)		Soma					Dendrite					
					Contacts (n)		Surface area (μm^2)	Density (n/ 100 µm2)		Contacts (n)		Total dendritic length (µm)	Surface area (μm^2)	Density (n/ 100 µm2)	
			VGAT	VGLUT1+2	VGAT	VGLUT1+2		VGAT	VGLUT1+2	VGAT	VGLUT1+2			VGAT	VGLUT1+2
SB															
	Rat 1	3	54	57	22	25	6133.47	0.36	0.41	32	32	181.20	4899.74	0.65	0.65
	Rat 2	3	119	98	26	23	6212.02	0.74	0.37	93	75	163.01	2796.32	3.33	2.68
	Rat 3	8	101	63	46	24	7187.41	0.50	0.33	54	39	110.78	3072.34	1.76	1.27
	Rat 4	3	130	113	36	33	6252.74	0.00	0.53	94	80	170.5	2809.13	3.35	2.85
Mean								**0.40**	**0.41**					**2.27**	**1.86**
SD								**0.31**	**0.08**					**1.31**	**1.07**
VSCT															
	Rat 1	3	5	43	2	22	4242.53	0.05	0.52	3	21	89.20	2029.15	0.15	1.03
	Rat 2	3	116	70	43	20	5004.42	0.86	0.40	73	50	267.05	5277.05	1.38	0.95
	Rat 3	8	120	61	51	18	6759.59	0.75	0.27	69	43	113.64	2970.82	2.32	1.45
	Rat 4	3	186	123	75	30	5676.91	1.32	0.53	112	94	186.65	4006.78	2.80	2.35
Mean								**0.75**	**0.43**					**1.66**	**1.44**
SD								**0.53**	**0.12**					**1.17**	**0.64**
ccDSCT															
	Rat 1	5	20	12	7	6	3699.14	0.19	0.16	13	7	105.32	2672.64	0.49	0.26
	Rat 2	4	14	11	6	5	2484.90	0.24	0.20	8	6	53.38	1211.87	0.66	0.50
	Rat 3	6	16	23	8	9	3179.10	0.25	0.28	8	14	47.32	1281.37	0.62	1.09
	Rat 4	5	18	23	7	5	3163.77	0.22	0.16	11	18	58.22	1244.22	0.88	1.45
Mean								**0.23**	**0.20**					**0.66**	**0.82**
SD								**0.03**	**0.06**					**0.16**	**0.54**
dhDSCT															
	Rat 1	4	9	32	4	12	2670.26	0.15	0.45	6	20	163.05	3168.71	0.19	0.63
	Rat 2	3	7	21	3	7	2141.25	0.14	0.33	5	14	124.45	1736.37	0.29	0.81
	Rat 3	4	19	16	8	6	2633.30	0.30	0.23	11	10	47.68	872.18	1.26	1.15
	Rat 4	3	46	51	14	10	3166.62	0.44	0.32	33	41	92	1834.52	1.80	2.23
Mean								**0.26**	**0.33**					**0.88**	**1.20**
SD								**0.14**	**0.09**					**0.78**	**0.72**

4.4 Discussion

The present results revealed considerable differences in the total number, density and distribution of inhibitory contacts on SB, VSCT, ccDSCT and dhDSCT neurons. When taken together with the demonstration of differences in glutamatergic terminals relaying excitatory input to these neurons (see chapter 3) (Shakya-Shrestha *et al.*, 2012), the results of the present study provide a new basis for understanding the morphological substrates of the types of information forwarded to the cerebellum by different populations of spinocerebellar tract neurons. As the results were qualitatively similar in samples of intracellularly labelled cat neurons in mid-lumbar segments and for retrogradely labelled rat neurons in thoraco-lumbar segments both in this and in the previous study, the conclusions of these studies apply to at least these two species and possibly even more generally.

4.4.1 Methodological issues

Several methodological issues need to be taken into consideration before evaluating the results of this study. One of these issues is that the data on excitatory terminals with VGLUT1 and VGLUT2 together were pooled, in contrast to the previous study (see chapter 3) in which distribution of these terminals was analysed separately. Terminals using glycine, GABA or co-expressing glycine and GABA, were all labelled with an antibody against VGAT which is highly expressed in both GABAergic and glycinergic nerve endings (Burger *et al.*, 1991; McIntire *et al.*, 1997; Chaudhry *et al.*, 1998; Wojcik *et al.*, 2006; Aubrey *et al.*, 2007). This approach enabled us to maximize labelling of both excitatory and inhibitory terminals and thus allowed the proportions of inhibitory and excitatory terminals to be defined with confidence.

Another methodological issue is that of the small size of the samples of neurons used for analysis of intracellularly labelled cat neurons. However, neurons identified electrophysiologically have a great advantage over neurons identified by retrograde labelling and location because they represent functionally investigated neurons characterised previously and therefore can be classified with greater confidence and morphological features of these neurons may therefore be more

reliably related to their functions. As mentioned in previous chapter (section 3.4.1), using electrophysiological criteria for classification of neurons while searching for cells to be labelled also enables subpopulations of particular interest to be selected, e.g. a subpopulation of SB cells with a dominant inhibitory input from peripheral afferents and monosynaptic input from RetST neurons (Burke *et al.*, 1971a; Jankowska *et al.*, 2010; Hammar *et al.*, 2011). Intracellular labelling additionally allows a much more complete visualization of the whole dendritic tree. These advantages to some extent compensate for the unavoidably restricted numbers of intracellularly labelled neurons in the present samples. It can also be relied upon the comparison with the samples of the same populations of spinocerebellar tract neurons (Shakya-Shrestha *et al.*, 2012) as the differences in the distribution of VGLUT1 and VGLUT2 contacts in the present study are consistent with those in previously separately analysed VGLUT1 and VGLUT2 contacts. Furthermore, qualitatively similar findings for small samples of well labelled cat neurons along with larger samples of less completely labelled rat neurons were consistent.

Further reasons for differences in the density of contacts on spinocerebellar tract neurons in the cat and in the rat have been discussed in Chapter 3.

4.4.2 Different density and pattern of inhibitory axonal contacts on different populations of spinocerebellar tract neurons

4.4.2.1 SB and VSCT neurons

Among the four populations of spinocerebellar tract neurons, SB and VSCT neurons showed highest densities of contacts formed by VGAT positive terminals, both in the cat and the rat. As VGAT should label all inhibitory terminals containing GABA and/or Glycine (Todd and Sullivan, 1990; Chaudhry *et al.*, 1998; Wojcik *et al.*, 2006), a high density of VGAT contacts on SB and VSCT neurons and relatively small proportion associated with ccDSCT and dhDSCT neurons provides a morphological substrate for differences in inhibition of these neurons found in electrophysiological studies. Electrophysiological studies revealed particularly strong inhibitory input to

SB and VSCT neurons which in some cells of these populations practically constitutes the exclusive input from the periphery (Eccles *et al.*, 1961a; Oscarsson, 1965; Burke *et al.*, 1971a; Lundberg and Weight, 1971; Hammar *et al.*, 2011; Shakya-Shrestha *et al.*, 2012). Inhibition of these neurons has been shown to be evoked to a great extent by collateral actions of premotor interneurons, most of which would mediate disynaptic inhibition from group Ia, Ib and II afferents (Eccles *et al.*, 1961a; Lundberg and Weight, 1971; Jankowska *et al.*, 2010). It has also long been suggested that the polysynaptic IPSPs from ipsilateral FRA is a common characteristic of all the neurons belonging to the VSCT (Eccles *et al.*, 1961a; Oscarsson, 1965). Similar evidence for the depression produced by Renshaw cells on SB and VSCT neurons has been demonstrated which were shown to act in parallel to motoneurons (Hultborn *et al.*, 1971a; Lundberg, 1971; Lindstrom and Schomburg, 1973; Lindstrom and Schomburg, 1974). The same interneurons would also mediate inhibition of spinocerebellar tract neurons from descending tract neurons (Baldissera and Roberts, 1976; Baldissera and ten Bruggencate, 1976; Hammar *et al.*, 2011; Jankowska *et al.*, 2011a). As the total number of premotor interneurons in any of these pathways may amount to not more than a thousand ((Alvarez and Fyffe, 2007) for Renshaw cells) and many interneurons mediate inhibition from several sources, the finding of several thousands of inhibitory terminals on individual SB or VSCT neurons requires comment. This could indicate either multiple contacts of individual interneurons, or contacts of a considerable number of interneurons on individual spinocerebellar tract neurons, or both. In the cat, the source of inhibitory terminals may be limited to spinal interneurons or propriospinal neurons in view of lack of evidence for projections of supraspinal inhibitory neurons to lumbar segments (Hammar *et al.*, 2011, Jankowska *et al.*, 2011a, b). However, in the rat some inhibitory terminals might also originate from a proportion of inhibitory RetS neurons projecting as far caudally as lumbar segments (Holstege and Bongers, 1991, A. Du Beau, S. Shakya Shrestha & D. J. Maxwell, In press).

A variety of inhibitory interneurons and proprioneurons might contribute to inhibition of individual spinocerebellar tract neurons. Premotor interneurons would include interneurons located in the ventral horn (e.g. Ia inhibitory interneurons and Renshaw cells) as well as in the intermediate zone (e.g. group I/ II interneurons).

This is indicated not only by electrophysiological evidence but also by morphological observations based on the demonstration of glycinergic inhibitory intermediate zone interneurons with input from group I and II afferents that have terminal projection areas in the intermediate zone and in laminae VII and VIII in addition to motor nuclei (Bannatyne *et al.*, 2009). Another potential source of inhibitory terminals might be inhibitory dorsal horn interneurons activated by group II muscle afferents with terminal arborisations both contralaterally and ipsilaterally (Bannatyne *et al.*, 2006) and commissural interneurons with direct input from RetS neurons which terminate outside motor nuclei in lamina VII and VIII (Bannatyne *et al.*, 2003). Propriospinal neurons potentially could include inhibitory neurons located in the C3 and C4 segments (Alstermark *et al.*, 1984) as well as other intersegmentally operating inhibitory interneurons (Liu *et al.*, 2010b).

4.4.2.2 ccDSCT and dhDSCT neurons

Inhibitory terminals on ccDSCT and dhDSCT neurons should likewise originate from spinal neurons but from a smaller range of interneuron populations including intermediate zone inhibitory premotor interneurons in pathways from group Ib and II afferents but not Ia inhibitory interneurons and Renshaw cells (Hongo *et al.*, 1983b; Jankowska and Puczynska, 2008; Krutki *et al.*, 2011). Another source of inhibitory input to these neurons might be dorsal horn interneurons relaying information from group II afferents which are shown to have terminal projections in laminae IV, V and VI of the dorsal horn (Bannatyne *et al.*, 2006; Bannatyne *et al.*, 2009). However, in contrast to SB and VSCT neurons inhibitory input from supraspinal neurons, in particular RetS neurons as discussed above would not be expected either in ccDSCT or in dhDSCT neurons, because hardly any input from RetS neurons has been found in them, at least in the cat (Hammar *et al.*, 2011). Nevertheless, in a specific subset of ccDSCT neurons, cortically evoked inhibition has been reported which were suggested to be mediated via inhibitory interneurons (Hantman and Jessell, 2010). The smaller numbers of inhibitory contacts on ccDSCT and dhDSCT neurons found in the present study might thus be related to generally weaker inhibitory input revealed in electrophysiological studies.

4.4.3 Proportions of Glycinergic and GABAergic/ Glycinergic axon terminals on intracellularly labelled neurons in the cat

It is widely accepted that the two isoforms of the GABA-synthesizing enzyme glutamic acid decarboxylase 65 and 67 are found within GABAergic presynaptic terminals (Kaufman *et al.*, 1991) and all GABAergic neurons in the spinal cord contain both isoforms of GAD (Soghomonian and Martin, 1998; Mackie *et al.*, 2003). Similarly, there is strong evidence for the presence of gephyrin at GABAergic/ glycinergic synapses (Mitchell *et al.*, 1993; Todd *et al.*, 1995). Therefore, GAD and gephyrin are known to be reliable markers of GABAergic axon terminals and GABAergic/ glycinergic receptors respectively (Mackie *et al.*, 2003). There is considerable evidence for the coexistence of GABA and glycine in axon terminals of the spinal cord (Ornung *et al.*, 1994; Taal and Holstege, 1994; Ornung *et al.*, 1996; Ornung *et al.*, 1998; Mackie *et al.*, 2003) but there is variation in the proportions of terminals containing both transmitters depending upon their location, origin, animal age and species. Todd *et al.* (1995) reported that the great majority of boutons that were presynaptic at gephyrin-immunoreactive synapses are glycine immunoreactive. However, it seems that gephyrin is not only present at glycinergic synapses as it is also found at the postsynaptic membrane of pure GABAergic boutons (Triller *et al.*, 1987; Mitchell *et al.*, 1993). Evidence for the presence of GAD positive terminals in apposition to gephyrin puncta has been reported in the ventral horn of the adult rat (Triller *et al.*, 1987). Such terminals were present on large cells which were presumed to be motoneurons. Ornung *et al.* (1996, 1998) found that almost all the GABAergic terminals contacting motoneurons also contained glycine in the adult cat spinal cord but that a sizable proportion of contacts were pure glycinergic and only a very small proportion contained GABA alone. The present results suggest that inhibitory input to SB, VSCT, ccDSCT and dhDSCT neurons is primarily from glycinergic neurons as many gephyrin puncta which were not apposed by GAD terminals were observed. This was confirmed by calculating the contact density of GAD/gephyrin synapses and subtracting this from the contact densities calculated for VGAT (see methods in section 4.2.3). In keeping with the evidence discussed above, it is likely that most of the GABA/gephyrin synapses observed in this study represent synapses that use both

GABA and glycine as neurotransmitters. Therefore at least two types of inhibitory neurons forming contacts with spinocerebellar tract neurons may mediate different actions on these cells. The predominance of glycinergic synapses is predicted from previous anatomical studies of the adult cat which have shown that inhibitory interneurons in the dorsal horn activated by group II afferents as well as intermediate zone interneurons with input from group I/ II afferents were almost entirely glycinergic (Bannatyne *et al.*, 2006; Bannatyne *et al.*, 2009). Similarly, inhibitory commissural interneurons mediating crossed actions of RetS neurons were glycinergic but not GABAergic (Bannatyne *et al.*, 2003). Further evidence has also been provided for the presence of glycine like immunoreactivity in axon terminals of Ia inhibitory interneurons and Renshaw cells (Fyffe, 1991a), both of which have collateral projections to motoneurons (Fyffe, 1991b; Schneider and Fyffe, 1992).

4.4.4 Functional consequences of various inhibitory input to different populations of spinocerebellar tract neurons

The findings of the present study provide a new basis for understanding the organization and functional connectivity of four different populations of spinocerebellar tract neurons in the lumbar enlargement of the cat and thoraco-lumbar spinal cord of the rat. The consequences of putative excitatory connectivity on these neurons have already been discussed (chapter 3). The pattern of inhibitory contacts on four different populations of spinocerebellar tract neurons is in strong agreement with previous morphological and electrophysiological data as discussed above. Summary diagram based on findings from the present and previous report (Shakya-Shrestha *et al.*, 2012) (chapter 3) showing putative connections of inhibitory and excitatory inputs to the four classes of spinocerebellar tract neurons are summarized in Figure 4-12.

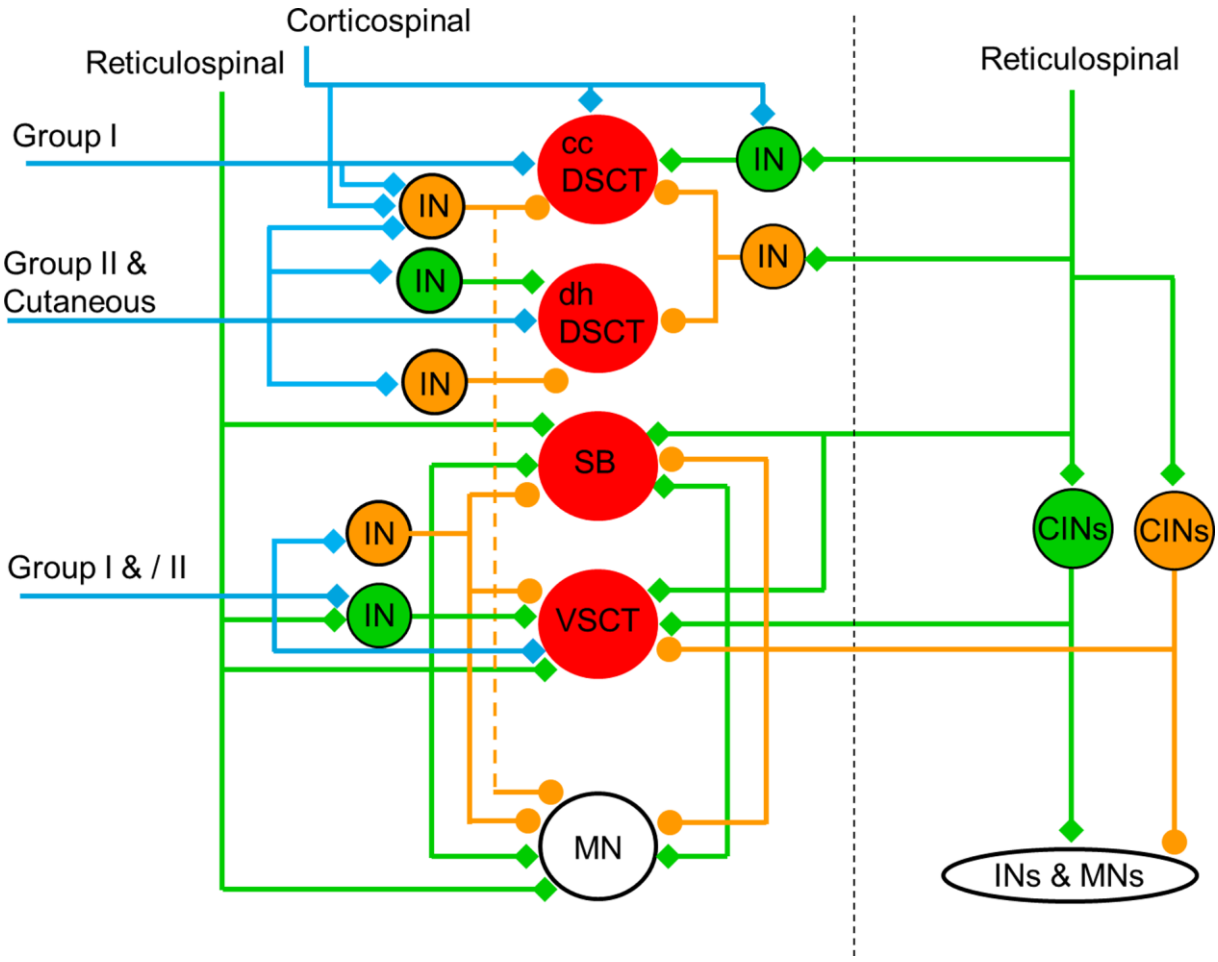

Figure 4-12 Summary of patterns of inhibitory and excitatory contacts formed with the four different populations of lumbar spinocerebellar tract neurons

Red circles represent Clarke's column dorsal spinocerebellar tract neurons (ccDSCT); dorsal horn dorsal spinocerebellar tract neurons (dhDSCT), spinal border neurons (SB), Ib-ventral spinocerebellar tract neurons (VSCT). Green circles represent excitatory interneurons in reflex pathways to motoneurons (MN) activated by primary afferents and descending systems. Blue lines and diamonds represent neurons that express vesicular glutamate transporter 1 (VGLUT1) in their axon terminals. Green lines and diamonds represent neurons that express vesicular glutamate transporter 2 (VGLUT2) in their axon terminals. Orange lines and circles represent neurons that express vesicular GABA transporter (VGAT) in their axon terminals. CINs, commissural interneurons; INs, interneurons; MNs, motoneurons.

The findings of a very high density of contacts formed by inhibitory axon terminals on SB and VSCT neurons complement findings of previous physiological studies. It can be considered that these populations of spinocerebellar tract neurons mainly monitor the degree of inhibition of motoneurons by premotor interneurons in pathways from group Ia, Ib and II afferents (Lundberg, 1971; Arshavsky *et al.*, 1972; Arshavsky *et al.*, 1984; Jankowska *et al.*, 2010). The probable diverse sources of VGAT contacts on these neurons are consistent with the hypothesis that they are components of a variety of functional networks. For example, as suggested by Jankowska *et al.* (2010) the inhibitory effects generated by premotor interneurons could be to decouple spinal interneuronal networks from cerebellar control, which might be of paramount importance under some behavioural conditions; such as during sequences of rhythmic locomotor or scratching movements. Similarly, the possibility that a certain proportion of inhibitory inputs to these neurons might be evoked from descending system (Baldissera and Roberts, 1975; Hammar *et al.*, 2011; Jankowska *et al.*, 2011a; Jankowska *et al.*, 2011b) could be of importance to prevent the errors in motor commands from higher centres and to adjust the commands relayed by RetS and RS neurons before errors are committed.

DSCT neurons have a contribution in forwarding information to the cerebellum regarding proprioceptive and extereoceptive sensory inputs. Firstly, the considerable proportion of VGAT contacts on ccDSCT neurons is consistent with previous evidence of disynaptic inhibition mediated via the same interneurons that mediate inhibition of hindlimb motoneurons from group I and/ or II afferents and would strongly support the conclusions drawn previously that not only VSCT neurons (Lundberg, 1971; Lindstrom and Schomburg, 1973), but also ccDSCT neurons monitor inhibitory interneuronal pathways to motoneurons (Hongo *et al.*, 1983a; Hongo *et al.*, 1983b; Jankowska and Puczynska, 2008). Despite the limited number of investigations on dhDSCT neurons relative to ccDSCT neurons, it can be considered that this group of neurons provides information on the activity of interneurons in inhibitory reflex pathways from group II afferents (Edgley and Jankowska, 1988; Bannatyne *et al.*, 2006) but, unlike ccDSCT neurons, the inhibitory effect produced by premotor interneurons on dhDSCT neurons was reported to be very weak (Krutki *et al.*, 2011). Finally, inhibitory input to ccDSCT

neurons derived by descending commands as discussed more recently (Hantman and Jessell, 2010) make the DSCT neurons an important candidate to integrate information from higher centres for motor planning and evaluation.

4.4.5 Functional consequences of differential distribution of inhibitory terminals

As judged by several features of IPSPs evoked in spinal motoneurons, IPSPs of different origin are evoked by inhibitory interneurons forming synapses at different locations. These different features include shapes of the IPSPs and their reversal potential, indicating that e.g. Renshaw cells terminate within the proximal dendrites of the motoneurons but Ia inhibitory interneurons closer to or on somata (Curtis and Eccles, 1959; Burke *et al.*, 1971b). A location close to the initial segment has been considered as particularly favourable for counteracting activation of the neurons. IPSPs evoked close to the initial segment may thus be most effective in preventing activation of the neurons, as an example, in the case of the arrest of firing of SB neurons during the rising phase and peak of IPSPs evoked in them by muscle afferents (Hammar *et al.*, 2011). The concentration of inhibitory synapses within 75 μm from the soma of SB neurons illustrated in Figure 4-6A and generally highest density of inhibitory terminals on the soma and proximal dendrites of SB neurons could serve this purpose. However, high concentrations of inhibitory terminals have been found within the region of the initial segment of not only SB but also other neurons even if they were generally lower indicating that activation of other spinocerebellar tract neurons might likewise be regulated in this way.

Distribution of inhibitory terminals along the whole surface of the neurons could be used for the purposes of integration of the excitatory and inhibitory inputs to spinocerebellar tract neurons and for tuning effects of excitatory terminals. The linearity of interactions between synaptic actions of the excitatory and inhibitory terminals would depend on distances between them (Rall *et al.*, 1967). Close relations between inhibitory and excitatory terminals indicated in Figures 4-3, 4-4, 4-5, 4-6 and 4-9 along not only the soma but also the whole length of the dendrites might be particularly relevant for such interactions. As illustrated in these figures

excitatory and inhibitory terminals were often located side by side, making interactions between synaptic potentials evoked by them most efficient. The irregular, clustered distribution of inhibitory terminals on dendrites of ccDSCT neurons which is best seen in Figure 4-11, is dissimilar to the parallel distribution of inhibitory and excitatory terminals observed on the other neurons and may be indicative of a particular kind of processing of information by these neurons. Excitatory input to ccDSCT neurons comes largely from VGLUT1-containing primary afferents (see chapter 3) (Shakya-Shrestha *et al.*, 2012). These terminals form 'giant' boutons with ccDSCT cells that are under very limited presynaptic inhibitory control (Walmsley *et al.*, 1985) and have very powerful 'all or nothing' excitatory effects. Clusters of inhibitory terminals on specific regions of dendritic trees could produce powerful shunting inhibition that may selectively modulate specific excitatory inputs. The spatially close locations of glycinergic and glutamatergic terminals might also be of importance for effects of glycine on NMDA sites of glutamatergic synapses (Berger *et al.*, 1998). The predominance of either the excitatory or inhibitory terminals on some of the dendrites, especially of ccDSCT and dhDSCT neurons might on the other hand be an indication of specialisation of some dendrites of these neurons (Korogod *et al.*, 2000).

4.4.6 Comparison of distribution of inhibitory terminals on spinocerebellar tract neurons and on other neurons

To the best of my knowledge this is the first report documenting the distribution of excitatory and inhibitory terminal contacts on extensively reconstructed dendritic trees of a specific group of neurons. Previous studies have concentrated on the cell bodies or short sections of dendrite (Ornung *et al.*, 1996; Ornung *et al.*, 1998). Distribution of inhibitory terminals on neurons has often been reported in fairly general terms previously. For example, Alvarez and Fyffe (2007) reported that "Renshaw cells uniquely displayed a high density of proximal inhibitory synapses". On spinal motoneurons, glycine positive terminals were reported to be widespread, similar to spinocerebellar tract neurons analysed presently, but it is difficult to make a direct comparison with these findings as information is given in terms of the proportions of terminals on the somatic (18-38%) and proximal dendritic (17-45%)

compartments (Destombes *et al.*, 1992). Perhaps the best studied type of neuron with respect to inhibitory input is the CA1 pyramidal cell of the hippocampus (e.g. (Klausberger and Somogyi, 2008). These cells are contacted by a diversity of inhibitory interneurons that target specific subcellular domains of pyramidal cells and have particular effects on their firing patterns. It can only be speculated at present on the origin, subcellular targets and effects of the inhibitory terminals that contact spinocerebellar tract cells. In future studies it would be of interest to determine the origin and properties of inhibitory contacts on initial axon segments which control activation of neurons and compare this with dendritic contacts where inhibitory input is utilised primarily for tuning of excitatory input.

In conclusion, the present findings are of relevance to understanding the functional organization of four populations of spinocerebellar tract neurons. This study shows that SB population of VSCT neurons with dominating inhibitory inputs from peripheral afferents have vast majority of contacts made by VGAT immunoreactive terminals. However similar proportions of inhibitory and excitatory contacts were associated with VSCT, ccDSCT and dhDSCT neurons though excitatory inputs dominated in ccDSCT and dhDSCT neurons. In all of the cells, the majority of inhibitory terminals were glycinergic. Variations in the density and distribution of inhibitory contacts found in this study may reflect differences in information on inhibitory processes forwarded by subtypes of spinocerebellar tract neurons to the cerebellum.

5 Origin of excitatory and inhibitory contacts on different populations of spinocerebellar tract neurons

5.1 Introduction

An understanding of how spinocerebellar tract neurons contribute to the control of motor behaviour from higher centres requires a full knowledge of the neural circuits in which different components of these neurons are involved. It has been demonstrated that different populations of spinocerebellar tract neurons receive direct and indirect inputs from proprio- and exteroceptors or network of intrinsic spinal neurons or various descending pathways (Oscarsson, 1965; Lundberg, 1971; Lindstrom and Schomburg, 1973; Arshavsky *et al.*, 1978b; Bosco and Poppele, 2001). These studies have also shown that if one component exclusively receives direct input from primary afferents then others may have dominating input from spinal interneurons or descending pathways. Addressing these issues, various electrophysiological studies have provided evidence for the origin of inputs to these neurons. For example, ccDSCT neurons have a major input from group Ia afferents (Eccles *et al.*, 1961b) while dhDSCT neurons are strongly activated by group II afferents (Edgley and Jankowska, 1988) whereas VSCT neurons including SB neurons are primarily modulated by Ia inhibitory interneurons (Eccles *et al.*, 1961a; Lundberg, 1971), Renshaw cells (Lindstrom and Schomburg, 1973) and also group I/ II interneurons (Jankowska *et al.*, 2010). Similarly, attempts have been made to investigate various sources of descending inputs to these neuronal populations (Hongo and Okada, 1967; Baldissera and Weight, 1969; Baldissera and Roberts, 1976; Fu *et al.*, 1977; Hantman and Jessell, 2010; Hammar *et al.*, 2011). It has been shown that ccDSCT neurons receive both excitatory and inhibitory inputs from CS neurons (Hantman and Jessell, 2010) and VSCT neurons are activated or inhibited by the action of RetS (Baldissera and Weight, 1969; Hammar *et al.*, 2011), VS (Baldissera and Roberts, 1976), CS (Fu *et al.*, 1977) and RS neurons (Jankowska *et al.*, 2011a). All the evidence suggests that the peripheral, spinal and supraspinal control of different populations of spinocerebellar tract neurons that anticipates their actions on motoneurons and interneurons of reflex pathways is of paramount

importance for coordinated movements evoked from higher centres. However, despite several indications for the existence of complex neuronal networks with a key role of spinocerebellar tract neurons in coding diverse signals and forwarding information to the cerebellum, morphological basis and the functional connectivity of spinocerebellar tract cells is poorly understood.

This issue was addressed with respect to the four different populations of spinocerebellar tract neurons. There were three principal aims: The first aim was to investigate the proportion of excitatory inputs originating from proprioceptors. The second aim was to characterize excitatory and inhibitory interneurons which formed contacts with spinocerebellar tract neuronal populations. Both of these aims were achieved by carrying out experiments in the cat and the rat. Finally, the third aim was to analyze the proportion of the inputs that originates directly from two major descending pathways (RetST and CST). A supplementary analysis was also carried out to characterize neurotransmitter phenotypes and termination patterns of VST and RST neurons (A. Du Beau, S. Shakya Shrestha & D. J. Maxwell, In Press).

The advances of various neurochemical markers specific for specific neuronal groups have aided in characterizing different populations of neurons. Improvements in immunohistochemical techniques allow identification of colocalisation patterns of these components and this approach can be used to provide information on the origin and functional properties of neurons. In the present study various neurochemical markers were used to establish the sources of excitatory and inhibitory contacts on four populations of spinocerebellar tract neurons. In order to address the first aim, two different markers were used: VGLUT1 and parvalbumin (PV). The reason for choosing these markers is that VGLUT1 is widely accepted to be expressed in the axon terminals of primary afferents including myelinated primary afferents (Varoqui *et al.*, 2002; Todd *et al.*, 2003; Alvarez *et al.*, 2004) and parvalbumin (PV) has likewise been known to be preferentially expressed in large-diameter primary afferents (Celio, 1990; Zhang *et al.*, 1990). Therefore, any terminals immunopositive for both of these markers are likely to have originated from proprioceptors. Similarly, previous studies have shown that immunoreactivities to different calcium binding proteins: calbindin (CB), calretinin (CR) and PV

(Garcia-Segura *et al.*, 1984; Celio, 1990; Zhang *et al.*, 1990; Resibois and Rogers, 1992; Rogers and Resibois, 1992) can be used to identify distinct neuronal populations in the central nervous system. It is also well established that VGAT labels GABAergic/ glycinergic axon terminals (Burger *et al.*, 1991; McIntire *et al.*, 1997; Chaudhry *et al.*, 1998) and VGLUT1 and VGLUT2 (Varoqui *et al.*, 2002; Todd *et al.*, 2003; Alvarez *et al.*, 2004) are the reliable markers for the glutamatergic nerve terminals. Therefore, combination of these markers (see Table 5-2) can be used to visualize their presence and colocalisation in particular neurons/ terminals which enables to characterize excitatory and inhibitory interneurons which formed contacts with different populations of spinocerebellar tract neurons. Thus this approach can be used to fulfil the second aim. Further, to address the third aim, excitatory and inhibitory inputs from labelled RetS and CS neurons can be characterized by using VGLUT1/2 and VGAT as mentioned above (see details in methods below). RetS terminals are known to be heterogeneous population, majority of which express VGLUT2 while a small proportion express VGAT while CS terminals exclusively express VGLUT1 (A. Du Beau, S. Shakya Shrestha & D.J. Maxwell, In press).

The study was conducted on electrophysiologically characterized spinocerebellar tract neurons in cats which were injected with a mixture of rhodamine-dextran and neurobiotin. In the rat, these neuronal populations were labelled by retrograde transport of CTb injected into the cerebellum. In addition, to address the third aim, RetS and CS terminals were identified by anterograde transport of CTb from the caudal medulla and hindlimb sensory motor cortex respectively in rats along with labelling of spinocerebellar tract neurons by retrograde injection of Fluorogold into the cerebellum. In order to compare the RetS inputs from medial versus lateral reticular formation, injections were made in two different sites of caudal medulla (MLF and CVLM). Different populations of spinocerebellar tract neurons were then classified according to their anatomical location which is similar to that of cat spinocerebellar tract neurons (Matsushita and Hosoya, 1979; Matsushita *et al.*, 1979).

5.2 Methods

All experimental procedures were approved by the Ethics committee as mentioned in Chapter 2.

5.2.1 Experimental procedures on cats

Surgical procedures, stimulation, identification and labelling of the four populations of spinocerebellar tract neurons in all animals were carried out following the procedures mentioned in detail in Chapter 2, Section 2.1.

5.2.2 Experimental procedures on rats

Stereotaxic surgery was performed on four adult male Sprague Dawley rats (250 – 350g) following the procedures described in detail in General experimental procedures (Chapter 2, Section 2.2). Retrograde injection with CTb was done at inter-aural co-ordinates -4.2 mm (anterior-posterior) and +2.0 mm (medio-lateral) at a dorso-ventral co-ordinate of +4.5 mm in the cerebellum (Paxinos and Watson, 1997). Injection sites were identified by using DAB as a chromogen and the location of site was determined with reference to the stereotaxic rat brain atlas (Paxinos and Watson, 1997) as described previously (see chapter 2, Section 2.2).

5.2.3 Immunohistochemistry, confocal microscopy, reconstructions and analysis

L3 – L6 segments of the cat and Th12 – L3 segments of the rat (see rationale in section 3.1) were cut into 50 µm thick transverse sections with a Vibratome (Oxford instruments, Technical products international Inc. USA) and processed following the procedure described in Section 2.1 and 2.2. Intracellularly labelled neurons with Neurobiotin and Rhodamine were first revealed using an Avidin-Rhodamine reaction and sections containing well labelled cells were selected with the help of florescence microscope. Both the cat and rat sections were then processed for immunocytochemistry.

AIM I: Investigation of the proportion of direct excitatory inputs from proprioceptors to different populations of spinocerebellar tract neurons

In order to fulfill this aim, immunohistochemical reactions were performed by using antibodies against VGLUT1 and one of the members of low molecular weight calcium binding proteins, PV in both species (see Introduction in section 5.1). Selected sections containing intracellularly labelled neurons in cats were first washed several times in PBS and thereafter incubated in a combination of primary antibodies containing rabbit anti-VGLUT1 and guinea pig anti-PV for 72 hours at 4º C. Following several washes in PBS, the sections were incubated in a combination of secondary antibodies coupled to Dylight 649 and Alexa 488 for 3 hours at room temperature to identify axon terminals containing VGLUT1 and PV respectively. They were then rinsed in PBS, mounted on glass slides and coverslipped with Vectashield. All antibodies were diluted in PBST (see Table 5-1 for details of antibodies used).

Table 5-1 Summary of the primary and secondary antibody combinations and concentrations used

	Primary antibody combination	Primary antibody concentration	Supplier	Secondary antibody combination	Secondary antibody concentration	Supplier
Cat	rbt VGLUT1	1:5000	Synaptic systems, UK	Dylight 649	1:500	Jackson ImmunoResearch, West Grove, USA
	gp PV	1:2500	M. Watanabe, Hokkaido University School of Medicine	Alexa 488	1:500	Molecular Probes, Eugene, USA
Rat	gt CTb	1:5000	List (quadratech)	Rh. Red	1:100	Jackson ImmunoResearch, West Grove, USA
	rbt VGLUT1	1:5000	Synaptic systems, UK	Dylight 649	1:500	Jackson ImmunoResearch, West Grove, USA
	gp PV	1:2500	M. Watanabe, Hokkaido University School of Medicine	Alexa 488	1:500	Molecular Probes, Eugene, USA

All secondary antibodies were raised in donkey and conjugated to Rh. Red, Rhodamine Red; Alexa 488, Alexa-fluor 488;Dylight 649; gp, guineapig; gt, goat; rbt, rabbit; CTb, B- subunit of cholera toxin; PV, Parvalbumin; VGLUT, Vesicular glutamate transporter

In both series of experiments in cats and rats, the sections were scanned by using three channels of a confocal laser scanning microscope following the procedure described in chapter 2, section 2.1. VGLUT1 immunoreactive terminals were imaged as blue, while terminals containing PV were visualized in green. Further, axon terminals expressing both the markers were imaged as turquoise. Reconstructions of neurons were done as described in chapter 2. VGLUT1, PV and VGLUT1+PV

contacts were plotted and the number of contacts was expressed per unit surface area of the neurons.

AIM II- Characterization of excitatory and inhibitory interneurons which formed contacts with different populations of spinocerebellar tract neurons

This aim was addressed by using antibodies raised against CB, CR and PV together with either VGAT or VGLUT1/ 2 (see section 5.1 and details in Table 5-2).

In the first series of experiment in cats this investigation was carried out with particular reference to SB and VSCT neurons. As demonstrated in chapter 3, these neuronal populations have major input from VGLUT2 positive terminals which probably originate principally from interneurons. This investigation was complemented by analyzing all four populations of spinocerebellar tract neurons in the rat. More generalized investigation of the proportion of excitatory and inhibitory inputs to these neuronal populations which were associated with different calcium binding proteins was done using different combinations of antibodies listed in Table 5-2 (Rat section). As shown in Table 5-2, a combination of VGLUT1 and VGLUT2 was used in this series of experiment to examine the excitatory nature of CB or CR containing terminals. Nevertheless, it is worth noting that CB and CR are expressed in interneurons in the spinal cord (Celio, 1990; Arvidsson *et al.*, 1992; Sanna *et al.*, 1993; Alvarez *et al.*, 2005; Liu *et al.*, 2010b), hence, all the axon terminals containing either or both of these proteins which co-express VGLUT1+2 can be considered to originate from interneurons. In addition, a proportion of the inhibitory contacts that originate from PV containing axon terminals were also examined in retrogradely labelled neurons in rats.

In a series of experiments in the cat, a sequential immunohistochemical technique was performed as described in chapter 2, section 2.3. Selected sections containing intracellularly labelled neurons were first reacted with the following antibodies: CB and CR (Cat section, group A and B in Table 5-2). The sections were then scanned using the confocal microscope and contacts were analysed as described in chapter 2, section 2.4. When analysis of sections with the initial combination of antibodies

was complete, sections were removed from the glass slides and following several washes in PBS, were sequentially incubated in either anti-VGLUT2 or anti-VGAT (Cat section, group A and B in Table 5-2). The sections were remounted and the field that was scanned previously was identified and re-scanned. By comparing the labelling before and after the sequential incubation, the additional staining for either VGLUT2 or VGAT could be detected. Axon terminals which were positive for both CB and either VGLUT2/ VGAT were magenta in colour as a consequence of the extra red labelling on the original blue while both CR and either VGLUT2/ VGAT immunoreactive terminals were yellow in colour because of a mixture of green (CR terminals) and red (VGLUT2/ VGAT terminals). Similarly, axon terminals which contained both of these calcium binding proteins when colocalised with either VGLUT2/ VGAT appeared in white.

In a second series of experiments in rats, sections containing retrogradely labelled cells with CTb were reacted with CTb antiserum along with one of the following antibodies: CB and VGLUT1+2/ VGAT (Rat section, group A & B in Table 5-2); CR and VGLUT1+2/ VGAT (Rat section, group C & D in Table 5-2) and PV and VGAT (Rat section, group E in Table 5-2). Terminals double-labelled with CB and CR could not be examined in this series of experiment because, no sequential incubation was performed unlike in the cat, instead sections were incubated separately in CB and CR either with VGLUT1+2 or VGAT. Therefore, using three colour imaging, all double labelled terminals with either CB/ CR/ PV and VGLUT1+2/ VGAT were visualized as turquoise.

Reconstructions of the neurons were made as described in chapter 2 (section 2.4). In intracellularly labelled cells in cats, contacts made by CB/ CR/ CB and CR terminals with or without colocalisation of VGLUT2/ VGAT were examined while in rats, appositions made by CB/ CR/ PV with or without co-expression of VGLUT1+2/ VGAT were examined. In both series of experiments, contact density of these terminals was calculated and expressed per 100 μm^2 of the neuronal surface area.

Table 5-2 Summary of the primary and secondary antibody combinations and concentrations used

	Primary antibody combination	Primary antibody concentration	Supplier	Secondary antibody combination	Secondary antibody concentration	Supplier	Sequential immuno-reaction	Secondary antibodies
Cat A	rbt CB	1:1000	Swant, Bellizona, Switzerland	Dylight 649	1:500	Jackson ImmunoResearch, West Grove, USA	gp VGLUT2 (1:5000)	Rh. Red
	gt CR	1:1000	Swant, Bellizona, Switzerland	Alexa 488	1:500	Molecular Probes, Eugene, USA		
B	rbt CB	1:1000	Swant, Bellizona, Switzerland	Dylight 649	1:500	Jackson ImmunoResearch, West Grove, USA	mo VGAT (1:5000)	Rh. Red
	gt CR	1:1000	Swant, Bellizona, Switzerland	Alexa 488	1:500	Molecular Probes, Eugene, USA		
Rat A	gt CTb	1:5000	List (quadratech)	Rh. Red	1:100	Jackson ImmunoResearch, West Grove, USA		
	gp VGLUT1 & 2	1:5000	Chemicon, Harlow, UK	Alexa 488	1:500	Molecular Probes, Eugene, USA		
	rbt CB	1:1000	Swant, Bellizona, Switzerland	Cy-5	1:100	Molecular Probes, Eugene, USA		
B	gt CTb	1:5000	List (quadratech)	Rh. Red	1:100	Jackson ImmunoResearch, West Grove, USA		
	mo VGAT	1:5000	Synaptic systems, UK	Alexa 488	1:500	Molecular Probes, Eugene, USA		
	rbt CB	1:1000	Swant, Bellizona, Switzerland	Cy-5	1:100	Molecular Probes, Eugene, USA		
C	mo CTb	1:250	A. Wikström, University of Gothenburg	Rh. Red	1:100	Jackson ImmunoResearch, West Grove, USA		
	rbt VGLUT1 & 2	1:5000	Synaptic systems, UK	Alexa 488	1:500	Molecular Probes, Eugene, USA		
	gt CR	1:1000	Swant, Bellizona, Switzerland	Cy-5	1:100	Molecular Probes, Eugene, USA		
D	mo CTb	1:250	A. Wikström, University of Gothenburg	Rh. Red	1:100	Jackson ImmunoResearch, West Grove, USA		
	rbt VGAT	1:5000	Synaptic systems, UK	Alexa 488	1:500	Molecular Probes, Eugene, USA		
	gt CR	1:1000	Swant, Bellizona, Switzerland	Cy-5	1:100	Molecular Probes, Eugene, USA		
E	mo CTb	1:250	A. Wikström, University of Gothenburg	Rh. Red	1:100	Jackson ImmunoResearch, West Grove, USA		
	rbt VGAT	1:5000	Synaptic systems, UK	Alexa 488	1:500	Molecular Probes, Eugene, USA		
	gt PV	1:1000	Swant, Bellizona, Switzerland	Dylight 649	1:500	Jackson ImmunoResearch, West Grove, USA		

All secondary antibodies were raised in donkey and conjugated to Rh. Red, Rhodamine Red; Cy-5, Cyanine 5.18; Alexa 488, Alexa-fluor 488;Dylight 649; gp, guineapig; gt, goat; rbt, rabbit; mo, mouse; CTb, B- subunit of cholera toxin;VGAT, Vesicular GABA transporter; VGLUT, Vesicular glutamate transporter

AIM III- Comparison of proportion of contacts that directly originates from the RetS and the CS pathways in the rat

This aim was fulfilled by utilizing a combination of tract tracing and immunohistochemistry in rats. Two different tracers were injected in different target sites in the same animal. Fluorogold (FG) was injected into the cerebellum to label spinocerebellar tract neurons and CTb was injected into one of the following: medial medulla, lateral medulla or hindlimb motor cortex to label the RetS and CS axon terminals in the spinal cord. This approach allowed me to establish direct connections between different descending pathways and different populations of spinocerebellar tract neurons. In addition immunohistochemistry was used to determine if contacts made by these terminals are excitatory or inhibitory. Therefore, in order to investigate direct monosynaptic excitatory and inhibitory inputs from the RetS pathway to spinocerebellar tract neurons, both VGLUT2 and VGAT was used whereas immunoreactivity against VGLUT1 alone was used for analysis of direct excitatory cortico-spinocerebellar connections (see section 5.1 and details in Table 5-3).

Experimental procedure for labelling RetS terminals and spinocerebellar tract neurons

The general surgical procedure used in this part of the study is similar to that described in chapter 2. Six adult male Sprague Dawley rats (250 – 350-g) were deeply anesthetized with an intraperitoneal injection of Ketamine and Xylazine (2:1 0.1ml/ 100g) and placed in a stereotaxic frame under strict aseptic conditions. The skin at the back of the head was cut in the midline and the skull was exposed. In order to label the RetS terminals and make comparison between the inputs from the medial versus lateral reticular formation, injections were made in two different sites of caudal medulla. In three rats, injections were made in the medial part of medulla in the MLF and in the other three rats injection was targeted to the caudal ventrolateral medulla (CVLM). For the first group of rats (MLF injection), a small burr hole was made on the left hand side at inter-aural co-ordinates -3.8 mm (anterior-posterior) and +0.1 mm (medio-lateral) (Paxinos and Watson, 1997). A

glass micropipette with a tip diameter of 20 µm filled with CTb (Sigma-Aldrich, Co., Poole, UK ;1% in distilled water; 200 nl) was aligned with the burr hole and inserted into the MLF at a dorso-ventral co-ordinate of +1.0 mm. Similarly, for the CVLM injection the injection micropipette was inserted in the left hand side at inter-aural co-ordinates -4.8 mm (anterior-posterior) and +1.8 mm (medio-lateral) at a dorso-ventral co-ordinate of -0.4 mm (Paxinos and Watson, 1997). CTb (200nl) was injected by pressure with a Pico Injector (World Precision Instruments, Sarasota, USA). The micropipette was left in place for 5 minutes after injection to prevent backflow of tracer and then removed. The pipette was then emptied by ejecting the remaining CTb in it and then cleaned by drawing distilled water and ejecting it several times. The outer surface of the tip was also cleaned by giving a gentle swab with distilled water. Following this, another burr hole was made on the same side at inter-aural co-ordinates -4.2 mm (anterior-posterior) and +2.0 mm (medio-lateral) (Paxinos and Watson, 1997) and the pipette was then filled with 4% FG (Fluorochrome, LLC, USA) in distilled water and inserted into the cerebellum at a dorso-ventral co-ordinate of +4.5 mm. On this occasion 50 nl of FG was ejected and the needle was left in place for 5 mins. The wound was sutured closed and all animals recovered uneventfully. Following 5-6 days survival period, the animals were perfused with 4% paraformaldehyde in 0.1M PB and the brain and the spinal cord were dissected. They were post-fixed with the same fixative overnight. The brain stem and the cerebellum were separated from the whole brain and cut into 100 µm coronal sections. MLF and CVLM injection sites were identified by using a DAB reaction as described in chapter 2. FG injections into the cerebellum were visualized directly under florescence microscope and photo-micrographed using an ultraviolet filter. Both injection sites were then identified with reference to the stereotaxic rat brain atlas of Paxinos and Watson (1997). Th12 - L3 segments of the spinal cord were cut into 50 µm transverse sections which underwent ethanol treatment immediately. The detailed procedures are described in chapter 2.

Retrogradely labelled rat spinocerebellar tract neurons were identified by the presence of FG and grouped into different populations based on their anatomical locations. Similarly, anterogradely labelled RetS terminals were identified by the presence of CTb from MLF/ CVLM injections. Four colour immunofluorescence was

performed in the selected sections by reacting them with antisera against FG and CTb along with the following antibodies: VGLUT2 and VGAT (group A in Table 5-3).

Table 5-3 Summary of the primary and secondary antibody combinations and concentrations used in the present study

	Primary antibody combination	Primary antibody concentration	Supplier	Secondary antibody combination	Secondary antibody concentration	Supplier
Rat A	gt CTb	1:5000	List (quadratech)	Rh. Red	1:100	Jackson ImmunoResearch, West Grove, USA
	gp FG	1:500	Fluorochrome, LLC, Denver, Colorado,	Dylight 488	1:500	Jackson ImmunoResearch, West Grove, USA
	rbt VGLUT2	1:5000	Chemicon, Harlow, UK	Dylight 649	1:500	Jackson ImmunoResearch, West Grove, USA
	mo VGAT	1:5000	Synaptic systems, UK	AV-PB	1:1000	Molecular Probes, Eugene, USA
B	gt CTb	1:5000	List (quadratech)	Rh. Red	1:100	Jackson ImmunoResearch, West Grove, USA
	gp FG	1:500	Fluorochrome, LLC, Denver, Colorado,	Dylight 488	1:500	Jackson ImmunoResearch, West Grove, USA
	rbt VGLUT1	1:5000	Synaptic systems, UK	Dylight 649	1:500	Jackson ImmunoResearch, West Grove, USA

All secondary antibodies were raised in donkey and conjugated to Rh. Red, Rhodamine Red; Dylight 649; dylight 488; AV-PB,Avidine pacific blu gp, guineapig; gt, goat; rbt, rabbit; CTb, B- subunit of cholera toxin; FG, fluorogold; VGAT, Vesicular GABA transporter; VGLUT, Vesicular glutamate transporter

The sections were scanned using four channels of a confocal microscope (LSM 700, Ziess, Germany). Due to the limitation of Neurolucida software, the images were analysed in three channels and images were reproduced in similar way. RetS terminals identified by the presence of CTb in them which were immunoreactive for VGLUT2 or VGAT were imaged as magenta due to the presence of blue (VGLUT2/ VGAT) over red (CTb). Reconstruction of the neurons were made following the procedure described in chapter 2 (section 2.4), contacts formed by CTb labelled RetS terminals with or without VGLUT2/ VGAT immunoreactions were counted and contact density was calculated which was expressed per 100 μm^2 of the neuronal surface area. It was also possible to estimate the percentages of RetS contacts that were either excitatory or inhibitory by utilizing quantitative data obtained for overall contact density of excitatory terminals which were VGLUT2 immunopositive and inhibitory contacts which expressed VGAT (from chapter 3 and 4). The sum of VGLUT2 expressing RetS contacts in both the MLF and CVLM injection can be converted into percentage by dividing it with overall VGLUT2 contact density and multiplying this by 100 which shows percentage of excitatory RetS contacts on spinocerebellar tract neurons. Percentage of VGAT expressing RetS contacts was also estimated in the same way.

Experimental procedure for labelling of CS terminals and spinocerebellar tract neurons

Anterograde labelling of CS axon terminals was performed in two adult Sprague Dawley rats as described for RetS terminals. In order to label the CS axon terminals, multiple injections of CTb (200 nl; 1% in distilled water) were made on the left hand side of the hindlimb region of the motor cortex at 3 locations: -1.0, -2.0 and -2.5 mm anterior-posterior, +2.0 mm medio-lateral and -2.0 mm dorso-ventral (bregma; Paxinos and Watson, 1997). We used bregma for this injection because this is considered as the most effective way to target the hindlimb region of the sensorimotor cortex (Neafsey *et al.*, 1986). Injection of the cerebellum with FG was performed in the same way as explained above for labelling of RetS terminals and spinocerebellar tract neurons. Similarly, identification of injection sites in the motor cortex with CTb, and the cerebellum with FG and sectioning of Th12-L3 spinal cord segments was also carried out as described above.

Different populations of spinocerebellar tract neurons were recognized by retrograde transport of FG according to their distinct anatomical locations. Likewise, CS axon terminals were identified by the presence of CTb in them. Selected sections were reacted with CTb and FG antibodies along with VGLUT1 antisera (group B in Table 5-3). Triple immunoflorescence was performed on these sections using a three channel confocal microscope. Contacts made by CTb labelled CS terminals which were also positive for VGLUT1 were imaged as magenta because of the presence of blue (VGLUT1) over red (CTb). Contacts made by these terminals were plotted. The density of terminals forming contacts was not calculated and only the absolute number of contacts per cell was recorded because very few contacts were present.

5.2.4 Statistical analysis

Data were expressed as mean ± SD. Multi-group comparisons were made by using a one way ANOVA followed by a *post hoc* Tukey's analysis as appropriate and two variable comparisons among the same population was made by using Student's *t* test. A $p < 0.05$ was considered to be statistically significant.

5.3 Results

5.3.1 Direct excitatory inputs from proprioceptors to different populations of spinocerebellar tract neurons

5.3.1.1 Glutamatergic terminals originating from proprioceptors on intracellularly labelled cat neurons

This part of the study was performed for 8 well-labelled spinocerebellar tract neurons from 3 adult cats. The sample included 2 VSCT neurons (cells a – b), 3 ccDSCT neurons (cells c – e) and 3 dhDSCT neurons (cells f – h). It is worth noting that SB neurons were not analysed because, these neuronal population are devoid of proprioceptive input (as discussed in chapter 3). However, all four populations of spinocerebellar tract neurons were analysed in a series of experiments in rats (see below).

Electrophysiological identification criteria have already been shown in Figure 3-1(chapter 3) and 4-1 (chapter 4). Similarly, the locations of cell bodies of the neurons analysed in this part of the study are shown in Figure 3-2 (chapter 3) which are represented by open circles.

Double immunoreactivity against VGLUT1 and PV was used as an indication of proprioceptive origin as described in the Methods (Section 5.2.3). The results showed considerable differences in proportions of contacts originating directly from proprioceptors. Representative examples of confocal microscope images showing immunocytochemical properties of axon terminals contacting labelled neurons (one from each population) are shown in Figure 5-1. One of the major findings was that the great majority of VGLUT1 contacts which were immunoreactive for PV were on ccDSCT neurons. Examples of the reconstructions of individual neurons are shown in Figure 5-2. The overall average density of VGLUT1 contacts that were colocalised with PV per 100 μm^2 of the soma and the dendritic tree of ccDSCT neurons was 0.97 ± 0.67 while that of dhDSCT neurons was 0.06 ± 0.06. This density was more than 15 times higher for ccDSCT neurons than dhDSCT neurons and was significantly

different ($p < 0.05$, Student's *t*-test). Similarly, in VSCT neurons, the overall average contact density of VGLUT1 positive terminals which contained PV was 0.12 per 100 μm^2. As there was no significant variation between the contact densities for soma and dendrites of the neurons analysed, data were expressed in terms of whole neuronal surface area. Detailed quantitative data are shown in Table 5-4. The bar graph in Figure 5-3A shows the overall contact density of VGLUT1 and PV double-labelled terminals associated with the three populations of neurons analyzed.

5.3.1.2 Glutamatergic terminals originating from proprioceptors on retrogradely labelled rat neurons

A photomicrograph of a coronal section of the cerebellum containing the CTb injection site and reconstructions of the injection sites for all four animals is shown in Figure 3-7 in chapter 3. A total of 72 spinocerebellar tract neurons included 17 SB, 17 VSCT, 17 ccDSCT and 21 dhDSCT neurons. All the cells comply with the selection criteria defined in previous chapters (chapter 3 & 4) which include well labelled cells located in the equivalent region where intracellularly labelled neurons are found in the cat. The locations of the cell bodies are shown in Figure 5-4. An illustration of VGLUT1 and PV contacts on these neuronal populations is shown in Figure 5-5.

Consistent with the results obtained from the cat experiment, ccDSCT neurons had the highest number of appositions made by VGLUT1 terminals which were also immunoreactive for PV. The contact density of VGLUT1 and PV co-expressing terminals on ccDSCT neurons was about 5 times higher than that associated with dhDSCT neurons and about 10 times higher than that found on SB and VSCT neurons. The overall average density of these contacts on ccDSCT neurons was 0.23 ± 0.12 per 100 μm^2 and that on dhDSCT neurons was 0.05 ± 0.07 per 100 μm^2. In contrast, in both SB and VSCT neurons, overall average density of contacts made by these terminals was 0.02 ± 0.34 per 100 μm^2. Detailed data are shown in Table 5-5. The overall average contact density of VGLUT1 axon terminals colocalised with PV was significantly higher on ccDSCT neurons in comparison with dhDSCT, VSCT and SB

neurons (ccDSCT versus dhDSCT neurons, $p < 0.05$; ccDSCT versus SB neurons $p < 0.01$; and ccDSCT versus VSCT neurons $p < 0.01$; ANOVA) as shown in Figure 5-3B.

Therefore, the proportion of contacts from VGLUT1 and PV double labelled axon terminals was highest in ccDSCT neurons in both cats and rats, thus providing direct evidence for a major input from proprioceptors to this neuronal population.

5.3.2 Glutamatergic and GABAergic/ glycinergic terminals originating from different types of interneurons on four types of spinocerebellar tract neurons

This aim was addressed with regards to the VSCT population of spinocerebellar tract neurons including SB neurons in cats and all four spinocerebellar tract neuronal populations in rats. An example of a CTb injection site in the cerebellum and reconstructions for all four rats is shown in Figure 3-7 in chapter 3. The location of cell bodies of all the neurons analysed are indicated with closed and open circles in Figure 5-6 (cat neurons) and closed circles Figure 5-4 (rat neurons) by different colours.

5.3.2.1 Sources of excitatory interneuronal inputs to intracellularly labelled SB and VSCT neurons in cats

In total, a sample of 5 well labelled spinocerebellar tract neurons was used for the detailed analysis which included 3 SB neurons (cells 1-3) and 2 VSCT neurons (cells 4-5). Figure 5-7 shows representative confocal images revealing VGLUT2 immunoreactive axon terminals which were also positive for CB and CR and reconstructions of individual cells showing the distribution of contacts made by CB, CR and CB/CR double labelled axon terminals with or without VGLUT2 labelling is shown in Figure 5-8.

The results of this study show that SB and VSCT neurons have a very small number of appositions made by VGLUT2 positive terminals which contained CB and/ or CR. As shown in Table 5-6, VSCT neurons have a relatively higher density of contacts

formed by CB containing VGLUT2 terminals than SB neurons. This density is about 5 times higher in VSCT neurons than that in SB neurons.

5.3.2.2 Sources of excitatory interneuronal inputs to retrogradely labelled spinocerebellar tract neurons in rats

In total, 150 spinocerebellar tract neurons that were retrogradely labelled were examined in this part of the study; 75 neurons were analysed for VGLUT1+2 and CB immuno-positive contacts and 75 of them were examined for contacts formed by VGLUT1+2 and CR labelled terminals. Among 75 neurons studied for contacts formed by VGLUT1+2 and CB immunoreactive terminals, there were 15 SB, 16 VSCT, 22 ccDSCT and 22 dhDSCT neurons. Similarly, a total of 75 neurons investigated for VGLUT1+2 and CR contacts included 17 SB, 16 VSCT, 25 ccDSCT and 17 dhDSCT neurons. Confocal microscope images showing the contacts made by VGLUT1+2 and CB labelled terminals and VGLUT1+2 and CR labelled terminals are shown in Figures 5-9 (A1-A4) and 5-9 (B1-B4) respectively.

Consistent with the results obtained from the cat experiment, the density of contacts formed by VGLUT1+2 terminals which contained either CB or CR was very low and among four populations of neurons, VSCT neurons had a higher density of appositions formed by VGLUT1+2 terminals expressing CB (0.03 ± 0.01 per 100 μm^2). In contrast, the mean density of contacts formed by CR containing VGLUT1+2 terminals was higher in ccDSCT neurons (0.04 ± 0.04 per 100 μm^2) but these differences were not significant. The average overall densities of contacts formed by VGLUT1+2 terminals containing CB or CR on all four neuronal populations are summarized in Table 5-7.

5.3.2.3 Sources of inhibitory interneuronal inputs to intracellularly labelled SB and VSCT neurons in cats

In total, a sample of 4 well labelled spinocerebellar tract neurons was used for the analysis. This included 2 SB neurons and 2 VSCT neurons. The locations of cell bodies of these neurons are indicated in Figure 5-6 by open circles. An example

showing VGAT immunoreactive axon terminals which were also positive for CB and CR is given in Figure 5-10. Similarly, reconstructions of individual cells showing the distribution of contacts made by CB, CR and CB and CR double labelled axon terminals with or without VGAT labelling are illustrated in Figure 5-11.

Quantitative analysis showed that SB and VSCT neurons have very few contacts made by VGAT immunoreactive terminals which contained CB and/ or CR. As shown in Table 5-8, SB neurons have more than 6 times the density of contacts made by VGAT terminals colocalised with CB than VSCT neurons (0.13 for SB cells as opposed to 0.02 per 100 μm^2 for VSCT neurons).

5.3.2.4 Sources of inhibitory interneuronal inputs to retrogradely labelled spinocerebellar tract neurons in rats

A total of 147 retrogradely labelled spinocerebellar tract neurons were analysed in rats of which 72 neurons were analysed for VGAT and CB contacts and 75 were analysed for appositions made by VGAT and CR terminals. Among 72 neurons studied for contacts formed by VGAT and CB immunoreactive terminals, there were 16 SB, 12 VSCT, 22 ccDSCT and 22 dhDSCT neurons. Similarly, a total of 75 neurons investigated for VGAT and CR contacts included 16 SB, 14 VSCT, 25 ccDSCT and 20 dhDSCT neurons. An additional 80 retrogradely labelled spinocerebellar tract neurons were analysed for appositions made by VGAT and PV immunoreactive terminals which included 23 SB, 15 VSCT, 22 ccDSCT and 20 dhDSCT neurons. As in the cat, SB neurons had about 3 times the density of contacts made by VGAT and CB double labelled axon terminals than VSCT neurons. dhDSCT neurons had 23 times the density of VGAT contacts that co-express CB than ccDSCT neurons a difference that was significantly higher (dhDSCT versus ccDSCT neurons, $p < 0.05$; dhDSCT versus SB neurons $p < 0.01$; and dhDSCT versus VSCT neurons $p < 0.01$; ANOVA). In contrast, the density of contacts made by VGAT and CR colocalised terminals was very small for all four neuronal populations. In addition, the average contact density of VGAT axon terminals immunoreactive for PV in SB neurons was 0.08 ± 0.07 per 100 μm^2 while in VSCT neurons the density was 0.06 ± 0.03 per 100 μm^2. Similarly, in ccDSCT and dhDSCT neurons, the average contact density of VGAT and

PV double labelled terminals were 0.02 and 0.06 per 100 μm^2 respectively. Figure 5-9 (C – F) shows immunohistochemical characteristics of VGAT terminals colocalised with CB/ CR/ PV on spinocerebellar tract neurons. Data summarizing the contact densities of VGAT terminals containing either of these calcium binding proteins are shown in Table 5-7.

Taken together with the results obtained from previous chapters (chapter 3 and 4), these results show that majority of spinal inputs to the four populations of spinocerebellar tract neurons are from pure glutamatergic and GABA/ glycinergic interneurons. Apparently, they receive very limited inputs from CB, CR and PV containing interneurons that are glutamatergic or GABA/ glycinergic.

5.3.3 Proportion of contacts that directly originates from the RetS and the CS pathways in the rat

5.3.3.1 Glutamatergic and GABAergic/ Glycinergic terminals originating from the RetS neurons on four types of spinocerebellar tract neurons

As specified in the methods section, medullary injections were made in two different sites to identify axon terminals originating from RetS neurons, one in the MLF and another in the CVLM. Connectivity between this pathway and retrogradely labelled spinocerebellar tract neurons was investigated by using immunohistochemistry and confocal microscopy. A photomicrograph of the injection site in the MLF/ CVLM and the cerebellum including reconstructions of each injection site for individual animals is shown in Figure 5-12 and Figure 5-13 respectively. The criteria for selection of neurons labelled with FG were the same as that for CTb labelled cells as explained above and in previous chapters. The locations of the cell bodies of all neurons analysed are indicated with closed circles of different colours in Figure 5-14.

Excitatory and inhibitory inputs originating from RetS axons descending from the MLF to spinocerebellar tract neurons in rats

A total of 160 spinocerebellar tract neurons were analysed which included 45 SB, 45 VSCT, 34 ccDSCT and 36 dhDSCT neurons. Examples of confocal microscope images for each of these neuronal populations are shown in Figure 5-15.

Quantitative analysis revealed that the overall average contact density of CTb labelled RetS axon terminals in SB neurons which expressed VGLUT2 was 0.03 ± 0.00 per 100μm^2 and of those which were immunoreactive for VGAT was 0.02 ± 0.01 per 100μm^2. In VSCT neurons, the average density of VGLUT2 positive RetS terminals was 0.04 ± 0.02 per 100μm^2 while that of VGAT expressing RetS terminals was 0.02 ± 0.01 per 100μm^2. In contrast, there were not any contacts made by VGLUT2 expressing RetS terminals on ccDSCT neurons and very small numbers in dhDSCT neurons. Similarly, the contact densities of VGAT expressing RetS terminals were very small for both ccDSCT and dhDSCT neurons. Detailed data are shown in Table 5-9.

Figure 5-16 (A & B) shows a comparison of the density of the contacts made by VGLUT2 and VGAT expressing RetS axon terminals in four populations of spinocerebellar tract neurons. This comparison showed a significantly higher density of VGLUT2 expressing RetS terminals for both SB ($p < 0.05$; ANOVA) and VSCT ($p < 0.01$; ANOVA) neurons than ccDSCT neurons. However, the difference in VGAT expressing RetS contacts on these neurons was not significant.

Excitatory and inhibitory inputs originating from the CVLM to retrogradely labelled spinocerebellar tract neurons in rats

Quantitative analysis was performed for a total of 199 retrogradely labelled spinocerebellar tract neurons that included 75 SB, 57 VSCT, 48 ccDSCT and 19 dhDSCT neurons. Images illustrating contacts formed by VGLUT2/ VGAT expressing RetS terminals on four populations of spinocerebellar tract neurons are shown in Figure 5-17.

The overall average density of appositions made by RetS terminals in SB neurons which were VGLUT2 positive was 0.07 ± 0.02 per 100μm^2 and that of VGAT expressing terminals was 0.01 ± 0.01 per 100μm^2. This difference was statistically significant ($p < 0.01$; Student's *t*-test). In VSCT neurons, the overall mean densities of RetS terminals positive for VGLUT2 and VGAT was 0.09 ± 0.01 and 0.02 ± 0.00 per 100μm^2 respectively. This difference was also highly significant ($p < 0.001$; Student's *t*-test). In contrast, both ccDSCT and dhDSCT neurons have very few contacts made by VGLUT2 RetS terminals and none from VGAT RetS terminals on them (Table 5-10).

The proportions of appositions made by RetS terminals that expressed either VGLUT2 or VGAT for four populations of spinocerebellar tract neurons are shown in Figure 5-16 (C & D). VSCT neurons have highest proportion of contacts made by VGLUT2 positive RetS terminals among other neurons. The contact densities of VGLUT2 expressing RetS terminals on both SB and VSCT neurons were significantly higher than that of ccDSCT and dhDSCT neurons (SB versus ccDSCT neurons, $p < 0.01$; SB versus dhDSCT neurons, $p < 0.01$; VSCT versus ccDSCT neurons, $p < 0.001$; VSCT versus dhDSCT neurons, $p < 0.001$; ANOVA). Similarly, the average densities of appositions formed by RetS terminals immunoreactive for VGAT on both SB and VSCT neurons were significantly higher than that of ccDSCT and dhDSCT neurons (SB versus ccDSCT neurons, $p < 0.05$; SB versus dhDSCT neurons, $p < 0.05$; VSCT versus ccDSCT neurons, $p < 0.01$; VSCT versus dhDSCT neurons, $p < 0.01$; ANOVA).

The present result also showed significant differences between the MLF and CVLM injections with respect to the proportion of contacts formed by VGLUT2 expressing RetS terminals on SB and VSCT neurons. However no difference was found for VGAT expressing RetS terminals. Nevertheless, the pattern of excitatory RetS inputs originating from axons descending from the MLF and the CVLM was consistent which showed highest proportion of inputs to the VSCT neurons. The average percentages of excitatory inputs originating from RetS pathway was 21.74% in SB neurons, 39.39% in VSCT neurons, 11.11% in ccDSCT neurons and 6.25% in dhDSCT neurons. On the other hand, the average percentages of inhibitory inputs derived from RetS

pathway was 7.50% in SB neurons, 5.33% in VSCT neurons, 4.35% in ccDSCT neurons and 7.69% in dhDSCT neurons.

In general, the majority of direct connections between RetS neurons and spinocerebellar tract neurons were excitatory in nature.

5.3.3.2 Glutamatergic terminals originating from the CS neurons on four types of spinocerebellar tract neurons

A photomicrograph of the injection site in the hindlimb motor cortex and the cerebellum and reconstructions of injection sites for individual animals is shown in Figure 5-18.

This part of the study is based on analysis of 167 spinocerebellar tract neurons in two rats which included 34 SB neurons, 41 VSCT neurons, 54 ccDSCT neuron and 38 dhDSCT neurons. The locations of cell bodies of these neurons are indicated in Figure 5-14. The average number of appositions made by VGLUT1 positive CS terminals on ccDSCT neurons was 1.16 per cell while that for dhDSCT neurons was 1.2/ cell. However, the average number of contacts made by these terminals on SB and VSCT neurons was 0.9 and 0.72 per cell. Confocal images of all four populations of spinocerebellar tract neurons revealing direct appositions made by CS terminals are shown in Figure 5-19.

Figure 5-1 Immunohistochemical characteristics of VGLUT1 and PV axon terminals in contact with intracellularly labelled spinocerebellar tract neurons

A-C*,** Single optical sections through the cell bodies of representative VSCT (Cell a), ccDSCT (Cell d) and dhDSCT (Cell g) neurons showing the presence of VGLUT1 (blue) and PV (green) immunoreactive terminals. The cell body and dendrites of intracellularly labelled cells are in red. ***A1-A4*; *B1-B4 and C1-C4*,** Projected images of dendritic trunks from cells shown in ***A*, *B and ***C*** respectively (areas encompassed in the boxes) illustrating contacts made by VGLUT1 terminals and VGLUT1 terminals co-expressing PV with the cell indicated by arrow heads and arrows respectively. Scale bar in ***A*-*C*** = 10 μm. Scale bar in ***A1-A4*, *B1-B4*** and ***C1-C4*** = 5 μm.

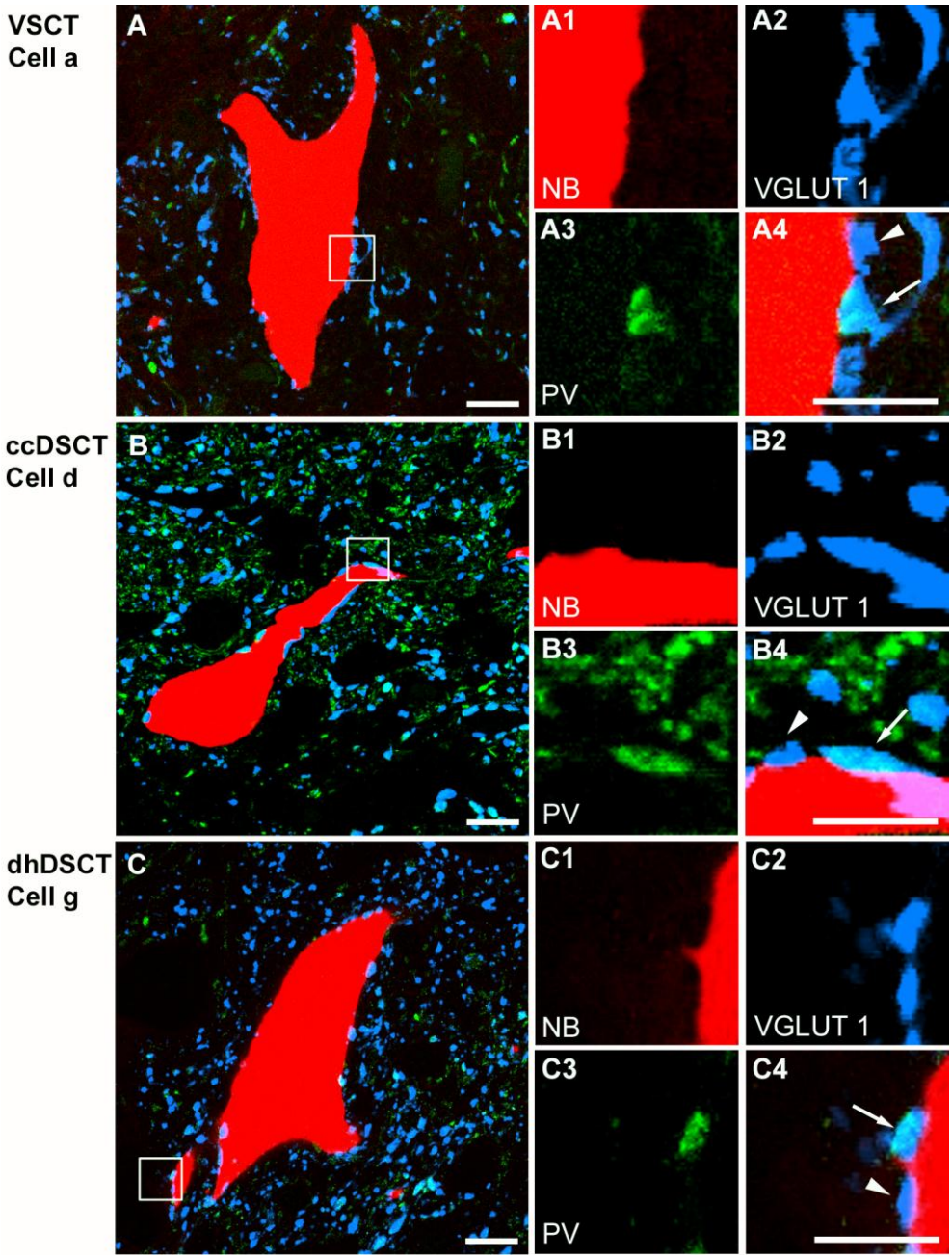
VSCT
Cell a
A
A1
NB
A2
VGLUT 1
A3
PV
A4
ccDSCT
Cell d
B
B1
NB
B2
VGLUT 1
B3
PV
B4
dhDSCT
Cell g
C
C1
NB
C2
VGLUT 1
C3
PV
C4

Figure 5-2 Reconstructions of spinocerebellar tract neurons illustrating the distribution patterns of VGLUT1, VGLUT1+PV and PV contacts

Reconstructions of spinocerebellar tract neurons showing the distributions of VGLUT1 (red), VGLUT1 colocalised with PV (purple) and PV (green) contacts throughout the dendritic trees. The reconstructions were made with Neurolucida for Confocal. All the small images without contacts plotted show the reconstructions of respective cells. Cell body and dendrites are shown in light grey. Scale bars = 50 μm for reconstructions with contacts plotted and 100 μm for reconstructions without contacts. All are oriented such that the midline is to the left and the lateral borders of the grey matter to the right. All the small images without contacts plotted show the reconstructions of the cells. Somata and dendrites are shown in dark grey.

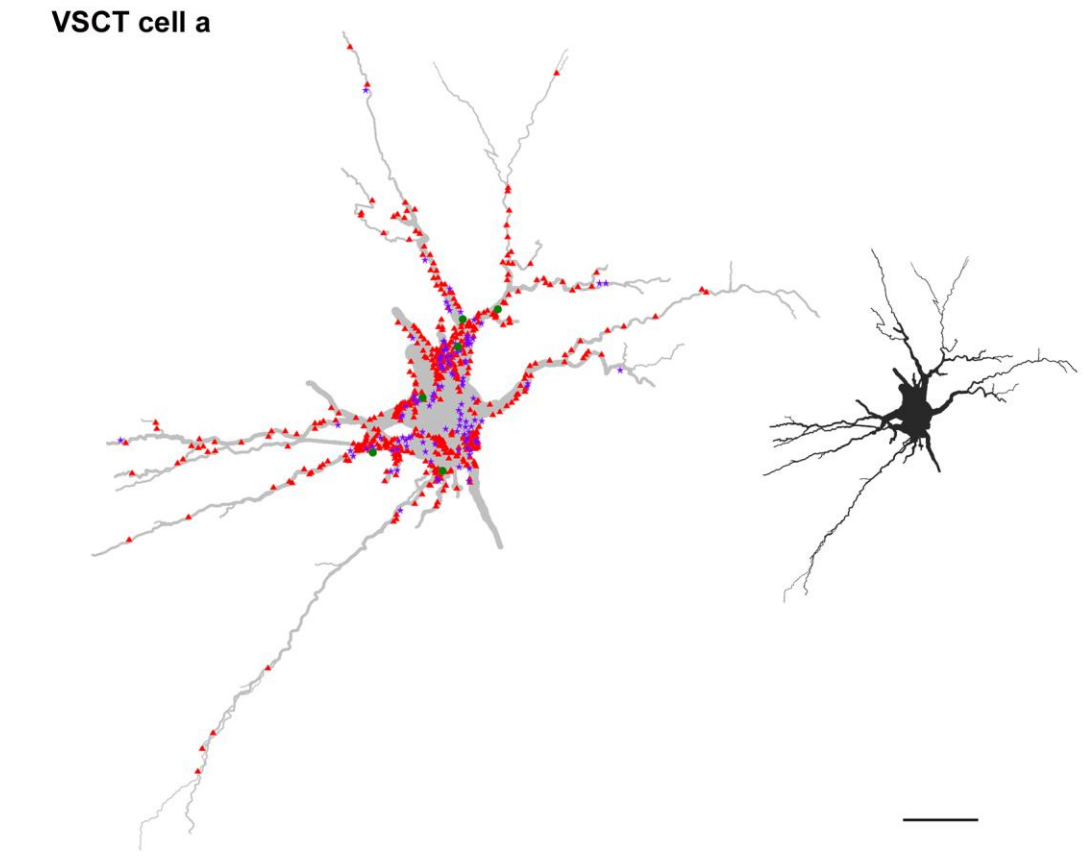
VSCT cell a

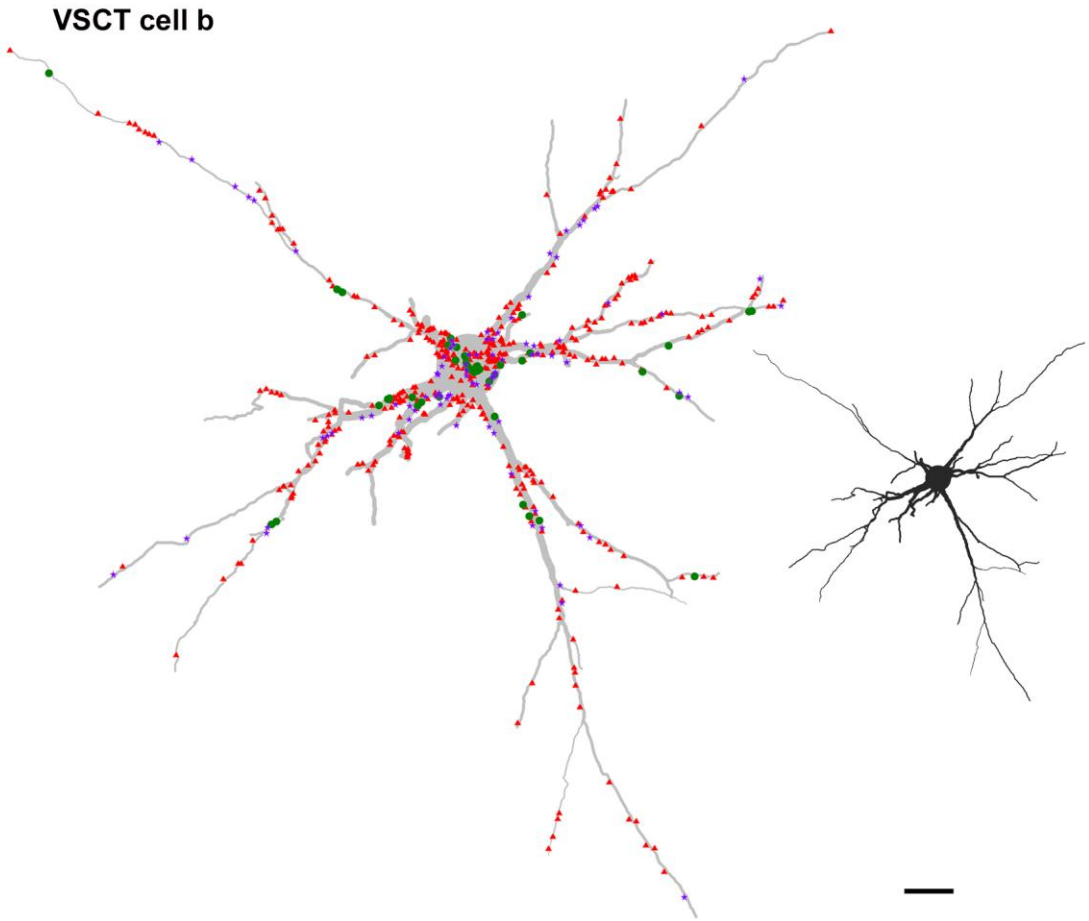
VSCT cell b

ccDSCT cell c

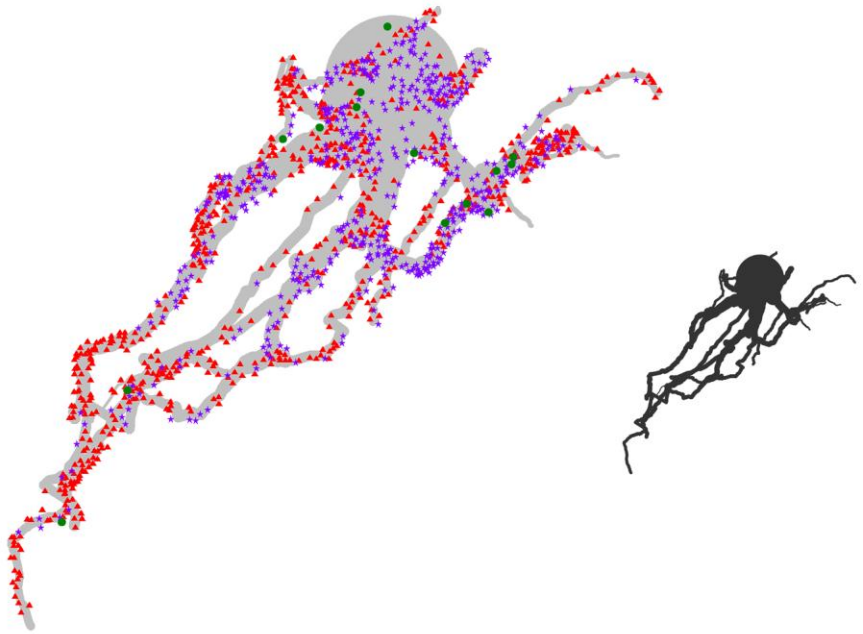

ccDSCT cell d

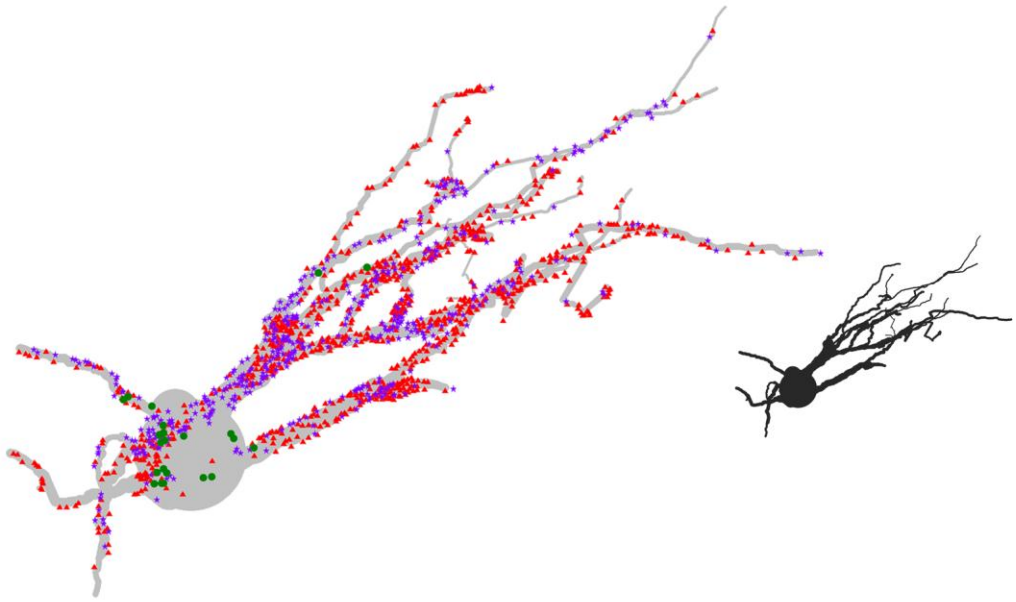

ccDSCT cell e

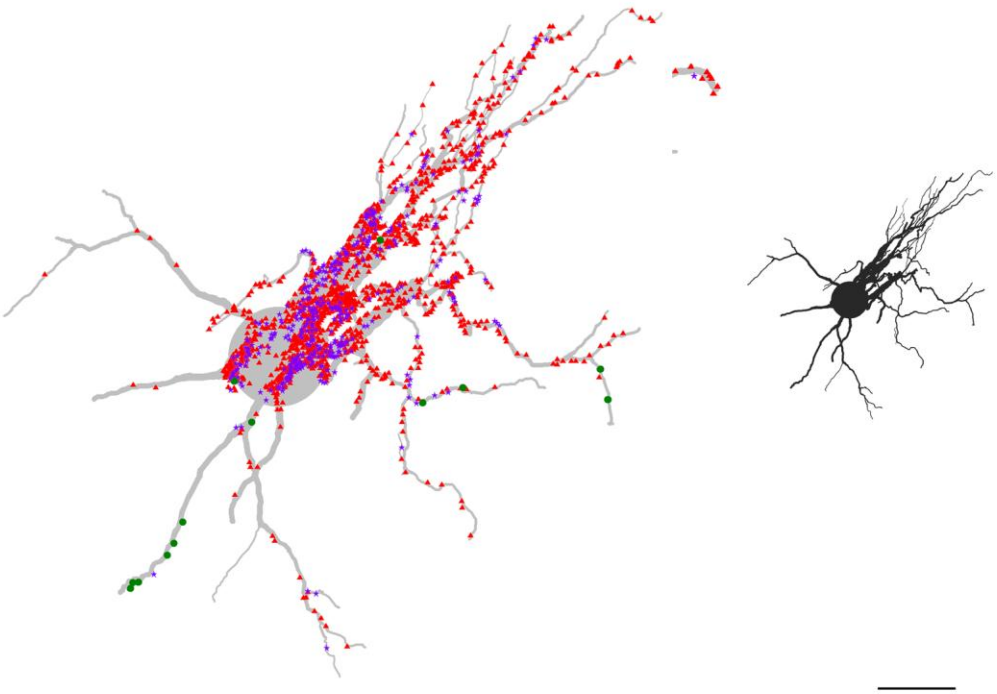

dhDSCT cell f

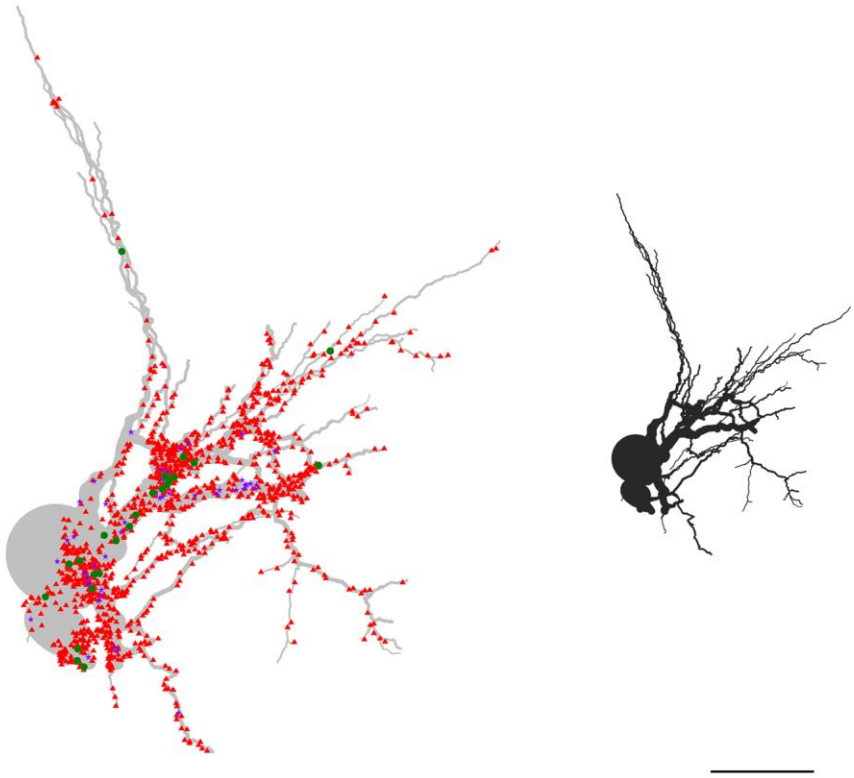

dhDSCT cell g

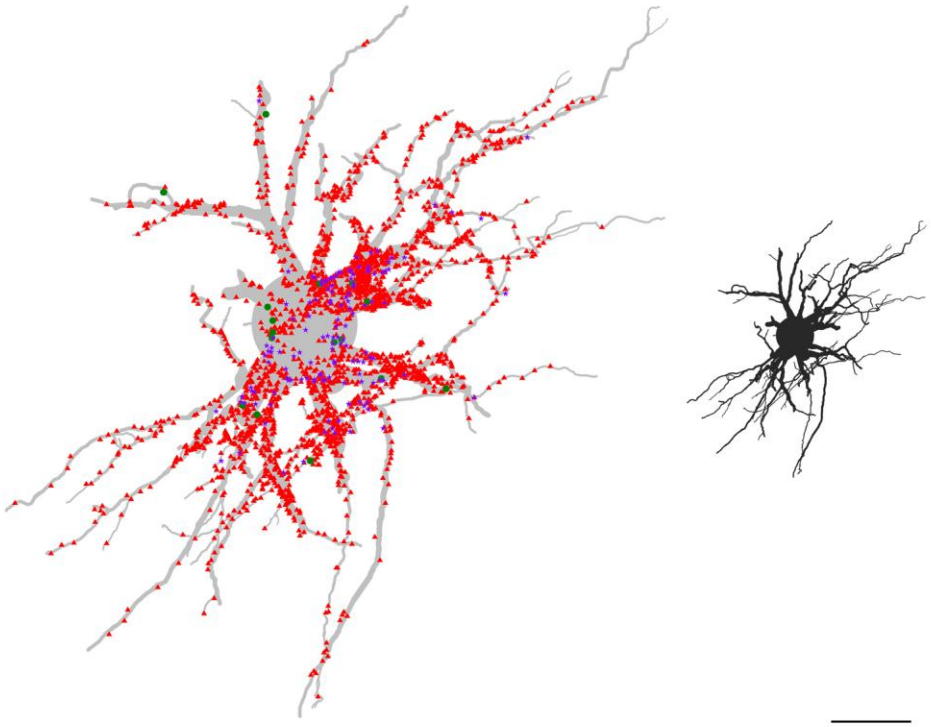

dhDSCT cell h

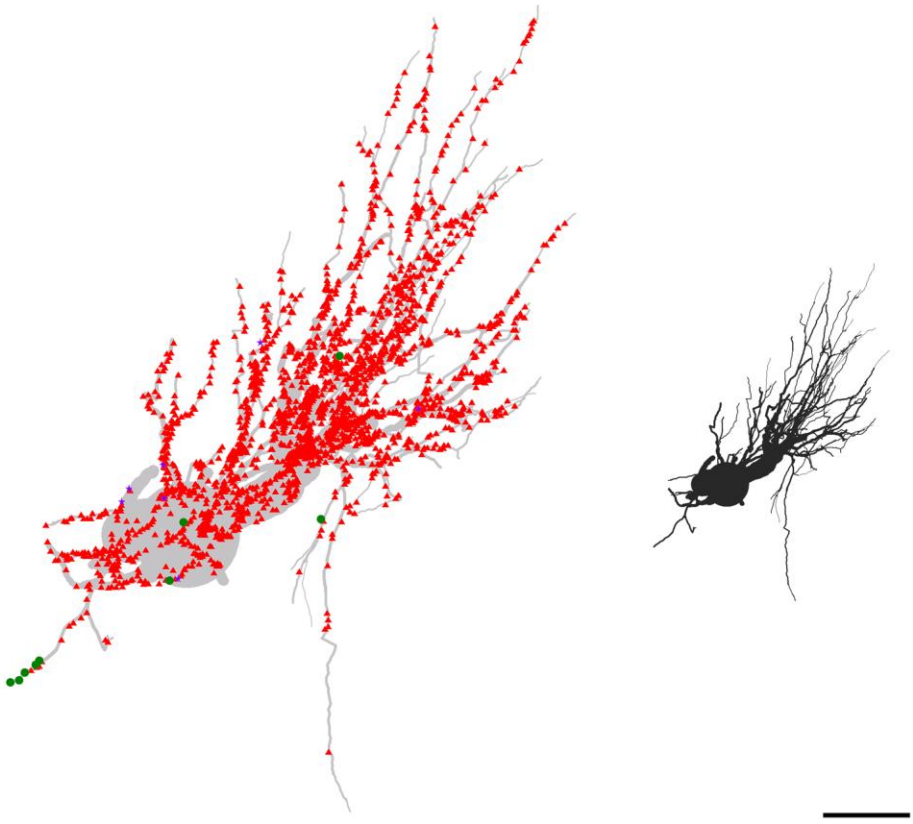

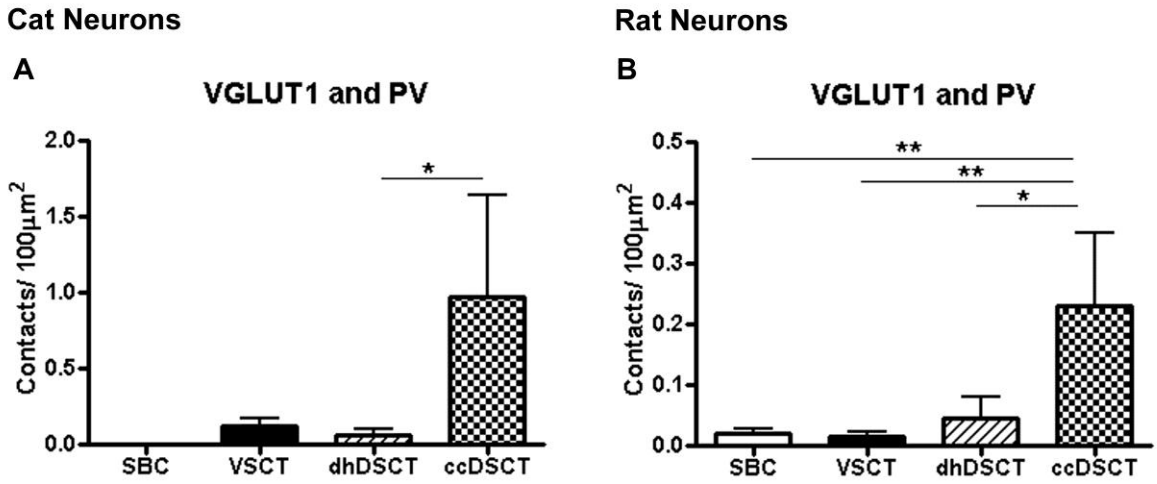

Figure 5-3 Comparison between the contact density of VGLUT1 and PV colocalised axon terminals in different populations of spinocerebellar tract neurons

***A*,** Differences in the overall contact density of VGLUT1 and PV colocalised terminals/ 100 μm^2 for the four different populations of spinocerebellar tract neurons in the cat. The contact density in ccDSCT neurons is significantly different from that on dhDSCT neurons ($p < 0.05$). All experiments were carried out in 4 cats (8 cells). Data presented as mean ± SD. ***B*,** Differences in the overall contact density of VGLUT1 and PV colocalised terminals/ 100 μm^2 in four different populations of spinocerebellar tract neurons in the rat. The contact density in ccDSCT neurons is significantly different from that on dhDSCT neurons ($p < 0.05$), VSCT neurons ($p < 0.01$) and SB neurons ($p < 0.01$). All experiments were carried out in 4 rats (72 cells). Data presented as mean ± SD. * denotes $p < 0.05$; ** denotes $p<0.01$ and *** denotes $p < 0.001$

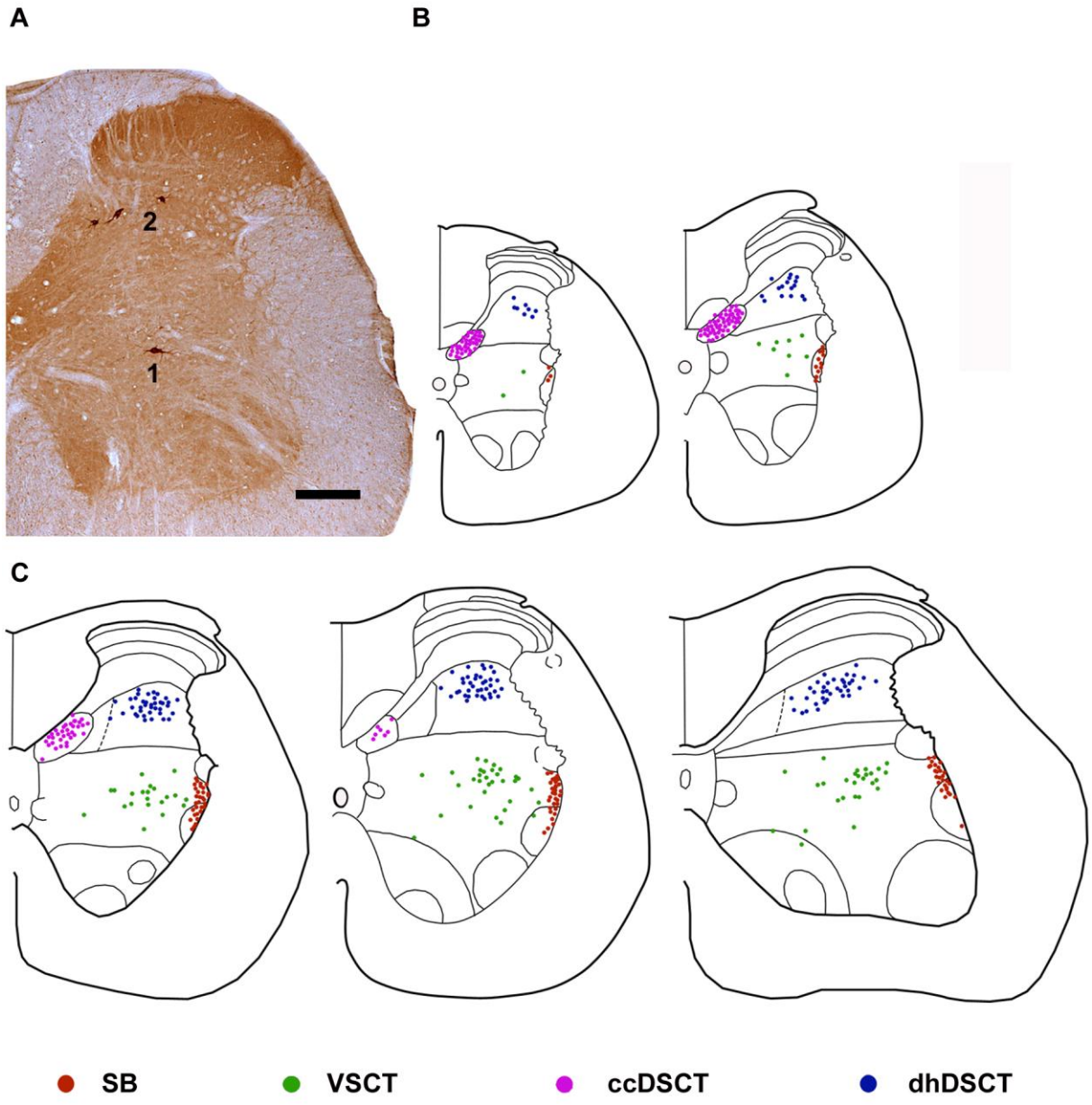

Figure 5-4 Locations of 449 analysed spinocerebellar tract neurons labelled retrogradely with CTb

A*,** A photomicrograph of a transverse section of the L3 segment of the rat spinal cord showing the location of one of the VSCT neurons (1) and dhDSCT neurons (2) identified by retrograde transport of CTb. ***B & C*,** Diagrams illustrating the locations of cell bodies of 449 cells analysed in the Th12 and Th13 segments and L1, L2 and L3 segments respectively. Scale bar in ***A 200 µm.

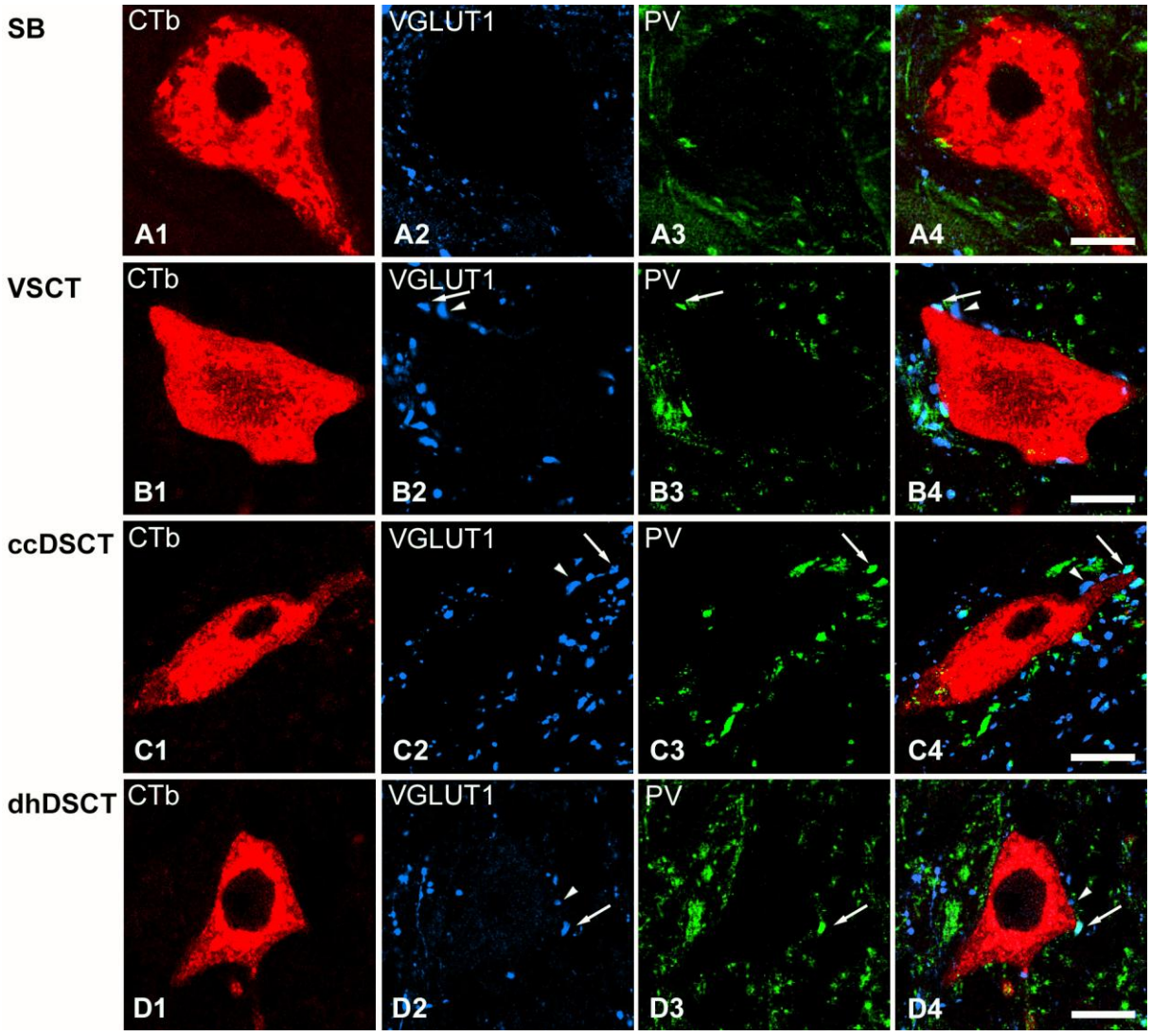

Figure 5-5 Immunohistochemical characteristics of VGLUT1 and PV axon terminals in contact with retrogradely labelled rat spinocerebellar tract neurons

A1-A4; B1-B4; C1-C4 and D1-D4, Single optical sections through the cell bodies of representative SB, VSCT, ccDSCT and dhDSCT neurons illustrating the presence of VGLUT1 (blue) and PV (green) immunoreactive terminals and contacts made by VGLUT1 (blue) and VGLUT1 terminals co-expressing PV (turquoise) immunoreactive terminals indicated by arrow heads and arrows respectively except in SB neurons. The cell body and dendrites of retrogradely labelled cells are in red. Scale bar in ***A-D*** = 20 μm.

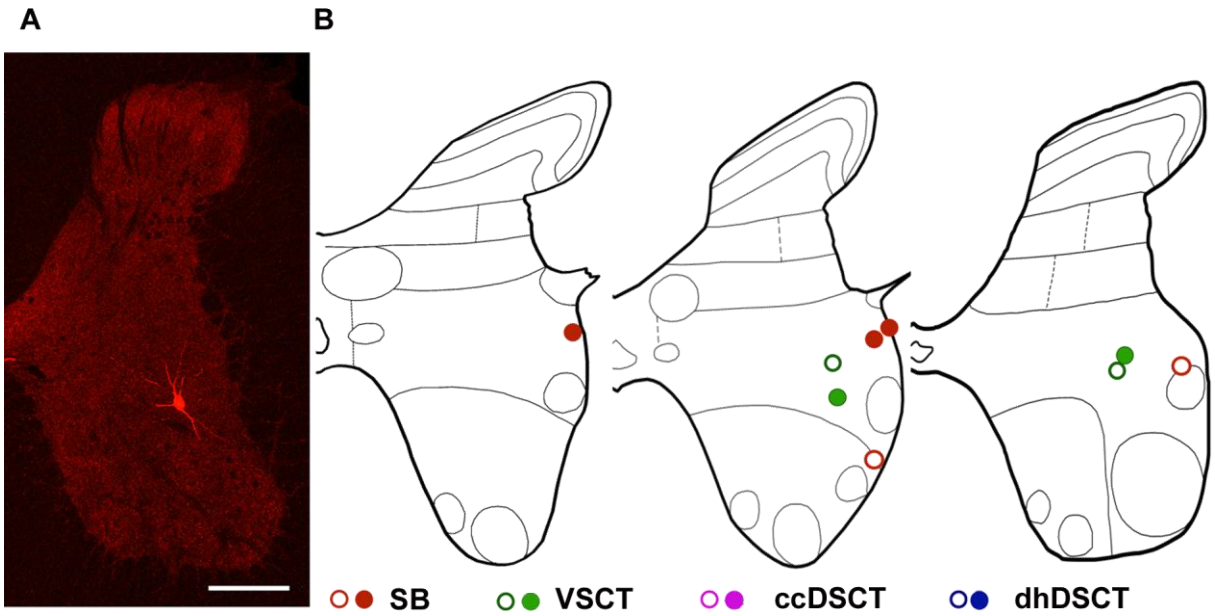

Figure 5-6 Locations of 9 intracellularly labelled spinocerebellar tract neurons

A, A low-magnification image of a transverse section of the L5 segment of the spinal cord showing the location of one of the VSCT neurons (cell 4). ***B***, Diagrams illustrating the locations of cell body of all 9 cells in the L3, L4 and L5 segments respectively. Closed circles indicate location of the 5 cells which were analysed for CB, CR and VGLUT2 while the open circles represent 4 cells which were analysed for CB, CR and VGAT only. Scale bar in ***A*** 400 μm.

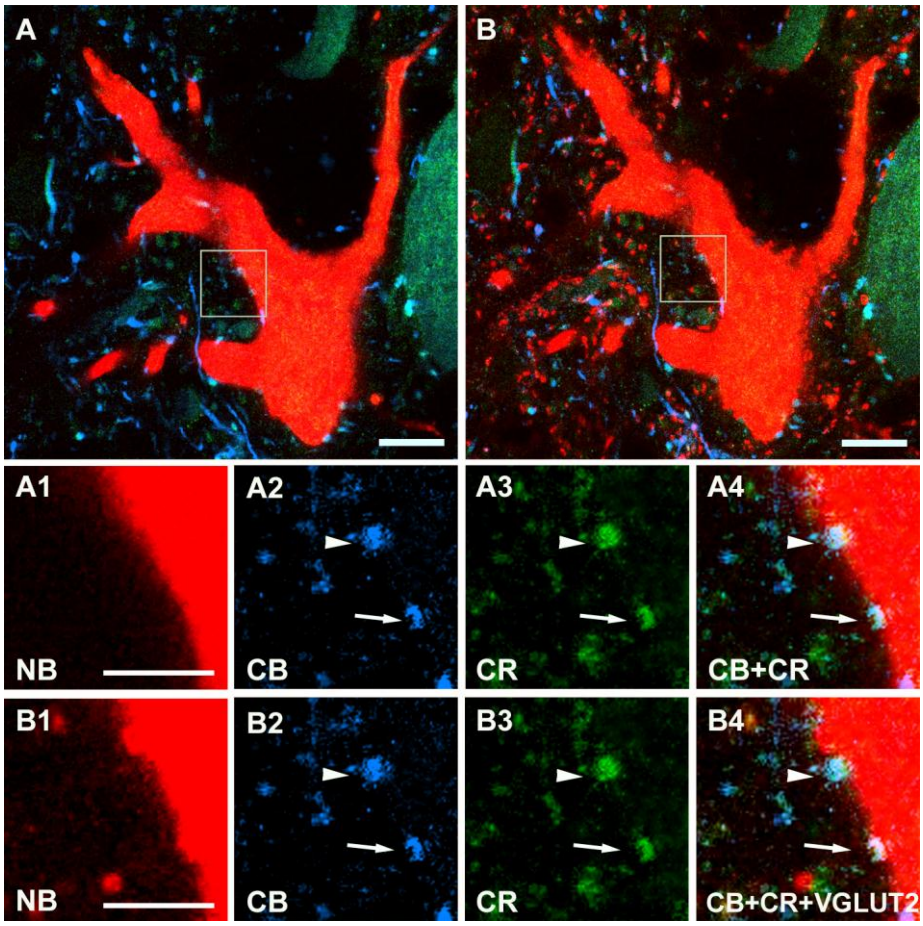

Figure 5-7 Sequential immunohistochemical characteristics of CB and CR terminals with VGLUT2 in contact with intracellularly labelled spinocerebellar tract neurons

A-B, A general overview of a single optical section through the cell bodies of representative SB neuron (Cell 3) before and after a reaction with sequentially reacted antibody against VGLUT2. Details of the areas demarcated by the boxes are shown in ***A1-A4*** and ***B1-B4***. ***A1-A4***, Single optical sections illustrating contacts made by CB and CR double labelled terminals with the cell. ***B1-B4***, Single optical sections of the same field that was rescanned after sequential incubation with antibody against VGLUT2. Arrows indicate CB and CR double labelled terminals which also had additional labelling with VGLUT2. Arrowhead indicates CB and CR double labelled terminals which did not have additional labelling with VGLUT2. Scale bar in ***A***, ***B*** = 10 μm. Scale bar in ***A1-A4 and B1-B4*** = 5 μm.

Figure 5-8 Reconstructions of spinocerebellar tract neurons illustrating the distribution patterns of CB, CR, CB+CR, CB+VGLUT2, CR+VGLUT2 and CB+CR+VGLUT2 contacts

Reconstructions of spinocerebellar tract neurons showing the distributions of CB (red), CB colocalised with VGLUT2 (blue), CR (green), CR colocalised with VGLUT2 (orange), CB double labelled with CR (purple) and CB and CR double labelled terminals colocalised with VGLUT2 (pink) contacts throughout the dendritic trees. The reconstructions were made with Neurolucida for Confocal. All the small images without contacts plotted show the reconstructions of respective cells. Cell body and dendrites are shown in light grey. Scale bars = 50 μm for reconstructions with contacts plotted and 100 μm for reconstructions without contacts. All are oriented such that the midline is to the left and the lateral borders of the grey matter to the right. All the small images without contacts plotted show the reconstructions of the cells. Somata and dendrites are shown in dark grey.

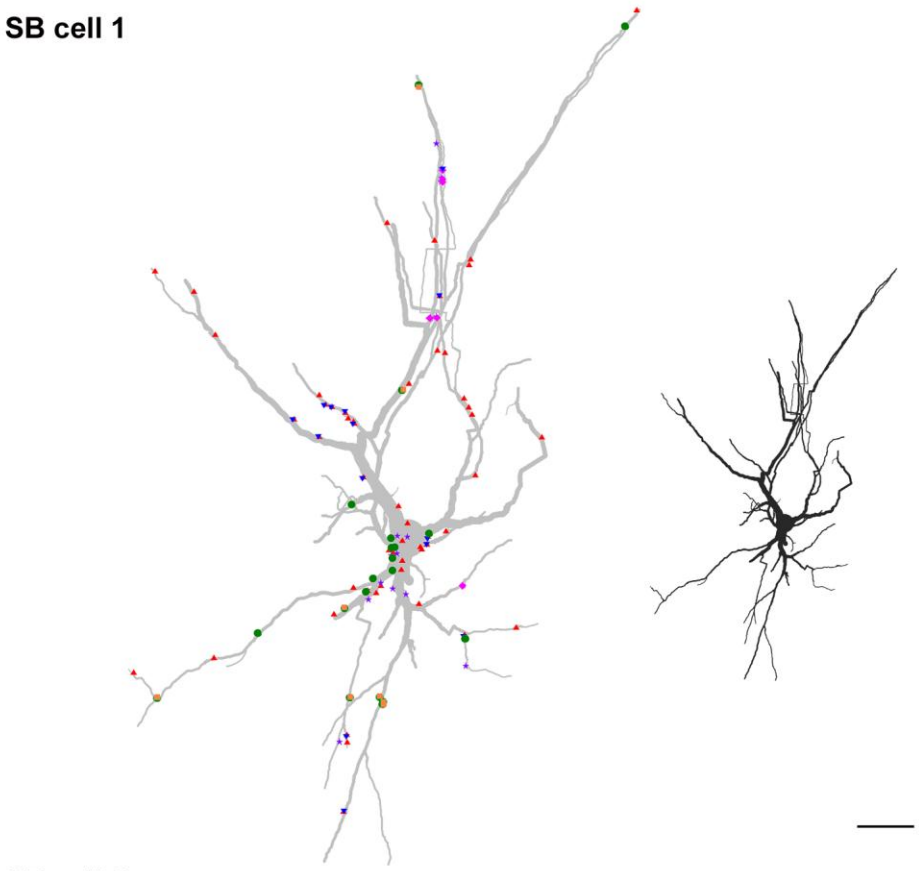
SB cell 1

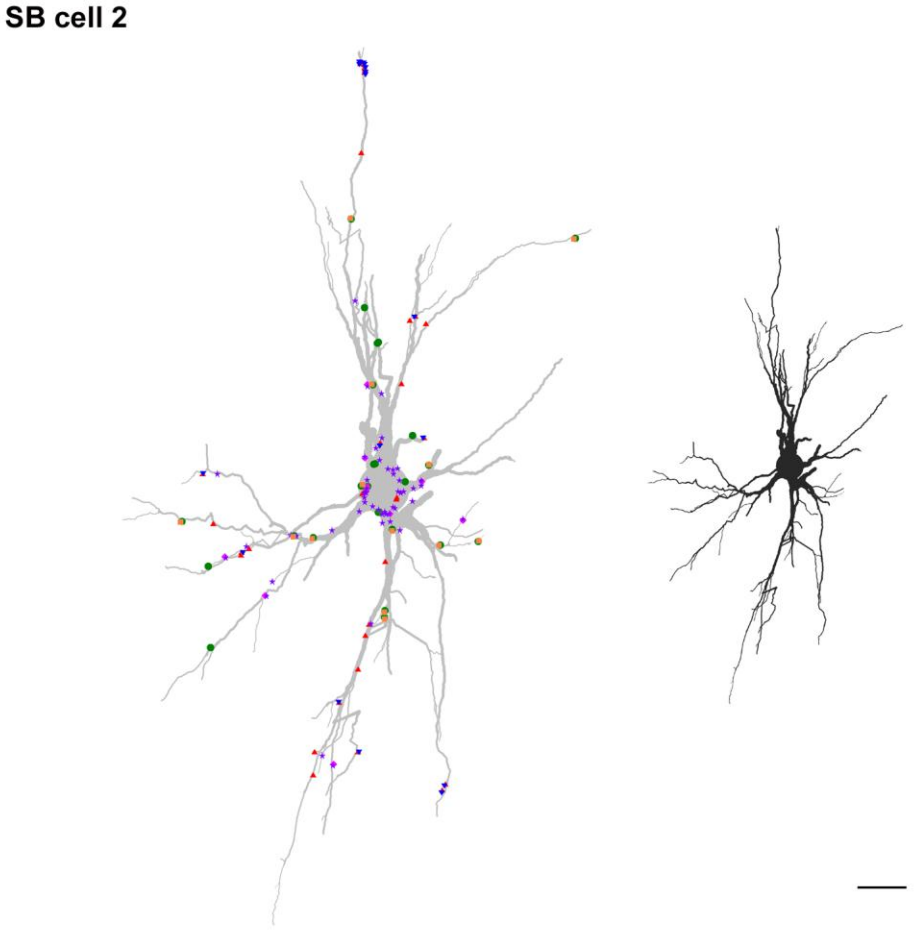
SB cell 2

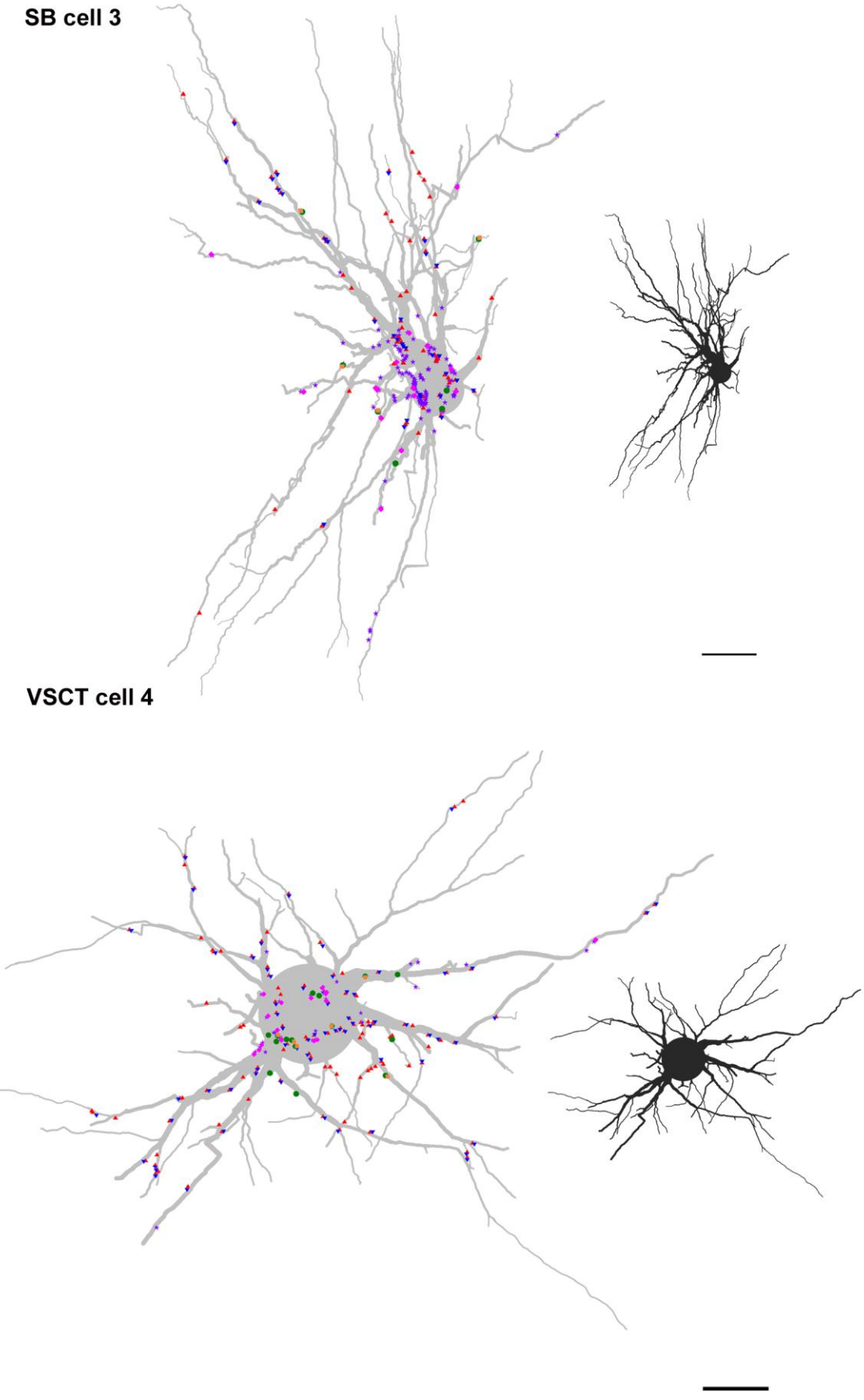
SB cell 3
VSCT cell 4

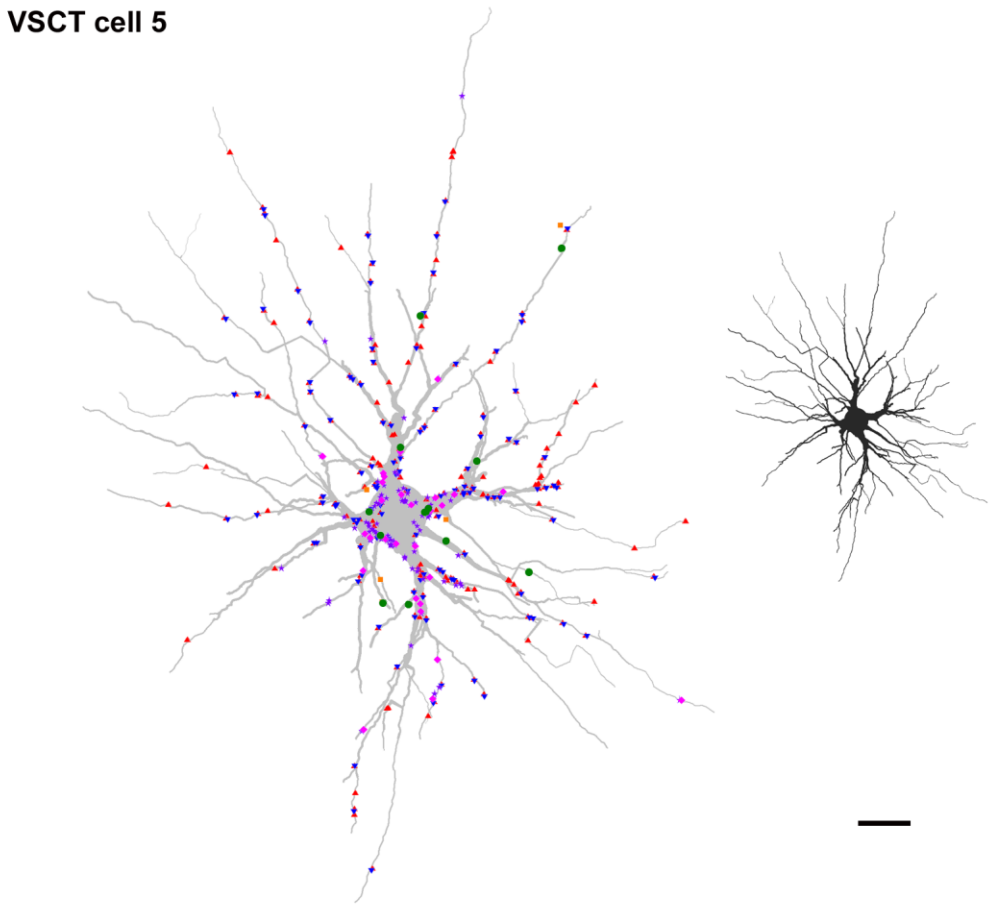
VSCT cell 5

Figure 5-9 Immunohistochemical characteristics of CB, CR and PV axon terminals with VGLUT1+2/ VGAT in contact with retrogradely rat labelled spinocerebellar tract neurons

A1-A4*; *B1-B4, Single optical sections through the cell bodies of representative VSCT and dhDSCT neurons illustrating the presence of CB/ CR (blue) and VGLUT1+2 (green) immunoreactive terminals and contacts made by VGLUT1+2 (green) and VGLUT1+2 terminals co-expressing CB/ CR (turquoise) immunoreactive terminals indicated by arrow heads and arrows respectively. ***C1-C4*; *D1-D4*, *E1-E4 and F1-F4*,** Single optical sections through the cell bodies of representative SB, dhDSCT, VSCT and SB neurons illustrating the presence of CB/ CR/ PV (blue) and VGAT (green) immunoreactive terminals and contacts made by VGAT (green) and VGAT terminals co-expressing CB/ CR/ PV (turquoise) immunoreactive terminals indicated by arrow heads and arrows respectively. The cell body and dendrites of retrogradely labelled cells are in red. Scale bar in ***A-F*** = 20 μm.

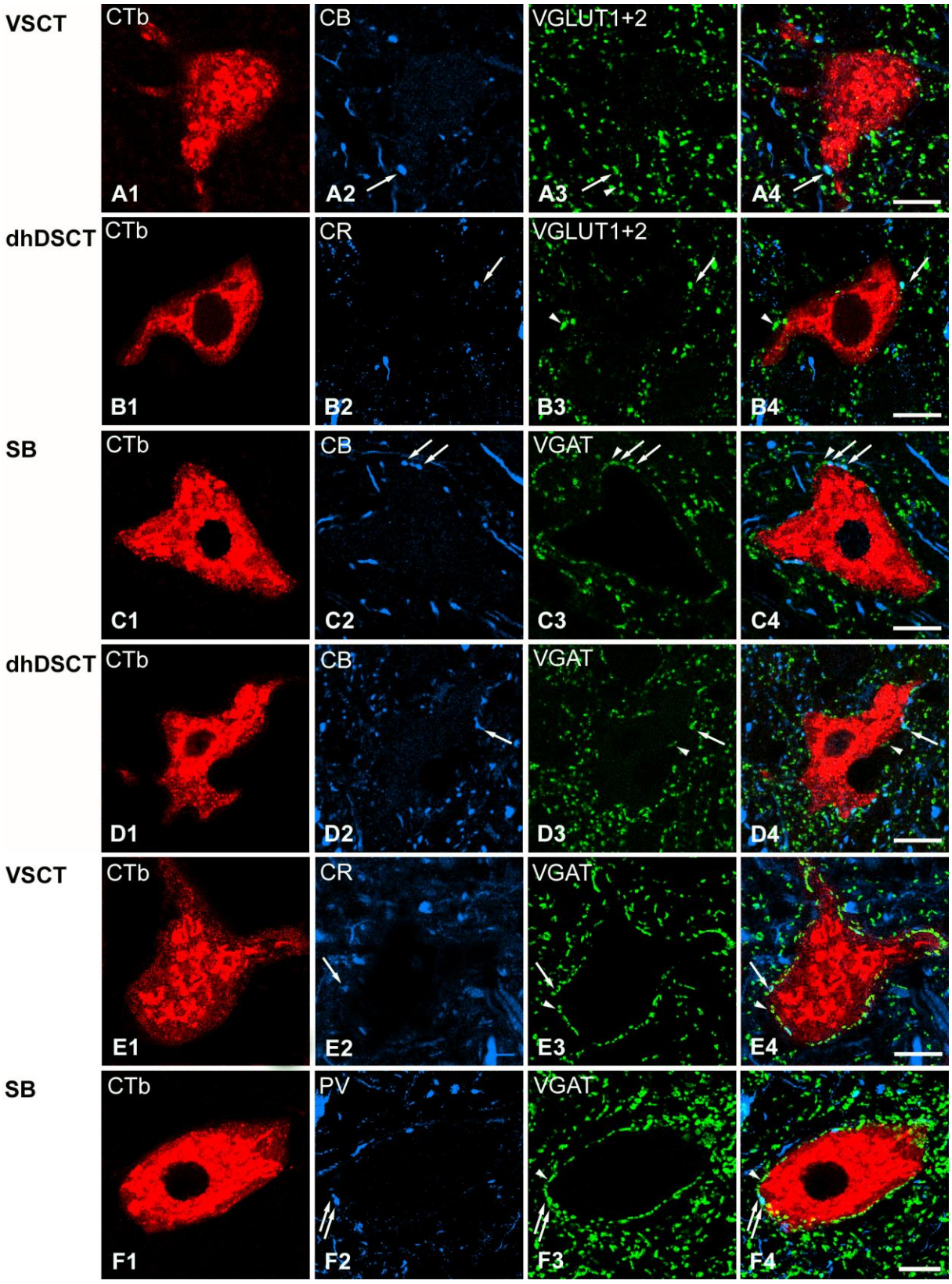
VSCT
CTb
CB
VGLUT1+2
A1
A2
A3
A4
dhDSCT
CTb
CR
VGLUT1+2
B1
B2
B3
B4
SB
CTb
CB
VGAT
C1
C2
C3
C4
dhDSCT
CTb
CB
VGAT
D1
D2
D3
D4
VSCT
CTb
CR
VGAT
E1
E2
E3
E4
SB
CTb
PV
VGAT
F1
F2
F3
F4

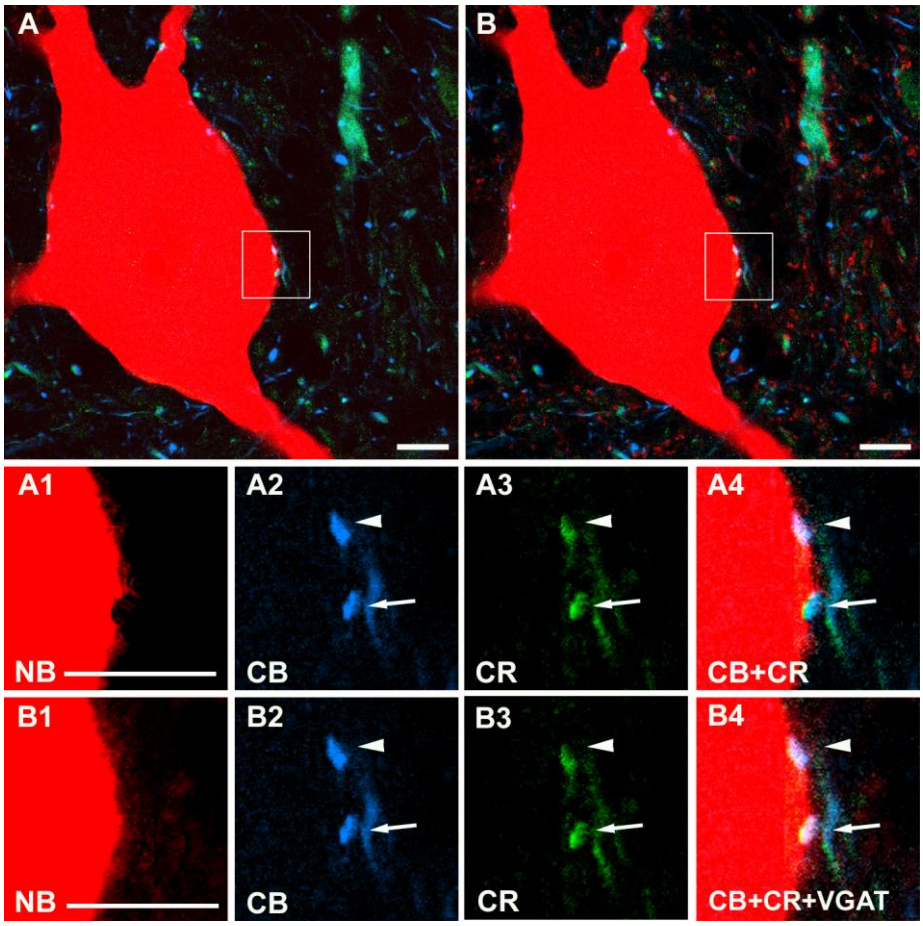

Figure 5-10 Sequential immunohistochemical characteristics of CB and CR terminals with VGAT in contact with intracellularly labelled spinocerebellar tract neurons

A-B, A general overview of a single optical section through the cell bodies of representative VSCT neuron (Cell IV) before and after a reaction with sequentially reacted antibody against VGAT. Details of the areas demarcated by the boxes are shown in ***A1-A4*** and ***B1-B4***. ***A1-A4***, Single optical sections illustrating contacts made by CB and CR double labelled terminals with the cell. ***B1-B4***, Single optical sections of the same field that was rescanned after sequential incubation with antibody against VGAT. Arrows indicate CB and CR double labelled terminals which also had additional labelling with VGAT. Arrowhead indicates CB and CR double labelled terminals which did not have additional labelling with VGAT. Scale bar in ***A***, ***B*** = 10 μm. Scale bar in ***A1-A4 and B1-B4*** = 5 μm.

Figure 5-11 Reconstructions of spinocerebellar tract neurons illustrating the distribution patterns of CB, CR, CB+CR, CB+VGAT, CR+VGAT and CB+CR+VGAT contacts

Reconstructions of spinocerebellar tract neurons showing the distributions of CB (red), CB colocalised with VGAT (blue), CR (green), CR colocalised with VGAT (orange), CB double labelled with CR (purple) and CB and CR double labelled terminals colocalised with VGAT (pink) contacts throughout the dendritic trees. The reconstructions were made with Neurolucida for Confocal. All the small images without contacts plotted show the reconstructions of respective cells. Cell body and dendrites are shown in light grey. Scale bars = 50 μm for reconstructions with contacts plotted and 100 μm for reconstructions without contacts. All are oriented such that the midline is to the left and the lateral borders of the grey matter to the right. All the small images without contacts plotted show the reconstructions of the cells. Somata and dendrites are shown in dark grey.

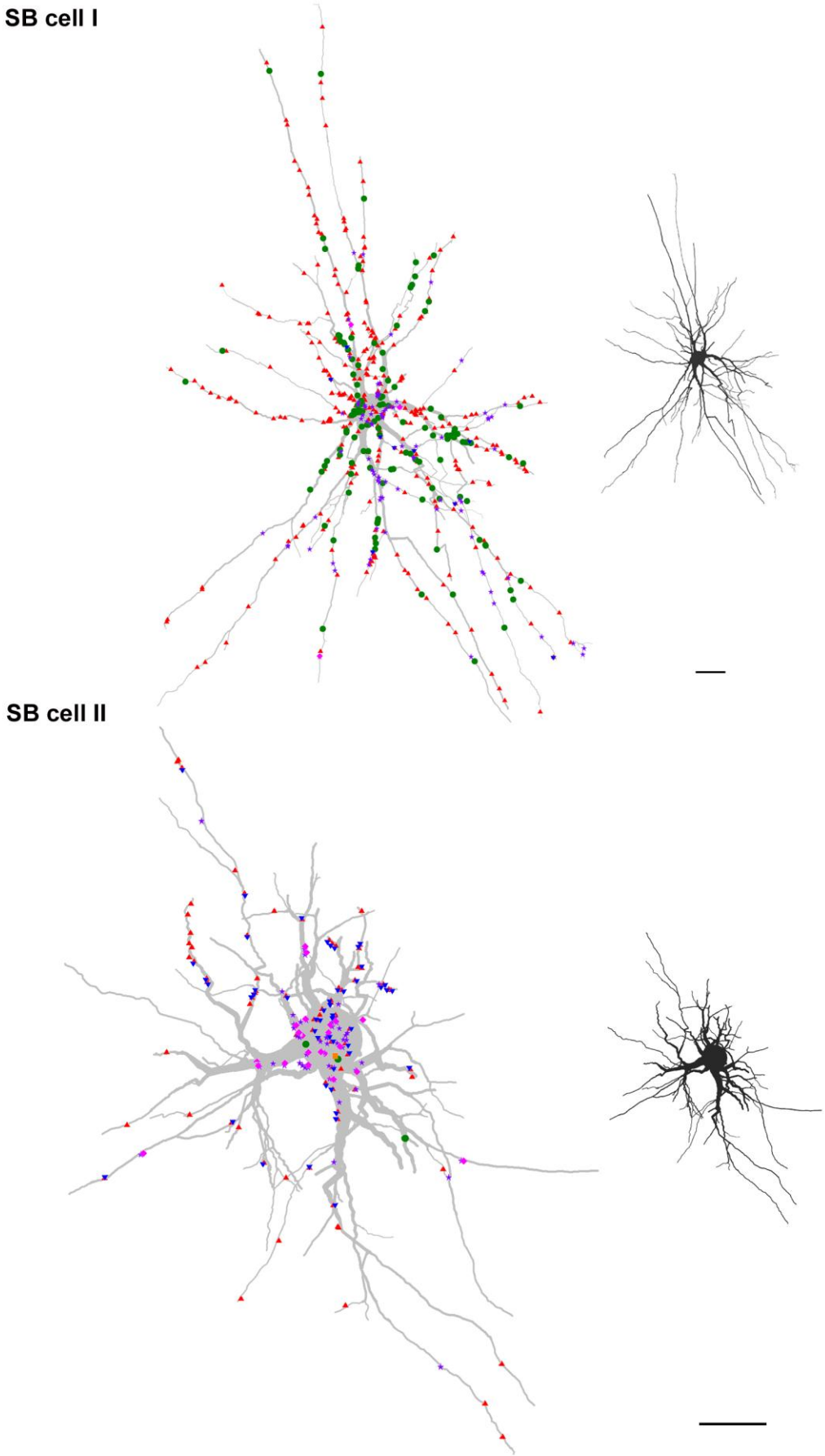
SB cell I
SB cell II

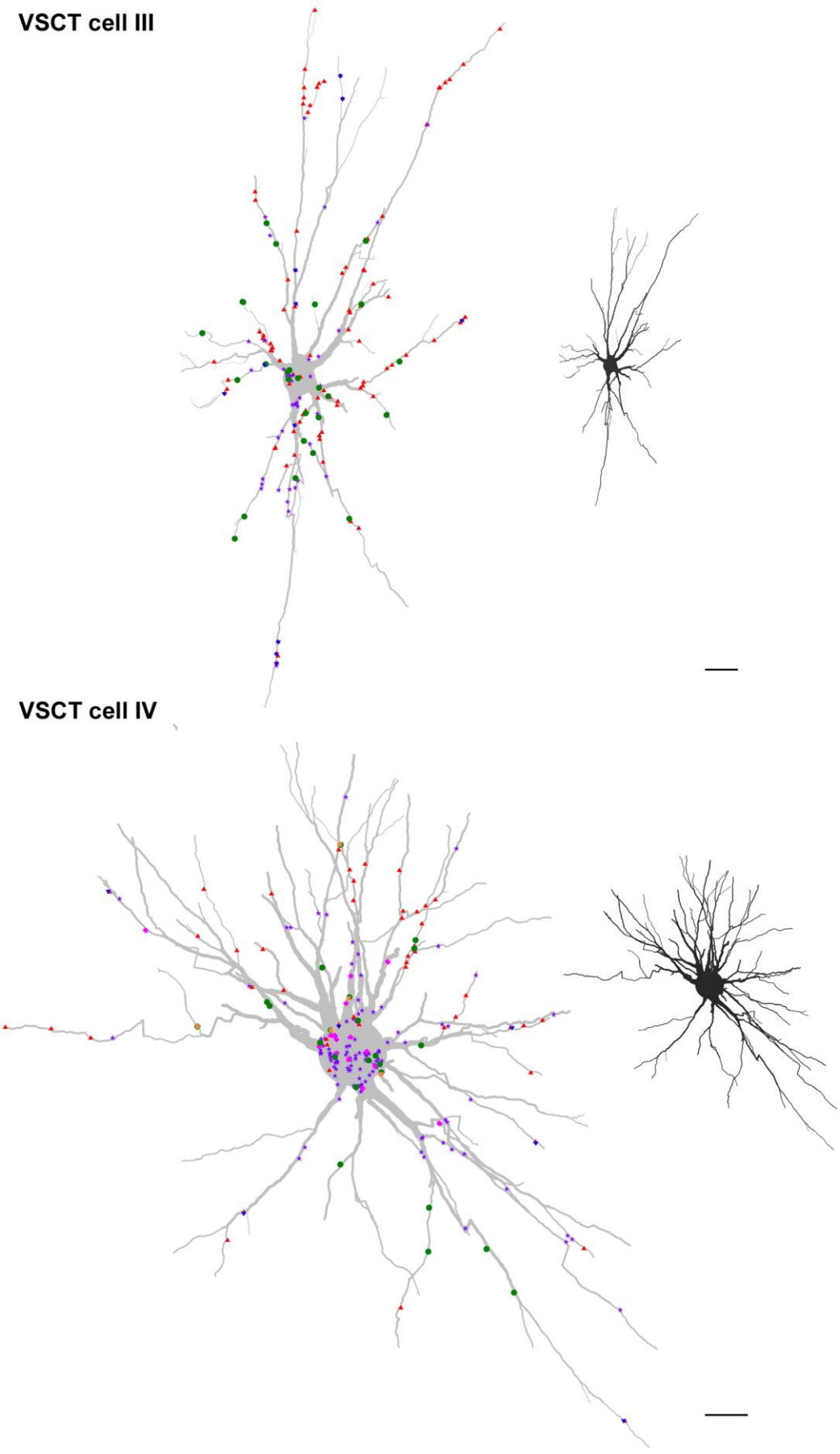
VSCT cell III
VSCT cell IV

Figure 5-12 Photomicrograph and reconstruction of a representative section of the rat brain illustrating an injection site in the cerebellum and the MLF

A*, *B*,** A photomicrograph of a coronal section of the brain showing an injection site in the cerebellum (FG) and the MLF (CTb) respectively. ***A1-A3*,** Reconstruction of the injection sites for all 3 animals. The black shaded area shows the FG injection site and the grey shaded area shows the maximum spread of the FG projected on a schematic drawing based on the atlas of Paxinos and Watson (1997). ***B1-B3*,** Reconstruction of the injection sites for all 3 animals. The black shaded area shows the CTb injection site and the grey shaded area shows the maximum spread of the CTb projected on a schematic drawing based on the atlas of Paxinos and Watson (1997). Scale bar in ***A*, *B 100 μm.

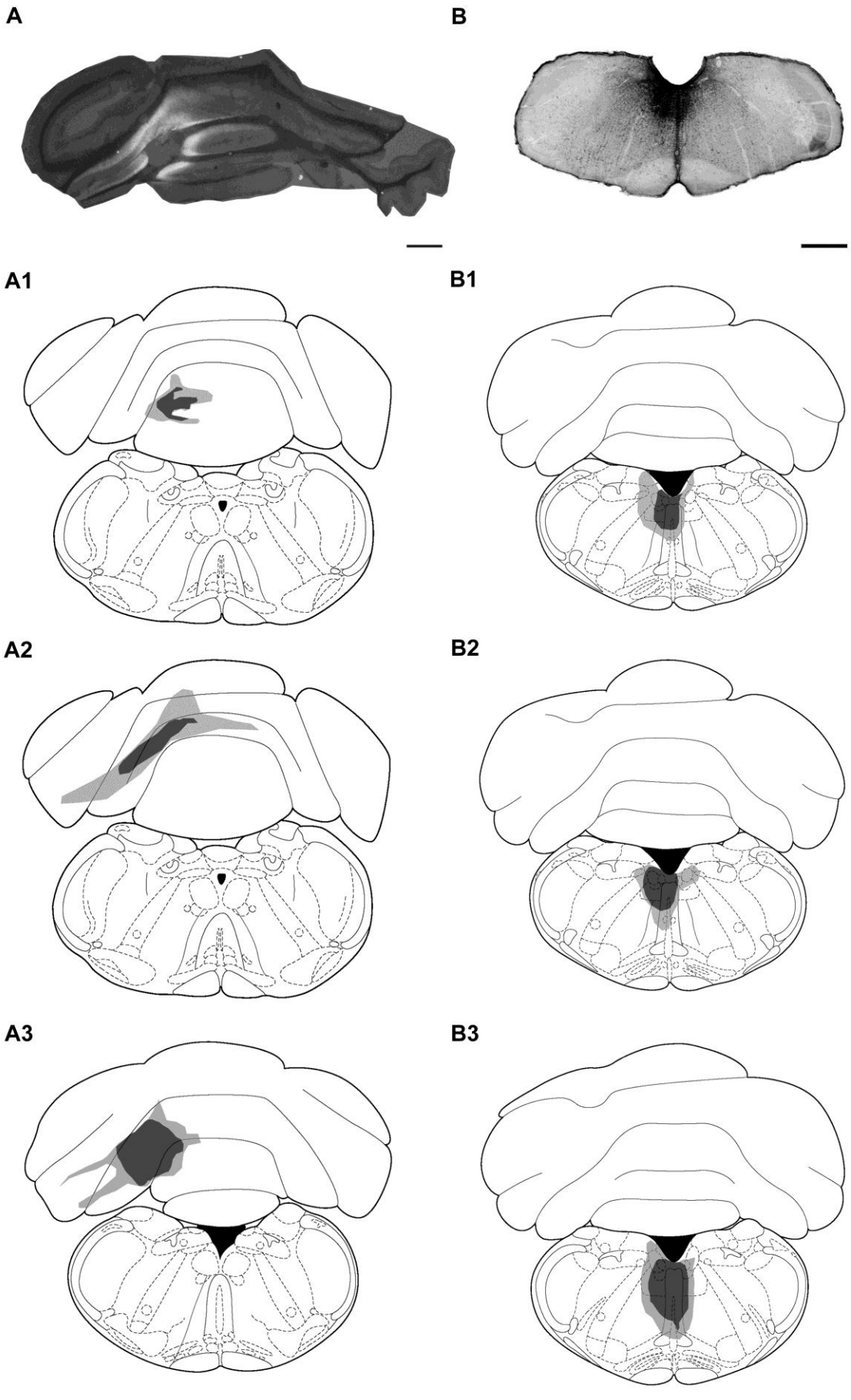
A
B
A1
B1
A2
B2
A3
B3

Figure 5-13 Photomicrograph and reconstruction of a representative section of the rat brain illustrating an injection site in the cerebellum and the CVLM

A*,*B*,** A photomicrograph of a coronal section of the brain showing an injection site in the cerebellum (FG) and the CVLM (CTb) respectively. ***A1-A3*,** Reconstruction of the injection sites for all 3 animals. The black shaded area shows the FG injection site and the grey shaded area shows the maximum spread of the FG projected on a schematic drawing based on the atlas of Paxinos and Watson (1997). ***B1-B3*,** Reconstruction of the injection sites for all 3 animals. The black shaded area shows the CTb injection site and the grey shaded area shows the maximum spread of the CTb projected on a schematic drawing based on the atlas of Paxinos and Watson (1997). Scale bar in ***A*, *B = 100 μm.

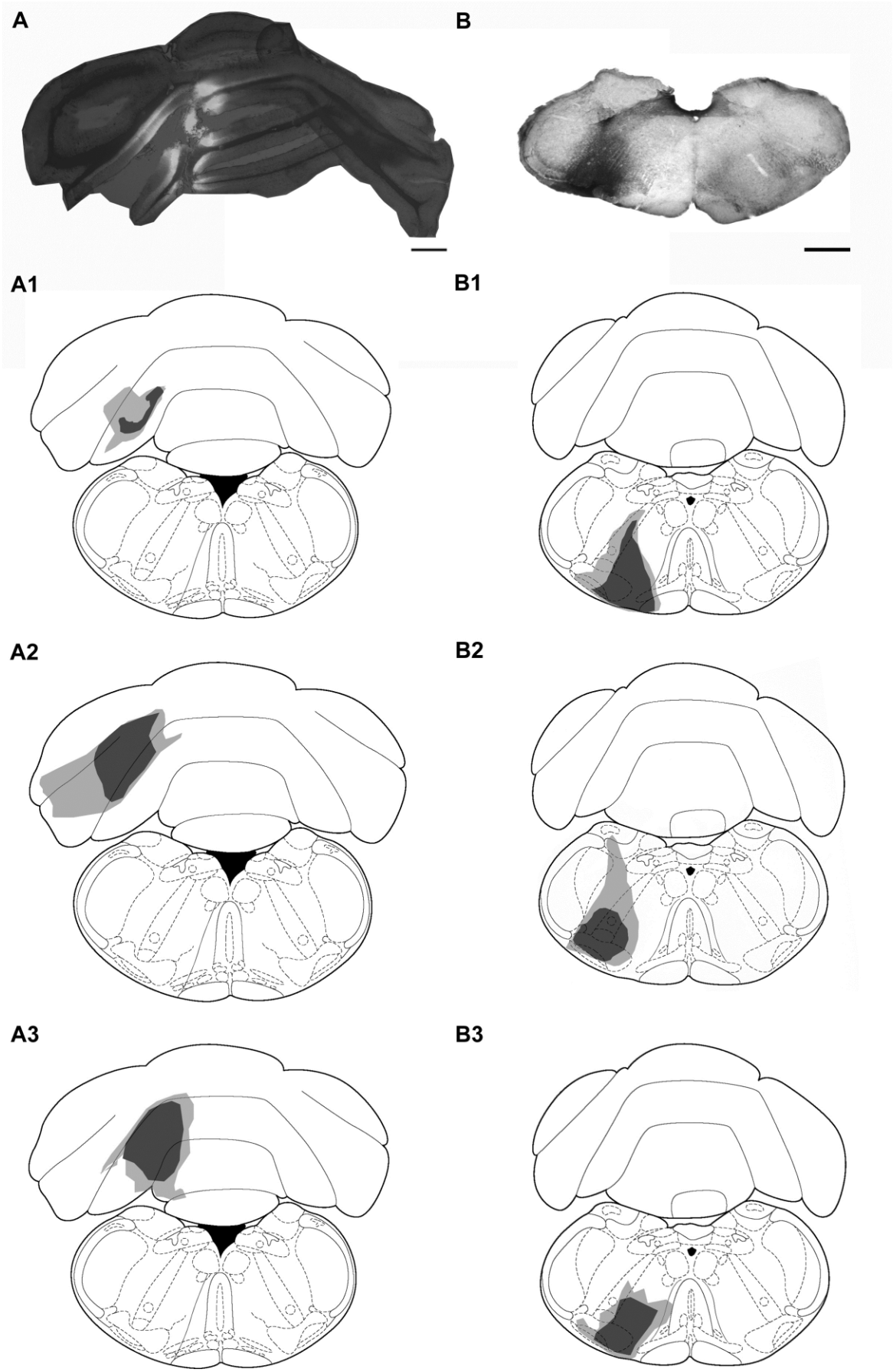
A
B
A1
B1
A2
B2
A3
B3

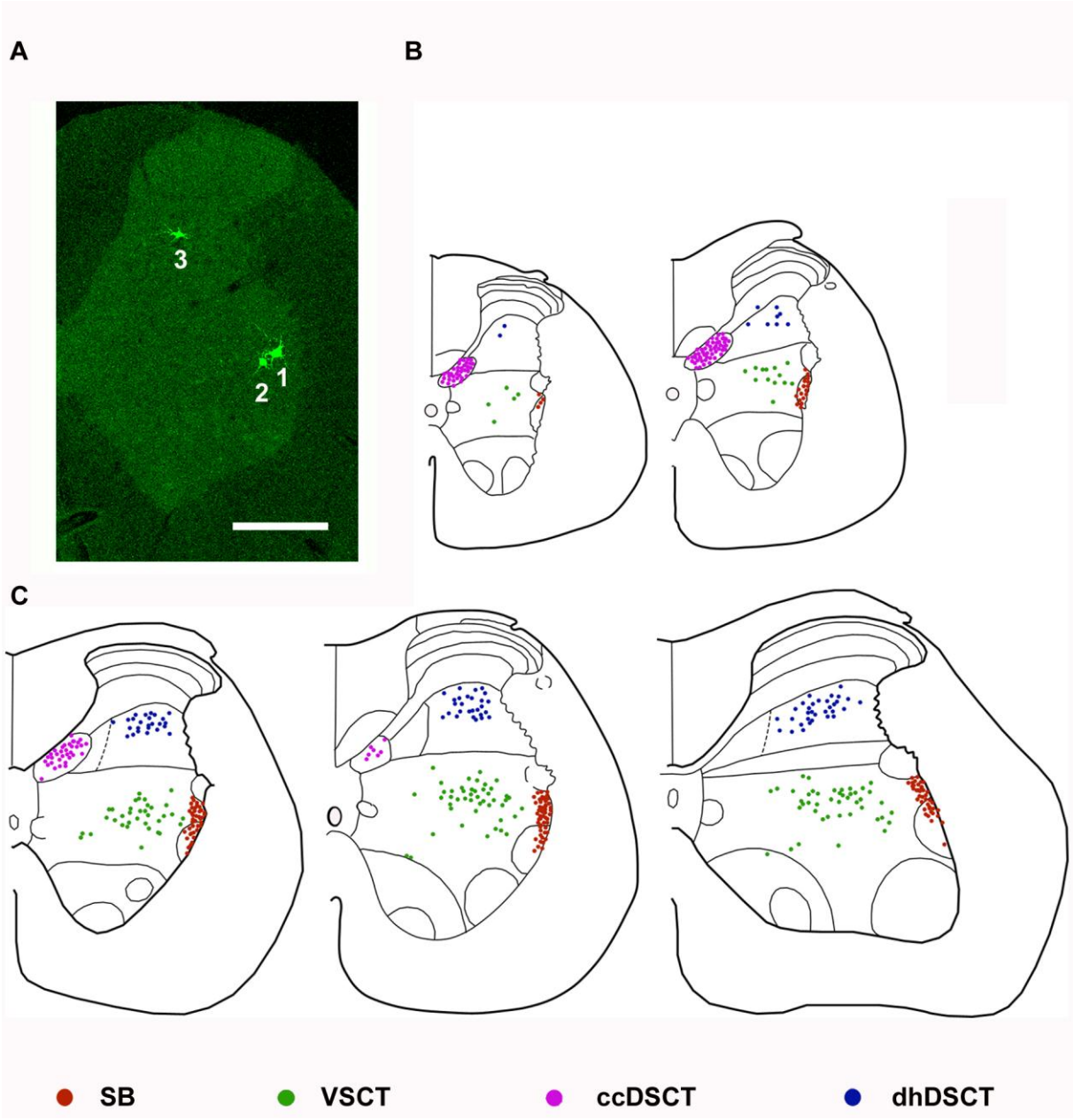

Figure 5-14 Locations of 526 analysed spinocerebellar tract neurons labelled retrogradely with FG

A*,** A photomicrograph of a transverse section of the L2 segment of the rat spinal cord showing the location of one of the SB neurons (1), VSCT neurons (2) and dhDSCT neurons (3) identified by retrograde transport of FG. ***B & C*,** Diagrams illustrating the locations of cell bodies of 526 cells analysed in the Th12 and Th13 segments and L1, L2 and L3 segments respectively. Scale bar in ***A 400 µm.

Figure 5-15 Immunohistochemical characteristics of RetS axon terminals labelled from the MLF injection in contact with retrogradely rat labelled spinocerebellar tract neurons

A-D*,** Single optical sections through the cell bodies of representative SB,VSCT, ccDSCT and dhDSCT neurons showing the presence of CTb (red) and VGLUT2 (blue) immunoreactive terminals. The cell body and dendrites of retrogradely labelled cells are in green. Scale bar in ***A-D = 20 µm. ***A1-A4; B1-B4; C1-C4, and D1-D4*,** Single optical section of soma/ dendritic trunks from cells shown in ***A*, *B*, *C*** and ***D*** respectively (areas encompassed in the boxes) illustrating contacts made by CTb terminals expressing VGLUT2 (magenta) with the cell. Scale bar in ***A1-A4*, *B1-B4*, *C1-C4*** and ***D1-D4*** = 5 µm. ***A'-D'*,** Single optical sections through the cell bodies of representative SB, VSCT, ccDSCT and dhDSCT neurons showing the presence of CTb (red) and VGAT (blue) immunoreactive terminals. Scale bar in ***A'-D'*** = 20 µm. The cell body and dendrites of retrogradely labelled cells are in green. ***A'1-A'4; B'1-B'4; C'1-C'4, and D'1-D'4*,** Single optical section of soma/ dendritic trunks from cells shown in ***A'*, *B'*, *C'*** and ***D'*** respectively (areas encompassed in the boxes) illustrating contacts made by CTb terminals expressing VGAT (magenta) with the cell. Scale bar in ***A'1-A'4*, *B'1-B'4*, *C'1-C'4*** and ***D'1-D'4*** = 5 µm.

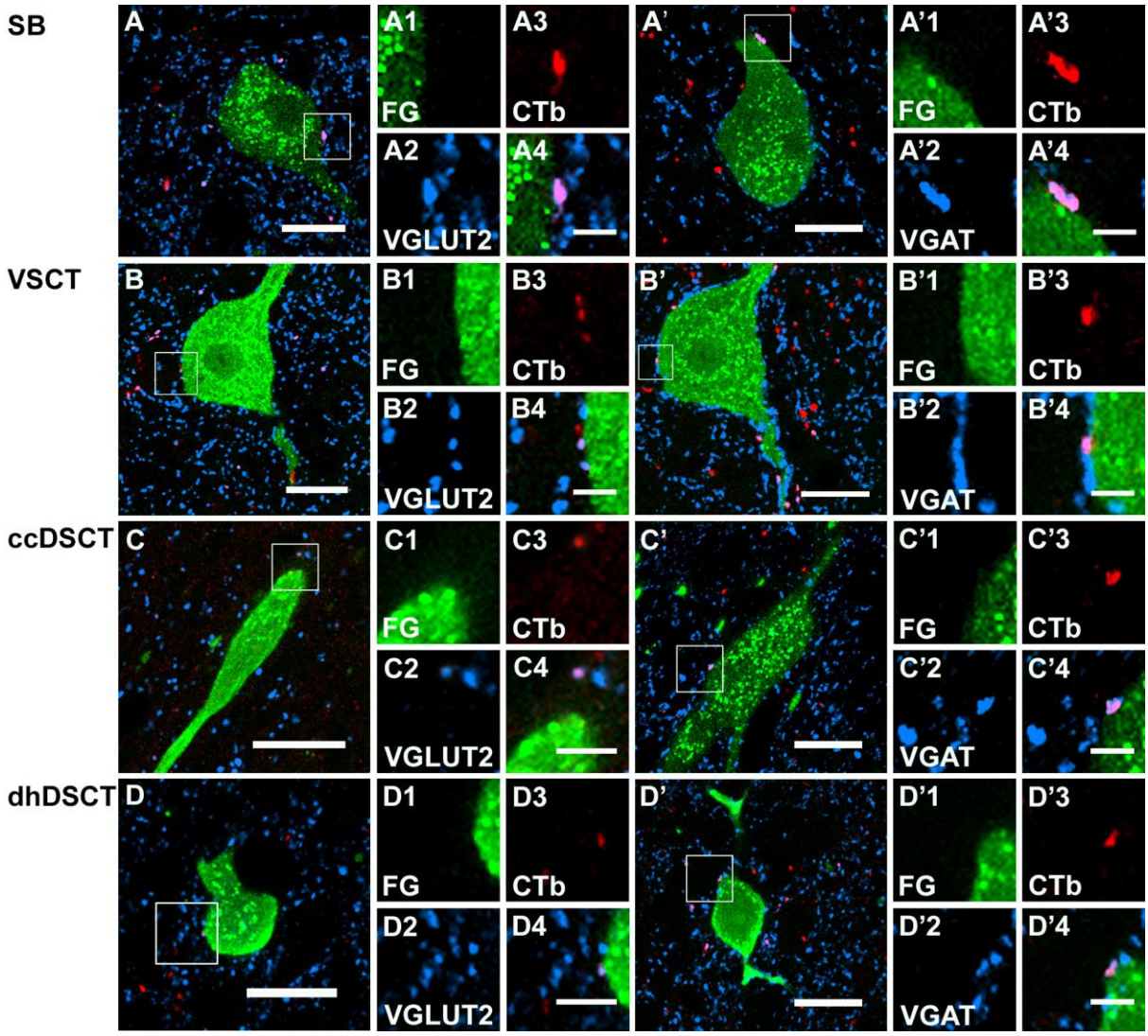
SB
VSCT
ccDSCT
dhDSCT
A
A1
FG
A3
CTb
A2
VGLUT2
A4
A'
A'1
FG
A'3
CTb
A'2
VGAT
A'4
B
B1
FG
B3
CTb
B2
VGLUT2
B4
B'
B'1
FG
B'3
CTb
B'2
VGAT
B'4
C
C1
FG
C3
CTb
C2
VGLUT2
C4
C'
C'1
FG
C'3
CTb
C'2
VGAT
C'4
D
D1
FG
D3
CTb
D2
VGLUT2
D4
D'
D'1
FG
D'3
CTb
D'2
VGAT
D'4

Figure 5-16 Comparison between the contact densities of RetS terminals labelled with VGLUT2 and VGAT in different populations of retrogradely labelled spinocerebellar tract neurons

***A*,** Differences in the overall contact density of RetS terminals labelled by transport of CTb from the MLF expressing VGLUT2 / 100 μm^2 for the four different populations of spinocerebellar tract neurons. The contact density in SB neurons is significantly different from that on ccDSCT neurons ($p < 0.05$). Similarly, the overall contact density in VSCT neurons is significantly different from that on ccDSCT neurons ($p < 0.01$). ***B*,** Differences in the overall contact density of RetS terminals labelled by transport of CTb from the MLF expressing VGAT / 100 μm^2 for the four different populations of spinocerebellar tract neurons. All experiments were carried out in 3 rats (160 cells). Data presented as mean ± SD. ***C*,** Differences in the overall contact density of RetS terminals labelled by transport of CTb from the CVLM expressing VGLUT2 / 100 μm^2 for the four different populations of spinocerebellar tract neurons. The contact density in SB neurons is significantly different from that on ccDSCT neurons ($p < 0.01$) and dhDSCT neurons ($p < 0.01$). Similarly, the overall contact density in VSCT neurons is significantly different from that on ccDSCT neurons ($p < 0.001$) and dhDSCT neurons ($p < 0.001$). ***D*,** Differences in the overall contact density of RetS terminals labelled by transport of CTb from the CVLM expressing VGAT / 100 μm^2 for the four different populations of spinocerebellar tract neurons. The contact density in SB neurons is significantly different from that on ccDSCT neurons ($p < 0.05$) and dhDSCT neurons ($p < 0.05$). Similarly, the overall contact density in VSCT neurons is significantly different from that on ccDSCT neurons ($p < 0.01$) and dhDSCT neurons ($p < 0.01$). All experiments were carried out in 3 rats (199 cells). Data presented as mean ± SD. * denotes $p<0.05$, ** denotes $p<0.01$ and *** denotes $p < 0.001$.

MLF Injection

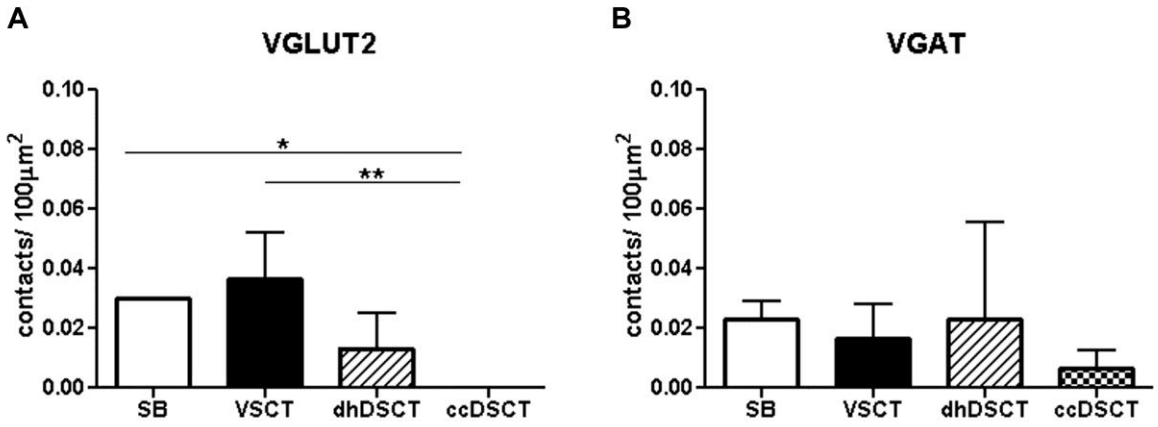

CVLM Injection

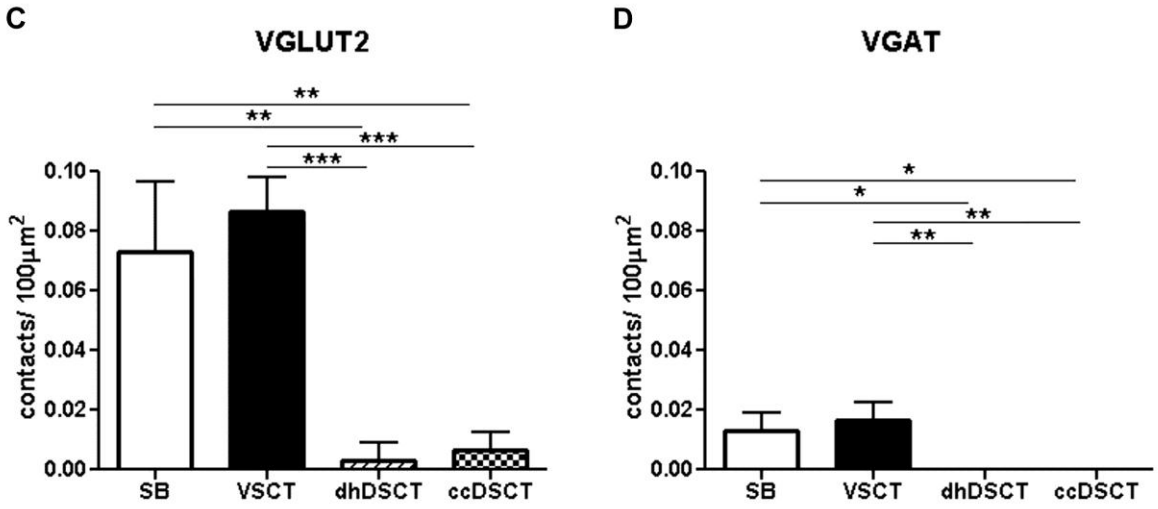

Figure 5-17 Immunohistochemical characteristics of RetS axon terminals labelled from the CVLM injection in contact with retrogradely labelled rat spinocerebellar tract neurons

A-D*,** Single optical sections through the cell bodies of representative SB, VSCT, ccDSCT and dhDSCT neurons showing the presence of CTb (red) and VGLUT2 (blue) immunoreactive terminals. The cell body and dendrites of retrogradely labelled cells are in green. Scale bar in ***A-D = 20 µm. ***A1-A4; B1-B4; C1-C4, and D1-D4*,** Single optical section of soma/ dendritic trunks from cells shown in ***A*, *B*, *C*** and ***D*** respectively (areas encompassed in the boxes) illustrating contacts made by CTb terminals expressing VGLUT2 (magenta) with the cell. Scale bar in ***A1-A4*, *B1-B4*, *C1-C4*** and ***D1-D4*** = 5 µm. ***A'-D'*,** Single optical sections through the cell bodies of representative SB, VSCT, ccDSCT and dhDSCT neurons showing the presence of CTb (red) and VGAT (blue) immunoreactive terminals. The cell body and dendrites of retrogradely labelled cells are in green. Scale bar in ***A'-D'*** = 20 µm. ***A'1-A'4; B'1-B'4; C'1-C'4, and D'1-D'4*,** Single optical section of soma/ dendritic trunks from cells shown in ***A'*, *B'*, *C'*** and ***D'*** respectively (areas encompassed in the boxes) illustrating contacts made by CTb terminals expressing VGAT (magenta) with the cell. Scale bar in ***A'1-A'4*, *B'1-B'4*, *C'1-C'4*** and ***D'1-D'4*** = 5 µm.

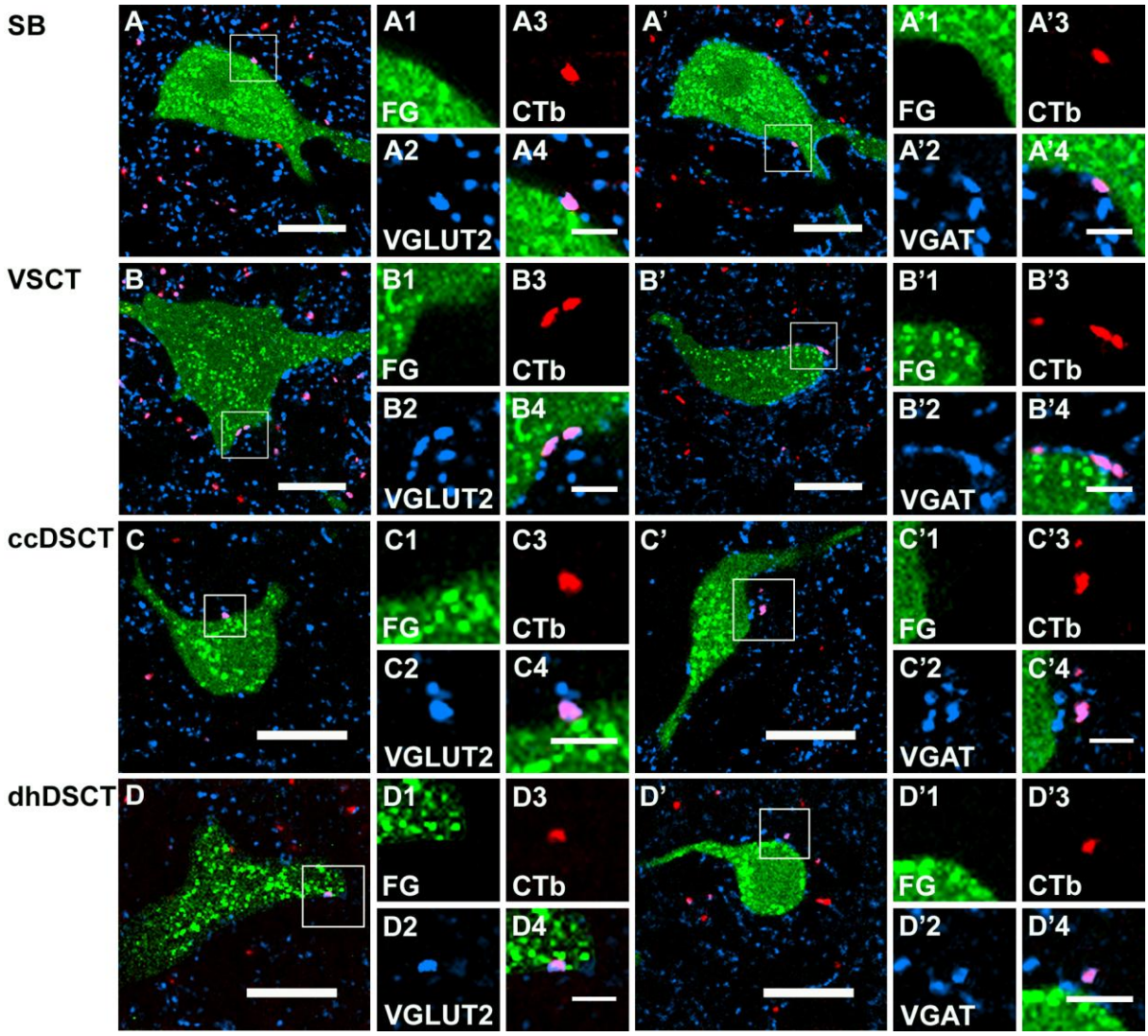
SB
VSCT
ccDSCT
dhDSCT
A
A1
FG
A3
CTb
A2
VGLUT2
A4
A'
A'1
FG
A'3
CTb
A'2
VGAT
A'4
B
B1
FG
B3
CTb
B2
VGLUT2
B4
B'
B'1
FG
B'3
CTb
B'2
VGAT
B'4
C
C1
FG
C3
CTb
C2
VGLUT2
C4
C'
C'1
FG
C'3
CTb
C'2
VGAT
C'4
D
D1
FG
D3
CTb
D2
VGLUT2
D4
D'
D'1
FG
D'3
CTb
D'2
VGAT
D'4

Figure 5-18 Photomicrograph and reconstruction of a representative section of the rat brain illustrating an injection site in the cerebellum and the sensorimotor cortex

A*, *B*,** A photomicrograph of a coronal section of the brain showing an injection site in the cerebellum (FG) and the sensorimotor cortex (CTb) respectively. ***A1-A3*,** Reconstruction of the injection sites for 2 animals. The black shaded area shows the FG injection site and the grey shaded area shows the maximum spread of the FG projected on a schematic drawing based on the atlas of Paxinos and Watson (1997). ***B1-B3*,** Reconstruction of the injection sites for 2 animals. The black shaded area shows the CTb injection site and the grey shaded area shows the maximum spread of the CTb projected on a schematic drawing based on the atlas of Paxinos and Watson (1997). Scale bar in ***A*, *B = 100 μm.

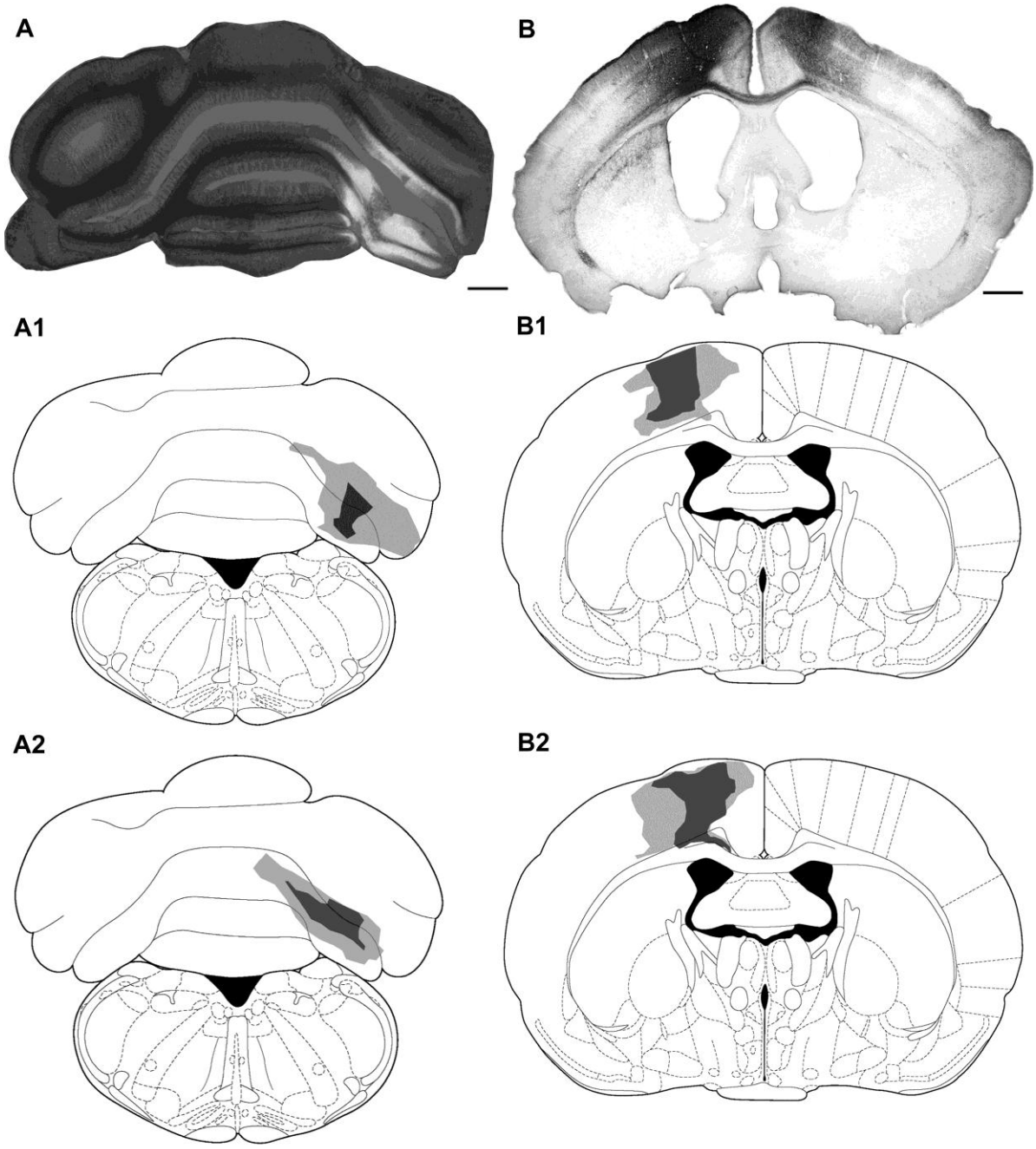
A
B
A1
B1
A2
B2

Figure 5-19 Immunohistochemical characteristics of CS axon terminals labelled from the sensorimotor cortex injection in contact with retrogradely labelled rat spinocerebellar tract neurons

A-D, Single optical sections through the cell bodies of representative SB, VSCT, ccDSCT and dhDSCT neurons showing the presence of CTb (red) and VGLUT1 (blue) immunoreactive terminals. The cell body and dendrites of retrogradely labelled cells are in green. ***A1-A4; B1-B4; C1-C4, and D1-D4***, Single optical section of soma/ dendritic trunks from cells shown in ***A***, ***B***, ***C*** and ***D*** respectively (areas encompassed in the boxes) illustrating contacts made by CTb terminals expressing VGLUT1 (turquoise) with the cell. Scale bar in ***A-D*** = 20 µm. Scale bar in ***A1-A4***, ***B1-B4***, ***C1-C4*** and ***D1-D4*** = 5 µm.

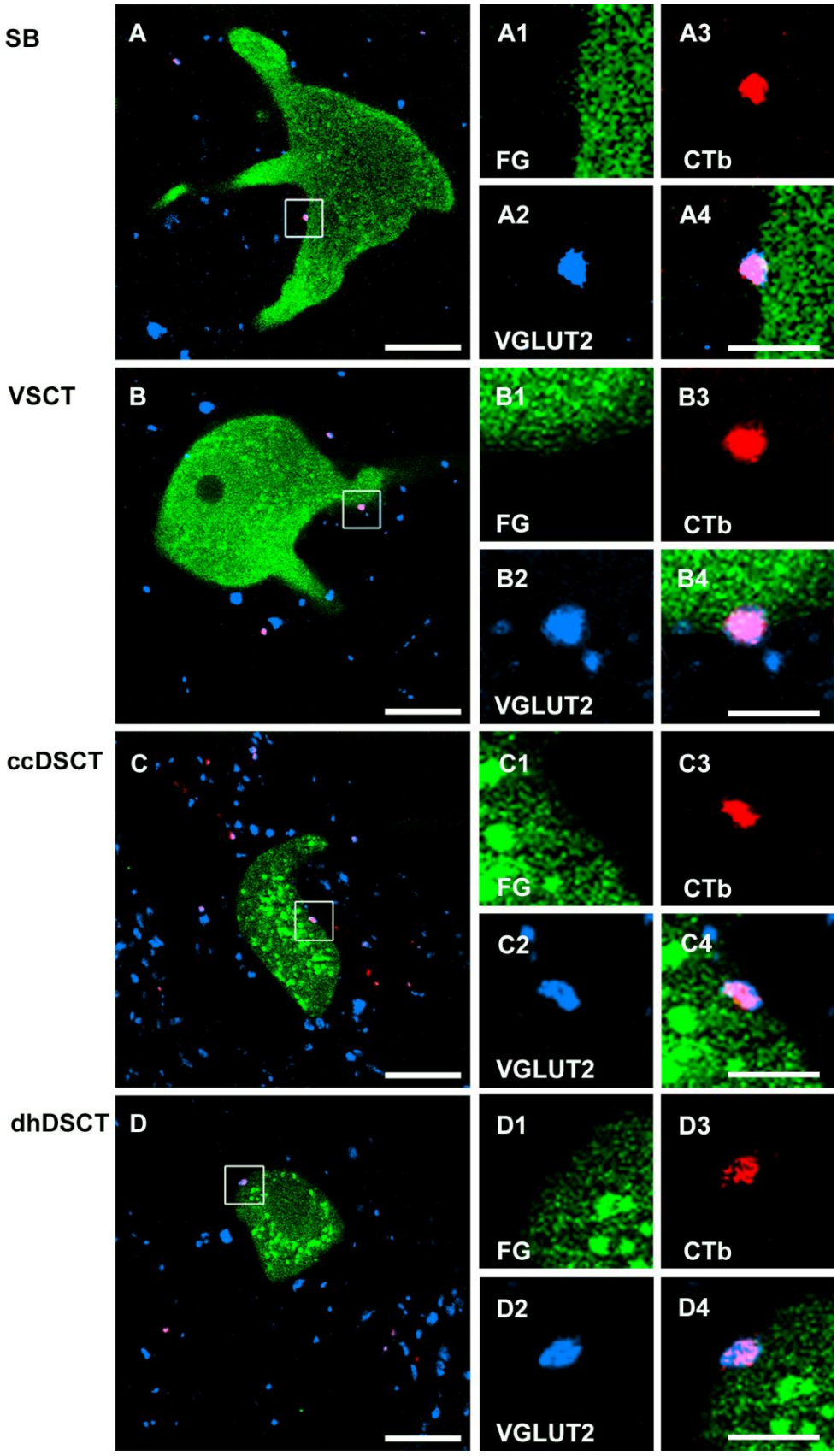
SB
A
A1
FG
A3
CTb
A2
VGLUT2
A4
VSCT
B
B1
FG
B3
CTb
B2
VGLUT2
B4
ccDSCT
C
C1
FG
C3
CTb
C2
VGLUT2
C4
dhDSCT
D
D1
FG
D3
CTb
D2
VGLUT2
D4

Table 5-4 The number and densities of VGLUT1, PV and VGLUT1+PV axon terminals in apposition with cell bodies and dendrites of different populations of spinocerebellar tract neurons in cats

Populations of Spinocerebellar tract neurons	Cell	Contacts (total number)			Total Surface area (μm^2)	Density (n/ 100 μm^2)		
		VGLUT1+PV	VGLUT1	PV		VGLUT1+PV	VGLUT1	PV
VSCT								
	Cell a	114	513	6	68810.69	0.17	0.75	0.01
	Cell b	89	400	44	126623.20	0.07	0.32	0.03
Mean						**0.12**	**0.53**	**0.02**
ccDSCT								
	Cell c	539	706	14	31616.57	1.70	2.23	0.04
	Cell d	471	884	22	56803.29	0.83	1.56	0.04
	Cell e	378	1316	13	98938.30	0.38	1.33	0.01
Mean						**0.97**	**1.71**	**0.03**
SD						**0.67**	**0.47**	**0.02**
dhDSCT								
	Cell f	47	1090	24	66975.08	0.07	1.63	0.04
	Cell g	137	2084	16	115321.10	0.12	1.81	0.01
	Cell h	7	2051	9	117383.54	0.01	1.75	0.01
Mean						**0.06**	**1.73**	**0.02**
SD						**0.06**	**0.09**	**0.01**

Table 5-5 The densities of VGLUT1, PV and VGLUT1+PV axon terminals in apposition with cell bodies and dendrites of different populations of spinocerebellar tract neurons in rats

Populations of Spinocerebellar tract neurons	Animal No.	No. of Cells	Average Density (n/ 100 μm^2)		
			VGLUT1 and PV	VGLUT1	PV
SB					
	Rat 1	2	0.00	0.16	0.03
	Rat 2	2	0.04	0.06	0.07
	Rat 3	6	0.02	0.02	0.01
	Rat 4	7	0.02	0.04	0.03
Mean			**0.02**	**0.07**	**0.04**
SD			**0.02**	**0.06**	**0.03**
VSCT					
	Rat 1	3	0.01	0.06	0.05
	Rat 2	2	0.04	0.11	0.03
	Rat 3	5	0.00	0.08	0.03
	Rat 4	7	0.01	0.21	0.01
Mean			**0.02**	**0.12**	**0.03**
SD			**0.02**	**0.07**	**0.02**
ccDSCT					
	Rat 1	4	0.34	0.29	0.00
	Rat 2	2	0.33	0.28	0.00
	Rat 3	6	0.12	0.22	0.01
	Rat 4	5	0.13	0.39	0.01
Mean			**0.23**	**0.30**	**0.01**
SD			**0.12**	**0.07**	**0.01**
dhDSCT					
	Rat 1	5	0.01	0.26	0.02
	Rat 2	2	0.02	0.13	0.03
	Rat 3	8	0.00	0.22	0.02
	Rat 4	6	0.15	0.01	0.01
Mean			**0.05**	**0.16**	**0.02**
SD			**0.07**	**0.11**	**0.01**

Table 5-6 The number and densities of CB, CR and VGLUT2 axon terminals in apposition with cell bodies and dendrites of different populations of spinocerebellar tract neurons in cats

Populations of Spinocerebellar tract neurons	Cell	Contacts (total number)						Total Surface area (μm^2)	Density (n/ 100µm2)					
		CB+VGLUT2	CR+VGLUT2	CB+CR+VGLUT2	CB	CR	CB+CR		CB+VGLUT2	CR+VGLUT2	CB+CR+VGLUT2	CB	CR	CB+CR
SB														
	Cell 1	15	8	6	38	12	11	75724.67	0.02	0.01	0.01	0.05	0.02	0.01
	Cell 2	16	13	10	17	12	40	101829.88	0.02	0.01	0.01	0.02	0.01	0.04
	Cell 3	32	4	16	33	3	109	120081.82	0.03	0.00	0.01	0.03	0.00	0.09
Mean									**0.02**	**0.01**	**0.01**	**0.03**	**0.01**	**0.05**
SD									**0.01**	**0.00**	**0.00**	**0.02**	**0.01**	**0.04**
VSCT														
	Cell 4	67	6	18	41	9	15	80448.55	0.08	0.01	0.02	0.05	0.01	0.02
	Cell 5	116	4	28	77	9	78	125093.84	0.09	0.00	0.02	0.06	0.01	0.06
Mean									**0.09**	**0.01**	**0.02**	**0.06**	**0.01**	**0.04**

Table 5-7 The densities of VGLUT1+2/VGAT and CB/CR/PV axon terminals in apposition with cell bodies and dendrites of different populations of spinocerebellar tract neurons in rats

Populations of Spinocerebellar tract neurons		Average Density (n/ 100 μm^2)				
		CB+VGLUT1+2	CR+VGLUT1+2	CB+VGAT	CR+VGAT	PV+VGAT
SB						
	Rat 1	0.01	0.00	0.33	0.14	0.10
	Rat 2	0.02	0.00	0.29	0.01	0.17
	Rat 3	0.01	0.00	0.03	0.01	0.04
	Rat 4	0.02	0.00	0.14	0.00	0.01
Mean		**0.02**	**0.00**	**0.20**	**0.04**	**0.08**
SD		**0.01**	**0.00**	**0.14**	**0.07**	**0.07**
VSCT						
	Rat 1	0.02	0.00	0.19	0.01	0.04
	Rat 2	0.02	0.00	0.06	0.00	0.10
	Rat 3	0.03	0.01	0.01	0.01	0.05
	Rat 4	0.03	0.02	0.06	0.03	0.05
Mean		**0.03**	**0.01**	**0.08**	**0.01**	**0.06**
SD		**0.01**	**0.01**	**0.08**	**0.01**	**0.03**
ccDSCT						
	Rat 1	0.00	0.04	0.03	0.00	0.03
	Rat 2	0.01	0.09	0.02	0.00	0.01
	Rat 3	0.03	0.01	0.00	0.01	0.04
	Rat 4	0.01	0.00	0.04	0.00	0.00
Mean		**0.01**	**0.04**	**0.02**	**0.00**	**0.02**
SD		**0.01**	**0.04**	**0.02**	**0.01**	**0.02**
dhDSCT						
	Rat 1	0.02	0.00	0.43	0.02	0.02
	Rat 2	0.02	0.00	0.70	0.02	0.14
	Rat 3	0.02	0.01	0.46	0.00	0.07
	Rat 4	0.01	0.00	0.24	0.00	0.01
Mean		**0.02**	**0.00**	**0.46**	**0.01**	**0.06**
SD		**0.01**	**0.01**	**0.19**	**0.01**	**0.06**

Table 5-8 The number and densities of CB, CR and VGAT axon terminals in apposition with cell bodies and dendrites of different populations of spinocerebellar tract neurons in cats

Populations of Spinocerebellar tract neurons	Cell	Contacts (total number)						Total Surface area (μm^2)	Density (n/ 100μm2)					
		CB+VGAT	CR+VGAT	CB+CR+VGAT	CB	CR	CB+CR		CB+VGAT	CR+VGAT	CB+CR+VGAT	CB	CR	CB+CR
SB														
	Cell I	9	0	4	126	314	87	144918.01	0.01	0.00	0.00	0.87	0.22	0.06
	Cell II	49	1	23	2	81	32	18763.64	0.26	0.01	0.12	0.11	0.43	0.17
Mean									**0.13**	**0.00**	**0.06**	**0.49**	**0.32**	**0.12**
VSCT														
	Cell III	26	98	44	26	98	44	97816.77	0.03	0.10	0.04	0.27	0.10	0.04
	Cell IV	18	45	112	18	45	112	177616.62	0.01	0.03	0.06	0.10	0.03	0.06
Mean									**0.02**	**0.06**	**0.05**	**0.18**	**0.06**	**0.05**

Table 5-9 The densities of RetS* axon terminals expressing VGLUT2 and VGAT in apposition with cell bodies and dendrites of different populations of retrogradely labelled spinocerebellar tract neurons in rats

Populations of Spinocerebellar tract neurons	Animal No.	No. of Cells	Average Density (n/ 100 µm2)		
			CTb+VGLUT2	CTb+VGAT	CTb
SB					
	Rat 1	16	0.03	0.02	0.00
	Rat 2	10	0.03	0.02	0.00
	Rat 3	19	0.03	0.03	0.00
Mean			**0.03**	**0.02**	**0.00**
SD			**0.00**	**0.01**	**0.00**
VSCT					
	Rat 1	11	0.02	0.01	0
	Rat 2	15	0.05	0.01	0
	Rat 3	19	0.04	0.03	0.00
Mean			**0.04**	**0.02**	**0.00**
SD			**0.02**	**0.01**	**0.00**
ccDSCT					
	Rat 1	8	0.00	0.01	0.00
	Rat 2	9	0.00	0.00	0.00
	Rat 3	17	0.00	0.01	0.00
Mean			**0.00**	**0.00**	**0.01**
SD			**0.00**	**0.01**	**0.01**
dhDSCT					
	Rat 1	9	0.02	0.01	0.00
	Rat 2	7	0.00	0.00	0.00
	Rat 3	20	0.02	0.06	0.00
Mean			**0.01**	**0.02**	**0.00**
SD			**0.01**	**0.03**	**0.00**

* denotes reticulospinal axon terminals labelled by injecting into the medial longitudinal fasciculus

Table 5-10 The densities of RetS axon terminals expressing VGLUT2 and VGAT in apposition with cell bodies and dendrites of different populations of retrogradely labelled spinocerebellar tract neurons in rats**

Populations of Spinocerebellar tract neurons	Animal No.	No. of Cells	Average Density (n/ 100 µm2)		
			CTb+VGLUT2	CTb+VGAT	CTb
SB					
	Rat 1	25	0.10	0.01	0.00
	Rat 2	21	0.06	0.01	0.00
	Rat 3	29	0.06	0.02	0.00
Mean			**0.07**	**0.01**	**0.00**
SD			**0.02**	**0.01**	**0.00**
VSCT					
	Rat 1	14	0.08	0.01	0
	Rat 2	21	0.1	0.02	0
	Rat 3	22	0.08	0.02	0.00
Mean			**0.09**	**0.02**	**0.00**
SD			**0.01**	**0.01**	**0.00**
ccDSCT					
	Rat 1	10	0.01	0.00	0.00
	Rat 2	3	0.01	0.00	0.00
	Rat 3	35	0.00	0.00	0.00
Mean			**0.01**	**0.00**	**0.00**
SD			**0.01**	**0.00**	**0.00**
dhDSCT					
	Rat 1	7	0.00	0.00	0.00
	Rat 2	3	0.01	0.00	0.00
	Rat 3	9	0.00	0.00	0.00
Mean			**0.00**	**0.00**	**0.00**
SD			**0.01**	**0.00**	**0.00**

** denotes reticulospinal axon terminals labelled by injecting into the caudal ventrolateral medulla

5.4 Discussion

The present investigation utilizing combined electrophysiological/ retrograde tract tracing and immunohistochemical methods has provided insights into sources of excitatory and inhibitory axonal contacts on four populations of spinocerebellar tract neurons. As discussed in previous chapters (chapter 3 and 4), inputs from VGLUT1 terminals dominate in ccDSCT neurons while the SB population of VSCT neurons principally has inhibitory inputs from GABA/ glycinergic nerve terminals and are also driven by spinal and supraspinal neurons. dhDSCT and VSCT neurons have mixed inputs. Results of this part of the study provide further information about sources of input to spinocerebellar tract cells.

5.4.1 A proportion of excitatory axonal contacts on different populations of spinocerebellar tract neurons originate from proprioceptors

The present morphological analysis revealed that ccDSCT neurons have higher proportions of contacts from VGLUT1 positive terminals which contained PV. PV is preferentially expressed by proprioceptive neurons (Zhang *et al.*, 1990; Alvarez *et al.*, 2004; Betley *et al.*, 2009). Studies combining immunocytochemistry and ganglionectomy have reported a significant reduction in PV like immunoreactivity in fibres following ganglionectomy ipsilateral to the surgery indicating their origin from primary afferents (Ren and Ruda, 1994) and VGLUT1 is expressed in primary afferent terminals including large myelinated afferents (Varoqui *et al.*, 2002; Todd *et al.*, 2003; Alvarez *et al.*, 2004). This evidence together with the present results implies that the majority of sensory inputs to ccDSCT neurons are derived from proprioceptors. In agreement with the findings from previous studies furthermore, it can be considered that all the PV terminals with VGLUT1 immunoreactivity in contact with ccDSCT neurons originate from group Ia afferents (Ishizuka *et al.*, 1979; Marsala *et al.*, 2007). This finding is also consistent with electrophysiological investigation of these neurons which shows that they receive strong monosynaptic input exclusively from group I afferents (Eccles *et al.*, 1961b). This feature of

ccDSCT neurons has also been corroborated in mice (Hantman and Jessell, 2010). Surprisingly, dhDSCT neurons which have major input from group II and cutaneous afferents possessed relatively few VGLUT1 contacts which coexpressed PV. This may indicate that group II input to these neurons is weaker than that from cutaneous afferents. Another possibility is that group II afferents might not express PV though its specificity to group I or II afferents have not been documented yet. Nevertheless, this observation indicates that dhDSCT neurons are functionally distinct from ccDSCT neurons. Similarly, in VSCT neurons, the considerable proportion of inputs from VGLUT1 and PV double labelled terminals is consistent with the physiological characteristics of these neurons (Burke *et al.*, 1971a; Lundberg and Weight, 1971). Likewise a small fraction of VGLUT1 contacts immunoreactive for PV on SB neurons is consistent with the very limited input from group Ia afferent found in these cells.

In addition to the explanations of the results discussed above, it is worthwhile to consider other possibilities as well. One possibility might be related to penetration of PV antibody though it seems unlikely because there is strong labelling in the surrounding tissue as shown in Figure 5-1. Another possibility might be that the antibody used in this study is only detecting a proportion of PV or PV is strongly expressed in neurons but weakly expressed in axon terminals. However, to date, these potential features of PV have not been documented and these possibilities remain to be resolved. Moreover, PV negative VGLUT1 contacts on these neuronal populations (in particular ccDSCT neurons) might have originated from CS neurons (Hantman and Jessell, 2010) (A. Du Beau, S. Shakya Shrestha and D. J. Maxwell, In press).

5.4.2 A proportion of glutamatergic and GABAergic/ glycinergic contacts on different populations of spinocerebellar tract neurons originate from distinct populations of interneurons

The findings show that a proportion of contacts on different populations of spinocerebellar tract neurons were made by CB and/ or CR and PV immuno-positive axon terminals; some of which were also positive for either VGLUT1+2 (VGLUT2 in

cat) or VGAT. Previous studies have demonstrated that calcium-binding proteins CB, CR and PV are widely distributed throughout the spinal cord grey matter (Antal *et al.*, 1990; Celio, 1990; Antal *et al.*, 1991; Ren *et al.*, 1993; Ichikawa *et al.*, 1994; Ren and Ruda, 1994). Although these proteins are known to play role in buffering intracellular Calcium (Ca^{2+}) fluxes and resistance to Ca^{2+} induced excitotoxicity (Andressen *et al.*, 1993; Airaksinen *et al.*, 1997; Edmonds *et al.*, 2000); very little is known about the functional role of neurons expressing these proteins in the spinal cord. Morphologically, CB immunoreactive neurons are found abundantly in the superficial dorsal horn, while CR positive neurons are found exclusively in laminae V-VI and VII-VIII (Antal *et al.*, 1990; Antal *et al.*, 1991; Ren *et al.*, 1993; Ichikawa *et al.*, 1994; Ren and Ruda, 1994). Similarly, cells that express both CB and CR are distributed throughout the length of the spinal cord but are more numerous at cervical and lumbar segments (Ren and Ruda, 1994; Morona *et al.*, 2006). PV positive neurons are found in all regions of spinal grey matter of the rat except in lamina I with abundant distribution in inner layer of lamina II, lamina III, internal basilar nucleus, central grey region and at the dorsomedial and ventromedial aspects of the lateral motor nuclei (Antal *et al.*, 1990; Ichikawa *et al.*, 1994).

SB and VSCT neurons

The results for both the cat and the rat show that SB and VSCT neurons have a considerable proportion of contacts made by VGAT and CB double labelled terminals. It has been reported that the axon terminals of Renshaw cells express CB (Arvidsson *et al.*, 1992; Sanna *et al.*, 1993; Alvarez *et al.*, 2005) and electrophysiological studies have shown that Renshaw cells have collateral actions on SB and VSCT neurons (Hultborn *et al.*, 1971a; Lindstrom and Schomburg, 1973; Lindstrom and Schomburg, 1974). Therefore VGAT axon terminals colocalised with CB which formed contact with SB and VSCT neurons might have originated from Renshaw cells. Furthermore, a proportion of VGAT contacts on these neurons in the cat experiments were colocalised with both CB and CR. This further shows that one of the parent sources of these terminals might be Renshaw cells as reported by Alvarez *et al.* (2005) who had demonstrated intense labelling of CB in Renshaw cells that also co-expressed CR. In addition, a small fraction of CR and VGAT

immunolabelled contacts in SB and VSCT neurons are likely to originate from propriospinal neurons (Liu *et al.*, 2010b).

Quantitative analysis also shows that VSCT neurons have a higher contact density of excitatory terminals which were colocalised with CB in both cats and rats. The proportion of contacts made by these terminals was relatively small in SB neurons. Similarly, both SB and VSCT neurons showed small contact densities of excitatory terminals which coexpressed either of CR or both CB and CR. This is indicative of different sources of inputs to these neurons. For instance, one of the potential sources of excitatory terminals expressing these proteins is likely to be propriospinal neurons (Liu *et al.*, 2010b). Another possibility might be that some of the CR containing terminals might have derived from commissural interneurons as shown in the occulomotor system (de la Cruz *et al.*, 1998). Similar observations for commissural CR positive cells in lamina VIII of rat spinal cord have been made by Liu *et al.* (2010b).

It has been shown that some V1 derived interneurons in the ventral horn express PV. These cells receive contacts from primary afferents as well as Renshaw cells and project to laminae IX, VII and the deep dorsal horn. They therefore resemble all the characters of Ia inhibitory interneurons (Alvarez *et al.*, 2005). Furthermore locations of PV immunoreactive cells in the ventral horn are similar to physiologically defined Ia inhibitory interneurons (Antal *et al.*, 1990). This study has revealed substantial density of contacts made by terminals that co-express VGAT and PV on both SB and VSCT neurons thus suggesting that they might originate from Ia inhibitory interneurons. Coexpression of CB, CR and PV in Renshaw cells has also been reported by Alvarez *et al.* (2005) but very few neurons in the ventral horn express high levels of PV in the mature spinal cord (Antal *et al.*, 1990; Zhang *et al.*, 1990; Ren and Ruda, 1994).

ccDSCT and dhDSCT neurons

The results show that ccDSCT neurons have a higher density of contacts formed by CR containing VGLUT1+2 axon terminals when compared with dhDSCT, SB and VSCT

neurons but few CR/ VGAT contacts were present on ccDSCT and dhDSCT neurons. Hence the majority of CR contacts on these cells are excitatory. As suggested by Liu *et al.* (2010 b), these terminals might have derived from CR cells in the ipsilateral dorsal horn which are likely to receive inputs from group I and II muscle afferents. In contrast, dhDSCT neurons exhibited significantly higher numbers of contacts formed by VGAT terminals with colocalised CB. Though at present, it is difficult to define the source of these terminals, it is likely that they originate from the group of CB positive cells in the dorsal horn which are within the area where field potentials of cutaneous and group II muscle afferents are evoked (Edgley and Jankowska, 1987a; Liu *et al.*, 2010b). CB and CR containing terminals that do not contain VGLUT or VGAT may contain other unknown neurotransmitters or neuropeptides. For instance, it has been shown that some CB containing neurons are also reactive for neuropeptides, such as neurotensin, Substance P, Enkephalin or Somatostatin (Yoshida *et al.*, 1990). Small numbers of contacts formed by VGAT axon terminals coexpressing PV were found in both ccDSCT and dhDSCT neurons. These PV and VGAT double labelled terminals might originate from inhibitory dorsal horn interneurons which are more likely to use GABA but not glycine as demonstrated by previous study (Antal *et al.*, 1991).

Moreover, it is worth noting that as a consequence of the limited sample of intracellularly labelled neurons in the cat, this part of the investigation was not performed on ccDSCT and dhDSCT neurons. However, as excitatory and inhibitory input patterns and the organization of these neuronal populations in the cat and the rat are comparable, it is likely that the sources of inhibitory and excitatory inputs to these cells are similar in both species.

Despite ample information about the distribution of cells positive for CB, CR and PV, it is difficult to confirm the precise origin of axon terminals. Similarly, information about the exact function of neurons containing CB/ CR/ PV in the spinal cord is sparse although their role in buffering intracellular calcium fluxes and resistance to calcium induced excitotoxicity have been established (Andressen *et al.*, 1993; Airaksinen *et al.*, 1997; Edmonds *et al.*, 2000). Further studies are necessary to elucidate the sources of CB, CR and PV immunoreactive terminals

which form contacts with different populations of spinocerebellar tract neurons and their role in afferent transmission from spinocerebellar pathways. Nevertheless, it can be concluded from the present findings that all four populations of spinocerebellar tract neurons receive inputs from diverse neuronal populations which might influence the cerebellum in different ways.

5.4.3 Reticulospinal and corticospinal neurons form direct contact with four types of spinocerebellar tract neurons in the rat

5.4.3.1 Glutamatergic and GABAergic/ glycinergic terminals originating from the RetS neurons form direct contacts on four types of spinocerebellar tract neurons

The present results reinforce electrophysiological evidence for monosynaptic connection between the neurons belonging to the RetS pathway and spinocerebellar tract neurons. The major finding is that the VSCT including the SB population of neurons have significantly higher numbers of contacts from VGLUT2 immunoreactive RetS axon terminals (from both the MLF and CVLM injections) than DSCT neurons (Figure 5-16; Tables 5-9 and 5-10). However, the contact density of VGAT expressing RetS terminals labelled by transport of CTb from the MLF was not significantly different among the four populations of spinocerebellar tract neurons while with the CVLM injection, the density of these terminals was significantly higher in SB and VSCT neurons when compared with DSCT neurons. Similarly, the proportion of contacts formed by VGLUT2 expressing RetS terminals was also higher than VGAT expressing terminals. This difference was statistically significant with respect to the axon terminals labelled by injecting into the CVLM.

SB and VSCT neurons

Higher proportions of VGLUT2 expressing RetS terminals on both SB and VSCT neurons is consistent with the EPSPs recorded in these neuronal populations following stimulation of axons descending in the MLF (Baldissera and Weight, 1969; Baldissera and Roberts, 1975; Hammar *et al.*, 2011). Similarly, the present results

are in strong agreement with anatomical evidence which has shown that medullary neurons descending to the ventral horn of the spinal cord in rats (Vetrivelan *et al.*, 2009) and mice (Martin *et al.*, 2011) are mostly glutamatergic. As most of the axons of RetS origin descend through the MLF (Nyberg-Hansen, 1965; Petras, 1967), actions evoked by MLF stimulation are likely to include axons originating from different regions of the reticular formation including the CVLM. Although, the inputs from CVLM to spinocerebellar tract neurons have not been investigated previously, higher number of appositions made by RetS terminals originating from the CVLM have been shown in the current study. However, the pattern of inputs from RetS terminals labelled by injecting into the CVLM resembled that of the MLF. A certain proportion of RetS contacts observed on VSCT neurons might originate from contralaterally descending axons in the MLF which is consistent with the monosynaptic coupling shown between contralaterally descending RetS axons and VSCT neurons (Hammar *et al.,* 2011). It is also worth noting that the injection in the MLF ipsilateral to the cerebellar injection site is located very close to the midline (medial-lateral = + 0.1mm) and spread of the tracer to the contralateral side is practically unavoidable. However, the main core of injection was in the ipsilateral side as shown in Figure 5-12 and all the analysis was performed on ipsilaterally located cells and terminals. Similar evidence for the crossed intraspinal axon collaterals of RetS neurons originating from various regions of reticular formation have been shown in previous studies (Nyberg-Hansen, 1965; Mitani *et al.*, 1988a; Mitani *et al.*, 1988b; Holstege, 1991; Matsuyama *et al.*, 1999; Jankowska *et al.*, 2003). Most of these collaterals were shown to form monosynaptic connections with motoneurons.

Contrary to the study of Hammar *et al.* (2011), the current results showed a small proportion of the contacts on both SB and VSCT neurons were made by RetS terminals containing VGAT. However, in agreement with these findings, direct inhibitory actions of MLF stimulation have been reported (Baldissera and Roberts, 1975). Furthermore, GABA and glycinergic projections from the ventromedial medulla to spinal motoneurons have been revealed in rats (Holstege, 1991; Holstege and Bongers, 1991). More recently, descending projections from the ventromedial medulla to the intermediate zone and ventral horn of the spinal cord have been

shown to contain both GABA and glycine (Hossaini *et al.*, 2012). Therefore, although the majority of inhibitory inputs to these neurons originate principally from inhibitory interneurons a small proportion may originate from the RetS pathway.

ccDSCT and dhDSCT neurons

Unlike SB and VSCT neurons, ccDSCT and dhDSCT neurons have fewer numbers of contacts made by VGLUT2 positive RetS terminals (Figure 5-16), although electrophysiological study (Hammar *et al.*, 2011) has found no evidence for monosynaptic EPSPs in these neurons following MLF stimulation. However, in contrast to the observations made by Hammar and her group (2011), both types of cell had a small proportion of appositions made by VGAT expressing RetS terminals. The reason for this discrepancy is not clear; one possible explanation is that some of the axonal populations labelled were contaminated with axons derived from cell sources in the adjacent area of injection site. However, this is not likely to be the case with MLF injections as inhibitory fibres from the medial VST (Nyberg-Hansen and Mascitti, 1964) and tectospinal tract descending through the MLF do not project as far caudally as the lumbar region (Nyberg-Hansen, 1964a; Nyberg-Hansen and Mascitti, 1964; Rose *et al.*, 1991). Another possible explanation could be that the very few contacts on these neurons might not be sufficient to excite or inhibit these neurons in experimental conditions used.

Functional considerations

Direct evidence for descending RetS projections to the spinocerebellar tract neurons supports the role of these neurons in the regulation of motor activity. The higher proportion of RetS inputs observed in VSCT neurons as compared to SB neurons is somewhat at variance with the conclusions of Hammar and her group (2011). The reason for this might be that the borderlines between these neurons are not very sharp. Also it is worth considering the technical differences in the approaches used (see chapter 3 and 4). Despite a small variation in the quantitative data, both SB and VSCT neurons might equally serve as the component of a highly specialized loop between neurons in the reticular formation and the cerebellum as

proposed by Hammar and colleagues (2011). It has been shown that activation of SB and VSCT neurons induced by MLF simulation is modulated by inhibitory action of primary afferents (Hammar *et al.*, 2011). In addition, it has been demonstrated that SB and VSCT neurons are inhibited by collateral actions of interneurons which also inhibit motoneurons (Lundberg, 1971; Lundberg and Weight, 1971; Lindstrom and Schomburg, 1973; Lindstrom and Schomburg, 1974). Therefore, it can be considered that feedback information conveyed by SB and VSCT neurons to the cerebellum will help the cerebellum to make corrective actions. Convergence of inputs from RetS neurons and peripheral afferents in the same SB and VSCT neuron could serve to prevent errors in descending commands. Further evidence for integration of inputs from PT neurons and the MLR by RetS neurons relaying information from these regions to SB and VSCT neurons (Jankowska *et al.*, 2011b) reveals a more specialised role for these neurons in monitoring descending commands for centrally initiated voluntary as well as locomotor movements relayed by RetS neurons.

Moreover, RetS inputs from the reticular formation in the CVLM might provide additional functional roles. Neurons in the lateral reticular nucleus (LRN) as a part of the CVLM receive inputs from various regions of the brain which includes cerebral cortices (motor and pre-motor areas), vestibular nuclei, red nucleus and spinal cord (Corvaja *et al.*, 1977; Hrycyshyn and Flumerfelt, 1981; Dietrichs *et al.*, 1985; Shokunbi *et al.*, 1986). This nucleus is often regarded as a precerebellar nucleus which has a major role in the control of motor activity and limb co-ordination, especially fine movements of forelimbs (Arshavsky *et al.*, 1978a; Ekerot, 1990). Whether it plays a similar role in hindlimb movement is yet to be established. Direct monosynaptic connections between terminals labelled by the uptake of CTb from the CVLM (LRN as shown in Figure 5-13) and spinocerebellar tract neurons, particularly SB and VSCT neurons might indicate that these neurons are likely to integrate and forward diverse supraspinal information to the cerebellum. RetS inputs to ccDSCT and dhDSCT neurons might also implicate these neurons in a similar role in providing the cerebellum with feedback information on the likely outcome of descending commands.

Similarly, with respect to the functional implications of VGAT expressing RetS contacts on spinocerebellar tract neurons, attempts have been made to explore the role of descending projections of ventromedial medulla in regulating muscle atonia during rapid eye movement sleep (Vetrivelan *et al.*, 2009). Whether, inhibitory RetS projections running through the MLF and descending from the CVLM have special functional significance or not is yet to be explored. However, in view of the very complex pattern of axonal projections of RetS neurons and interconnections between them (Nyberg-Hansen, 1965; Mitani *et al.*, 1988a; Mitani *et al.*, 1988b; Holstege, 1991; Matsuyama *et al.*, 1999; Jankowska *et al.*, 2003), precise conclusions regarding the influence of particular population of RetS neurons cannot be drawn. Nevertheless, findings of the present study showing diverse inputs suggest a highly complex functional organization of the spinocerebellar pathway.

5.4.3.2 Glutamatergic terminals originating from the CS neurons form direct contacts on four types of spinocerebellar tract neurons

All populations of the spinocerebellar tract neurons receive monosynaptic input from CS neurons. The DSCT neurons have higher numbers of CS terminal appositions when compared with VSCT neurons, including SB neurons.

Electrophysiological studies have provided evidence for both rapid excitation and prolonged inhibition of DSCT neurons evoked by CS neurons (Hongo and Okada, 1967; Hongo *et al.*, 1967). The present results are consistent with these studies. Although, these studies did not distinguish between different subtypes of DSCT neurons, it is likely that the analysis of neurons located at caudal lumbar segments might include at least a proportion of dhDSCT neurons. Caudal lumbar levels are devoid of cc and DSCT neurons at this level receive excitatory inputs from cutaneous and group II afferents (Edgley and Jankowska, 1988). Therefore, VGLUT1 expressing CS contacts on dhDSCT neurons corroborate findings of previous *in-vivo* studies in cats. Furthermore, excitatory cortical inputs to ccDSCT neurons have been revealed in a recent study (Hantman and Jessell, 2010). These authors suggested that different subsets of ccDSCT neurons could be defined with respect to the extent of cortical inputs. This could be one of the explanations for variation

in the number of CS contacts on ccDSCT neurons found in the current study. The current findings are also consistent with respect to the terminal distribution pattern of CS neurons which form dense arborisations in laminae III - VII (Brown, 1971; Antal, 1984; Casale *et al.*, 1988; Liang *et al.*, 1991; A. Du Beau, S. Shakya Shrestha & D. J. Maxwell, In press). Thus in addition to the dominant excitatory drive from primary afferents to DSCT neurons, they also integrate substantial input from CS neurons.

Although, most of the previous studies were focused on DSCT neurons, current anatomical analysis has revealed VGLUT1 labelled CS terminal appositions on both populations of VSCT neurons (Figure 5-19). The average number of contacts was lower than that found in DSCT neurons but this would be predicted from the sparse number of CS terminals seen in the ventral horn (Brown, 1971; Antal, 1984; Casale *et al.*, 1988; Liang *et al.*, 1991; A. Du Beau, S. Shakya Shrestha & D. J. Maxwell, In press). In agreement with the present findings, a physiological study reported EPSPs of shorter latency in VSCT neurons evoked by volleys of CST, although polysynaptic excitation dominated (Fu *et al.*, 1977). Despite the scarce evidence for direct cortical input to SB and VSCT neurons, VGLUT1 contacts on SB neurons are likely to be derived from CS neurons. This can be considered as a plausible explanation because most VGLUT1 contacts on VSCT neurons are known to be of primary afferent origin (Eccles *et al.*, 1961a; Hubbard and Oscarsson, 1962) but SB neurons analyzed in this study were virtually devoid of such input (see chapter 3 for detailed discussion).

Functional considerations

The result of the present study suggests that DSCT neurons in addition to relaying simple sensory information to the cerebellum, also serve to integrate cortical inputs. Therefore, in support of the suggestions made by Hantman and Jessel (2010), the existence of direct coupling between DSCT neurons and CS neurons can play a key role in anticipating peripherally derived sensory feedback and relay this information to the cerebellum. Although there is no evidence for direct connections between CST and hindlimb motoneurons, monosynaptic connections between CS

pathway and SB and VSCT neurons as shown in the present study might also serve a similar function to DSCT neurons. However the difference might be that they serve to monitor consequences of cortical inputs to interneurons (Fu *et al.*, 1977).

In conclusion, the functional organization of the spinocerebellar pathway is extremely complex, and is still poorly understood. This is largely due to the lack of information about sources of inputs to the neurons belonging to this pathway. Results of the present study provide further evidence that excitatory and inhibitory inputs to spinocerebellar tract neurons have specific and overlapping origins from the periphery, spinal and supraspinal levels. Likewise, there is a difference in excitatory and inhibitory axonal contact patterns among different populations of spinocerebellar tract neurons. ccDSCT and dhDSCT neurons predominantly receive direct input from large myelinated primary afferents with additional input from CS neurons which might anticipate incoming proprioceptive inputs. In contrast, SB and VSCT neurons principally integrate interneuronal inputs which are primarily glutamatergic or GABA/ glycinergic. In addition, they have substantial input from the RetS pathway and are likely to provide the cerebellum with information on the likely outcome of RetS actions on motoneurons and help the cerebellum to adjust the descending commands accordingly. ccDSCT and dhDSCT neurons have limited input originating from RetS neurons; likewise, SB and VSCT neurons appear to have small numbers of contacts made by CS terminals. The circuit diagram in Figure 5-20 summarizes the putative connections between different neurons originating from various peripheral, spinal and supraspinal sources with the four populations of spinocerebellar tract neurons. This information should help to understand their functional organization and clarify their role in neural networks contributing to coordinated motor activities.

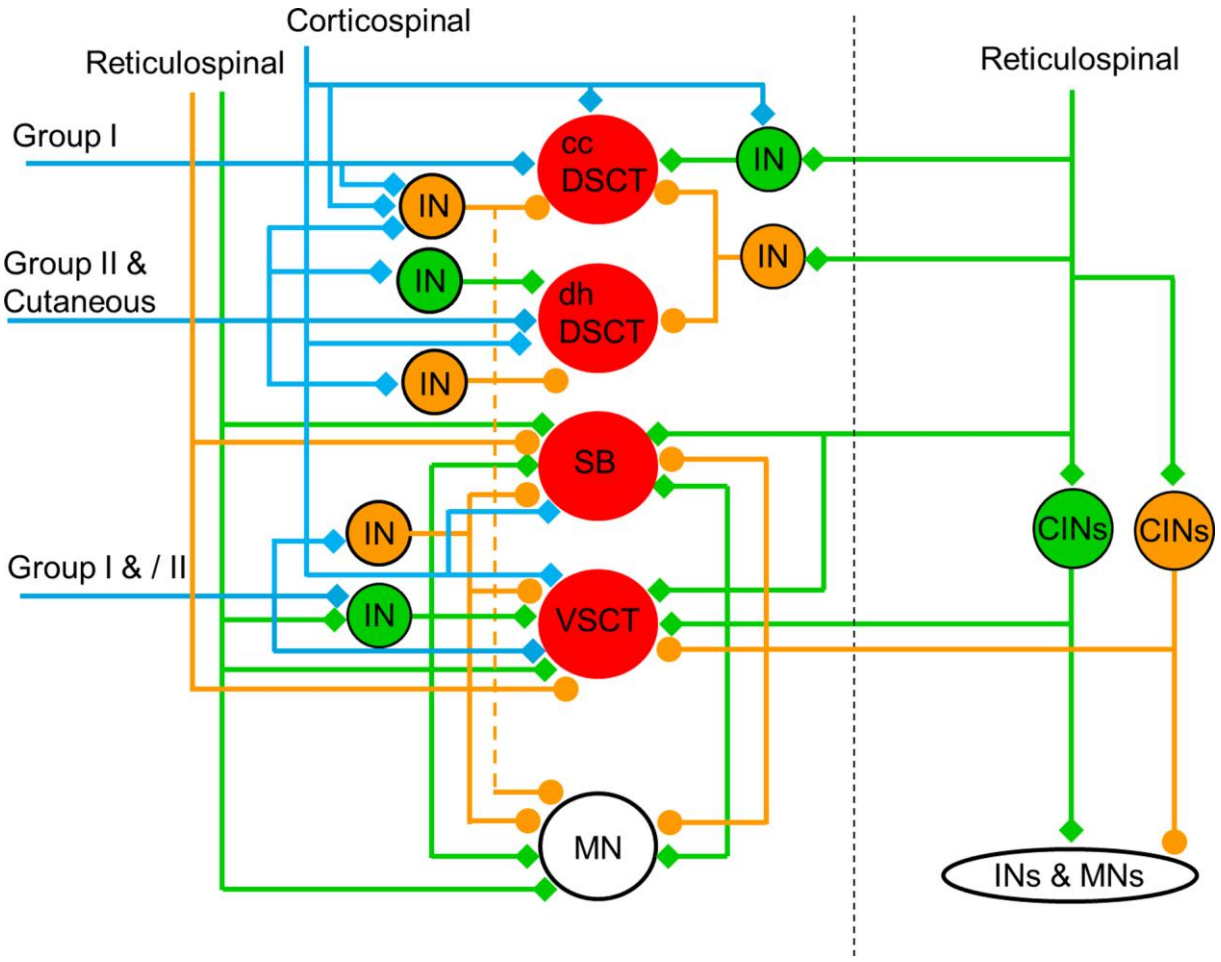

Figure 5-20 Summary of patterns and origin of inhibitory and excitatory contacts formed with the four different populations of lumbar spinocerebellar tract neurons

Red circles represent Clarke's column dorsal spinocerebellar tract neurons (ccDSCT); dorsal horn dorsal spinocerebellar tract neurons (dhDSCT), spinal border neurons (SB), Ib-ventral spinocerebellar tract neurons (VSCT). Green circles represent excitatory interneurons in reflex pathways to motoneurons (MN) activated by primary afferents and descending systems. Blue lines and diamonds represent neurons that express vesicular glutamate transporter 1 (VGLUT1) in their axon terminals. Green lines and diamonds represent neurons that express vesicular glutamate transporter 2 (VGLUT2) in their axon terminals. Orange lines and circles represent neurons that express vesicular GABA transporter (VGAT) in their axon terminals. CINs, commissural interneurons; INs, interneurons; MNs, motoneurons.

6 General Discussion

The cerebellum receives information from various parts of the body including the hindlimbs through the spinocerebellar pathways. Neurons giving rise to this pathway are modulated by proprioceptors, exteroceptors, intrinsic spinal neurons and descending systems. Although there are overlapping functions among spinocerebellar tract neurons to a certain extent, there exist distinct subsets within these neuronal populations. Therefore, the overall aim of this study was to investigate input properties of the hindlimb component of the spinocerebellar tract. To address this issue, I have investigated four types of spinocerebellar tract neurons in the lumbar enlargement of the cat and in the thoraco-lumbar spinal cord of the rat. The four different populations of spinocerebellar tract neurons have distinct functional organization. A number of studies (Oscarsson, 1965; Lundberg, 1971; Lindstrom and Schomburg, 1973; Arshavsky *et al.*, 1978b; Bosco and Poppele, 2001; Hantman and Jessell, 2010; Hammar *et al.*, 2011) have established that spinocerebellar tract neurons forward highly diverse information on peripheral afferent inputs, on the operation of interneuronal networks involved in sensorimotor integration, on feedback information on descending commands and their motor outputs. However, this current study demonstrated for the first time marked differences in morphological organisation with respect to their proposed input properties. Despite the highly complex input properties of these neurons, a good correlation was observed between electrophysiological and morphological properties.

The majority of excitatory terminals making appositions with SB neurons with predominant inhibitory input from primary afferents and VSCT neurons with peripheral input from group Ib afferents were VGLUT2 positive. The number of appositions made by VGLUT1 positive terminals was insignificant in SB neurons but was substantial in VSCT neurons. In contrast to these groups of neurons, ccDSCT neurons with monosynaptic input from group Ia afferents and dhDSCT neurons with input from group II and cutaneous afferents received a majority of excitatory contacts from VGLUT1 expressing axon terminals. It is generally accepted that VGLUT1 labels primary afferent terminals while VGLUT2 is expressed in spinal

interneuron terminals (Varoqui *et al.*, 2002; Todd *et al.*, 2003; Alvarez *et al.*, 2004) and axon terminals of descending pathways except the CST (A. Du Beau, S. Shakya Shrestha & D. J. Maxwell, In press). The contact density and distribution pattern was consistent for both cats and rats (refer Figure 3-5). In support of these findings, previous electrophysiological studies have demonstrated that both SB and VSCT neurons are sometimes di- and poly- synaptically excited from muscle, tendon organ and cutaneous afferents (Eccles *et al.*, 1961a; Lundberg and Oscarsson, 1962; Lundberg, 1971). This suggests that VGLUT2 terminals could originate from excitatory interneurons mediating indirect actions of primary afferents upon these neurons. As shown by Jankowska *et al.* (2010), the results of the present study also indicate that VSCT neurons including SB neurons are subject to activation by collateral actions of excitatory premotor interneurons with input from group I/ II afferents. Despite the higher density of contacts from VGLUT2 positive terminals, in particular on SB neurons, no EPSPs were recorded following stimulation of tested nerves but they were evoked from the MLF stimulation. Thus, a considerable proportion of VGLUT2 contacts on SB and VSCT neurons might be derived from RetS pathways and this would be predicted from electrophysiological studies (Baldissera and ten Bruggencate, 1976; Hammar *et al.*, 2011). Similarly, a small fraction of VGLUT1 contacts on SB neurons fully comply with the characteristic feature of rostrally located SB neurons (Burke *et al.,* 1971; Jankowska *et al.,* 2010; Hammar *et al.,* 2011) and a substantial number of VGLUT1 appositions on VSCT neurons is consistent with excitation from group Ib afferents. However, another possible source of these terminals could be the CST (Fu *et al.*, 1977).

The morphological findings of the present study show that ccDSCT and dhDSCT neurons have a major input from VGLUT1 expressing terminals and again this complements evidence from previous physiological studies (Eccles *et al.*, 1961b; Edgley and Jankowska, 1988) indicating that both these neuronal populations receive strong monosynaptic input from primary afferents but ccDSCT neurons mainly receive input from group I afferents (Eccles *et al.*, 1961b) whereas dhDSCT neurons receive input from group II and cutaneous afferents (Edgley and Jankowska, 1988). Likewise, the lack of VGLUT2 contacts on ccDSCT neurons which contrasts with the considerable contact density on dhDSCT neurons is consistent with

physiological evidence for di-synaptic EPSPs recorded in dhDSCT cells from stimuli applied within motor nuclei (Krutki *et al.*, 2011) and further supplements the suggestion that these two neuronal populations are functionally different entities. In addition, a proportion of VGLUT2 appositions on these neurons might originate from RetS neurons (Hammar *et al.*, 2011) while some VGLUT1 contacts could be of CS terminals (Hantman and Jessell, 2010). Taken together, these findings suggest that DSCT neurons principally integrate inputs from primary afferents while VSCT neurons forward information on spinal actions of descending commands depending upon the degree of inhibition of motoneurons as discussed in chapter 3. Nevertheless, although VSCT neurons, including SB neurons, play a principal role in monitoring actions of inhibitory premotor interneurons on motoneurons, excitatory inputs to these neurons mediated via yet undefined spinal neurons might likewise provide the cerebellum with important information.

Having established differences in excitatory axonal contact patterns on the four populations of spinocerebellar tract neurons, the second aim of my study was to make a similar comparison of the inhibitory axonal contacts by using markers for GABAergic/ glycinergic terminals (Todd and Sullivan, 1990; Chaudhry *et al.*, 1998; Wojcik *et al.*, 2006). This part of the study revealed considerable differences in the inhibitory axonal contact pattern among the four populations. SB neurons showed the highest contact densities of VGAT terminals whereas VSCT, ccDSCT and dhDSCT neurons had similar proportions of inhibitory and excitatory contacts on them in both the cat and the rat. Strong inhibitory inputs to SB and VSCT neurons have been shown to be evoked by collateral actions of premotor interneurons with inputs from group Ia, Ib and II afferents (Eccles *et al.*, 1961a; Lundberg and Weight, 1971; Bannatyne *et al.*, 2006; Bannatyne *et al.*, 2009; Jankowska *et al.*, 2010) and also from descending tract neurons (Baldissera and Roberts, 1976; Baldissera and ten Bruggencate, 1976; Hammar *et al.*, 2011; Jankowska *et al.*, 2011a). It has also been shown that Renshaw cells which have collateral actions on motoneurons also inhibit VSCT neurons (Hultborn *et al.*, 1971a; Lundberg, 1971; Lindstrom and Schomburg, 1973; Lindstrom and Schomburg, 1974). Likewise, a proportion of VGAT contacts on ccDSCT and dhDSCT neurons originate from spinal neurons including intermediate zone inhibitory premotor interneurons in pathways from group Ib and II afferents

but not Ia inhibitory interneurons and Renshaw cells (Hongo *et al.*, 1983b; Jankowska and Puczynska, 2008; Krutki *et al.*, 2011). Another source of inhibitory input to these neurons might be dorsal horn interneurons relaying information from group II afferents which have terminal projections in laminae IV, V and VI of the dorsal horn (Bannatyne *et al.*, 2006; Bannatyne *et al.*, 2009). Finally, the CS pathway might also be one of the potential sources of inhibition of these neurons as suggested by Hantman and Jessel (2010).

Glycinergic or GABAergic or GABAergic/ glycinergic inputs to these neuronal populations were characterized by using markers for GAD (Soghomonian and Martin, 1998; Mackie *et al.*, 2003) and gephyrin (Mackie *et al.*, 2003) in the cat. The majority of gephyrin puncta were not apposed by GAD terminals which suggest that inhibitory input to SB, VSCT, ccDSCT and dhDSCT neurons is primarily from glycinergic neurons. In keeping with the evidence (Triller *et al.*, 1987; Mitchell *et al.*, 1993; Todd *et al.*, 1995; Ornung *et al.*, 1996; Ornung *et al.*, 1998) discussed in chapter 4, (section 4.4.3), it is likely that most of the GABA/gephyrin synapses observed in this study represent synapses that use both GABA and glycine as neurotransmitters. Therefore at least two types of inhibitory neuron form contacts with spinocerebellar tract neurons. The current result is also consistent with anatomical studies in the adult cat (Bannatyne *et al.*, 2006; Bannatyne *et al.*, 2009) which have shown that inhibitory interneurons in the dorsal horn, activated by group II afferents as well as intermediate zone interneurons with input from group I/ II afferents, were almost entirely glycinergic. These findings indicate the potential diverse sources of VGAT contacts on these neurons and show, in particular, that SB and VSCT neurons monitor spinal interneuronal networks involved in various reflex pathways and descending commands.

The third aim of the study was to investigate the origin of excitatory and inhibitory contacts on the four types of neurons. Three potential sources were investigated: proprioceptors, different types of interneurons and descending pathways (RetST and CST). Among the four populations of spinocerebellar tract neurons, ccDSCT neurons had the highest proportion of contacts formed by VGLUT1 terminals also labelled for PV in both the cat and the rat. This indicates that majority of the

sensory inputs to ccDSCT neurons are derived from proprioceptors (Zhang *et al.*, 1990; Alvarez *et al.*, 2004; Betley *et al.*, 2009). This finding is consistent with electrophysiological properties of these neurons which show that these neurons receive strong monosynaptic input exclusively from group I afferents (Eccles *et al.*, 1961b). Relatively smaller proportions of VGLUT1 and PV co-expressing terminals were found on dhDSCT neurons. The most plausible explanation for this might be that the neurons analysed in the current study have either less group II inputs than cutaneous inputs or that PV does not label group II afferents terminals (see details in chapter 5). Nevertheless, this result confirms that dhDSCT neurons are functionally distinct from ccDSCT neurons. Similarly, in SB and VSCT neurons, the small numbers of VGLUT1/ PV terminals observed is consistent with the physiological characteristics of these neurons (Burke *et al.*, 1971a; Lundberg and Weight, 1971).

Very small numbers of excitatory and inhibitory contacts on all four populations of spinocerebellar tract neurons originated from CB/ CR/ PV expressing neurons. Calcium binding proteins are suggested to label distinct groups of neurons within the spinal cord (Antal *et al.*, 1990; Antal *et al.*, 1991; Ren *et al.*, 1993; Ichikawa *et al.*, 1994; Ren and Ruda, 1994; Alvarez *et al.*, 2005). For instance, CB is expressed in Renshaw cells in the ventral horn (Arvidsson *et al.*, 1992; Sanna *et al.*, 1993; Alvarez *et al.*, 2005) whereas CR as well as both CB/ CR expression was reported in propriospinal neurons (Liu *et al.*, 2010b) and PV is suggested to label Ia inhibitory interneurons in the ventral horn (Antal *et al.*, 1990; Anelli and Heckman, 2005). Therefore, a small proportion of excitatory/ inhibitory terminals co-expressing CB/ CR/ PV may originate from these sources. dhDSCT neurons had significantly higher numbers of contacts formed by VGAT terminals with colocalised CB and it is likely that they originate from CB positive cells in the dorsal horn which are within the area where field potentials of cutaneous and group II muscle afferents are evoked (Edgley and Jankowska, 1987a; Liu *et al.*, 2010b). However, due to the paucity of information on the origin and function of CB/ CR/ PV containing neurons, further studies are necessary to explore their role in afferent transmission to spinocerebellar pathways. The very small numbers of appositions made by excitatory and inhibitory terminals colocalised with CB/ CR/ PV on spinocerebellar

neurons (see chapter 3, 4 & 5 for details) indicates that they principally receive inputs from glutamatergic and GABAergic/ glycinergic neurons that do not contain these calcium binding proteins.

In rats, VSCT cells (including the SB population) have significantly higher numbers of contacts from VGLUT2 immunoreactive RetS axon terminals than DSCT neurons. This finding is in agreement with previous electrophysiological studies which showed EPSPs in SB and VSCT neurons evoked by stimulation of RetS axons descending from the MLF (Baldissera and Weight, 1969; Baldissera and Roberts, 1975; Hammar *et al.*, 2011). Similarly, an anatomical study has shown that medullary neurons which have descending projections to the ventral horn of the spinal cord are mostly glutamatergic (Vetrivelan *et al.*, 2009) but in contradiction to evidence for the absence of monosynaptic inhibitory inputs to these neurons in cats (Hammar *et al.*, 2011), evidence was found for a small proportion of contacts made by VGAT expressing RetS terminals. Nevertheless, this finding is consistent with a study which showed direct inhibitory actions of MLF stimuli on these neurons (Baldissera and Roberts, 1975). Furthermore, GABA/glycinergic projections from the ventromedial medulla to the spinal motoneurons have been established previously (Holstege, 1991; Holstege and Bongers, 1991) and descending projections from the ventromedial medulla to the intermediate zone and ventral horn of the spinal cord have been shown to contain both GABA and glycine (Hossaini *et al.*, 2012).

Activation of SB and VSCT neurons induced by MLF simulation is modulated by inhibitory actions of primary afferents (Hammar *et al.*, 2011). In addition, it has also been demonstrated that SB and VSCT neurons are inhibited by collateral actions of interneurons inhibiting motoneurons (Lundberg, 1971; Lundberg and Weight, 1971; Lindstrom and Schomburg, 1973; Lindstrom and Schomburg, 1974). Therefore, it can be considered that such feedback information conveyed by SB and VSCT neurons to the cerebellum will enable the cerebellum to take corrective actions. Convergence of inputs from RetS neurons and peripheral afferents if they exist in individual SB and VSCT neurons, could serve to prevent errors in descending commands. Therefore VSCT neurons may serve as a vital component in a highly specialized loop between neurons in the reticular formation and the cerebellum as

proposed by Hammar and colleagues (2011). Similarly, RetS contacts to ccDSCT and dhDSCT neurons might implicate a similar role for these neurons in providing the cerebellum with feedback information on the outcome of descending RetS commands.

Evidence for monosynaptic connections between the CS pathway and different populations of spinocerebellar tract neurons was also found. The DSCT population of spinocerebellar tract neurons had higher numbers of CS appositions in comparison to VSCT neurons. This observation is consistent with previous electrophysiological studies in DSCT neurons (Hongo and Okada, 1967; Hongo *et al.*, 1967). Similarly, excitatory cortical inputs to ccDSCT neurons have been revealed by recent study in the mouse (Hantman and Jessell, 2010). Although, most studies were focused on DSCT neurons, the present anatomical analysis also revealed small numbers of CS terminal appositions on both populations of VSCT neurons consistent with previous physiological study (Fu *et al.*, 1977). Thus the present study provides further details of the functional circuitry of spinocerebellar tract neurons which suggests that DSCT neurons in addition to relaying simple sensory information to the cerebellum also serve to integrate cortical inputs (see chapter 5). In agreement with the suggestions made by Hantman and Jessel (2010), the existence of direct coupling between DSCT and CS neurons can play a key role in anticipating peripherally derived sensory feedback and relay this information to the cerebellum. Similarly, direct connections between the CS pathway and SB and VSCT neurons might also serve a similar function to that of DSCT neurons but the difference might be that they monitor sensory consequences of cortical inputs to interneurons (Fu *et al.*, 1977).

There are several indications that a major source of excitatory input to SB and VSCT neurons is from descending systems (Baldissera and Weight, 1969; Baldissera and Roberts, 1975; Baldissera and Roberts, 1976; Hammar *et al.*, 2011; Jankowska *et al.*, 2011b; Jankowska *et al.*, 2011a). It can also be considered that a certain proportion of VGLUT2 positive contacts might have originated from VS and RS pathways in addition to those from the RetST. The evidence to support this suggestion is that VS, RS and RetS neurons express VGLUT2 in their axon terminals

(A. Du Beau, S. Shakya Shrestha & D. J. Maxwell, In press) and as VS terminals terminate in lamina VII- VIII (Holstege and Kuypers, 1982) and RS terminals in laminae V – VII (Antal *et al.*, 1992), VSCT and SB neurons are potential postsynaptic targets. Similarly, descending actions on hindlimb motoneurons relayed by RetS, PT and RS neurons may be monitored directly by VSCT and SB neurons in cats (Hammar *et al.*, 2011; Jankowska *et al.*, 2011b; Jankowska *et al.*, 2011a). Labelling of these terminals by injecting tracer into vestibular nuclei/ red nucleus together with retrograde tract tracing of spinocerebellar neurons would be useful to refine the present findings.

Previous studies have shown that RetS neurons activate neurons of swimming circuits in the brainstem and spinal cord that initiate locomotion in Xenopus tadpoles (Soffe *et al.*, 2009) as well as in zebrafish (Fetcho *et al.*, 2008) and lamprey (Dubuc *et al.*, 2008; Le Ray *et al.*, 2011). Likewise, these neurons are shown to co-relay voluntary movements (Jankowska and Edgley, 2006; Schepens *et al.*, 2008; Riddle and Baker, 2010) which are involved in the control of movement of hand and finger as well as of proximal muscles (Riddle *et al.*, 2009; Riddle and Baker, 2010). Recently, it has been demonstrated that RetS neurons convey information regarding centrally initiated voluntary and locomotor movements to the SB and VSCT neurons (Jankowska *et al.*, 2011b). These authors showed that PT and MLR stimulation evoked longer latency EPSPs in these neurons in parallel with EPSPs generated by stimulation of RetS neurons in the MLF suggesting that the effects from the PT and the MLR are mediated by same RetS neurons. Therefore, information about these commands forwarded by spinocerebellar tract neurons might have a crucial influence in the cerebellar control of voluntary movement. Further, it has been shown that RST and CST neurons act together to initiate voluntary movements and RST neurons may contribute in substituting some functions of CST neurons after injury to the PT (Ghez, 1975; Gibson *et al.*, 1985; Cheney *et al.*, 1991; van Kan and McCurdy, 2001). Previous evidence has also shown that RST neurons also have a role in centrally initiated locomotion (Arshavsky *et al.*, 1988; Lavoie and Drew, 2002). Recently, Jankowska *et al.* (2011a) have demonstrated monosynaptic and disynaptic coupling between RS neurons and SB and VSCT neurons in the cat. These authors have proposed that descending actions

of RST neurons on hindlimb motoneurons are also likely to be monitored more directly by SB and VSCT neurons. Moreover, the very few VGLUT1 contacts on SB and VSCT neurons and substantial inputs from VGLUT2 terminals, indicates that in addition to forwarding descending commands on voluntary movement relayed via RetS neurons to the cerebellum, SB and VSCT neurons might be components of a more direct pathway to relay this information.

The present study was done by combining intracellular labelling of electrophysiologically characterized cells in cats/ retrograde labelling in rats and immunohistochemistry using various neurochemical markers. There are various neurochemical markers which are specific to axon terminals (for eg, VGLUT1, VGLUT2, VGAT; see chapter 4) and whole neurons including axon terminals (for eg, CB, CR, PV; see chapter 5). Therefore, by combining the techniques which labels cells and terminals, it is possible to determine whether particular groups of spinocerebellar tract neurons are apposed by axon terminals immunoreactive for specific neurochemical markers. Different criteria for considering immunolabelled varicosities in close apposition to the labelled cells can be used to define them as putative contacts in confocal microscopy studies (Jankowska *et al.,* 1995b). Two main criteria can be used: an immunoreactive varicosity can be considered to be a genuine contact 1) if images of two labelled structures in same optical plane were juxtaposed with no intervening space between them provided optimal setting of the confocal microscope (for eg, aperture, intensity) 2) if during examination of three-dimensional reconstructions, the immunoreactive terminal and the cell remained in contact without any intervening space between them when rotated. The numbers of contacts counted following consistent strict criteria are considered to be underestimates rather than overestimates of the actual numbers of contacts because of various degree of penetration of antibodies used throughout the thickness of the sections. However, such problem is less likely to occur in the present study because intensities of immunolabelling were consistent throughout the sections analysed in both the cat and the rat. Nevertheless, future studies can also be advanced by combining confocal microscopy with investigation at an ultrastructural level using electron microscopy to refine the findings from the present study. In addition, simultaneous recording from presynaptic neuron and

labelling this neuron together with labelling of spinocerebellar tract neurons; combination of retrograde labelling of spinocerebellar tract neurons and anterograde labelling of various presynaptic fibres using different tracers; transneuronal labelling would allow detailed characterization of specific interactions between the major components of the neuronal circuitry.

In conclusion, the present findings provide a better basis for understanding the functional organization of different subsets of spinocerebellar tract neurons. The major role of VSCT neurons, including SB neurons, is to regulate intra- and supra-spinal inputs to spinal motoneurons by providing feed-back information to the cerebellum. Likewise, ccDSCT and dhDSCT neurons seem to have a crucial role in the regulation of proprioceptive sensory processing. This information is essential to understand the specific role of these neuronal populations in the highly specialized spino-cerebellar loop. This research has thrown up many questions in need of further investigation. It would be interesting to further investigate if inputs from different populations of these neurons converge on the same cerebellar target neurons or in different sites and, ultimately, how this information is integrated by the cerebellum.

References

Airaksinen MS, Thoenen H and Meyer M (1997). "Vulnerability of midbrain dopaminergic neurons in calbindin-D28k-deficient mice: lack of evidence for a neuroprotective role of endogenous calbindin in MPTP-treated and weaver mice." Eur J Neurosci **9**(1): 120-127.

Akaike T (1983). "Neuronal organization of the vestibulospinal system in the cat." Brain Res **259**(2): 217-227.

Alstermark B, Lundberg A, Pinter M and Sasaki S (1987). "Vestibular effects in long C3-C5 propriospinal neurones." Brain Res **404**(1-2): 389-394.

Alstermark B, Lundberg A and Sasaki S (1984). "Integration in descending motor pathways controlling the forelimb in the cat. 10. Inhibitory pathways to forelimb motoneurones via C3-C4 propriospinal neurones." Experimental brain research. Experimentelle Hirnforschung. Experimentation cerebrale **56**(2): 279-292.

Alvarez FJ, Dewey DE, Harrington DA and Fyffe RE (1997). "Cell-type specific organization of glycine receptor clusters in the mammalian spinal cord." J Comp Neurol **379**(1): 150-170.

Alvarez FJ and Fyffe RE (2007). "The continuing case for the Renshaw cell." The Journal of physiology **584**(Pt 1): 31-45.

Alvarez FJ, Jonas PC, Sapir T, Hartley R, Berrocal MC, Geiman EJ, Todd AJ and Goulding M (2005). "Postnatal phenotype and localization of spinal cord V1 derived interneurons." J Comp Neurol **493**(2): 177-192.

Alvarez FJ, Villalba RM, Zerda R and Schneider SP (2004). "Vesicular glutamate transporters in the spinal cord, with special reference to sensory primary afferent synapses." J Comp Neurol **472**(3): 257-280.

Alvina K and Khodakhah K (2010). "The therapeutic mode of action of 4-aminopyridine in cerebellar ataxia." J Neurosci **30**:7258–7268.

Andén NE, Jukes MGM, Lundberg A and Vyklicky L (1966). "The Effect of DOPA on the Spinal Cord. 1. Influence on Transmission from Primary Aflerents." Acta Physiologica Scandinavica **67**(3-4): 373-386.

Andressen C, Blumcke I and Celio MR (1993). "Calcium-binding proteins: selective markers of nerve cells." Cell Tissue Res **271**(2): 181-208.

Anelli R and Heckman CJ (2005). "The calcium binding proteins calbindin, parvalbumin, and calretinin have specific patterns of expression in the gray matter of cat spinal cord." Journal of neurocytology **34**(6): 369-385.

Antal M (1984). "Termination areas of corticobulbar and corticospinal fibres in the rat." J Hirnforsch **25**(6): 647-659.

Antal M, Freund TF and Polgar E (1990). "Calcium-binding proteins, parvalbumin- and calbindin-D 28k-immunoreactive neurons in the rat spinal cord and dorsal root ganglia: a light and electron microscopic study." J Comp Neurol **295**(3): 467-484.

Antal M, Polgar E, Chalmers J, Minson JB, Llewellyn-Smith I, Heizmann CW and Somogyi P (1991). "Different populations of parvalbumin- and calbindin-D28k-immunoreactive neurons contain GABA and accumulate 3H-D-aspartate in the dorsal horn of the rat spinal cord." J Comp Neurol **314**(1): 114-124.

Antal M, Sholomenko GN, Moschovakis AK, Storm-Mathisen J, Heizmann CW and Hunziker W (1992). "The termination pattern and postsynaptic targets of rubrospinal fibers in the rat spinal cord: a light and electron microscopic study." J Comp Neurol **325**(1): 22-37.

Arshavsky Y, I., Gelfand IM, Orlovsky GN, Pavlova GA and Popova LB (1984). "Origin of signals conveyed by the ventral spino-cerebellar tract and spino-reticulo-cerebellar pathway." Exp Brain Res **54**(3): 426-431.

Arshavsky YI, Berkinblit MB, Fukson OI, Gelfand IM and Orlovsky GN (1972). "Origin of modulation in neurones of the ventral spinocerebellar tract during locomotion." Brain Res **43**(1): 276-279.

Arshavsky YI, Gelfand IM, Orlovsky GN and Pavlova GA (1978a). "Messages conveyed by spinocerebellar pathways during scratching in the cat. I. Activity of neurons of the lateral reticular nucleus." Brain Research **151**(3): 479-491.

Arshavsky YI, Gelfand IM, Orlovsky GN and Pavlova GA (1978b). "Messages conveyed by spinocerebellar pathways during scratching in the cat. II. Activity of neurons of the ventral spinocerebellar tract." Brain Res **151*b***(3): 493-506.

Arshavsky YI, Orlovsky GN and Perret C (1988). "Activity of rubrospinal neurons during locomotion and scratching in the cat." Behavioural Brain Research **28**(1-2): 193-199.

Arvidsson U, Ulfhake B, Cullheim S, Ramirez V, Shupliakov O and Hokfelt T (1992). "Distribution of calbindin D28k-like immunoreactivity (LI) in the monkey ventral horn: do Renshaw cells contain calbindin D28k-LI?" J Neurosci **12**(3): 718-728.

Aubrey KR, Rossi FM, Ruivo R, Alboni S, Bellenchi GC, Le Goff A, Gasnier B and Supplisson S (2007). "The transporters GlyT2 and VIAAT cooperate to determine the vesicular glycinergic phenotype." J Neurosci **27**(23): 6273-6281.

Baldissera F and Roberts WJ (1975). "Effects on the ventral spinocerebellar tract neurones from Deiters' nucleus and the medial longitudinal fascicle in the cat." Acta Physiol Scand **93**(2): 228-249.

Baldissera F and Roberts WJ (1976). "Effects from the vestibulospinal tract on transmission from primary afferents to ventral spino-cerebellar tract neurones." Acta Physiol Scand **96**(2): 217-232.

Baldissera F and ten Bruggencate G (1976). "Rubrospinal effects on ventral spinocerebellar tract neurones." Acta Physiol Scand **96**(2): 233-249.

Baldissera F and Weight F (1969). "Descending monosynaptic connexions to spinal border cells." Acta Physiologica Scandinavica **76**: 28-29A.

Bannatyne BA, Edgley SA, Hammar I, Jankowska E and Maxwell DJ (2003). "Networks of inhibitory and excitatory commissural interneurons mediating crossed reticulospinal actions." Eur J Neurosci **18**(8): 2273-2284.

Bannatyne BA, Edgley SA, Hammar I, Jankowska E and Maxwell DJ (2006). "Differential projections of excitatory and inhibitory dorsal horn interneurons relaying information from group II muscle afferents in the cat spinal cord." J Neurosci **26**(11): 2871-2880.

Bannatyne BA, Liu TT, Hammar I, Stecina K, Jankowska E and Maxwell DJ (2009). "Excitatory and inhibitory intermediate zone interneurons in

pathways from feline group I and II afferents: differences in axonal projections and input." J Physiol **587**(Pt 2): 379-399.

Basbaum AI, Clanton CH and Fields HL (1978). "Three bulbospinal pathways from the rostral medulla of the cat: an autoradiographic study of pain modulating systems." J Comp Neurol **178**(2): 209-224.

Basbaum AI and Fields HL (1979). "The origin of descending pathways in the dorsolateral funiculus of the spinal cord of the cat and rat: Further studies on the anatomy of pain modulation." The Journal of Comparative Neurology **187**(3): 513-531.

Beitz AJ and Ecklund LJ (1988). "Colocalization of fixative-modified glutamate and glutaminase but not GAD in rubrospinal neurons." J Comp Neurol **274**(2): 265-279.

Berger AJ, Dieudonné S and Ascher P (1998). "Glycine uptake governs glycine site occupancy at NMDA receptors of excitatory synapses." Journal of neurophysiology **80**(6): 3336-3340.

Betley JN, Wright CV, Kawaguchi Y, Erdelyi F, Szabo G, Jessell TM and Kaltschmidt JA (2009). "Stringent specificity in the construction of a GABAergic presynaptic inhibitory circuit." Cell **139**(1): 161-174.

Boehme CC (1968). "The neural structure of Clarke's nucleus of the spinal cord." J Comp Neurol **132**(3): 445-461.

Bosco G and Poppele RE (1997). "Representation of multiple kinematic parameters of the cat hindlimb in spinocerebellar activity." J Neurophysiol **78**(3): 1421-1432.

Bosco G and Poppele RE (1999). "Low sensitivity of dorsal spinocerebellar neurons to limb movement speed." Exp Brain Res **125**(3): 313-322.

Bosco G and Poppele RE (2001). "Proprioception from a spinocerebellar perspective." Physiol Rev **81**(2): 539-568.

Bosco G, Rankin A and Poppele R (1996). "Representation of passive hindlimb postures in cat spinocerebellar activity." J Neurophysiol **76**(2): 715-726.

Bowker RM, Steinbusch HW and Coulter JD (1981). "Serotonergic and peptidergic projections to the spinal cord demonstrated by a combined retrograde HRP histochemical and immunocytochemical staining method." Brain Res **211**(2): 412-417.

Bowker RM, Westlund KN and Coulter JD (1982). "Origins of serotonergic projections to the lumbar spinal cord in the monkey using a combined retrograde transport and immunocytochemical technique." Brain Res Bull **9**(1-6): 271-278.

Bras H, Cavallari P and Jankowska E (1988). "Demonstration of initial axon collaterals of cells of origin of the ventral spinocerebellar tract in the cat." J Comp Neurol **273**(4): 584-592.

Brink E, Harrison PJ, Jankowska E, McCrea DA and Skoog B (1983). "Post-synaptic potentials in a population of motoneurones following activity of single interneurones in the cat." J Physiol **343**: 341-359.

Brösamle C and Schwab ME (1997). "Cells of origin, course, and termination patterns of the ventral, uncrossed component of the mature rat corticospinal tract." The Journal of Comparative Neurology **386**(2): 293-303.

Brown LT, Jr. (1971). "Projections and termination of the corticospinal tract in rodents." Exp Brain Res **13**(4): 432-450.

Burger PM, Hell J, Mehl E, Krasel C, Lottspeich F and Jahn R (1991). "GABA and glycine in synaptic vesicles: storage and transport characteristics." Neuron **7**(2): 287-293.

Burke R, Lundberg A and Weight F (1971a). "Spinal border cell origin of the ventral spinocerebellar tract." Exp Brain Res **12**(3): 283-294.

Burke RE, Fedina L and Lundberg A (1971b). "Spatial synaptic distribution of recurrent and group Ia inhibitory systems in cat spinal motoneurones." The Journal of physiology **214**(2): 305-326.

Cabaj A, Stecina K and Jankowska E (2006). "Same spinal interneurons mediate reflex actions of group Ib and group II afferents and crossed reticulospinal actions." Journal of neurophysiology **95**(6): 3911-3922.

Casale EJ, Light AR and Rustioni A (1988). "Direct projection of the corticospinal tract to the superficial laminae of the spinal cord in the rat." The Journal of Comparative Neurology **278**(2): 275-286.

Cavallari P, Edgley SA and Jankowska E (1987). "Post-synaptic actions of midlumbar interneurones on motoneurones of hind-limb muscles in the cat." J Physiol **389**: 675-689.

Celio MR (1990). "Calbindin D-28k and parvalbumin in the rat nervous system." Neuroscience **35**(2): 375-475.

Cerminara NL and Apps R (2010). "Behavioural significance of cerebellar modules." Cerebellum **10**:484-494.

Chaudhry FA, Reimer RJ, Bellocchio EE, Danbolt NC, Osen KK, Edwards RH and Storm-Mathisen J (1998). "The vesicular GABA transporter, VGAT, localizes to synaptic vesicles in sets of glycinergic as well as GABAergic neurons." J Neurosci **18**(23): 9733-9750.

Cheema SS, Rustioni A and Whitsel BL (1984). "Light and electron microscopic evidence for a direct corticospinal projection to superficial laminae of the dorsal horn in cats and monkeys." The Journal of Comparative Neurology **225**(2): 276-290.

Cheney PD, Fetz EE and Mewes K (1991). "Neural mechanisms underlying corticospinal and rubrospinal control of limb movements." Prog Brain Res **87**:213-252.

Coffey GL, Godwin-Austen RB, Macgillivray BB and Sears TA (1971). "The form and distribution of the surface evoked responses in cerebellar cortex from intercostal nerves in the cat." The Journal of physiology **212**(1): 129-145.

Cooke JD, Larson B, Oscarsson O and Sjolund B (1971a). "Organization of afferent connections to cuneocerebellar tract." Exp Brain Res **13**(4): 359-377.

Cooke JD, Larson B, Oscarsson O and Sjolund B (1971b). "Origin and termination of cuneocerebellar tract." Exp Brain Res **13**(4): 339-358.

Corvaja N, Grofová I, Pompeiano O and Walberg F (1977). "The lateral reticular nucleus in the cat--I. An experimental anatomical study of its spinal and supraspinal afferent connections." Neuroscience **2**(4): 537-553.

Coulter JD, Bowker RM, Wise SP, Murray EA, Castiglioni AJ and Westlund KN (1979). "Cortical, tectal and medullary descending pathways to the cervical spinal cord." Prog Brain Res **50**: 263-279.

Curfs MH, Gribnau AA and Dederen PJ (1996). "Direct cortico-motoneuronal synaptic contacts are present in the adult rat cervical spinal cord and are first established at postnatal day 7." Neurosci Lett **205**(2): 123-126.

Curtis DR and Eccles JC (1959). "The time courses of excitatory and inhibitory synaptic actions." The Journal of physiology **145**(3): 529-546.

Czarkowska J, Jankowska E and Sybirska E (1981). "Common interneurones in reflex pathways from group 1a and 1b afferents of knee flexors and extensors in the cat." The Journal of physiology **310**: 367-380.

D'Angelo E (2011). "NEURAL CIRCUITS OF THE CEREBELLUM: HYPOTHESIS FOR FUNCTION." Journal of Integrative Neuroscience **10** (3):317-352.

Daniel H, Billard JM, Angaut P and Batini C (1987). "The interposito-rubrospinal system. Anatomical tracing of a motor control pathway in the rat." Neuroscience research **5**(2): 87-112.

Davies HE and Edgley SA (1994). "Inputs to group II-activated midlumbar interneurones from descending motor pathways in the cat." J Physiol **479 (Pt 3)**: 463-473.

de la Cruz RR, Pastor AM, Martinez-Guijarro FJ, Lopez-Garcia C and Delgado-Garcia JM (1998). "Localization of parvalbumin, calretinin, and calbindin D-28k in identified extraocular motoneurons and internuclear neurons of the cat." J Comp Neurol **390**(3): 377-391.

Destombes J, Horcholle-Bossavit G and Thiesson D (1992). "Distribution of glycinergic terminals on lumbar motoneurons of the adult cat: an ultrastructural study." Brain research **599**(2): 353-360.

Dietrichs E, Haines DE and Qvist H (1985). "Indirect hypothalamo-cerebellar pathway? Demonstration of hypothalamic efferents to the lateral reticular nucleus." Experimental brain research. Experimentelle Hirnforschung. Experimentation cerebrale **60**(3): 483-491.

Dubuc R, Brocard F, Antri M, Fénelon K, Gariépy JF, Smetana R, Ménard A, Le Ray D, Viana Di Prisco G, Pearlstein E, Sirota MG, Derjean D, St-Pierre M, Zielinski B, Auclair F and Veilleux D (2008). "Initiation of locomotion in lampreys." Brain research reviews **57**(1): 172-182.

Duysens J, Loeb GE and Weston BJ (1980). "Crossed flexor reflex responses and their reversal in freely walking cats." Brain Research **197**(2): 538-542.

Eccles JC, Eccles RM and Lundberg A (1957). "The convergence of monosynaptic excitatory afferents on to many different species of alpha motoneurones." J Physiol **137**(1): 22-50.

Eccles JC, Fatt P, Landgren S and Winsbury GJ (1954). "Spinal cord potentials generated by volleys in the large muscle afferents." J Physiol **125**(3): 590-606.

Eccles JC, Hubbard JI and Oscarsson O (1961a). "Intracellular recording from cells of the ventral spinocerebellar tract." J Physiol **158**: 486-516.

Eccles JC, Oscarsson O and Willis WD (1961b). "Synaptic action of group I and II afferent fibres of muscle on the cells of the dorsal spinocerebellar tract." J Physiol **158**: 517-543.

Eccles RM and Lundberg A (1958). "Integrative pattern of Ia synaptic actions on motoneurones of hip and knee muscles." The Journal of physiology **144**(2): 271-298.

Eccles RM and Lundberg A (1959). "Synaptic actions in motoneurons by afferents which may evoke the flexion reflex." Archives Italiennes de Biologie **97**: 199-221.

Eccles RM and Lundberg A (1959). "Supraspinal control of interneurones mediating spinal reflexes." The Journal of physiology **147**: 565-584.

Edgley SA and Gallimore CM (1988). "The morphology and projections of dorsal horn spinocerebellar tract neurones in the cat." J Physiol **397**: 99-111.

Edgley SA and Jankowska E (1987a). "Field potentials generated by group II muscle afferents in the middle lumbar segments of the cat spinal cord." J Physiol **385**: 393-413.

Edgley SA and Jankowska E (1987b). "An interneuronal relay for group I and II muscle afferents in the midlumbar segments of the cat spinal cord." J Physiol **389**: 647-674.

Edgley SA and Jankowska E (1988). "Information processed by dorsal horn spinocerebellar tract neurones in the cat." J Physiol **397**: 81-97.

Edgley SA, Jankowska E and Hammar I (2004). "Ipsilateral actions of feline corticospinal tract neurons on limb motoneurons." The Journal of neuroscience : the official journal of the Society for Neuroscience **24**(36): 7804-7813.

Edgley SA, Jankowska E, Krutki P and Hammar I (2003). "Both dorsal horn and lamina VIII interneurones contribute to crossed reflexes from feline group II muscle afferents." J Physiol **552**(Pt 3): 961-974.

Edgley SA, Jankowska E and Shefchyk S (1988). "Evidence that mid-lumbar neurones in reflex pathways from group II afferents are involved in locomotion in the cat." The Journal of physiology **403**: 57-71.

Edmonds B, Reyes R, Schwaller B and Roberts WM (2000). "Calretinin modifies presynaptic calcium signaling in frog saccular hair cells." Nat Neurosci **3**(8): 786-790.

Ekerot CF (1990). "The lateral reticular nucleus in the cat. VI. Excitatory and inhibitory afferent paths." Experimental brain research. Experimentelle Hirnforschung. Experimentation cerebrale **79**(1): 109-119.

Elger CE, Speckman EJ, Caspers H and Janzen RWC (1977). "Cortico-Spinal Connections in the Rat. I. Monosynaptic and Polysynaptic Responses of Cervical Motoneurons to Epicortical Stimulation." Exp Brain Res **28**: 385-404.

Fedina L and Hultborn H (1972). "Facilitation from ipsilateral primary afferents of interneuronal transmission in the Ia inhibitory pathway to motoneurones." Acta physiologica Scandinavica **86**(1): 59-81.

Feldman AG and Orlovsky GN (1975). "Activity of interneurons mediating reciprocal 1a inhibition during locomotion." Brain research **84**(2): 181-194.

Fern R, Harrison PJ and Riddell JS (1988). "The dorsal column projection of muscle afferent fibres from the cat hindlimb." Journal of Physioloy **401**:97-113.

Fetcho JR, Higashijima S and McLean DL (2008). "Zebrafish and motor control over the last decade." Brain research reviews **57**(1): 86-93.

Fu TC, Jankowska E and Lundberg A (1975). "Reciprocal La inhibition during the late reflexes evoked from the flexor reflex afferents after DOPA." Brain research **85**(1): 99-102.

Fu TC, Jankowska E and Tanaka R (1977). "Effects of Volleys in Cortico-spinal Tract Fibres on Ventral Spino-cerebellar Tract Cells in the Cat." Acta Physiologica Scandinavica **100**(1): 1-13.

Fyffe RE (1991a). "Glycine-like immunoreactivity in synaptic boutons of identified inhibitory interneurons in the mammalian spinal cord." Brain research **547**(1): 175-179.

Fyffe RE (1991b). "Spatial distribution of recurrent inhibitory synapses on spinal motoneurons in the cat." Journal of neurophysiology **65**(5): 1134-1149.

Garcia-Segura LM, Baetens D, Roth J, Norman AW and Orci L (1984). "Immunohistochemical mapping of calcium-binding protein immunoreactivity in the rat central nervous system." Brain Res **296**(1): 75-86.

Ghez C (1975). "Input-output relations of the red nucleus in the cat." Brain Res **98**, 93–308.

Gibson AR, Houk JC and Kohlerman NJ (1985). "Magnocellular red nucleus activity during different types of limb movement in the macaque monkey." J Physiol **:**527–549.

Giuffrida R and Rustioni A (1989). "Glutamate and aspartate immunoreactivity in corticospinal neurons of rats." The Journal of Comparative Neurology **288**(1): 154-164.

Glickstein M, Sultan F and Voogd J (2009). "Functional localization in the cerebellum." Cortex **47**:5980.

Grant G (1962a). "Projection of the external cuneate nucleus onto the cerebellum in the cat: an experimental study using silver methods." Exp Neurol **5**: 179-195.

Grant G (1962b). "Spinal course and somatotopically localized termination of the spinocerebellar tracts. An experimental study in the cat." Acta physiologica Scandinavica. Supplementum **56**(193): 1-61.

Grant G, Wiksten B, Berkley KJ and Aldskogius H (1982). "The location of cerebellar-projecting neurons within the lumbosacral spinal cord in the cat. An anatomical study with HRP and retrograde chromatolysis." J Comp Neurol **204**(4): 336-348.

Grant G and Xu Q (1988). "Routes of entry into the cerebellum of spinocerebellar axons from the lower part of the spinal cord. An experimental anatomical study in the cat." Exp Brain Res **72**(3): 543-561.

Grillner S and Hongo T (1972). "Vestibulospinal effects on motoneurones and interneurones in the lumbosacral cord." Prog Brain Res **37**: 243-262.

Grillner S, Hongo T and Lund S (1970). "The vestibulospinal tract. Effects on alpha-motoneurones in the lumbosacral spinal cord in the cat." Exp Brain Res **10**(1): 94-120.

Grillner S and Lund S (1968). "The origin of a descending pathway with monosynaptic action on flexor motoneurones." Acta Physiol Scand **74**(3): 274-284.

Gustafsson B and Lindstrom S (1973). "Recurrent control from motor axon collaterals of Ia inhibitory pathways to ventral spinocerebellar tract neurones." Acta Physiol Scand **89**(4): 457-481.

Ha H and Liu CN (1968). "Cell origin of the ventral spinocerebellar tract." The Journal of comparative neurology **133**(2): 185-206.

Hammar I, Chojnicka B and Jankowska E (2002). "Modulation of responses of feline ventral spinocerebellar tract neurons by monoamines." J Comp Neurol **443**(3): 298-309.

Hammar I, Krutki P, Drzymala-Celichowska H, Nilsson E and Jankowska E (2011). "A trans-spinal loop between neurones in the reticular formation and in the cerebellum." J Physiol **589**(Pt 3): 653-665.

Hammar I and Maxwell DJ (2002). "Serotoninergic and noradrenergic axons make contacts with neurons of the ventral spinocerebellar tract in the cat." J Comp Neurol **443**(3): 310-319.

Hantman AW and Jessell TM (2010). "Clarke's column neurons as the focus of a corticospinal corollary circuit." Nat Neurosci **13**(10): 1233-1239.

Harrison PJ and Jankowska E (1985). "Sources of input to interneurones mediating group I non-reciprocal inhibition of motoneurones in the cat." The Journal of physiology **361**: 379-401.

Harrison PJ, Jankowska E and Johannisson T (1983). "Shared reflex pathways of group I afferents of different cat hind-limb muscles." The Journal of physiology **338**: 113-128.

Harrison PJ, Jankowska E and Zytnicki D (1986). "Lamina VIII interneurones interposed in crossed reflex pathways in the cat." J Physiol **371**: 147-166.

Hayes NL and Rustioni A (1981). "Descending projections from brainstem and sensorimotor cortex to spinal enlargements in the cat. Single and double retrograde tracer studies." Exp Brain Res **41**(2): 89-107.

Holmqvist B, Oscarsson O and Rosén I (1963a). "Functional Organization of the Cuneocerebellar Tract in the Cat." Acta Physiologica Scandinavica **58**(2-3): 216-235.

Holmqvist B, Oscarsson O and Uddenberg N (1963b). "Organization of Ascending Spinal Tracts Activated from Forelimb Afferents in the Cat." Acta Physiologica Scandinavica **58**(1): 68-76.

Holstege G (1987). "Anatomical evidence for an ipsilateral rubrospinal pathway and for direct rubrospinal projections to motoneurons in the cat." Neuroscience Letters **74**(3): 269-274.

Holstege G and Kuypers HG (1982). "The anatomy of brain stem pathways to the spinal cord in cat. A labeled amino acid tracing study." Prog Brain Res **57**: 145-175.

Holstege JC (1991). "Ultrastructural evidence for GABAergic brain stem projections to spinal motoneurons in the rat." The Journal of neuroscience : the official journal of the Society for Neuroscience **11**(1): 159-167.

Holstege JC (1996). "The ventro-medial medullary projections to spinal motoneurons: ultrastructure, transmitters and functional aspects." Progress in brain research **107**: 159-181.

Holstege JC and Bongers CM (1991). "A glycinergic projection from the ventromedial lower brainstem to spinal motoneurons. An ultrastructural double labeling study in rat." Brain Research **566**(1-2): 308-315.

Holstege JC and Kuypers HG (1987a). "Brainstem projections to lumbar motoneurons in rat--I. An ultrastructural study using autoradiography and the combination of autoradiography and horseradish peroxidase histochemistry." Neuroscience **21**(2): 345-367.

Holstege JC and Kuypers HG (1987b). "Brainstem projections to spinal motoneurons: an update." Neuroscience **23**(3): 809-821.

Hongo T, Jankowska E and Lundberg A (1969). "The rubrospinal tract. I. Effects on alpha-motoneurones innervating hindlimb muscles in cats." Exp Brain Res **7**(4): 344-364.

Hongo T, Jankowska E and Lundberg A (1972). "The rubrospinal tract. IV. Effects on interneurones." Experimental brain research. Experimentelle Hirnforschung. Experimentation cerebrale **15**(1): 54-78.

Hongo T, Jankowska E, Ohno T, Sasaki S, Yamashita M and Yoshida K (1983a). "Inhibition of dorsal spinocerebellar tract cells by interneurones in upper and lower lumbar segments in the cat." J Physiol **342**: 145-159.

Hongo T, Jankowska E, Ohno T, Sasaki S, Yamashita M and Yoshida K (1983b). "The same interneurones mediate inhibition of dorsal spinocerebellar tract cells and lumbar motoneurones in the cat." J Physiol **342**: 161-180.

Hongo T, Kudo N, Sasaki S, Yamashita M, Yoshida K, Ishizuka N and Mannen H (1987). "Trajectory of group Ia and Ib fibers from the hind-limb muscles at the L3 and L4 segments of the spinal cord of the cat." J Comp Neurol **262**(2): 159-194.

Hongo T and Okada Y (1967). "Cortically evoked pre- and postsynaptic inhibition of impulse transmission to the dorsal spinocerebellar tract." Exp Brain Res **3**(2): 163-177.

Hongo T, Okada Y and Sato M (1967). "Corticofugal influences on transmission to the dorsal spinocerebellar tract from hindlimb primary afferents." Exp Brain Res **3**(2): 135-149.

Hossaini M, Goos JA, Kohli SK and Holstege JC (2012). "Distribution of Glycine/GABA Neurons in the Ventromedial Medulla with Descending Spinal Projections and Evidence for an Ascending Glycine/GABA Projection." PloS one **7**(4): e35293.

Houchin J, Maxwell DJ, Fyffe RE and Brown AG (1983). "Light and electron microscopy of dorsal spinocerebellar tract neurones in the cat: an intracellular horseradish peroxidase study." Quarterly journal of experimental physiology (Cambridge, England) **68**(4): 719-732.

Hrycyshyn AW and Flumerfelt BA (1981). "A light microscopic investigation of the afferent connections of the lateral reticular nucleus in the cat." The Journal of Comparative Neurology **197**(3): 477-502.

Hubbard JI and Oscarsson O (1961). "Localization of the cells of origin of the ventral spino-cerebellar tract." Nature **189**: 157-158.

Hubbard JI and Oscarsson O (1962). "Localization of the cell bodies of the ventral spino-cerebellar tract in lumbar segments of the cat." J Comp Neurol **118**: 199-204.

Huisman AM, Kuypers HGJM and Verburgh CA (1981). "Quantitative differences in collateralization of the descending spinal pathways from red nucleus and other brain stem cell groups in rat as demonstrated with the multiple fluorescent retrograde tracer technique." Brain Research **209**(2): 271-286.

Hultborn H, Illert M and Santini M (1976a). "Convergence on interneurones mediating the reciprocal Ia inhibition of motoneurones. I. Disynaptic Ia inhibition of Ia inhibitory interneurones." Acta physiologica Scandinavica **96**(2): 193-201.

Hultborn H, Illert M and Santini M (1976b). "Convergence on interneurones mediating the reciprocal Ia inhibition of motoneurones. II. Effects from segmental flexor reflex pathways." Acta Physiol Scand **96**(3): 351-367.

Hultborn H, Illert M and Santini M (1976c). "Convergence on interneurones mediating the reciprocal Ia inhibition of motoneurones. III. Effects from supraspinal pathways." Acta Physiol Scand **96**(3): 368-391.

Hultborn H, Jankowska E and Lindstrom S (1971a). "Recurrent inhibition from motor axon collaterals of transmission in the Ia inhibitory pathway to motoneurones." J Physiol **215**(3): 591-612.

Hultborn H, Jankowska E and Lindstrom S (1971b). "Recurrent inhibition of interneurones monosynaptically activated from group Ia afferents." J Physiol **215**(3): 613-636.

Hultborn H, Jankowska E and Lindström S (1971c). "Relative contribution from different nerves to recurrent depression of Ia IPSPs in motoneurones." The Journal of physiology **215**(3): 637-664.

Ichikawa H, Deguchi T, Nakago T, Jacobowitz DM and Sugimoto T (1994). "Parvalbumin, calretinin and carbonic anhydrase in the trigeminal and spinal primary neurons of the rat." Brain Res **655**(1-2): 241-245.

Ishizuka N, Mannen H, Hongo T and Sasaki S (1979). "Trajectory of group Ia afferent fibers stained with horseradish peroxidase in the lumbosacral spinal cord of the cat: three dimensional reconstructions from serial sections." J Comp Neurol **186**(2): 189-211.

Ito M, Udo M and Mano N (1970). "Long inhibitory and excitatory pathways converging onto cat reticular and Deiters' neurons and their relevance to reticulofugal axons." J Neurophysiol **33**(2): 210-226.

Ito M (2006). "Cerebellar circuitry as a neuronal machine." Prog Neurobiol **78**:272-303.

Jankowska E (1992). "Interneuronal relay in spinal pathways from proprioceptors." Prog Neurobiol **38**(4): 335-378.

Jankowska E (2008). "Spinal interneuronal networks in the cat: elementary components." Brain research reviews **57**(1): 46-55.

Jankowska E, Bannatyne BA, Stecina K, Hammar I, Cabaj A and Maxwell DJ (2009). "Commissural interneurons with input from group I and II muscle afferents in feline lumbar segments: neurotransmitters, projections and target cells." J Physiol **587**(Pt 2): 401-418.

Jankowska E and Edgley SA (2006). "How can corticospinal tract neurons contribute to ipsilateral movements? A question with implications for recovery of motor functions." Neuroscientist **12**(1): 67-79.

Jankowska E and Edgley SA (2010). "Functional subdivision of feline spinal interneurons in reflex pathways from group Ib and II muscle afferents; an update." Eur J Neurosci **32**(6): 881-893.

Jankowska E, Edgley SA, Krutki P and Hammar I (2005). "Functional differentiation and organization of feline midlumbar commissural interneurones." J Physiol **565**(Pt 2): 645-658.

Jankowska E, Hammar I, Djouhri L, Heden C, Szabo Lackberg Z and Yin XK (1997). "Modulation of responses of four types of feline ascending tract neurons by serotonin and noradrenaline." Eur J Neurosci **9**(7): 1375-1387.

Jankowska E, Hammar I, Slawinska U, Maleszak K and Edgley SA (2003). "Neuronal basis of crossed actions from the reticular formation on feline hindlimb motoneurons." J Neurosci **23**(5): 1867-1878.

Jankowska E, Johannisson T and Lipski J (1981). "Common interneurones in reflex pathways from group 1a and 1b afferents of ankle extensors in the cat." The Journal of physiology **310**: 381-402.

Jankowska E, Krutki P and Hammar I (2010). "Collateral actions of premotor interneurons on ventral spinocerebellar tract neurons in the cat." J Neurophysiol **104**(4): 1872-1883.

Jankowska E, Krutki P, Lackberg ZS and Hammar I (1995a). "Effects of serotonin on dorsal horn dorsal spinocerebellar tract neurons." Neuroscience **67**(2): 489-495.

Jankowska E and Lindström S (1972). "Morphology of interneurones mediating Ia reciprocal inhibition of motoneurones in the spinal cord of the cat." The Journal of physiology **226**(3): 805-823.

Jankowska E, Maxwell DJ, Dolk S, Krutki P, Belichenko PV and Dahlstrom A (1995b). "Contacts between serotoninergic fibres and dorsal horn spinocerebellar tract neurons in the cat and rat: a confocal microscopic study." Neuroscience **67**(2): 477-487.

Jankowska E, Nilsson E and Hammar I (2011a). "Do spinocerebellar neurones forward information on spinal actions of neurones in the feline red nucleus?" J Physiol.

Jankowska E, Nilsson E and Hammar I (2011b). "Processing information related to centrally initiated locomotor & voluntary movements by feline spinocerebellar neurones." J Physiol.

Jankowska E, Padel Y and Tanaka R (1976). "Disynaptic inhibition of spinal motoneurones from the motor cortex in the monkey." The Journal of physiology **258**(2): 467-487.

Jankowska E and Puczynska A (2008). "Interneuronal activity in reflex pathways from group II muscle afferents is monitored by dorsal spinocerebellar tract neurons in the cat." J Neurosci **28**(14): 3615-3622.

Jankowska E, Simonsberg IH and Chojnicka B (1998). "Modulation of information forwarded to feline cerebellum by monoamines." Annals of the New York Academy of Sciences **860**: 106-109.

Jankowska E, Stecina K, Cabaj A, Pettersson LG and Edgley SA (2006). "Neuronal relays in double crossed pathways between feline motor cortex and ipsilateral hindlimb motoneurones." J Physiol **575**(Pt 2): 527-541.

Jansen JK and Rudjord T (1965). "Dorsal spinocerebellar tract: response pattern of nerve fibers to muscle stretch." Science **149**(688): 1109-1111.

Johansson H and Silfvenius H (1977). "Axon-collateral activation by dorsal spinocerebellar tract fibres of group I relay cells of nucleus Z in the cat medulla oblongata." J Physiol **265**(2): 341-369.

Kaufman DL, Houser CR and Tobin AJ (1991). "Two forms of the gamma-aminobutyric acid synthetic enzyme glutamate decarboxylase have distinct intraneuronal distributions and cofactor interactions." Journal of neurochemistry **56**(2): 720-723.

Kim JH, Ebner TJ and Bloedel JR (1986). "Comparison of response properties of dorsal and ventral spinocerebellar tract neurons to a physiological stimulus." Brain Res **369**(1-2): 125-135.

Klausberger T and Somogyi P (2008). "Neuronal diversity and temporal dynamics: the unity of hippocampal circuit operations." Science (New York, N.Y.) **321**(5885): 53-57.

Kneisley LW, Biber MP and LaVail JH (1978). "A study of the origin of brain stem projections to monkey spinal cord using the retrograde transport method." Experimental Neurology **60**(1): 116-139.

Korogod SM, Kulagina IB, Horcholle-Bossavit G, Gogan P and Tyc-Dumont S (2000). "Activity-dependent reconfiguration of the effective dendritic field of motoneurons." The Journal of Comparative Neurology **422**(1): 18-34.

Korogod SM and Tyc-Dumont S (2010). Electrical dynamics of the dendritic space, Cambridge University Press.

Krutki P, Jankowska E and Edgley SA (2003). "Are crossed actions of reticulospinal and vestibulospinal neurons on feline motoneurons mediated by the same or separate commissural neurons?" The Journal of neuroscience : the official journal of the Society for Neuroscience **23**(22): 8041-8050.

Krutki P, Jelen S and Jankowska E (2011). "Do premotor interneurons act in parallel on spinal motoneurons and on dorsal horn spinocerebellar and spinocervical tract neurons in the cat?" J Neurophysiol **105**(4): 1581-1593.

Kuang RZ and Kalil K (1990). "Branching patterns of corticospinal axon arbors in the rodent." The Journal of Comparative Neurology **292**(4): 585-598.

Kuchler M, Fouad K, Weinmann O, Schwab ME and Raineteau O (2002). "Red nucleus projections to distinct motor neuron pools in the rat spinal cord." J Comp Neurol **448**(4): 349-359.

Kuno M, Munoz-Martinez EJ and Randic M (1973a). "Sensory inputs to neurones in Clarke's column from muscle, cutaneous and joint receptors." J Physiol **228**(2): 327-342.

Kuno M, Munoz-Martinez EJ and Randic M (1973b). "Synaptic action on Clarke's column neurones in relation to afferent terminal size." J Physiol **228**(2): 343-360.

Kuypers HG (1960). "Central cortical projections to motor and somato-sensory cell groups. An experimental study in the rhesus monkey." Brain **83**: 161-184.

Kuypers HG (1964). "THE DESCENDING PATHWAYS TO THE SPINAL CORD, THEIR ANATOMY AND FUNCTION." Progress in brain research **11**: 178-202.

Kuze B, Matsuyama K, Matsui T, Miyata H and Mori S (1999). "Segment-specific branching patterns of single vestibulospinal tract axons arising from the lateral vestibular nucleus in the cat: A PHA-L tracing study." J Comp Neurol **414**(1): 80-96.

Landgren S and Silfvenius H (1970). **"**The projection of group I muscle afferents from the hindlimb to the contralateral thalamus of the cat.**"** Acta Physiol Scand **80**:l0A.

Landgren S and Silfvenius H (1971). "Nucleus Z, the medullary relay in the projection path to the cerebral cortex of group I muscle afferents from the cat's hind limb." J Physiol **218**(3): 551-571.

Laporte Y and Lundberg A (1956). "Functional organization of the dorsal spino-cerebellar tract in the cat. III. Single fibre recording in Flechsig's fasciculus

on adequate stimulation of primary afferent neurons." Acta Physiol Scand **36**(1-2): 204-218.

Laporte Y, Lundberg A and Oscarsson O (1956a). "Functional organization of the dorsal spino-cerebellar tract in the cat. I. Recording of mass discharge in dissected Flechsig's fasciculus." Acta Physiol Scand **36**(1-2): 175-187.

Laporte Y, Lundberg A and Oscarsson O (1956b). "Functional organization of the dorsal spino-cerebellar tract in the cat. II. Single fibre recording in Flechsig's fasciculus on electrical stimulation of various peripheral nerves." Acta Physiol Scand **36**(1-2): 188-203.

Lavoie S and Drew T (2002). "Discharge characteristics of neurons in the red nucleus during voluntary gait modifications: a comparison with the motor cortex." J Neurophysiol **88**:1791–1814.

Lawrence DG and Hopkins DA (1976). "The development of motor control in the rhesus monkey: evidence concerning the role of corticomotoneuronal connections." Brain **99**(2): 235-254.

Lawrence DG and Kuypers HG (1968). "The functional organization of the motor system in the monkey. I. The effects of bilateral pyramidal lesions." Brain **91**(1): 1-14.

Le Ray D, Juvin L, Ryczko D and Dubuc R (2011). "Supraspinal control of locomotion: the mesencephalic locomotor region." Progress in brain research **188**: 51-70.

Li X-G, Florence SL and Kaas JH (1990). "Areal Distributions of Cortical Neurons Projecting to Different Levels of the Caudal Brain Stem and Spinal Cord in Rats." Somatosensory & Motor Research **7**(3): 315-335.

Liang FY, Moret V, Wiesendanger M and Rouiller EM (1991). "Corticomotoneuronal connections in the rat: evidence from double-labeling of motoneurons and corticospinal axon arborizations." J Comp Neurol **311**(3): 356-366.

Lindstrom S and Schomburg ED (1973). "Recurrent inhibition from motor axon collaterals of ventral spinocerebellar tract neurones." Acta Physiol Scand **88**(4): 505-515.

Lindstrom S and Schomburg ED (1974). "Group I inhibition in Ib excited ventral spinocerebellar tract neurones." Acta Physiol Scand **90**(1): 166-185.

Liu TT, Bannatyne BA, Jankowska E and Maxwell DJ (2010a). "Properties of axon terminals contacting intermediate zone excitatory and inhibitory premotor interneurons with monosynaptic input from group I and II muscle afferents." J Physiol **588**(Pt 21): 4217-4233.

Liu TT, Bannatyne BA and Maxwell DJ (2010b). "Organization and neurochemical properties of intersegmental interneurons in the lumbar enlargement of the adult rat." Neuroscience **171**(2): 461-484.

Lloyd DP and McIntyre Ak (1950). "Dorsal column conduction of group I muscle efferent impulses and their relay through Clarke's column." J Neurophysiol **13**(1): 39-54.

Low JS, Mantle-St John LA and Tracey DJ (1986). "Nucleus z in the rat: spinal afferents from collaterals of dorsal spinocerebellar tract neurons." J Comp Neurol **243**(4): 510-526.

Lundberg A (1971). "Function of the ventral spinocerebellar tract. A new hypothesis." Exp Brain Res **12**(3): 317-330.

Lundberg A, Malmgren K and Schomburg ED (1975). "Convergence from Ib, cutaneous and joint afferents in reflex pathways to motoneurones." Brain research **87**(1): 81-84.

Lundberg A, Malmgren K and Schomburg ED (1978). "Role of joint afferents in motor control exemplified by effects on reflex pathways from Ib afferents." The Journal of physiology **284**: 327-343.

Lundberg A, Malmgren K and Schomburg ED (1987). "Reflex pathways from group II muscle afferents. 2. Functional characteristics of reflex pathways to alpha-motoneurones." Experimental brain research. Experimentelle Hirnforschung. Experimentation cerebrale **65**(2): 282-293.

Lundberg A and Oscarsson O (1956). "Functional organization of the dorsal spinocerebellar tract in the cat. IV. Synaptic connections of afferents from Golgi tendon organs and muscle spindles." Acta Physiol Scand **38**(1): 53-75.

Lundberg A and Oscarsson O (1960). "Functional organization of the dorsal spino-cerebellar tract in the cat. VII. Identification of units by antidromic activation from the cerebellar cortex with recognition of five functional subdivisions." Acta Physiol Scand **50**: 356-374.

Lundberg A and Oscarsson O (1962). "Functional organization of the ventral spino-cerebellar tract in the cat. IV. Identification of units by antidromic activation from the cerebellar cortex." Acta Physiol Scand **54**: 252-269.

Lundberg A and Weight F (1971). "Functional organization of connexions to the ventral spinocerebellar tract." Exp Brain Res **12**(3): 295-316.

Lundberg A and Winsbury G (1960). "Functional Organization of the Dorsal Spino-Cerebellar Tract in the Cat." Acta Physiologica Scandinavica **49**(2-3): 165-170.

Mackie M, Hughes DI, Maxwell DJ, Tillakaratne NJ and Todd AJ (2003). "Distribution and colocalisation of glutamate decarboxylase isoforms in the rat spinal cord." Neuroscience **119**(2): 461-472.

Mann MD (1971). "Axons of dorsal spinocerebellar tract which respond to activity in cutaneous receptors." J Neurophysiol **34**(6): 1035-1050.

Marsala J, Lukácová N, Kolesár D, Sulla I, Galik J and Marsala M (2007). "The distribution of primary nitric oxide synthase- and parvalbumin-immunoreactive afferents in the dorsal funiculus of the lumbosacral spinal cord in a dog." Cellular and molecular neurobiology **27**(4): 475-504.

Martin EM, Devidze N, Shelley DN, Westberg L, Fontaine C and Pfaff DW (2011). "Molecular and neuroanatomical characterization of single neurons in the mouse medullary gigantocellular reticular nucleus." J Comp Neurol **519**(13): 2574-2593.

Martin GF, Cabana T and Humbertson AO, Jr. (1981). "Evidence for collateral innervation of the cervical and lumbar enlargements of the spinal cord by single reticular and raphe neurons. Studies using fluorescent markers in double-labeling experiments on the North American opossum." Neurosci Lett **24**(1): 1-6.

Martin GF, Humbertson AO, Jr., Laxson LC, Panneton WM and Tschismadia I (1979a). "Spinal projections from the mesencephalic and pontine reticular formation in the North American Opossum: a study using axonal transport techniques." J Comp Neurol **187**(2): 373-399.

Martin GF, Humbertson AO, Laxson C and Panneton WM (1979b). "Evidence for direct bulbospinal projections to laminae IX, X and the inter-mediolateral cell column. Studies using axonal transport techniques in the North American opossum." Brain Research **170**(1): 165-171.

Martin GF, Vertes RP and Waltzer R (1985). "Spinal projections of the gigantocellular reticular formation in the rat. Evidence for projections from different areas to laminae I and II and lamina IX." Experimental Brain Research **58**(1): 154-162.

Massion J (1967). "The mammalian red nucleus." Physiol Rev **47**(3): 383-436.

Matsushita M (1988). "Spinocerebellar projections from the lowest lumbar and sacral-caudal segments in the cat, as studied by anterograde transport of wheat germ agglutinin-horseradish peroxidase." J Comp Neurol **274**(2): 239-254.

Matsushita M (1999). "Projections from the upper lumbar cord to the cerebellar nuclei in the rat, studied by anterograde axonal tracing." J Comp Neurol **412**(4): 633-648.

Matsushita M and Gao X (1997). "Projections from the thoracic cord to the cerebellar nuclei in the rat, studied by anterograde axonal tracing." J Comp Neurol **386**(3): 409-421.

Matsushita M and Hosoya Y (1979). "Cells of origin of the spinocerebellar tract in the rat, studied with the method of retrograde transport of horseradish peroxidase." Brain Res **173**(2): 185-200.

Matsushita M and Hosoya Y (1982). "Spinocerebellar projections to lobules III to V of the anterior lobe in the cat, as studied by retrograde transport of horseradish peroxidase." J Comp Neurol **208**(2): 127-143.

Matsushita M, Hosoya Y and Ikeda M (1979). "Anatomical organization of the spinocerebellar system in the cat, as studied by retrograde transport of horseradish peroxidase." J Comp Neurol **184**(1): 81-106.

Matsushita M and Ikeda M (1980). "Spinocerebellar projections to the vermis of the posterior lobe and the paramedian lobule in the cat, as studied by retrograde transport of horseradish peroxidase." J Comp Neurol **192**(1): 143-162.

Matsushita M and Okado N (1981). "Spinocerebellar projections to lobules I and II of the anterior lobe in the cat, as studied by retrograde transport of horseradish peroxidase." J Comp Neurol **197**(3): 411-424.

Matsushita M, Tanami T and Yaginuma H (1984). "Differential distribution of spinocerebellar fiber terminals within the lobules of the cerebellar anterior lobe in the cat: an anterograde WGA-HRP study." Brain Res **305**(1): 157-161.

Matsushita M and Yaginuma H (1989). "Spinocerebellar projections from spinal border cells in the cat as studied by anterograde transport of wheat germ agglutinin-horseradish peroxidase." J Comp Neurol **288**(1): 19-38.

Matsuyama K, Mori F, Kuze B and Mori S (1999). "Morphology of single pontine reticulospinal axons in the lumbar enlargement of the cat: a study using the anterograde tracer PHA-L." J Comp Neurol **410**(3): 413-430.

Matsuyama K, Nakajima K, Mori F, Aoki M and Mori S (2004). "Lumbar commissural interneurons with reticulospinal inputs in the cat: morphology and discharge patterns during fictive locomotion." The Journal of Comparative Neurology **474**(4): 546-561.

Matthews PBC (1964). "Muscle spindles and their motor control." Physiol Rev **44**: 219-288.

Maxwell DJ, Christie WM, Ottersen OP and Storm-Mathisen J (1990). "Terminals of group Ia primary afferent fibres in Clarke's column are enriched with L-glutamate-like immunoreactivity." Brain Res **510**(2): 346-350.

Maxwell DJ and Jankowska E (1996). "Synaptic relationships between serotonin-immunoreactive axons and dorsal horn spinocerebellar tract cells in the cat spinal cord." Neuroscience **70**(1): 247-253.

Maxwell DJ, Kerr R, Jankowska E and Riddell JS (1997). "Synaptic connections of dorsal horn group II spinal interneurons: synapses formed with the interneurons and by their axon collaterals." J Comp Neurol **380**(1): 51-69.

McGonigle DJ, Maxwell DJ, Shehab SA and Kerr R (1996). "Evidence for the presence of neurokinin-1 receptors on dorsal horn spinocerebellar tract cells in the rat." Brain Res **742**(1-2): 1-9.

McIntire SL, Reimer RJ, Schuske K, Edwards RH and Jorgensen EM (1997). "Identification and characterization of the vesicular GABA transporter." Nature **389**(6653): 870-876.

McIntyre AK, Proske U and Rawson JA (1985). "Pathway to the cerebral cortex for impulses from tendon organs in the cat's hind limb." J Physiol **369**: 115-126.

Meyer G, Kirsch J, Betz H and Langosch D (1995). "Identification of a gephyrin-binding motif on the glycine receptor b subunit." Neuron **15**:563–572.

Miller MW (1987). "The origin of corticospinal projection neurons in rat." Experimental brain research. Experimentelle Hirnforschung. Experimentation cerebrale **67**(2): 339-351.

Mitani A, Ito K, Mitani Y and McCarley RW (1988a). "Descending projections from the gigantocellular tegmental field in the cat: cells of origin and their brainstem and spinal cord trajectories." The Journal of Comparative Neurology **268**(4): 546-566.

Mitani A, Ito K, Mitani Y and McCarley RW (1988b). "Morphological and electrophysiological identification of gigantocellular tegmental field neurons with descending projections in the cat: II. Bulb." The Journal of Comparative Neurology **274**(3): 371-386.

Mitchell K, Spike RC and Todd AJ (1993). "An immunocytochemical study of glycine receptor and GABA in laminae I-III of rat spinal dorsal horn." J Neurosci **13**(6): 2371-2381.

Molander C, Xu Q and Grant G (1984). "The cytoarchitectonic organization of the spinal cord in the rat. I. The lower thoracic and lumbosacral cord." J Comp Neurol **230**(1): 133-141.

Morona R, Lopez JM and Gonzalez A (2006). "Calbindin-D28k and calretinin immunoreactivity in the spinal cord of the lizard Gekko gecko: Colocalization with choline acetyltransferase and nitric oxide synthase." Brain Res Bull **69**(5): 519-534.

Neafsey EJ, Bold EL, Haas G, Hurley-Gius KM, Quirk G, Sievert CF and Terreberry RR (1986). "The organization of the rat motor cortex: a microstimulation mapping study." Brain Research **396**(1): 77-96.

Nyberg-Hansen R (1964a). "THE LOCATION AND TERMINATION OF TECTOSPINAL FIBERS IN THE CAT." Experimental Neurology **9**: 212-227.

Nyberg-Hansen R (1964b). "Origin and Termination of Fibers from the Vestibular Nuclei Descending in the Medial Longitudinal Fasciculus. an Experimental Study with Silver Impregnation Methods in the Cat." J Comp Neurol **122**: 355-367.

Nyberg-Hansen R (1965). "Sites and Mode of Termination of Reticulo-Spinal Fibers in the Cat. an Experimental Study with Silver Impregnation Methods." J Comp Neurol **124**: 71-99.

Nyberg-Hansen R and Mascitti TA (1964). "Sites and Mode of Termination of Fibers of the Vestibulospinal Tract in the Cat. an Experimental Study with Silver Impregnation Methods." J Comp Neurol **122**: 369-383.

Ornung G, Ottersen OP, Cullheim S and Ulfhake B (1998). "Distribution of glutamate-, glycine- and GABA-immunoreactive nerve terminals on dendrites in the cat spinal motor nucleus." Experimental brain research. Experimentelle Hirnforschung. Experimentation cerebrale **118**(4): 517-532.

Ornung G, Shupliakov O, Lindå H, Ottersen OP, Storm-Mathisen J, Ulfhake B and Cullheim S (1996). "Qualitative and quantitative analysis of glycine- and GABA-immunoreactive nerve terminals on motoneuron cell bodies in the cat spinal cord: a postembedding electron microscopic study." The Journal of comparative neurology **365**(3): 413-426.

Ornung G, Shupliakov O, Ottersen OP, Storm-Mathisen J and Cullheim S (1994). "Immunohistochemical evidence for coexistence of glycine and GABA in nerve terminals on cat spinal motoneurones: an ultrastructural study." Neuroreport **5**(8): 889-892.

Osborn CE and Poppele RE (1983). "Cross-correlation analysis of the response of units in the dorsal spinocerebellar tract (DSCT) to muscle stretch and contraction." Brain Res **280**(2): 339-342.

Oscarsson O (1957). "Functional Organization of the Ventral Spino-Cerebellar Tract in the Cat.: I. Electrophysiological Identification of the Tract." Acta Physiologica Scandinavica **38**(2): 145-165.

Oscarsson O (1965). "Functional Organization of the Spino- and Cuneocerebellar Tracts." Physiol Rev **45**: 495-522.

Oscarsson O and Uddenberg N (1964). "Identification of a Spinocerebellar Tract Activated from Forelimb Afferents in the Cat." Acta Physiol Scand **62**: 125-136.

Oscarsson O and Uddenberg N (1965). "Properties of Afferent Connections to the Rostral Spinocerebellar Tract in the Cat." Acta Physiol Scand **64**: 143-153.

Paxinos G and Watson C (1997). The rat brain in stereotaxic coordinates. New York, Academic Press.

Pearson JC, Sedivec MJ, Dewey DE and Fyffe RE (2000). "Light microscopic observations on the relationships between 5-hydroxytryptamine-immunoreactive axons and dorsal spinocerebellar tract cells in Clarke's column in the cat." Experimental brain research. Experimentelle Hirnforschung. Experimentation cerebrale **130**(3): 320-327.

Peterson BW (1979). "Reticulospinal projections to spinal motor nuclei." Annu Rev Physiol **41**: 127-140.

Peterson BW, Maunz RA, Pitts NG and Mackel RG (1975). "Patterns of projection and braching of reticulospinal neurons." Exp Brain Res **23**(4): 333-351.

Petras JM (1967). "Cortical, tectal and tegmental fiber connections in the spinal cord of the cat." Brain Res **6**(2): 275-324.

Petras JM (1977). "Spinocerebellar neurons in the rhesus monkey." Brain research **130**(1): 146-151.

Petras JM and Cummings JF (1977). "The origin of spinocerebellar pathways. II. The nucleus centrobasalis of the cervical enlargement and the nucleus dorsalis of the thoracolumbar spinal cord." J Comp Neurol **173**(4): 693-716.

Pfeiffer F, Simler R, Grenninlogh G and Betz H (1984). "Monoclonal antibodies and peptide mapping reveal structural similarities between the subunits of the glycine receptor of rat spinal cord." Proc Natl Acad Sci, USA **81**:7224-7227.

Pijpers A, Apps R, Pardoe J, Voogd J and Ruigrok TJ (2006). "Precise spatial relationships between mossy fibers and climbing fibers in rat cerebellar cortical zones." J Neurosci **26**:12067-12080.

Pompeiano O and Brodal A (1957). "Experimental demonstration of a somatotopical origin of rubrospinal fibers in the cat." The Journal of Comparative Neurology **108**(2): 225-251.

Poppele RE, Rankin A and Eian J (2003). "Dorsal spinocerebellar tract neurons respond to contralateral limb stepping." Exp Brain Res **149**(3): 361-370.

Prentice SD and Drew T (2001). "Contributions of the reticulospinal system to the postural adjustments occurring during voluntary gait modifications." Journal of neurophysiology **85**(2): 679-698.

Rall W (1977). Core conductor theory and cable properties of neurons. The Nervous System. Kandel ER. Washington, American Physiological Society**:** 39-97.

Rall W, Burke RE, Smith TG, Nelson PG and Frank K (1967). "Dendritic location of synapses and possible mechanisms for the monosynaptic EPSP in motoneurons." J Neurophysiol **30**(5): 1169-1193.

Randic M, Miletic V and Loewy AD (1981). "A morphological study of cat dorsal spinocerebellar tract neurons after intracellular injection of horseradish peroxidase." J Comp Neurol **198**(3): 453-466.

Randic M, Myslinski NR and Gordon JH (1976). "Spinal localization of neurons receiving inputs from cutaneous afferents in the cat hindlimb." Brain Res **105**(3): 573-577.

Reed WR, Shum-Siu A and Magnuson DS (2008). "Reticulospinal pathways in the ventrolateral funiculus with terminations in the cervical and lumbar enlargements of the adult rat spinal cord." Neuroscience **151**(2): 505-517.

Ren K and Ruda MA (1994). "A comparative study of the calcium-binding proteins calbindin-D28K, calretinin, calmodulin and parvalbumin in the rat spinal cord." Brain Res Brain Res Rev **19**(2): 163-179.

Ren K, Ruda MA and Jacobowitz DM (1993). "Immunohistochemical localization of calretinin in the dorsal root ganglion and spinal cord of the rat." Brain Res Bull **31**(1-2): 13-22.

Resibois A and Rogers JH (1992). "Calretinin in rat brain: an immunohistochemical study." Neuroscience **46**(1): 101-134.

Réthelyi M (1970). "Ultrastructural synaptology of Clarke's column." Experimental brain research. Experimentelle Hirnforschung. Experimentation cerebrale **11**(2): 159-174.

Rexed B (1954). "A cytoarchitectonic atlas of the spinal cord in the cat." J Comp Neurol **100**(2): 297-379.

Riddle CN and Baker SN (2010). "Convergence of pyramidal and medial brain stem descending pathways onto macaque cervical spinal interneurons." Journal of neurophysiology **103**(5): 2821-2832.

Riddle CN, Edgley SA and Baker SN (2009). "Direct and indirect connections with upper limb motoneurons from the primate reticulospinal tract." The Journal of neuroscience : the official journal of the Society for Neuroscience **29**(15): 4993-4999.

Robbins A, Schwartz-Giblin S and Pfaff DW (1992). "Reticulospinal and reticuloreticular pathways for activating the lumbar back muscles in the rat." Experimental Brain Research **92**(1): 46-58.

Rogers JH and Resibois A (1992). "Calretinin and calbindin-D28k in rat brain: patterns of partial co-localization." Neuroscience **51**(4): 843-865.

Rose PK, MacDonald J and Abrahams VC (1991). "Projections of the tectospinal tract to the upper cervical spinal cord of the cat: a study with the anterograde tracer PHA-L." The Journal of Comparative Neurology **314**(1): 91-105.

Rose PK, Tourond JA and Donevan AH (1996). "Morphology of single vestibulospinal collaterals in the upper cervical spinal cord of the cat: III collaterals originating from axons in the ventral funiculus ipsilateral to their cells of origin." J Comp Neurol **364**(1): 16-31.

Sakai ST, Davidson AG and Buford JA (2009). "Reticulospinal neurons in the pontomedullary reticular formation of the monkey (Macaca fascicularis)." Neuroscience **163**(4): 1158-1170.

Sanna PP, Celio MR, Bloom FE and Rende M (1993). "Presumptive Renshaw cells contain decreased calbindin during recovery from sciatic nerve lesions." Proc Natl Acad Sci U S A **90**(7): 3048-3052.

Schepens B and Drew T (2004). "Independent and convergent signals from the pontomedullary reticular formation contribute to the control of posture and movement during reaching in the cat." Journal of neurophysiology **92**(4): 2217-2238.

Schepens B, Stapley P and Drew T (2008). "Neurons in the pontomedullary reticular formation signal posture and movement both as an integrated behavior and independently." Journal of neurophysiology **100**(4): 2235-2253.

Schneider SP and Fyffe RE (1992). "Involvement of GABA and glycine in recurrent inhibition of spinal motoneurons." Journal of neurophysiology **68**(2): 397-406.

Schomburg ED and Steffens H (1988). "The effect of DOPA and clonidine on reflex pathways from group II muscle afferents to alpha-motoneurones in the cat." Experimental brain research. Experimentelle Hirnforschung. Experimentation cerebrale **71**(2): 442-446.

Schor RH, Suzuki I, Timerick SJ and Wilson VJ (1986). "Responses of interneurons in the cat cervical cord to vestibular tilt stimulation." J Neurophysiol **56**(4): 1147-1156.

Shakya-Shrestha S, Bannatyne BA, Jankowska E, Hammar I, Nilsson E and Maxwell DJ (2012). "Excitatory inputs to four types of spinocerebellar tract neurons in the cat and the rat thoraco-lumbar spinal cord." The Journal of physiology **590**(Pt 7): 1737-1755.

Shamboul KM (1980). "Lumbosacral predominance of vestibulospinal fibre projection in the rat." J Comp Neurol **192**(3): 519-530.
Sherrington CS (1906). The Integrative Action of the Nervous System. New Haven, CT: Yale Univ. Press.
Shieh JY, Leong SK and Wong WC (1983). "Origin of the rubrospinal tract in neonatal, developing, and mature rats." The Journal of Comparative Neurology **214**(1): 79-86.
Shinoda Y, Sugiuchi Y, Izawa Y and Hata Y (2006). "Long descending motor tract axons and their control of neck and axial muscles." Prog Brain Res **151**: 527-563.
Shokunbi MT, Hrycyshyn AW and Flumerfelt BA (1986). "A horseradish peroxidase study of the rubral and cortical afferents to the lateral reticular nucleus in the rat." The Journal of Comparative Neurology **248**(3): 441-454.
Snyder RL, Faull RL and Mehler WR (1978). "A comparative study of the neurons of origin of the spinocerebellar afferents in the rat, cat and squirrel monkey based on the retrograde transport of horseradish peroxidase." J Comp Neurol **181**(4): 833-852.
Soffe SR, Roberts A and Li WC (2009). "Defining the excitatory neurons that drive the locomotor rhythm in a simple vertebrate: insights into the origin of reticulospinal control." The Journal of physiology **587**(Pt 20): 4829-4844.
Soghomonian JJ and Martin DL (1998). "Two isoforms of glutamate decarboxylase: why?" Trends in pharmacological sciences **19**(12): 500-505.
Strominger RN, McGiffen JE and Strominger NL (1987). "Morphometric and experimental studies of the red nucleus in the albino rat." The Anatomical record **219**(4): 420-428.
Sugiuchi Y, Izawa Y and Shinoda Y (1995). "Trisynaptic inhibition from the contralateral vertical semicircular canal nerves to neck motoneurons mediated by spinal commissural neurons." J Neurophysiol **73**(5): 1973-1987.
Suzuki I, Timerick SJ and Wilson VJ (1985). "Body position with respect to the head or body position in space is coded by lumbar interneurons." J Neurophysiol **54**(1): 123-133.
Taal W and Holstege JC (1994). "GABA and glycine frequently colocalize in terminals on cat spinal motoneurons." Neuroreport **5**(17): 2225-2228.
Tapper DN, Mann MD, Brown PB and Cogdell B (1975). "Cells of origin of the cutaneous subdivision of the dorsal spinocerebellar tract." Brain Res **85**(1): 59-63.
Todd AJ, Hughes DI, Polgar E, Nagy GG, Mackie M, Ottersen OP and Maxwell DJ (2003). "The expression of vesicular glutamate transporters VGLUT1 and VGLUT2 in neurochemically defined axonal populations in the rat spinal cord with emphasis on the dorsal horn." Eur J Neurosci **17**(1): 13-27.
Todd AJ, Spike RC, Chong D and Neilson M (1995). "The relationship between glycine and gephyrin in synapses of the rat spinal cord." Eur J Neurosci **7**(1): 1-11.
Todd AJ and Sullivan AC (1990). "Light microscope study of the coexistence of GABA-like and glycine-like immunoreactivities in the spinal cord of the rat." J Comp Neurol **296**(3): 496-505.
Tohyama M, Sakai K, Salvert D, Touret M and Jouvet M (1979a). "Spinal projections from the lower brain stem in the cat as demonstrated by the

horseradish peroxidase technique. I. Origins of the reticulospinal tracts and their funicular trajectories." Brain Research **173**(3): 383-403.

Tohyama M, Sakai K, Touret M, Salvert D and Jouvet M (1979b). "Spinal projections from the lower brain stem in the cat as demonstrated by the horseradish peroxidase technique. II. Projections from the dorsolateral pontine tegmentum and raphe nuclei." Brain Res **176**(2): 215-231.

Tracey DJ and Walmsley B (1984). "Synaptic input from identified muscle afferents to neurones of the dorsal spinocerebellar tract in the cat." J Physiol **350**: 599-614.

Triller A, Cluzeaud F and Korn H (1987). "gamma-Aminobutyric acid-containing terminals can be apposed to glycine receptors at central synapses." J Cell Biol **104**(4): 947-956.

Valtschanoff JG, Weinberg RJ and Rustioni A (1993). "Amino acid immunoreactivity in corticospinal terminals." Exp Brain Res **93**(1): 95-103.

van Kan PL and McCurdy ML (2001). "Role of primate magnocellular red nucleus neurons in controlling hand preshaping during reaching to grasp." J Neurophysiol **85**:1461–1478.

Varoqui H, Schafer MK, Zhu H, Weihe E and Erickson JD (2002). "Identification of the differentiation-associated Na+/PI transporter as a novel vesicular glutamate transporter expressed in a distinct set of glutamatergic synapses." J Neurosci **22**(1): 142-155.

Vetrivelan R, Fuller PM, Tong Q and Lu J (2009). "Medullary circuitry regulating rapid eye movement sleep and motor atonia." The Journal of neuroscience : the official journal of the Society for Neuroscience **29**(29): 9361-9369.

Waldron HA and Gwyn DG (1969). "Descending nerve tracts in the spinal cord of the rat. I. Fibers from the midbrain." The Journal of Comparative Neurology **137**(2): 143-153.

Walmsley B (1989). "Synaptic potentials evoked in cat dorsal spinocerebellar tract neurones by impulses in single group I muscle afferents." J Physiol **415**: 423-431.

Walmsley B and Nicol MJ (1990). "Location and morphology of dorsal spinocerebellar tract neurons that receive monosynaptic afferent input from ankle extensor muscles in cat hindlimb." J Neurophysiol **63**(2): 286-293.

Walmsley B and Nicol MJ (1991). "The effects of Ca2+, Mg2+ and kynurenate on primary afferent synaptic potentials evoked in cat spinal cord neurones in vivo." J Physiol **433**: 409-420.

Walmsley B, Wieniawa-Narkiewicz E and Nicol MJ (1985). "The ultrastructural basis for synaptic transmission between primary muscle afferents and neurons in Clarke's column of the cat." J Neurosci **5**(8): 2095-2106.

Walmsley B, Wieniawa-Narkiewicz E and Nicol MJ (1987). "Ultrastructural evidence related to presynaptic inhibition of primary muscle afferents in Clarke's column of the cat." J Neurosci **7**(1): 236-243.

Waltzer R and Martin GF (1984). "Collateralization of reticulospinal axons from the nucleus reticularis gigantocellularis to the cerebellum and diencephalon. A double-labelling study in the rat." Brain Res **293**(1): 153-158.

Wilson VJ, Ezure K and Timerick SJ (1984). "Tonic neck reflex of the decerebrate cat: response of spinal interneurons to natural stimulation of neck and vestibular receptors." J Neurophysiol **51**(3): 567-577.

Wilson VJ and Peterson BW (1978). "Peripheral and central substrates of vestibulospinal reflexes." Physiol Rev **58**(1): 80-105.

Wilson VJ and Yoshida M (1969). "Comparison of effects of stimulation of Deiters' nucleus and medial longitudinal fasciculus on neck, forelimb, and hindlimb motoneurons." J Neurophysiol **32**(5): 743-758.

Wirth FP, O'Leary JL, Smith JM and Jenny AB (1974). "Monosynaptic corticospinal-motoneuron path in the raccoon." Brain Res **77**(2): 344-348.

Wojcik SM, Katsurabayashi S, Guillemin I, Friauf E, Rosenmund C, Brose N and Rhee JS (2006). "A shared vesicular carrier allows synaptic corelease of GABA and glycine." Neuron **50**(4): 575-587.

Xu Q and Grant G (1994). "Course of spinocerebellar axons in the ventral and lateral funiculi of the spinal cord with projections to the anterior lobe: an experimental anatomical study in the cat with retrograde tracing techniques." The Journal of comparative neurology **345**(2): 288-302.

Xu Q and Grant G (2005). "Course of spinocerebellar axons in the ventral and lateral funiculi of the spinal cord with projections to the posterior cerebellar termination area: an experimental anatomical study in the cat, using a retrograde tracing technique." Exp Brain Res **162**(2): 250-256.

Yaginuma H and Matsushita M (1986). "The projection fields of spinal border cells in the cerebellar anterior lobe in the cat: an anterograde WGA-HRP study." Brain Res **384**(1): 175-179.

Yoshida S, Senba E, Kubota Y, Hagihira S, Yoshiya I, Emson PC and Tohyama M (1990). "Calcium-binding proteins calbindin and parvalbumin in the superficial dorsal horn of the rat spinal cord." Neuroscience **37**(3): 839-848.

Zhang JH, Morita Y, Hironaka T, Emson PC and Tohyama M (1990). "Ontological study of calbindin-D28k-like and parvalbumin-like immunoreactivities in rat spinal cord and dorsal root ganglia." J Comp Neurol **302**(4): 715-728.

List of Publications

Shakya Shrestha S, Bannatyne BA, Jankowska E, Hammar I, Nilsson E & Maxwell DJ (2012). "Excitatory inputs to four types of spinocerebellar tract neurons in the cat and the rat thoraco-lumbar spinal cord." *The Journal of physiology* **590,** 1737-1755.

Shakya Shrestha S, Bannatyne BA, Jankowska E, Hammar I, Nilsson E & Maxwell DJ (2012). "Inhibitory inputs to four types of spinocerebellar tract neurons in the cat spinal cord." *Neuroscience,* in press.

Du Beau A, Shakya Shrestha S, Bannatyne BA, Jalicy SM, Linnen S & Maxwell DJ (2012). "Neurotransmitter phenotypes of descending systems in the rat lumbar spinal cord." *Neuroscience,* in press.